Title
Macromolecules for the Delivery of Cancer Chemotherapeutics

Author
van der Poll, Derek Gregory

Publication Date
2010

Peer reviewed|Thesis/dissertation

Macromolecules for the Delivery of Cancer Chemotherapeutics

by

Derek Gregory van der Poll

A dissertation submitted in partial satisfaction of the

requirements for the degree of

Doctor of Philosophy

in

Chemistry

in the

Graduate Division

of the

University of California, Berkeley

Committee in charge:

Professor Jean M. J. Fréchet, Chair
Professor Kenneth Raymond
Professor Jhih-Wei Chu

Fall 2010

Macromolecules for the Delivery of Cancer Chemotherapeutics

Abstract

Macromolecules for the Delivery of Cancer Chemotherapeutics

by

Derek Gregory van der Poll

Doctor of Philosophy in Chemistry

University of California, Berkeley

Professor Jean M. J. Fréchet, Chair

Chemotherapy is the practice of treating cancer with antineoplastic drugs. In general, these drugs are highly toxic, and in many patients the side effects from therapy become so severe that treatment is stopped before full tumor remission has occurred. Further, chemotherapeutics usually have poor water solubility and short circulation lifetimes, which makes it difficult to get a significant fraction of the injected dose to the tumor site. The use of polymers as delivery vehicles for drugs is a strategy for improving the efficacy and reducing the side effects of toxic cancer drugs. The design of an ideal polymeric system for drug delivery is an active area of research and PEGylated dendrimers are among the most promising. Here we report the design, synthesis and biological evaluation of a biodegradable and versatile PEGylated dendrimer. We also report the preliminary results of a project involving hyaluronic acid functionalized liposomes.

Chapter 1 is a brief overview of the background and history of polymers in drug delivery. The relevance of dendrimers is described in the context of other polymer delivery systems that have begun the transition into clinical development.

Chapter 2 describes the synthesis and characterization of a PEGylated dendrimer that is biodegradable, robust, and has a nine step synthesis to drug loaded material. The polymer was functionalized with the drug, doxorubicin, and evaluated in mice. The *in vivo* chemotherapy experiment in Balb/c mice inoculated with murine C26 colon carcinoma resulted in nine out of ten long fully cured mice.

Chapter 3 describes the application of PEGylated dendrimers with platinum therapeutics. In order to increase the number of drug attachment sites on the dendrimer, the dendrimer core is used as a macroinitiator to carry out a ring-opening radial growth polymerization of the *N*-carboxy anhydride of glutamic acid. The terminal amines are then PEGylated and platinum chelators are attached to the glutamic acid side chains. Preliminary biological evaluation revealed that the polymer released platinum too quickly and therefore did not significantly improve the efficacy of the drug. This information was what inspired the research in chapter 4.

Chapter 4 presents the synthesis and characterization of a small library of polymer bound platinum chelators. The chelators were loaded with diaminocyclohexane platinate (DACHPt). Differences in the ring size and ligand strength are examined in relation to drug release rate and cytotoxity. The most promising chelators were taken forward and evaluated in the C26 colon carcinoma model alongside the clinical drug, cisplatin, as a positive control.

Chapter 5 outlines an attempt to develop a new class of platinum (II) drugs that are specially tailored for polymeric drug delivery. A small library of heterocyclic diamine ligands functionalized with a ketone moiety was synthesized. The ligands were loaded with platinum (II) and the complexes were screened for their *in vitro* toxicity. The complexes with high potency were attached to polymers via a hydrazone bond and evaluated *in vivo*.

Chapter 6 outlines a new synthetic approach toward hyaluronic acid (HA) functionalized liposomes. HA, a naturally occurring polysaccharide is specific ligand for the CD44 receptor which is overexpressed on a number of cancer cell types. Using oxime chemistry, lipid molecules were attached to various lengths of HA oligomers at their reducing ends. The glycolipids were then incorporated into fluorescently labeled liposomes. The cells preferentially internalized the HA-targeted liposomes and did not internalize non-targeted control liposomes.

Table of Contents

Dedications

To my parents, Jan and Henny van der Poll.

Acknowledgements

I acknowledge the contributions to this research made by my advisor, Jean Fréchet. He has provided great advice and insight into the work described in this dissertation. Under Professor Fréchet's guidance I have been exposed to science at the highest level. I will always be grateful for having the opportunity to be a part of his lab.

I am also very grateful for the opportunity to collaborate with Professor Francis Szoka at the University of California, San Francisco. It has been an invaluable experience to be part of a collaborative team of outstanding scientists.

I would also like to acknowledge the few individuals who have directly contributed to the work described in this dissertation: Heidi Kieler-Ferguson, William Floyd, Katherine Jerger, Dr. Steven Guillaudeu, Dr. Megan Fox, Dr. Daniel Poulsen, Dr. Cameron Lee, Professor Elizabeth Gillies, and Yarah Haidar. I am also grateful to the leadership provided by Dr. Justin Mynar during Professor Fréchet's time at KAUST.

I would like to thank all of the great friends, both in and out of lab, that have made my time in Berkeley so enjoyable. There are too many to mention. I especially thank my parents, Jan and Henny van der Poll, for endless encouragement and support. Also, I thank my brothers: Herbert, Maarten, and Thomas, for making sure I maintain some interests outside of science. Finally, I thank Tara Yacovitch for bringing happiness to my life no matter how well or how poorly my experiments are going.

Chapter 1 – Introduction to Polymers in Drug Delivery

Abstract

The use of polymers in drug delivery is an active field of research in both academia and in industry. Polymers have found a number of applications in the biomedical field that have profoundly improved the quality of life for people with a wide range of health problems. Chapter 1 is a short overview of the role polymers have played as delivery vehicles for bioactive agents. Advances in polymer materieals for delivery of small molecule chemotherapeutics are emphasized. The state of clinically relevant polymers as well as fundamental research in structure-property relationships of polymers are discussed.

Introduction

In the past century, advances in polymer science have made an enormous impact on society. Manipulating a polymer structure at the molecular level can allow access to materials with a breadth of properties from Styrofoam all the way to Kevlar. In addition to being key components in industrial and consumer products, polymers have a growing role in the biomedical field. A few examples of polymer uses in healthcare include prostheses, medical devices and contact lenses. More recently, synthetic polymers are being used to create nanoscopic therapeutics such as polymer-protein conjugates,[1] polymer-drug,[2] or polymer-nucleic acid[3,4] conjugates to treat various disease targets. The first successful implementation of polymer therapeutics came from conjugation of water soluble linear polymers to proteins. Biotechnology has offered many peptide, protein, and antibody therapeutics; but, they suffer from a few limitations including short plasma residence times and poor stability *in vivo*. Attachment of poly(ethylene) glycol (PEG) to a protein increases the protein's hydrodynamic volume thereby increasing its blood circulation time. The PEG chains also provide a protective coating for the protein, which prevents uptake by the reticuloendothelial system (RES) and prevents enzymatic degradation of the protein during circulation. Great progress has been made in the chemistry of protein PEGylation which has led to improved efficacy of protein therapeutics.[5] Since the first PEGylated protein reached the market in 1990,[6] the clinical impact of polymer-protein conjugates has continued to grow as more and more polymer-protein therapeutics achieve FDA approval and help treat diseases in people.

Like proteins, small molecule drugs benefit from polymer conjugation. Chemotherapy is commonly associated with severe side effects that are sometimes life threatening and also reduce the quality of life for the patient. The systemic toxicity caused by cancer drugs is a major limitation of chemotherapy. Small molecule cancer drugs are usually poorly soluble, have a short plasma residence and no specificity for the tumor site. A drug that is attached to a hydrophilic polymer has improved solubility and an increased blood circulation time because the drug takes on the pharmacokinetic properties of the polymer while reducing metabolism by the RES. Additionally, polymer-drug conjugates passively target tumor sites via enhanced permeation and retention (EPR) effect.[7,8] These characteristics of polymer-drug conjugates allow for more of the injected dose accumulating at the tumor tissue, which provides improved efficacy and decreased side effects.[9,10] In comparison to protein-polymer therapeutics, the design of polymer-drug conjugates brings on new challenges and considerations. For example, Neulasta™ is a recombinant human megakaryocyte colony stimulating factor that is composed of 19 kDa protein attached to a single 20 kDa PEG chain.[11] If the same polymer attachment strategy is taken for the chemotherapeutic, doxorubicin, a 543 Da drug would be conjugated to a 20 kDa PEG chain. The polymer conjugate would have 2.6 wt% loading of active pharmaceutical ingredient, which means that 1 gram of polymer is required for a 26 milligram dose of doxorubicin to be administered. This has driven the search for polymeric carriers that can carry multiple copies of a drug and ultimately increase the therapeutic payload.

Polymeric Architectures in Drug Delivery

Ringsdorf postulated that linear polymers can be functionalized with a drug molecule that is then selectively released inside the cell.[12] Interestingly, polymeric delivery of small molecule drugs was originally seen as an opportunity to improve cell specificity of small molecule hydrophobic drugs even before the EPR effect was discovered.[2] The important design features for a new polymeric carrier are the size or hydrodynamic volume, pharmacokinetic profile,

capacity for high drug loading, low toxicity, low polydispersity index (PDI), simple synthesis and characterization, and biodegradability.[13] Currently, there are many different drug vehicles being explored for cancer therapy.[14] They can be broadly characterized by four descriptors: linear, branched, unimolecular, and self-assembled. Figure 1 shows a few key examples of polymer materials studied for drug delivery and how they fit in to the 4 categories. [15-39] Each material has advantages and disadvantages in regard to the design criteria described above. To date, liposomes, linear polymers and polymer micelles are the furthest along in their clinical development.

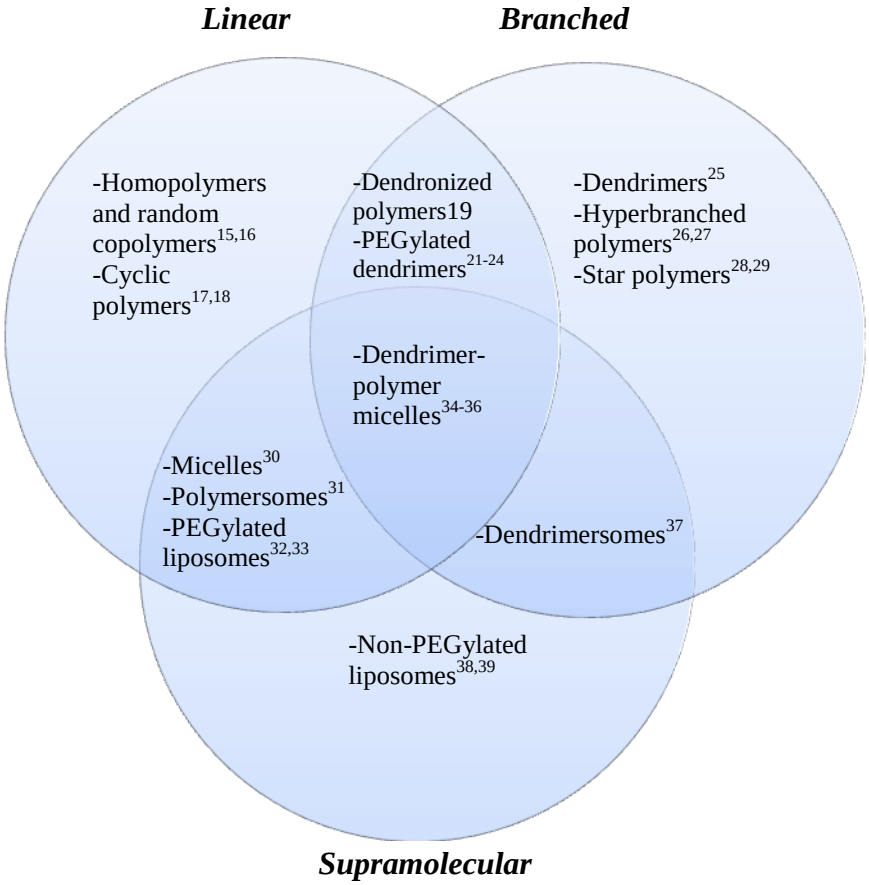

Figure 1. A diagram that divides the types of delivery vehicles based on their molecular architecture and solution properties.

Liposomes

The most successful and clinically relevant delivery vehicle for small molecule drugs is the liposome.[40] Liposomes are spherical lipid bilayers with aqueous interiors.[41] The development of sterically stabilized liposomes that have PEG chains displayed on their surface resulted in "stealth" liposomes that avoided opsonization and clearance by the RES.[33,42] Sterically stabilized liposomes with doxorubicin encapsulated (Doxil, U.S.; Caelyx, Europe) were developed by Sequus Pharmaceuticals and have achieved FDA approval. Liposomes are usually in the 80-100 nm size range and can carry a relatively high payload of drug in their interiors. Since the discovery of liposomes, academia and industry have been pushing the frontiers of liposome

technology with different therapeutic payloads, imaging agents and active targeting towards a myriad of diseases.[32]

Linear Polymers

The biggest advantage of linear polymers over other delivery systems is their simplicity. While self-assembled liposomes can have issues of poor stability and rapid drug release, linear polymers are amenable to covalent attachment of various drug molecules through stimuli responsive drug linkages.[43] There are many different linear polymers that have been studied for drug delivery, and several have reached clinical trials including PEGylated drugs[44] and polyglutamic acid-drug conjugates[45]. The most extensively studied linear polymer drug delivery system is poly(2-hydroxypropyl methacrylamide) (HPMA), a water soluble polymer originally developed in the labs of Jindrich Kopecek.[46] HPMA polymers functionalized with doxorubicin[47,48], paclitaxel[49], camptothecin[50] and platinum drugs[51,52] have been entered into clinical trials (Figure 2). The polymers in solution typically have hydrodynamic radii of 2-10 nm.

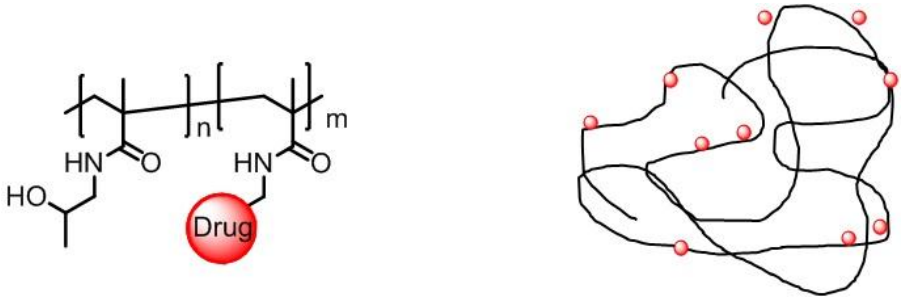

Figure 2. A representative drug loaded HPMA copolymer structure and a cartoon of is solution phase morphology.

An enormous amount of research has been carried out on these polymers in recent years focusing on demonstrating improved efficacy of the polymer-drug and investigation into the chemistry of drug attachment and programmed drug release. In a recent series of interesting reviews, Ruth Duncan and coworkers detail the challenges these polymers have faced during clinical trials.[53-56] Polymer therapeutics are considered a new chemical entitiy (NCE) by the regulatory agencies and the fate of each component of the conjugate is scrutinized very strictly. The molecular weight heterogeneity of each sample, the statistical distribution of each comonomer along the backbone, and lack of degradability of the HPMA backbone presents challenges when convincing regulatory agencies of the safety and reproducibility of the polymer therapeutic. While the likelihood for HPMA drugs to receive FDA approval is uncertain, over the last 30 years Duncan and her team paved the way for future polymer therapeutics to make the transition from the chemistry lab to the clinic.

Polymeric Micelles

Polymeric micelles are composed of linear, amphiphilic block copolymers. They benefit from simple preparation, high drug loading capacity and a core shell architecture were the hydrophilic block shields the payload contained at the micelle core either covalently[57] or encapsulated[58] at the core through hydrophobic interactions.[59] Professor Kazunori Kataoka has developed polymeric micelles which are composed of PEG-poly(aspartic acid) copolymers. The

aspartic acid block is rendered hydrophobic as the side chain is functionalized with a benzyl ester which forms water soluble aggregates ranging from 20-100 nm in size.[30] The Japanese company, NanoCarrier®, has PEG-poly(amino acid) copolymers in development for chemotherapeutic delivery, protein delivery, siRNA delivery. Challenges facing micelles for clinical approval are the stability of the self assembly during storage, control over drug release, and a safe and reproducible preparation protocol.

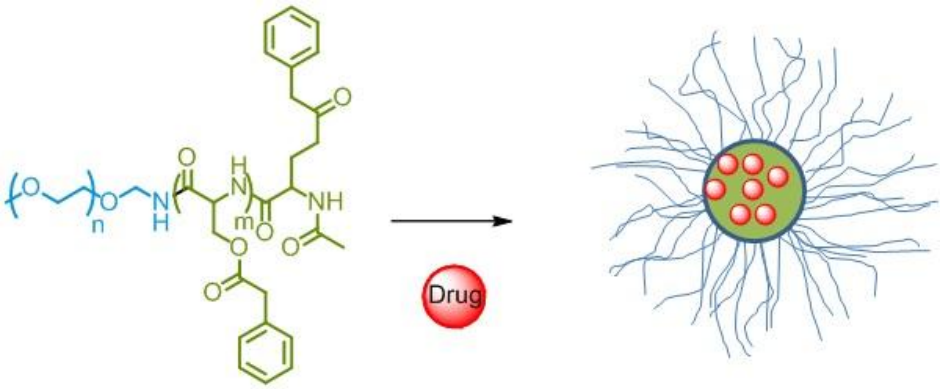

Figure 3. Structure of a PEG-poly(Asp(OBn)) block copolymer and a cartoon of the self-assembled architecture.

Dendrimers

Dendrimers are branched polymers that are capable of addressing the limitations of linear polymers and micelles at the cost of being more complicated to synthesize. Advantages of dendrimers include that they have multiple functional handles at their periphery that can be functionalized with a controlled number of drugs, targeting groups, or solubilizing groups.[60] They are prepared by a stepwise iterative synthesis, which ensures a monodisperse or nearly monodisperse sample with batch-to-batch reproducibility. A low PDI is an important feature for a polymeric material to be considered for clinical applications because variations in the polymer molecular weights from batch-to-batch can result in unpredictable and irreproducible pharmacokinetic properties. The earliest work on dendritic polymers dates back to Vogtle et al in 1978.[61] Currently, the most common techniques for dendrimer synthesis are convergent[62] and divergent[63] methods which have been used extensively to make dendrimers with many different properties for various applications.[64,65]

Dendrimers generally have three distinct parts: the core, the interior, and the periphery. Amphiphilic dendrimers have been made that are hydrophobic at their core and hydrophilic at their periphery enabling them to encapsulated hydrophobic small molecule drugs in their interiors.[66,67] Alternatively, drug molecules can be covalently,[68,69] or sometimes noncovalently,[70] attached to the functional groups at dendrimer periphery. These constructs are successful demonstrations of how dendrimers can bear a large and well-defined payload of drug and facilitate cell uptake. A drawback to these systems is that they are still relatively low molecular weight entities and the drug is often exposed at the dendrimer periphery so they are still excreted fairly quickly and can be recognized by the RES.[71]

The limitations of dendrimer-drug conjugates has led to the design of PEGylated dendrimers—a new class of dendrimer-linear polymer hybrid that is about 10 nm in diameter and takes on a core-shell architecture in solution where the PEG chains form a high molecular

weight, water soluble sheath around the cargo loaded at dendrimer core.[72,73] The desire to attach solubilizing groups and drugs to a single carrier has driven the design of dendrimers with multiple and orthogonal functionality.[21,74,75] Gillies and coworkers synthesized a library of "bow-tie" PEGylated dendrimers to investigate how the number of PEG chains and the molecular weight of each individual PEG chain affects the pharmacokinetics and biodistribution of PEGylated dendrimers (Figure 4).[76] Interestingly, it was found that a dendrimer with eight 5 kDa PEG chains (~40 kDa) had a blood circulation half-life of 31 hours while a dendrimer with two 20 kDa PEG chains (~40 kDa) had a half-life of only 1.5 hours. This trend held true for a library of eight different PEGylated dendrimers of varied PEG length and molecular weight. The accepted mechanism of renal filtration for neutral linear polymers relies on polymer reputation through the pores of the glomerulus.[77] Therefore, the deformability of a polymer affects the rate of renal clearance in addition to hydrodynamic volume. This explains why a linear polymer can permeate the glomerulus much more easily than a highly branched polymer. In a later study, the "bow-tie" polymer was functionalized with doxorubicin attached via a pH-sensitive hydrazone bond and provided a full cure in mice bearing C26 colon carcinoma.[9]

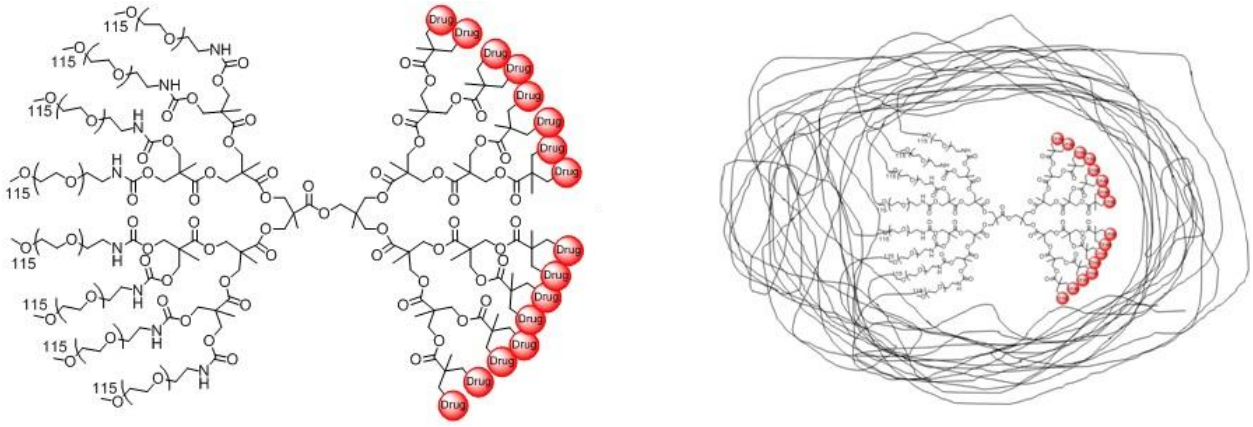

Figure 4. Chemical structure of a ~40 kDa bow-tie polymer and a cartoon of its solution phase morphology.

PEGylated dendrimers have emerged as a powerful and elegant vehicle for drug delivery applications and may become clinically relevant in the future. Many of the best performing systems still suffer from lengthy syntheses that would be difficult to implement in an industrial setting. Also, currently there are many promising drugs that cannot be attached to a polymer support in a controlled way that also offers selective or triggered drug release. The results produced thus far by dendrimers in drug delivery warrant continued research by interdisciplinary teams. The following chapters describe work toward developing a streamlined dendrimer synthesis, stimuli-responsive attachment strategies for new promising drugs and use of targeting ligands in liposome therapeutics.

References

(1) Harris, J. M.; Chess, R. B. *Nat Rev Drug Discov* **2003**, *2*, 214-221.
(2) Duncan, R. *Nat Rev Drug Discov* **2003**, *2*, 347-360.

(3) Nguyen, D. N.; Green, J. J.; Chan, J. M.; Longer, R.; Anderson, D. G. *Adv Mater* **2009**, *21*, 847-867.
(4) Ferber, D. *Science* **2001**, *294*, 1638-1642.
(5) Roberts, M. J.; Bentley, M. D.; Harris, J. M. *Adv Drug Deliver Rev* **2002**, *54*, 459-476.
(6) Levy, Y.; Hershfield, M. S.; Fernandezmejia, C.; Polmar, S. H.; Scudiery, D.; Berger, M.; Sorensen, R. U. *J Pediatr* **1988**, *113*, 312-317.
(7) Seymour, L. W. *Crit Rev Ther Drug* **1992**, *9*, 135-187.
(8) Matsumura, Y.; Maeda, H. *Cancer Res* **1986**, *46*, 6387-6392.
(9) Lee, C. C.; Gillies, E. R.; Fox, M. E.; Guillaudeu, S. J.; Frechet, J. M. J.; Dy, E. E.; Szoka, F. C. *P Natl Acad Sci USA* **2006**, *103*, 16649-16654.
(10) Seymour, L. W.; Ulbrich, K.; Strohalm, J.; Kopecek, J.; Duncan, R. *Biochem Pharmacol* **1990**, *39*, 1125-1131.
(11) Kinstler, O.; Molineux, G.; Treuheit, M.; Ladd, D.; Gegg, C. *Adv Drug Deliver Rev* **2002**, *54*, 477-485.
(12) Bader, H.; Ringsdorf, H.; Schmidt, B. *Angew Makromol Chem* **1984**, *123*, 457-485.
(13) Fox, M. E.; Szoka, F. C.; Frechet, J. M. J. *Accounts Chem Res* **2009**, *42*, 1141-1151.
(14) Peer, D.; Karp, J. M.; Hong, S.; FaroKHzad, O. C.; Margalit, R.; Langer, R. *Nat Nanotechnol* **2007**, *2*, 751-760.
(15) Tomlinson, R.; Heller, J.; Brocchini, S.; Duncan, R. *Bioconjugate Chem* **2003**, *14*, 1096-1106.
(16) Duncan, R. *Nat Rev Cancer* **2006**, *6*, 688-701.
(17) Nasongkla, N.; Chen, B.; Macaraeg, N.; Fox, M. E.; Frechet, J. M. J.; Szoka, F. C. *J Am Chem Soc* **2009**, *131*, 3842-3843.
(18) Chen, B.; Jerger, K.; Frechet, J. M. J.; Szoka, F. C. *J Control Release* **2009**, *140*, 203-209.
(19) Lee, C. C.; Yoshida, M.; Frechet, J. M. J.; Dy, E. E.; Szoka, F. C. *Bioconjugate Chem* **2005**, *16*, 535-541.
(20) Lim, J.; Guo, Y.; Rostollan, C. L.; Stanfield, J.; Hsieh, J. T.; Sun, X. K.; Simanek, E. E. *Mol Pharmaceut* **2008**, *5*, 540-547.
(21) Guillaudeu, S. J.; Fox, M. E.; Haidar, Y. M.; Dy, E. E.; Szoka, F. C.; Frechet, J. M. J. *Bioconjugate Chem* **2008**, *19*, 461-469.
(22) Fox, M. E.; Guillaudeu, S.; Frechet, J. M. J.; Jerger, K.; Macaraeg, N.; Szoka, F. C. *Mol Pharmaceut* **2009**, *6*, 1562-1572.
(23) van der Poll, D. G.; Kieler-Ferguson, H. M.; Floyd, W. C.; Guillaudeu, S. J.; Jerger, K.; Szoka, F. C.; Frechet, J. M. *Bioconjugate Chem* **2010**, *21*, 764-773.
(24) Kono, K.; Kojima, C.; Hayashi, N.; Nishisaka, E.; Kiura, K.; Wataral, S.; Harada, A. *Biomaterials* **2008**, *29*, 1664-1675.
(25) Medina, S. H.; El-Sayed, M. E. H. *Chem Rev* **2009**, *109*, 3141-3157.
(26) Voit, B. *J Polym Sci Pol Chem* **2000**, *38*, 2505-2525.
(27) Haxton, K. J.; Burt, H. M. *Dalton T* **2008**, 5872-5875.
(28) Fukukawa, K. I.; Rossin, R.; Hagooly, A.; Pressly, E. D.; Hunt, J. N.; Messmore, B. W.; Wooley, K. L.; Welch, M. J.; Hawker, C. J. *Biomacromolecules* **2008**, *9*, 1329-1339.
(29) Wang, F.; Bronich, T. K.; Kabanov, A. V.; Rauh, R. D.; Roovers, J. *Bioconjugate Chem* **2005**, *16*, 397-405.
(30) Kataoka, K.; Harada, A.; Nagasaki, Y. *Adv Drug Deliver Rev* **2001**, *47*, 113-131.
(31) Meng, F. H.; Zhong, Z. Y.; Feijen, J. *Biomacromolecules* **2009**, *10*, 197-209.

(32) Torchilin, V. P. *Nat Rev Drug Discov* **2005**, *4*, 145-160.
(33) Papahadjopoulos, D.; Allen, T. M.; Gabizon, a.; Mayhew, E.; Matthay, K.; Huang, S. K.; Lee, K. D.; Woodle, M. C.; Lasic, D. D.; Redemann, C.; Martin, F. J. *P Natl Acad Sci USA* **1991**, *88*, 11460-11464.
(34) Gillies, E. R.; Frechet, J. M. J. *Pure Appl Chem* **2004**, *76*, 1295-1307.
(35) Gillies, E. R.; Frechet, J. M. J. *Bioconjugate Chem* **2005**, *16*, 361-368.
(36) Gillies, E. R.; Jonsson, T. B.; Frechet, J. M. J. *J Am Chem Soc* **2004**, *126*, 11936-11943.
(37) Percec, V.; Wilson, D. A.; Leowanawat, P.; Wilson, C. J.; Hughes, A. D.; Kaucher, M. S.; Hammer, D. A.; Levine, D. H.; Kim, A. J.; Bates, F. S.; Davis, K. P.; Lodge, T. P.; Klein, M. L.; DeVane, R. H.; Aqad, E.; Rosen, B. M.; Argintaru, A. O.; Sienkowska, M. J.; Rissanen, K.; Nummelin, S.; Ropponen, J. *Science* **2010**, *328*, 1009-1014.
(38) Rosenthal, E.; Poizot-Martin, I.; Saint-Marc, T.; Spano, J. P.; Cacoub, P. *Am J Clin Oncol* **2002**, *25*, 57-9.
(39) Zhang, L.; Gu, F. X.; Chan, J. M.; Wang, A. Z.; Langer, R. S.; Farokhzad, O. C. *Clin Pharmacol Ther* **2008**, *83*, 761-769.
(40) Allen, T. M.; Cullis, P. R. *Science* **2004**, *303*, 1818-1822.
(41) Bangham, A. D.; Standish, M. M.; Watkins, J. C. *J Mol Biol* **1965**, *13*, 238-239.
(42) Gabizon, A. A. *Clin Cancer Res* **2001**, *7*, 223-225.
(43) Haag, R.; Kratz, F. *Angew Chem Int Edit* **2006**, *45*, 1198-1215.
(44) Rowinsky, E. K.; Rizzo, J.; Ochoa, L.; Takimoto, C. H.; Forouzesh, B.; Schwartz, G.; Hammond, L. A.; Patnaik, A.; Kwiatek, J.; Goetz, A.; Denis, L.; McGuire, J.; Tolcher, A. W. *Journal of Clinical Oncology* **2003**, *21*, 148-157.
(45) Bhatt, R. L.; de Vries, P.; Tulinsky, J.; Bellamy, G.; Baker, B.; Singer, J. W.; Klein, P. *J Med Chem* **2003**, *46*, 190-193.
(46) Kopecek, J. *Polymers in Medicine* **1977**, *7*, 191-221.
(47) Vasey, P. A.; Kaye, S. B.; Morrison, R.; Twelves, C.; Wilson, P.; Duncan, R.; Thomson, A. H.; Murray, L. S.; Hilditch, T. E.; Murray, T.; Burtles, S.; Fraier, D.; Frigerio, E.; Cassidy, J.; Comm, C. R. C. P. I. I. *Clin Cancer Res* **1999**, *5*, 83-94.
(48) Seymour, L. W.; Ferry, D. R.; Anderson, D.; Hesslewood, S.; Julyan, P. J.; Poyner, R.; Doran, J.; Young, A. M.; Burtles, S.; Kerr, D. J.; Clin, C. R. C. P. I.-I. *Journal of Clinical Oncology* **2002**, *20*, 1668-1676.
(49) Meerum Terwogt, J. M.; ten Bokkel Huinink, W. W.; Schellens, J. H.; Schot, M.; Mandjes, I. A.; Zurlo, M. G.; Rocchetti, M.; Rosing, H.; Koopman, F. J.; Beijnen, J. H. *Anticancer Drugs* **2001**, *12*, 315-23.
(50) Sarapa, N.; Britto, M. R.; Speed, W.; Jannuzzo, M.; Breda, M.; James, C. A.; Porro, M.; Rocchetti, M.; Wanders, A.; Mahteme, H.; Nygren, P. *Cancer Chemoth Pharm* **2003**, *52*, 424-430.
(51) Rice, J. R.; Gerberich, J. L.; Nowotnik, D. P.; Howell, S. B. *Clin Cancer Res* **2006**, *12*, 2248-2254.
(52) Rademaker-Lakhai, J. M.; Terret, C.; Howell, S. B.; Baud, C. M.; de Boer, R. F.; Pluim, D.; Beijnen, J. H.; Schellens, J. H. M.; Droz, J. P. *Clin Cancer Res* **2004**, *10*, 3386-3395.
(53) Duncan, R.; Vicent, M. J. *Adv Drug Deliver Rev* **2010**, *62*, 272-282.
(54) Duncan, R. *Adv Drug Deliver Rev* **2009**, *61*, 1131-1148.
(55) Vicent, M. J.; Ringsdorf, H.; Duncan, R. *Adv Drug Deliv Rev* **2009**, *61*, 1117-20.
(56) Gaspar, R.; Duncan, R. *Adv Drug Deliver Rev* **2009**, *61*, 1220-1231.

(57) Bae, Y.; Nishiyama, N.; Fukushima, S.; Koyama, H.; Yasuhiro, M.; Kataoka, K. *Bioconjugate Chem* **2005**, *16*, 122-130.
(58) Kataoka, K.; Matsumoto, T.; Yokoyama, M.; Okano, T.; Sakurai, Y.; Fukushima, S.; Okamoto, K.; Kwon, G. S. *J Control Release* **2000**, *64*, 143-153.
(59) Torchilin, V. P. *Pharm Res* **2007**, *24*, 1-16.
(60) Gillies, E. R.; Frechet, J. M. J. *Drug Discov Today* **2005**, *10*, 35-43.
(61) Buhleier, E.; Wehner, W.; Vogtle, F. *Synthesis-Stuttgart* **1978**, 155-158.
(62) Hawker, C. J.; Frechet, J. M. J. *J Am Chem Soc* **1990**, *112*, 7638-7647.
(63) Tomalia, D. A.; Baker, H.; Dewald, J.; Hall, M.; Kallos, G.; Martin, S.; Roeck, J.; Ryder, J.; Smith, P. *Polym J* **1985**, *17*, 117-132.
(64) Bosman, A. W.; Janssen, H. M.; Meijer, E. W. *Chem Rev* **1999**, *99*, 1665-1688.
(65) Grayson, S. M.; Frechet, J. M. J. *Chem Rev* **2001**, *101*, 3819-3867.
(66) Naylor, A. M.; Goddard, W. A.; Kiefer, G. E.; Tomalia, D. A. *J Am Chem Soc* **1989**, *111*, 2339-2341.
(67) Kolhe, P.; Misra, E.; Kannan, R. M.; Kannan, S.; Lieh-Lai, M. *Int J Pharm* **2003**, *259*, 143-160.
(68) Khandare, J. J.; Jayant, S.; Singh, A.; Chandna, P.; Wang, Y.; Vorsa, N.; Minko, T. *Bioconjugate Chem* **2006**, *17*, 1464-1472.
(69) Kono, K.; Liu, M. J.; Frechet, J. M. J. *Bioconjugate Chem* **1999**, *10*, 1115-1121.
(70) Malik, N.; Evagorou, E. G.; Duncan, R. *Anti-Cancer Drug* **1999**, *10*, 767-776.
(71) De Jesus, O. L. P.; Ihre, H. R.; Gagne, L.; Frechet, J. M. J.; Szoka, F. C. *Bioconjugate Chem* **2002**, *13*, 453-461.
(72) Gillies, E. R.; Frechet, J. M. J. *J Am Chem Soc* **2002**, *124*, 14137-14146.
(73) Margerum, L. D.; Campion, B. K.; Koo, M.; Shargill, N.; Lai, J. J.; Marumoto, A.; Sontum, P. C. *J Alloy Compd* **1997**, *249*, 185-190.
(74) Goodwin, a. P.; Lam, S. S.; Frechet, J. M. J. *J Am Chem Soc* **2007**, *129*, 6994-6995.
(75) Killops, K. L.; Campos, L. M.; Hawker, C. J. *J Am Chem Soc* **2008**, *130*, 5062-5063.
(76) Gillies, E. R.; Dy, E.; Frechet, J. M. J.; Szoka, F. C. *Mol Pharmaceut* **2005**, *2*, 129-138.
(77) Rennke, H. G.; Venkatachalam, M. A. *J Clin Invest* **1979**, *63*, 713-717.

Chapter 2 - Design, Synthesis and Biological Evaluation of a Robust, Biodegradable Dendrimer

Abstract

PEGylated dendrimers are attractive for biological applications due to their tunable pharmacokinetics and ability to carry multiple copies of bioactive molecules. The rapid and efficient synthesis of a robust and biodegradable PEGylated dendrimer based on a polyester-polyamide hybrid core is described. The architecture is designed to avoid destructive side-reactions during dendrimer preparation while maintaining biodegradability. Therefore, a dendrimer functionalized with doxorubicin (Dox) was prepared from commercial starting materials in nine, high-yielding linear steps. Both the dendrimer and Doxil™ were evaluated in parallel using equimolar dosage in the treatment of C26 murine colon carcinoma, leading to statistically equivalent results with most mice tumor-free at the end of the sixty day experiment. The attractive features of this dendritic drug carrier are its simple synthesis, biodegradability, and versatility for application to a variety of drug payloads with high drug loadings.

Introduction

The use of macromolecular carries for delivery of chemotherapeutics originated from the hypothesis that polymers may be used to improve both the solubility and the blood circulation time of small molecule drugs.[1,2] It was later discovered that macromolecules have the additional benefit of increased accumulation in tumor tissue as a result of the leaky vasculature surrounding rapidly growing neoplasm—a concept known as the enhanced permeation and retention (EPR) effect.[3,4] Thus, macromolecular carriers can provide both enhanced pharmacokinetics and a passive targeting mechanism, characteristics that may be used to increase the efficacy of small molecule drugs. To this end, carrier systems such as linear polymers, micellar assemblies, liposomes, polymersomes and dendrimers have been studied in an effort to determine an ideal drug carrier.[5-14] Important design features[9] include a long blood circulation time, high tumor-accumulation, high drug-loading, low toxicity, low polydispersity index and simple preparation. Considering the above criteria, PEGylated dendrimers.[15,16] constitute an attractive platform because their size and degree of branching can be precisely controlled and they can be furnished with multiple functional appendages for the attachment of solubilizing groups as well as drugs. Dendritic drug carriers based on polyesters,[17-19] polyamines,[20, 21] melamines or triazines,[22-24] PAMAM,[25-30] and other polyamides[31-33] have all been explored and recently reviewed.[14] Polyesters constitute a very attractive class of materials because they are biodegradable; however, the hydrolytic susceptibility of the ester bond can make the synthesis of drug conjugates somewhat challenging. The hydrolysis rates of polyesters can vary dramatically depending on the hydrophobicity of the monomer, steric environment, and the reactivity of functional groups located within the dendrimer.[34] In contrast, polyamide and polyamine dendrimers can withstand a much wider selection of synthetic manipulations, but do not degrade as easily in the body and are thus more prone to long-term accumulation *in vivo*.[35] Currently, challenges facing the biological application of dendrimers are their lengthy syntheses and the need to synthesize nontoxic, biodegradable dendrimers that are still resilient to reaction conditions encountered during their synthesis and modification. To date, accessing a universal, biodegradable, highly soluble, unimolecular carrier capable of achieving a high drug loading and low polydispersity remains difficult.

In recent studies, we have determined that dendrimers based on a 2,2-bis(hydroxymethyl) propanoic acid (bis-HMPA) monomer unit that have been functionalized with eight 5 kDa poly(ethylene glycol) (PEG) chains[18] are biocompatible, facilitate high tumor accumulation, have long circulation half-lives, and are capable of high drug loading.[36] An asymmetric bis-HMPA PEGylated dendrimer functionalized with doxorubicin via a pH sensitive acyl hydrazone bond demonstrated outstanding antitumor activity in mice bearing murine C26 colon carcinoma.[17] Despite these promising *in vivo* results, further evaluation of this asymmetric carrier in biological models was made difficult due to its lengthy synthesis.[37] We were interested in transposing the beneficial features[9] of this PEGylated dendrimer onto a simpler and more readily prepared carrier. Initial approaches toward this goal involved simplified multifunctional dendrimers based on bis-HMPA,[38,39] however, some issues still remained as undesired backbone degradation was observed during the attachment of certain drugs.

Herein, we describe the design evolution of three dendrimers that resulted in the creation of a new PEGylated dendrimer, which circumvented the synthetic and biological limitations presented by the polyester and polyamide dendrimers. We report a very efficient synthesis that

combines the biocompatibility of bis-HMPA dendrimers with the robustness of polyamide dendrimers, yielding a hybrid scaffold capable of translation into clinical studies.

Results and Discussion

Synthesis of Polyester Dendrimer

Polyester dendrimers based on bis(HMPA) monomer units are an attractive scaffold for biological applications because they are non-immunogenic, biodegradable, and non-toxic.[36] Scheme 1 outlines the synthesis of a core-functionalized PEGylated dendrimer developed by Guillaudeu *et al*.[39] Briefly, the tetrafunctional pentaerythritol core **1** was modified with a benzylidene-protected bis(HMPA) monomer **2** to afford the first generation dendrimer **3**. After removal of the protecting groups via hydrogenolysis, the eight peripheral hydroxyl groups were functionalized with orthogonally protected aspartic acid to give **6**. Subsequent deprotection of the amino groups of **6** followed by PEGylation with the 5 kDa PEG electrophiles gave dendrimer **8**. Removal of the benzyl ester protecting groups of **8** via hydrogenolysis afforded dendrimer **9** with eight carboxylic acids moieties available for potential drug attachment. Initial attempts at the functionalization of this dendrimer with *t*-butyl carbazate or glutamic acid derivative **10** were unsuccessful as degradation of the dendrimer was observed during this reaction.

Scheme 1. Synthesis of Symmestrically PEGylated Dendrimer.

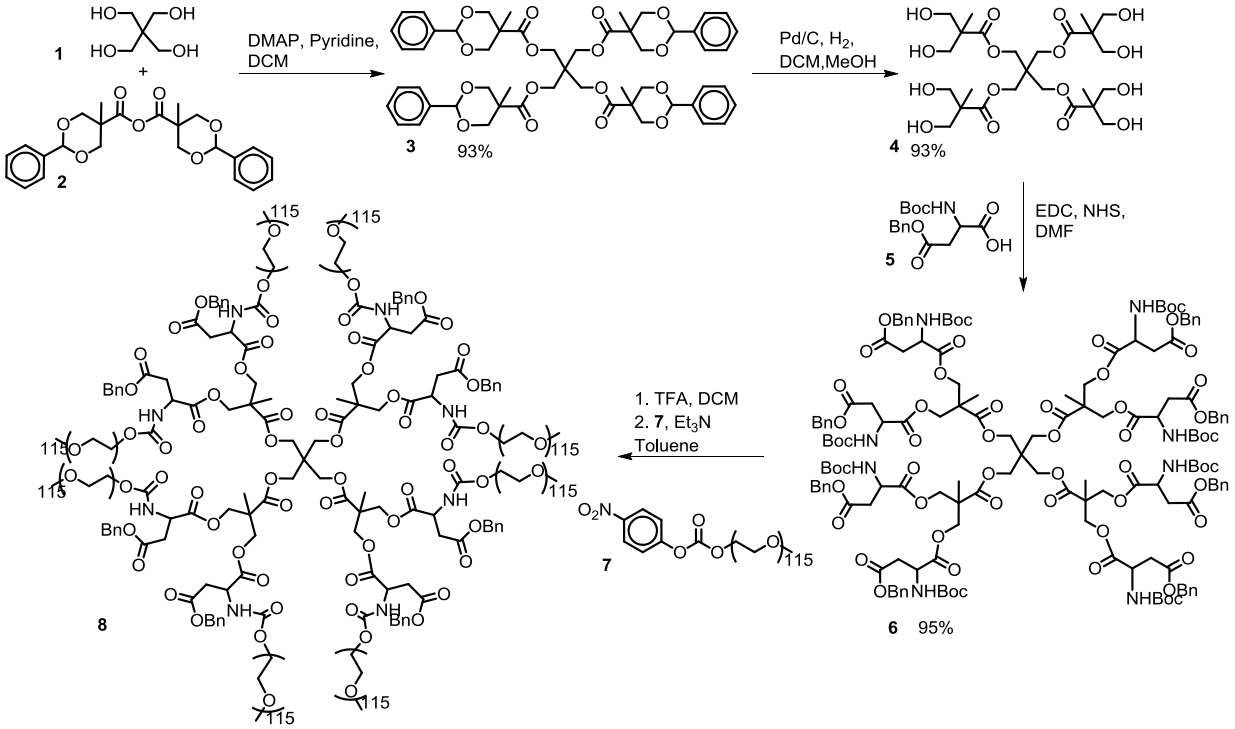

In order to gain insight into the degradation pathway, we prepared the dendrimer probe **11** and attempted to functionalize its aspartic acid chain-ends with *t*-butyl carbazate. Probe molecule **11** was selected instead of PEGylated dendrimer **9** as progress of its reaction could be more easily monitored by MALDI-ToF since it does not contain PEG chains (Figure 1). As a result of a degradation side reaction, only a small amount of the target product was formed, leading to the appearance of lower molecular weight products with molecular weights decreasing

in increments of 329 amu; this was likely due to the occurrence of intramolecular cyclization reactions as proposed in Figure 1.

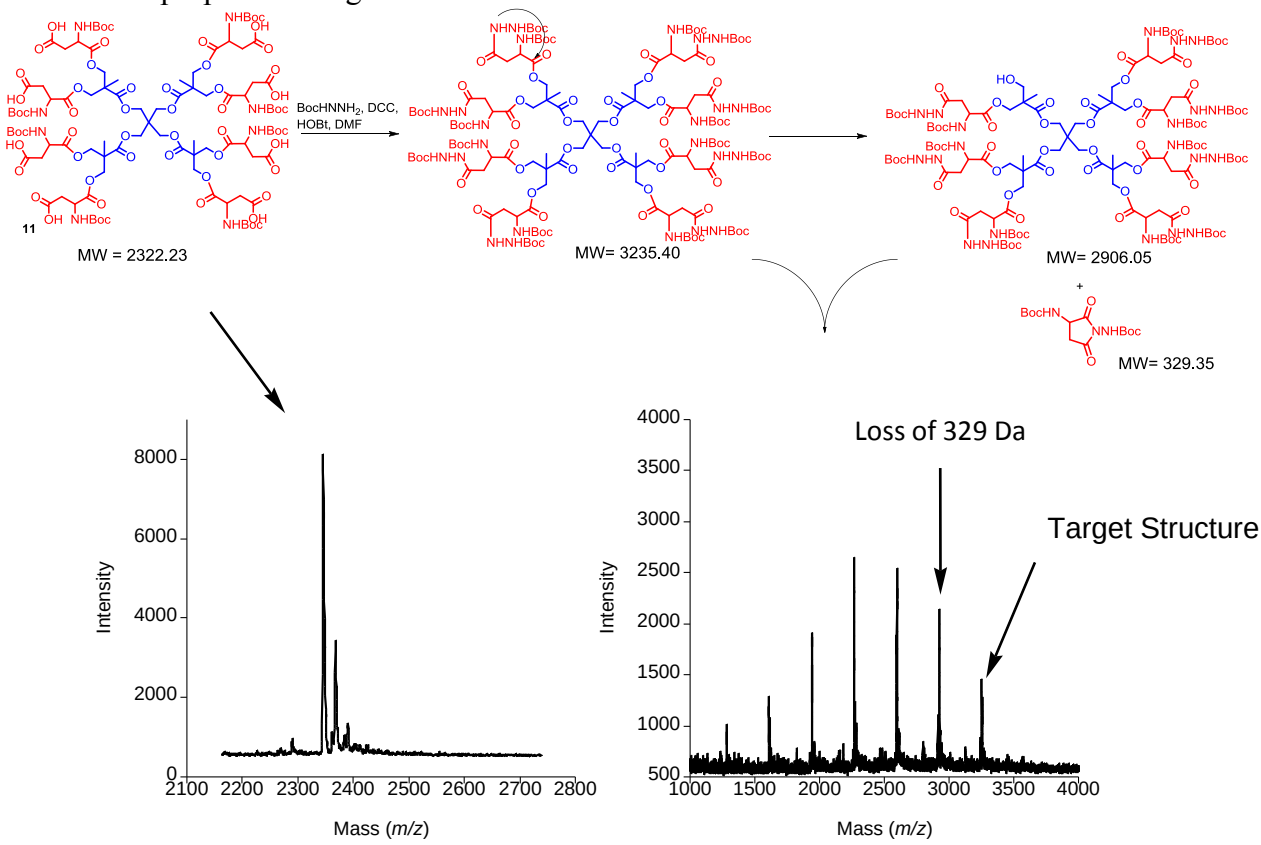

Figure 1. Proposed degradation pathway for polyester dendrimer.

This type of cyclization reaction on benzyl ester-protected aspartic acid residues is documented in the peptide literature and additives have been developed to suppress such reactions.[44] For example, pentachlorophenol (PCP) has been used to decrease the production of the aminosuccinyl by-product by inhibiting amide deprotonation. Under these buffered conditions, the primary amines are still available to react with *p*-nitrophenyl (PNP) carbonates and other electrophiles. The use of PCP as an additive proved beneficial in our hands as it allowed the functionalization of the carboxylic acid side chains of dendrimer **9** with protected nucleophile **10** to give dendrimer **12**. Finally, doxorubicin hydrazone conjugate **14** was obtained after removal of the Boc groups from the hydrazide linkers in **12** and condensation of the resulting amines with the ketone group of doxorubicin **13**. In order to determine how rapidly this polyester architecture breaks down under physiological conditions, **12** was incubated in PBS buffer at 37 ^{o}C and changes in molecular weight were monitored by SEC. Unfortunately, the α-amino esters at the periphery proved to be too unstable for *in vivo* applications because after 10 hours significant degradation was observed. For this reason, we began exploring alternative dendrimer scaffolds based on polyamides.

Scheme 2. Linker attachment and Dox loading.

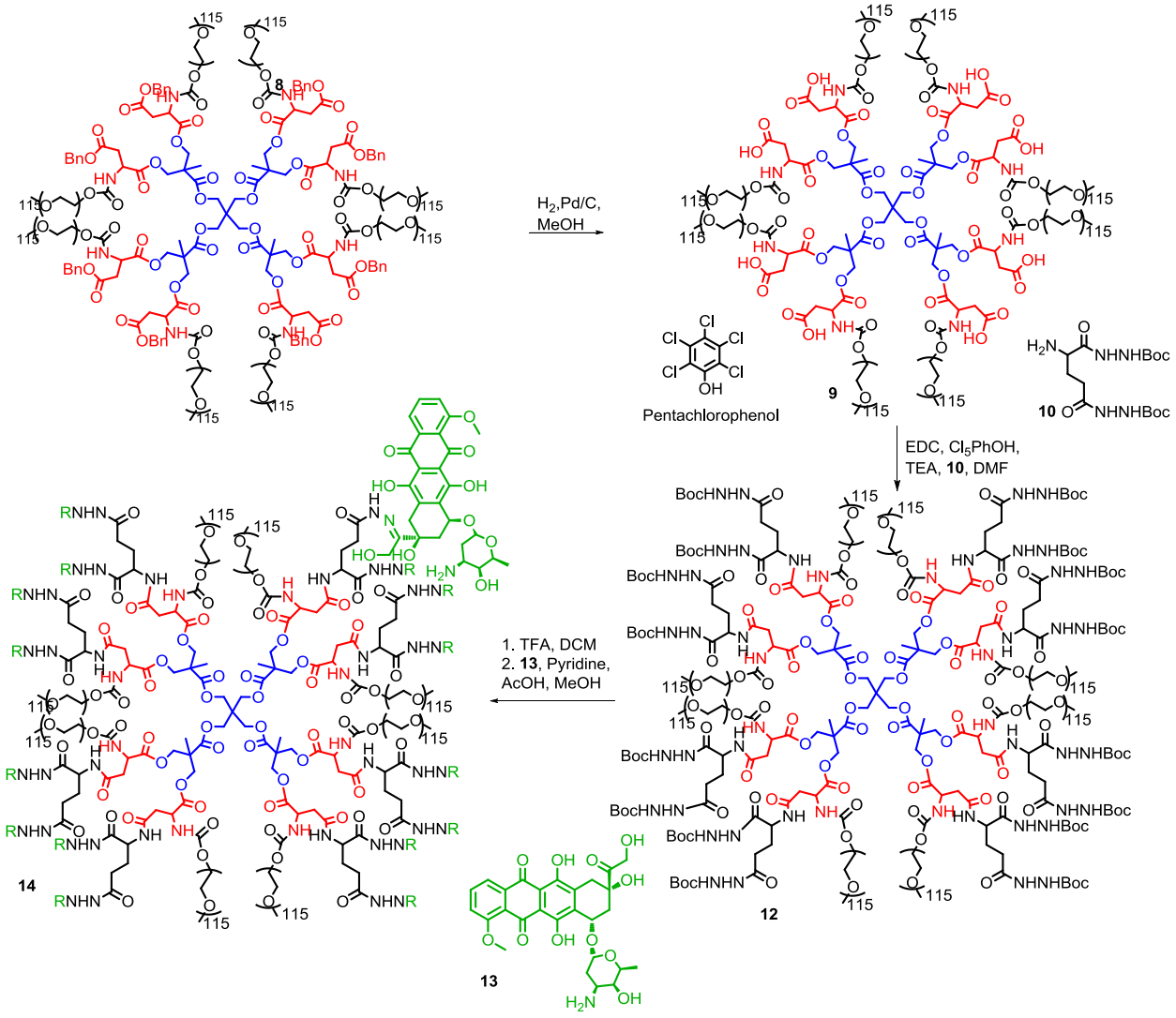

Synthesis of Polylysine Dendrimer

In contrast to polyester dendrimers, polyamide dendrimers are less susceptible to hydrolysis, but this increased stability may hamper their break down *in vivo*. Recently, Fox *et al.* functionalized a PEGylated polylysine with camptothecin and observed complete tumor remission in transgenic mice with HT-29 human colon carcinoma.[41] While the degradation of amide bonds in linear peptides *in vivo* is well established, the fate of branched, acylated, and PEGylated polyamide dendrimers is less certain as proteases may not be able to access amide bonds near the core of the structure. However, even incomplete degradation of the carrier may be permissible for drug delivery applications if the by-products are non-toxic.[45,46] In order to apply the polylysine carrier used by Fox[41] to the delivery of doxorubicin, dendrimer **18** with a protected hydrazide had to be prepared.

Scheme 3. PEGylated polylysine synthesis.

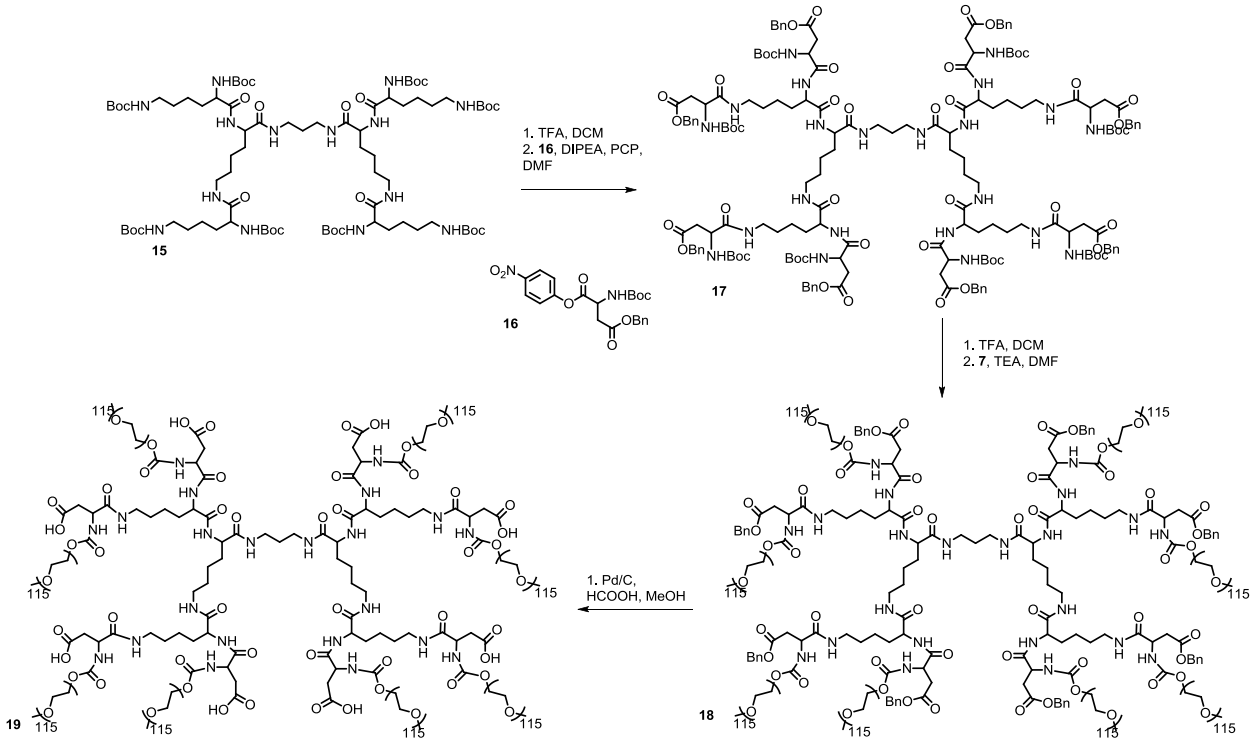

Lysine dendrimer **15**, first synthesized by Denkewalter[47] in 1982 was used as the starting material. Its peripheral amines were acylated with PNP-Asp(Bn)Boc to afford dendrimer **17** (Scheme 3). It is worth noting that the PCP additive was also needed when attaching aspartic acid to the G_2 lysine periphery. Otherwise, a 5-membered amino succinyl byproduct can form via amidolysis of the benzyl ester protected side chain. Deprotection of the amino groups of the aspartate termini and PEGylation with PEG-*p*-nitrophenyl carbonate afforded **18**. Unfortunately, the coupling of *t*-butyl carbazate to the deprotected side chain carboxylic acid terminal moieties (**19**) led to the appearance of degradation byproducts such as **20** (Figure 2). Monitoring of the reaction by size exclusion chromatography (Figure 2) showed the formation of lower molecular weight by products - presumably formed as a result of attack of the hydrazide nitrogens onto the carbamate linkers to PEG, thus forming a six-membered cyclic by-product and releasing PEG.

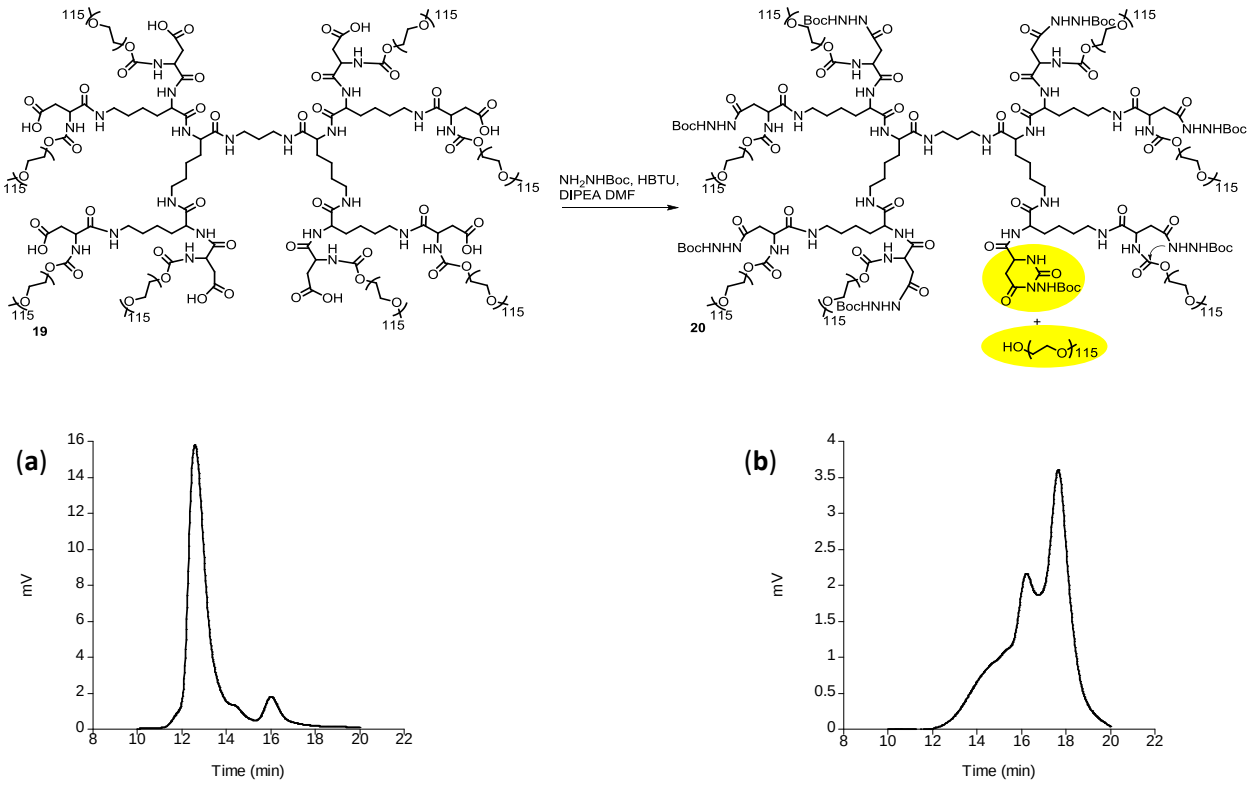

Figure 2. PEGylated polylysine degradation: (a) SEC of compound **19**, (b) SEC of reaction mixture.

This side reaction could be circumvented in two ways: (i) replacement of the carbamate in **18** with a more stable amide linkage by using carboxymethyl terminated PEG instead of a PNP carbamate; or (ii) use of a glutamic acid spacer between the nucleophilic hydrazides and the relatively labile carbamate linkages to PEG. The latter route requires more synthetic operations, but had the added benefit of doubling the number of hydrazides through which drug molecules can be attached. In Scheme 4, PEGylation of dendrimer **17** with carboxymethyl-PEG afforded dendrimer **28**, which had PEG attached through the amide linkage. The benzyl ester protecting groups were removed via hydrogenolysis and the free acids were functionalized with *t*-butyl carbazate to give dendrimer **29**.

Scheme 4. PEGylation via amide bond formation for a more stable architecture.

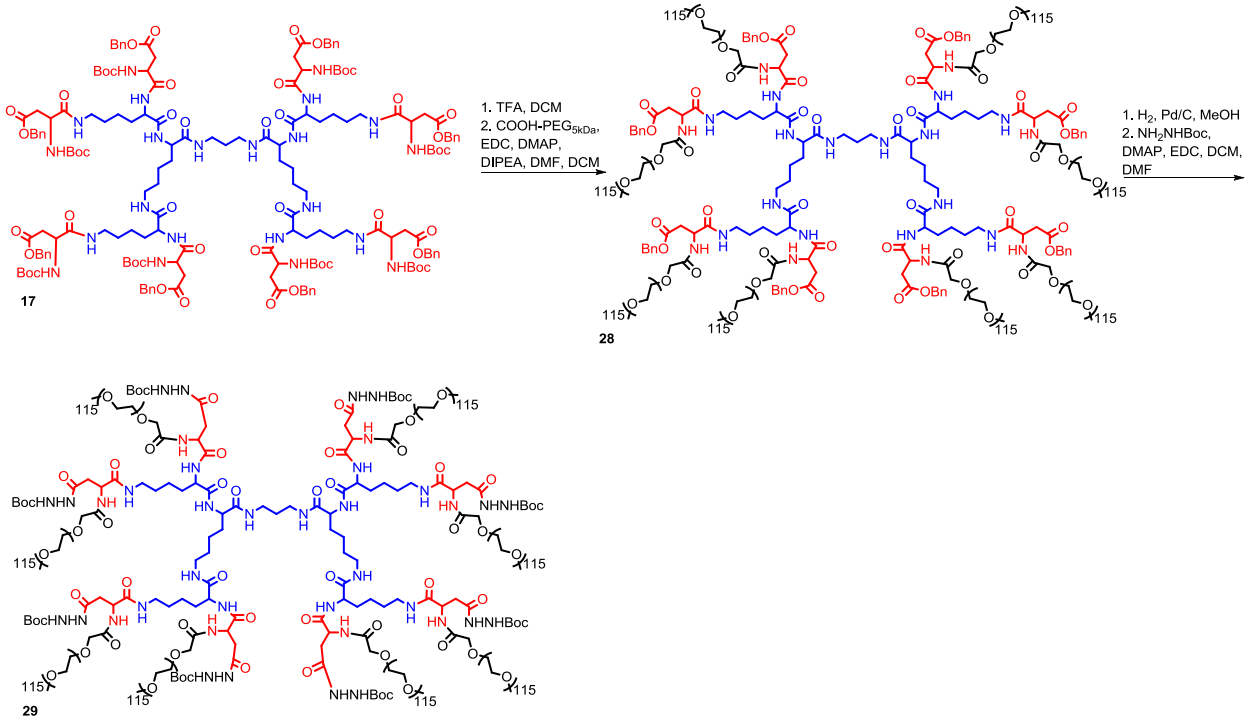

An alternate approach involved attachment of a glutamic acid spacer (**10**) to dendrimer **18** as shown in Scheme 5. Subsequent deprotection of the hydrazides allowed for up to 16 doxorubicin molecules to be attached.

Scheme 5. Drug attachment through bifunctional hydrazide drug linker.

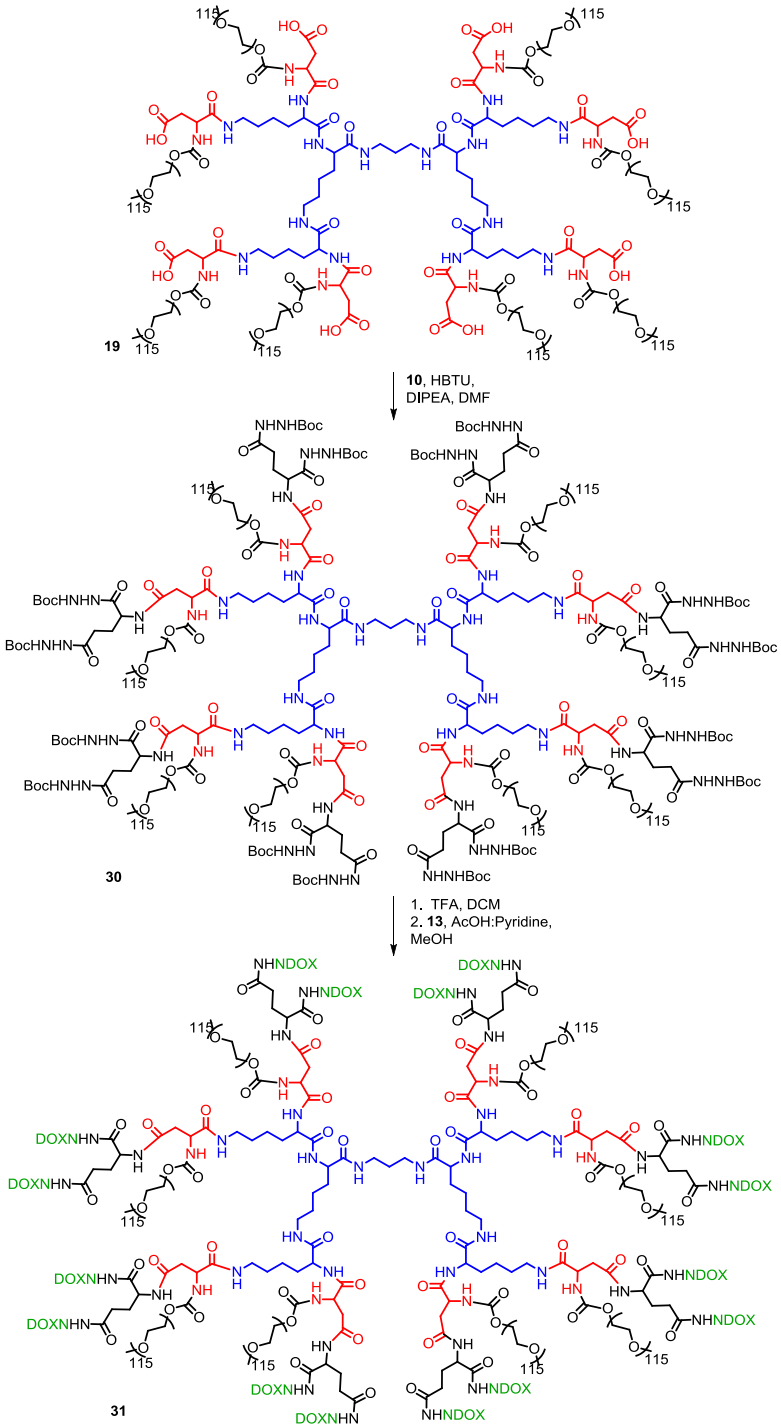

Scheme 6. Side reaction occurring between residual trifluoroacetic acid and PNP-activated esters.

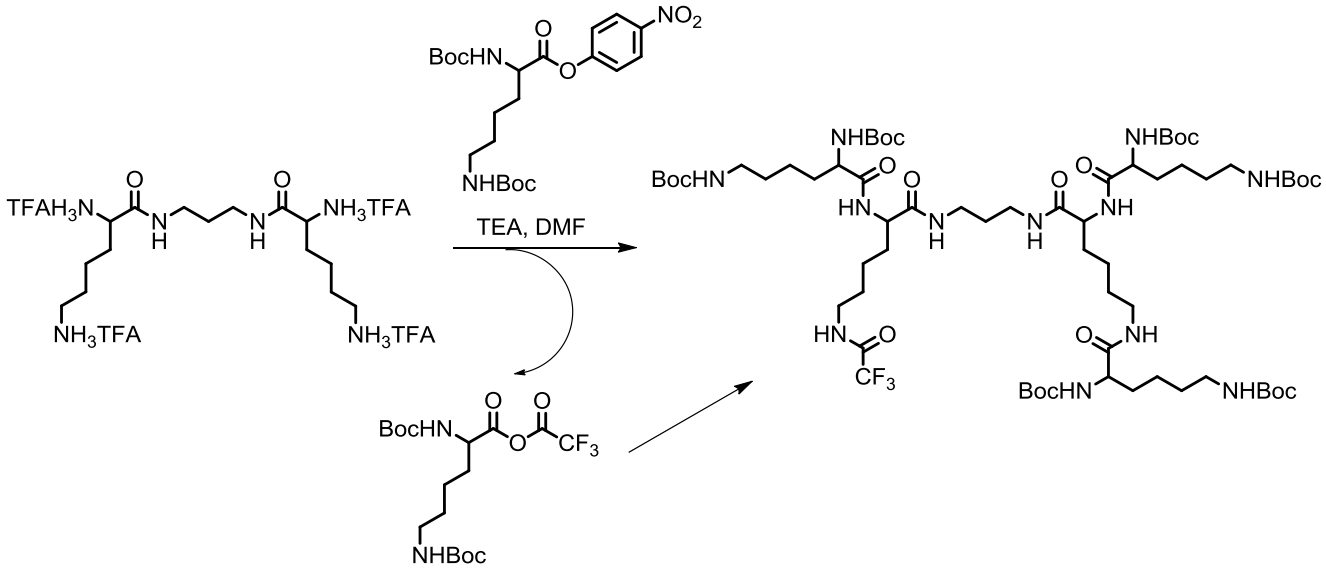

During the synthesis of polylysine dendrimers, we observed an additional side reaction that may be of interest to other polymer and dendrimer chemists. Complete removal of trifluoroacetic acid (TFA) after Boc deprotection steps was found to be critical; otherwise, TFA was found to add into the activated ester to form a mixed anhydride, which can cap the peripheral amines as the trifluoroacetamide. This side reaction was identified by MALDI-ToF analysis, and it was determined that the TFA counter ions on the dendrimer starting material do not cause this to occur.

Synthesis of Hybrid Ester-Amide Dendrimer

The important lessons learned from the synthesis of both the polyester and polyamide carriers ultimately led us to consider a hybrid approach that combines their separate virtues in one scaffold. It appears that the combination of a hydrolytically degradable ester core and a more chemically resistant amide periphery might be ideal for the construction of PEGylated drug conjugates. Furthermore, the early designs we tested (*vide supra*) also underscored the importance of avoiding the positioning nucleophilic sites at a 5- or 6-atom distance from potential leaving groups.[43] Hybrid dendrimer **24** (Scheme 4), representing such an architecture was obtained in three simple steps in 81% overall yield, and without any chromatographic purification.

Synthesis of the hybrid carrier began by treatment of pentaerythritol **1** with the *p*-nitrophenyl ester of lysine **21** (Scheme 4). The amine protecting groups of the resulting dendrimer **22** were then removed and the molecule was provided with "differentiated end functionalities" by reacting each of its eight primary amino groups with orthogonally protected PNP-glutamic acid **23**. Glutamic acid was selected over aspartic acid for the following reasons: (i) pentachlorophenol was no longer needed to prevent amidolysis of the benzyl ester group, since formation of the 6-membered amino succinyl byproduct was not observed; and (ii) *t*-butyl carbazate could be attached directly to the glutamic acid side chain without any degradation as cyclization of the acyl hydrazide onto the carbamate to form a 7-membered ring was not an

issue. Eight 5 kDa PEG chain were then installed on the dendrimer periphery via a carbamate linkage. This was accomplished by quantitative removal of the Boc protecting groups and subsequent PEGylation with one equivalent (per amine) of PNP-PEG (Scheme 4). The PEGylation reaction was carried out for two days, at which time, piperidine was added to quench any unreacted PNP-PEG, and then acetic andydride was added to acylate any remaining primary amines on the dendrimer scaffold. The resulting PEGylated dendrimer **25** was purified via precipitation into ether to give a polymer with MW ~40,000 Da and PDI < 1.1, with an average particle size of 12 nm as determined by dynamic light scattering (DLS). Finally, residual linear PEG could be removed by dialysis using 100,000 MW cut-off dialysis tubing in water.

The benzyl ester protected side chains of the glutamic acid moieties in **25** were removed via hydrogenolysis, and the resultant carboxylic acids were treated with *t*-butyl carbazate and 1-ethyl-3-(3-dimethylaminopropyl)carbodiimide (EDC) to give dendrimer **26** with eight protected hydrazides available for drug attachment. Finally, target drug conjugate **27** was successfully obtained from the protected precursor **26** by removal of the Boc groups and subsequent condensation with doxorubicin in 5% pyridine/acetic acid solution of methanol at 60 ^{o}C.

Scheme 5. Synthesis of drug loaded PEGylated ester-amide dendrimer.

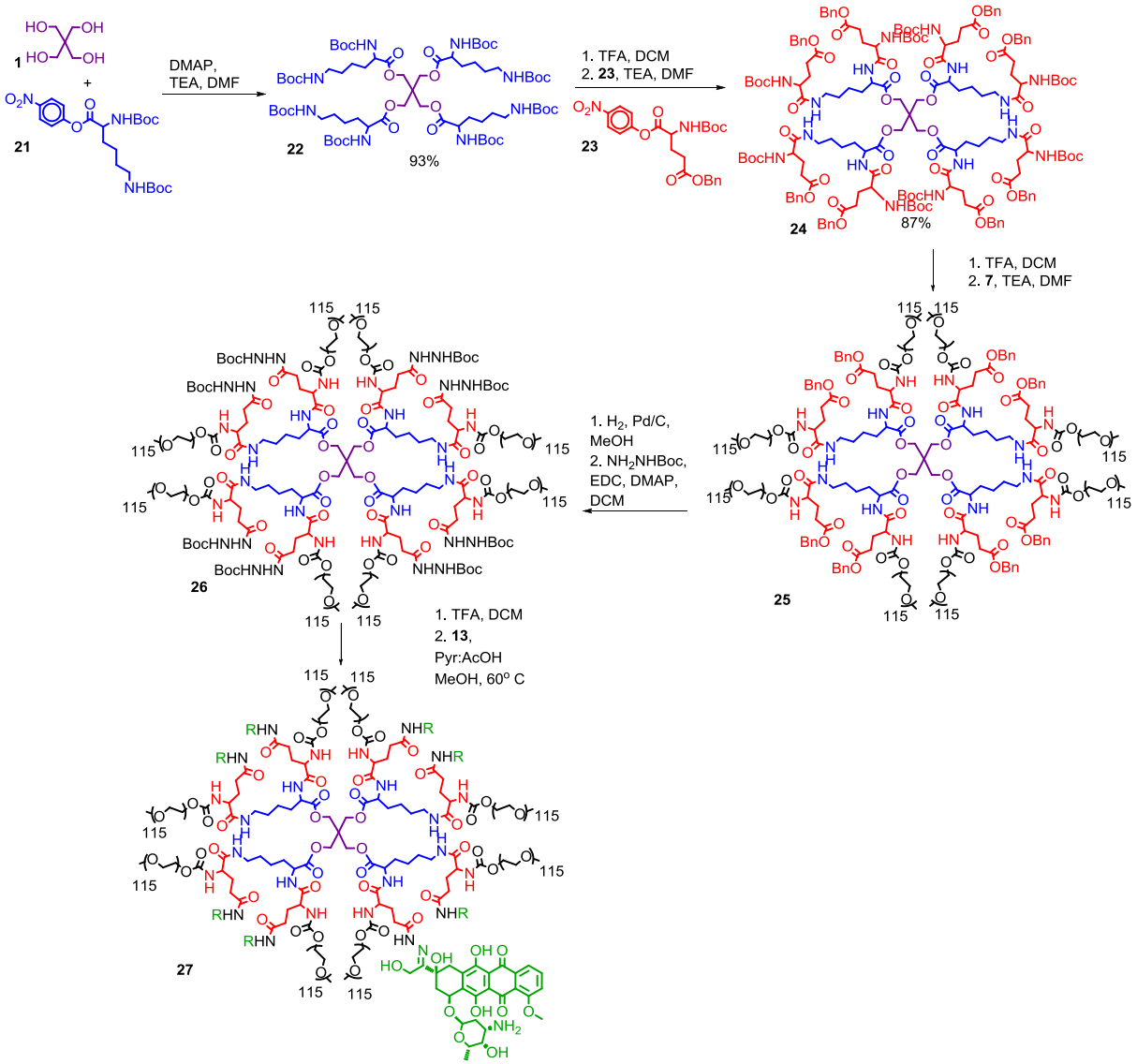

The degradation profile of the ester-amide dendrimer hybrid was evaluated under physiological conditions. Polymer **26** was incubated at 37 °C in phosphate buffer at physiological pH and the molecular weight was monitored over 20 days by size exclusion chromatography (Figure 4a). As expected, the polymer degraded into 10 kDa and 5 kDa fragments as a result of the slow hydrolysis of both ester and carbamate moieties. Given that the threshold for renal clearance for linear polymers is estimated to be near 45,000 Daltons,[48] cleavage of the 40,000 Dalton branched polymer following delivery of its payload contributes to prevent its long-term accumulation. The observed degradation profile is promising as it suggests that hybrid dendrimer **26** is sufficiently stable to allow for selective tumor uptake, yet can be eventually broken down and cleared.[9] It is also noteworthy that the drug is attached to a narrow population of polymeric material and that no significant amount of free drug is present as confirmed by the absence of a peak corresponding to free drug at 590 nm in the UV-vis trace of the conjugate (Figure 4b).

Figure 3. (a) Size exclusion chromatographs of **26** in pH 7.4 PBS buffer at 37 °C. (b) UV-vis size exclusion chromatograph of **27** at 590 nm.

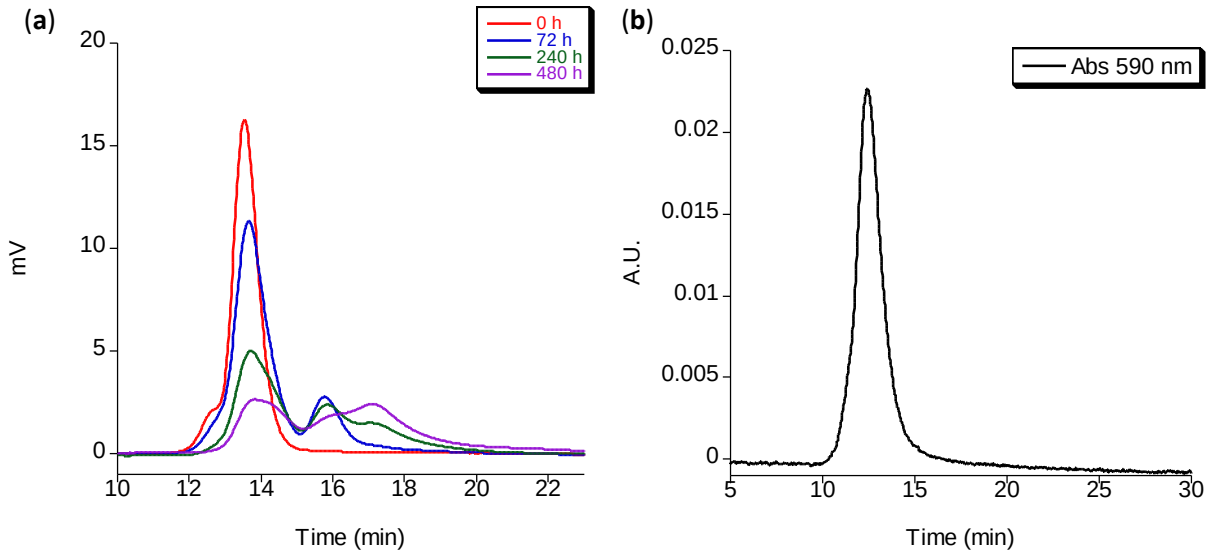

Carrier drug loading was determined via UV-vis spectroscopy and could be varied from 6-10 wt/wt% depending on how many equivalents of doxorubicin were used in the loading step. Doxorubicin was chosen for attachment because it is a well-established and highly effective chemotherapeutic agent[49] that can benefit from conjugation to a carrier to decrease its innate cardiotoxicity. It is important to note that a variety of drugs, prodrugs, or other biological agents may potentially be attached to dendritic carriers based on **25** through its latent carboxylic acid side chains.

Drug Release Rates and *In Vitro* Toxicity of Ester-Amide Dendrimer.

An important characteristic of our drug carrier is that the drug is covalently bound via a stimulus responsive linkage. The pH-dependence for the rate of hydrolysis of the hydrazone bond we formed is well studied,[43,50,51] and we could confirm that the drug would be selectively released under acidic conditions similar to those found in the lysosome.[43] At pH 7.4, less than 5% of drug was released over 48 hours while the half-life of hydrolysis at pH 5 was 22 hours (Figure 4a).

The *in vitro* cytotoxicity tests showed that **26** remained non-toxic toward C26 cells at a concentration of 5 mg/mL (Figure 4b). When Dox was conjugated to the carrier, a ten fold decrease in toxicity was observed over the free Dox ($IC_{50(\mathbf{27})}$ = 529.6 +/- 3.8 nM; $IC_{50(Dox)}$ = 52.4 +/- 12.7 nM). The decrease in toxicity may be attributed to the slower rate of uptake of the ester-amide carrier compared to free Dox and hydrolysis of the drug from the carrier.

Figure 4. a) Drug release rate measure at ph 5 (squares) and pH 7.4 (diamonds). b) Cell viability versus drug-free carrier concentration for Dox (green), **27** (blue) and **26** (red).

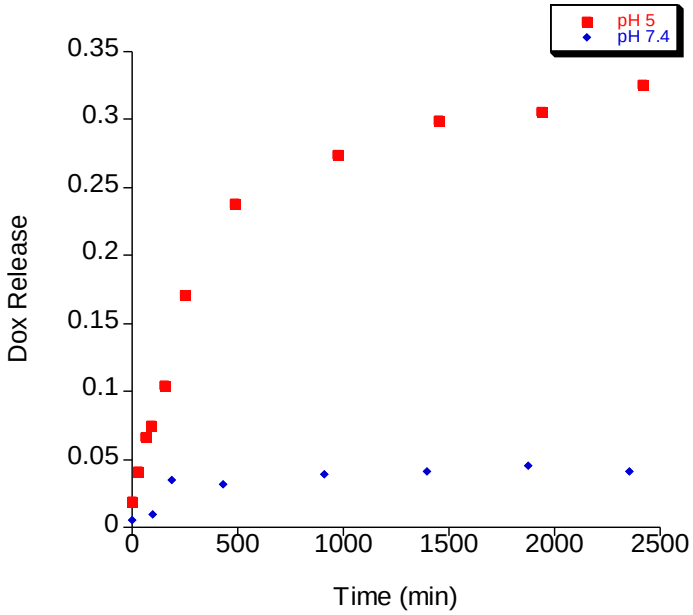

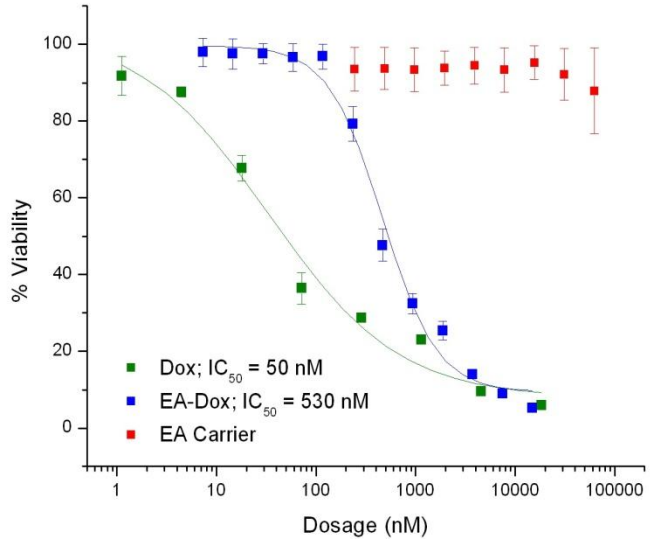

Biodistribution in Tumored Mice.

The biodistribution of the ester-amide dendrimer was determined in C26 tumored female Balb/C mice Figure. Mice were injected with 8 mg Dox eq/kg, formulated as Doxil™ or **27**. After 48 h, Dox accumulation within the tumor was 5.5 $\pm$ 0.7 % ID/g of tissue, whereas, accumulation in the vital organs was less than 2 % ID/g of tissue. This result is comparable to accumulation seen with previous carriers in our group.[36,39] Furthermore, a measurable level of Dox was found to remain within the tumor tissue after one week with little accumulation within the vital organs. Mice injected with **27** or Doxil™ had comparable tumor accumulation after one week, 3.7 $\pm$ 0.51 % ID/g of tissue and 5.27 $\pm$ 5.19 % ID/g of tissue respectively. The ester-amide dendrimer showed lower accumulation within the spleen than Doxil™. Lowering Dox

accumulation in the vital organs is important for reducing systemic toxicity, while uptake by tumor tissue must be maintained to promote treatment efficacy.

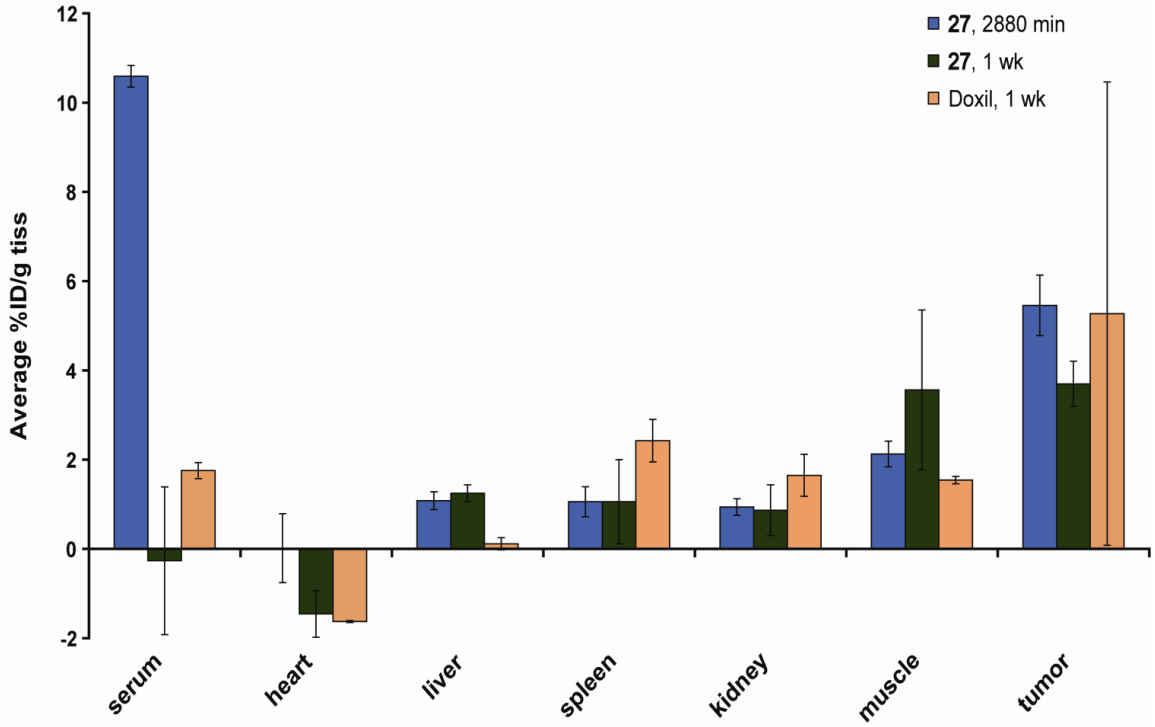

Figure 5. 48 hour and 1 week biodistribution of **27** and 1 week biodistribution of Doxil in mice with s.c. C26 colon carcinoma.

Chemotherapy Study in Tumored Mice.

A dose-response experiment was performed in C26 tumored Balb/C mice; four treatment groups were investigated, Doxil™ (20 mg Dox/kg) and **27** (10, 15, and 20 mg Dox/kg). Dose-dependent survival was observed and all three groups treated with **27** showed significant tumor growth delay (TGD) and prolonged survival (Table 1, Figure 5). Mice treated with 20 mg Dox/kg had 9 out of 10 mice tumor free at the end of the study (day 60), with TGD of 229% ($p< 0.0001$) and median survival time of 60 days. The 15 mg Dox/kg and 10 mg Dox/kg treatment groups had 175% ($p< 0.0001$), and 74% TGD ($p< 0.0001$) and a median survival time of 60, and 33 days respectively. Doxil™ had 8 out of 10 mice alive at day 60, but the two deaths appeared to be due to treatment-related toxicity. Weight loss due to treatment toxicity was on average not severe, with a mean weight loss of 6.4% for Doxil™ and 4.3% for **27** (20 mg Dox/kg). This result is comparable to the chemotherapy experiment with the asymmetrically PEGylated dendrimer vs Doxil™, both administered at 20 mg Dox/kg[17] In this earlier study, there was complete tumor regression with the asymmetrically PEGylated dendrimer carrier with and a single toxic death due to Doxil™. The current and former study both indicate that Dox-loaded PEGylated dendrimer carriers are as effective as Doxil™ against the C26 tumor model. The ester-amide dendrimer **27** may exhibit less toxicity than Doxil™ at equivalent Dox dosages and its biodegradability and streamlined synthesis offer significant advantages over previous dendrimer scaffolds.

Table 1. In vivo efficacy of ester amide dendrimer conjugate and controls against Balb/C mice with C26 colon carcinoma.

Treatment Group	No. mice	Dose (mg/kg)	Mean TGD (%)	Median survival time (days)	TRD	LTS
PBS	10			20	0	0
Doxil	10	20	245[a]	60[a]	2	8
27	10	20	229[a]	60[a]	0	9
27	10	15	175[a]	60[a]	0	6
27	10	10	74[b]	33[a]	0	1

TGD, tumor growth delay, calculate from time of growth to 400 mm^3; TRD, treatment-related death; LTS, long term survivors; [a] Compared to PBS, $P \leq 0.0001$. [b] Compared to PBS, $P = 0.004$.

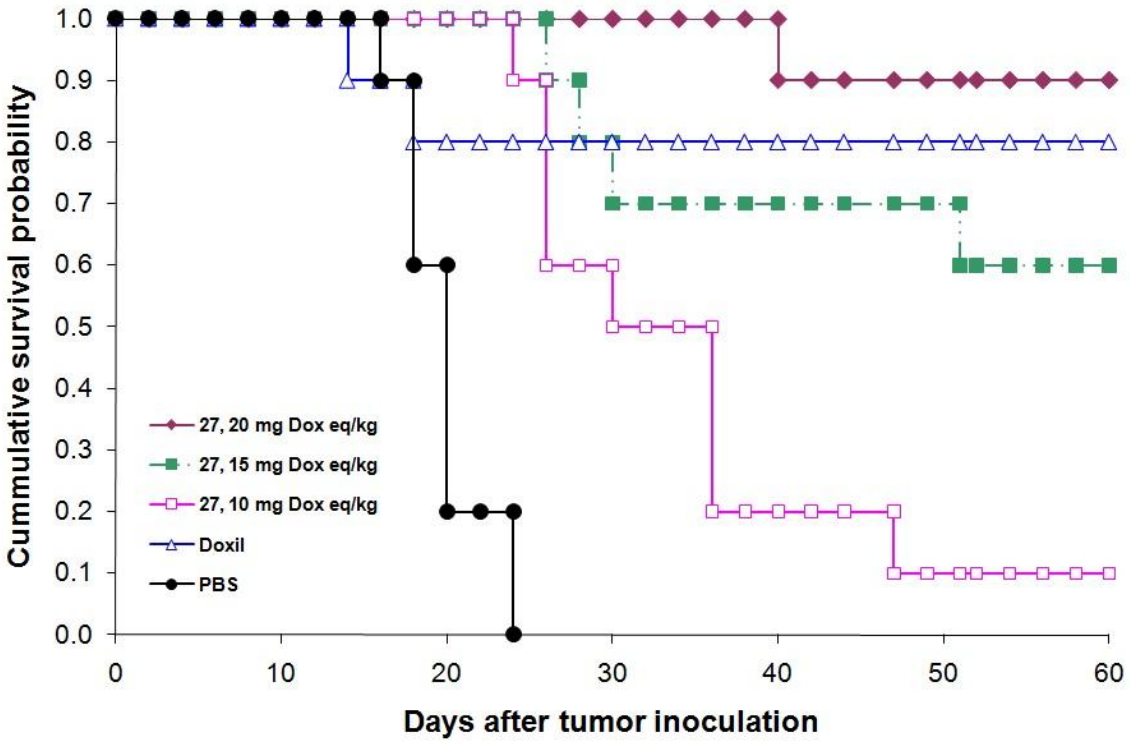

Figure 6. Survival probability versus time for Balb/C mice bearing s.c. C26 colon carcinoma after a single injection of PEGylated polyester-amide Dox conjugate or control. Mice were treated 8 days after tumoring. diamonds, 27 (20 mg Dox equiv/kg); squares, 27 (15 mg Dox equiv/kg); boxes, 27 (10 mg Dox equiv/kg); triangles, Doxil (20 mg Dox equiv/kg); circles, PBS.

Conclusion

In conclusion, the attractive features of polyester and polyamide dendrimers have been combined to form a robust yet degradable polyvalent macromolecular scaffold that can be prepared in a scalable fashion. The final drug loaded dendrimer is made entirely from commercial starting materials in nine high-yielding steps, four of which are near quantitative deprotection steps. No chromatographic steps are required during the dendrimer preparation. This scaffold will be studied with additional tumor models and drugs and shows promise as a clinically relevant delivery vehicle.

Materials and Methods

Materials. Materials were used as obtained from commercial sources unless otherwise noted. Poly(ethylene glycol) was purchased from Laysan Biosciences Inc. Amino acid derivatives were purchased from Bachem. Dimethylformamide (DMF), pyridine, and CH_2Cl_2 for syntheses were purged 1 h with nitrogen and further dried by passing them through commercially available push stills (Glass Contour). Solvents were removed under reduced pressure using a rotary evaporator or by vacuum pump evacuation. Compounds **2, 3, 4;**[19] **6**, **8**, **9;**[39] **10;**[40] **15**, **17**, **18, 19**[41] were synthesized according to published procedures.

Characterization. NMR spectra were recorded on Bruker AV 300, AVB 400, AVQ 400, or DRX 500 MHz instruments. Spectra were recorded in $CDCl_3$ or D_2O solutions and were referenced to TMS or the solvent residual peak and taken at ambient temperature. Elemental analyses were performed at the UC Berkeley Mass Spectrometry Facility. MALDI-TOF MS was performed on a PerSeptive Biosystems Voyager-DE using the following matrices: *trans*-3-indoleacrylic acid (IAA) for *tert*-butyloxycarbonyl (Boc) protected dendrimers; or 2,5-dihyroxybenzoic acid (DHB) for amine-terminated dendrimers. Samples were prepared by diluting dendrimer solutions (~1 M) 40-fold in 100 mM matrix solutions in tetrahydrofuran and spotting 0.5 μL on the sample plate. Size exclusion chromatography (SEC) was performed using one of three systems:

SEC System A: a Waters 515 pump, a Waters 717 autosampler, a Waters 996 Photodiode Array detector (210-600 nm), and a Waters 2414 differential refractive index (RI) detector. SEC was performed at 1.0 mL/min in a PLgel Mixed B (10 μm) and a PLgel Mixed C (5 μm) column (Polymer Laboratories, both 300 x 7.5 mm), in that order, using DMF with 0.2% LiBr as the mobile phase and linear PEO (4,200-478,000 MW) as the calibration standards. The columns were thermostated at 70 °C.

SEC System B: The same equipment as System A, but performed at 1.0 mL/min in two SDV Linear S (5 μm) columns (Polymer Standards Service, 300 x 8 mm) using DMF with 0.2% LiBr as the mobile phase.

SEC System C: A Waters Alliance separation module 2695 (sample compartment maintained at 37.0 ± 3.0 ^{o}C), a Waters 410 differential RI detector, a Waters 996 photodiode array detector (λ = 486 nm), and a Shodex OHpak SB-804 HQ SEC column. An isocratic flow rate of 0.7 mL/min was used with a mobile phase composed of 70%/30%/0.05% water/acetonitrile/formic acid.

Doxorubicin loading was quantified using a Lambda 35 UV-vis spectrometer (PerkinElmer, Wellesley, MA). Measurements were performed in sealed, standard 1-cm quartz cells in millipore water at room temperature.

Animal and Tumor Models. All animal experiments were performed in compliance with National Institutes of Health guidelines for animal research under a protocol approved by the Committee on Animal Research at the University of California (San Francisco, CA) (UCSF). C26 colon carcinoma cells obtained from the UCSF cell culture facility were cultured in RPMI medium 1640 containing 10% FBS. Female BALB/c mice were obtained from Simonsen Laboratories, Inc. (Gilroy, CA).

EA-G_1-Lys(Boc)$_8$ (22). Pentaerythritol (353mg, 2.6 mmol), BocLys(Boc)-ONp (5.500 g, 11.8 mmol) and DMAP (125 mg, 1.0 mmol) were added to a 20 ml reaction vial. Under a nitrogen atmosphere, DMF (5.5 mL) and triethylamine (1.6 mL, 11.5 mmol) were added and the reaction stirred for 48 h. MALDI-ToF analysis confirmed the reaction had gone to completion. *N*,*N*-dimethylethylene diamine (300 µL, 4.1 mmol) was added to quench excess PNP esters. After 10 min, the mixture was diluted with ether (200 mL) and washed with three 100 mL portions of 1M NaOH, three 100 mL portions of 1M $NaHSO_4$, 100 mL DI water, and 100 mL of brine. The organic layer was dried over Na_2SO_4 and evaporated to dryness to give **22** (3.455 g, 93% yield) as a white foam. ^{1}H NMR (400 MHz, $CDCl_3$): δ 1.26-1.49 (m, 88H), 1.58-1.83 (m, 8H), 3.09-3.11 (m, 8H), 4.08-4.18 (m, 12H), 4.80 (s, 4H), 5.3-5.6 (br d, 4H). ^{13}C NMR (100 MHz, $CDCl_3$): δ 22.5, 28.3, 28.4, 29.6, 31.5, 39.9, 53.4, 62.2, 79.0, 79.8, 155.7, 156.1. Calc $[M]^+$ ($C_{69}H_{124}N_8O_{24}$) *m/z* = 1448.87. Found MALDI-ToF $[M+Na]^+$ *m/z* = 1470.0.

EA-G_1-Lys(NH_3TFA)$_8$ (22a). Compound **22** (209 mg, 144 µmol) was dissolved in 1:1 TFA:DCM for 1 h. Quantitative deprotection was confirmed by MALDI-ToF analysis. The solvents were removed under reduced pressure to give **22a** as a gummy solid in quantitative yield. ^{1}H NMR (400 MHz, MeOD): δ 1.40-1.60 (m, 8H), 1.67-1.75 (m, 8H), 1.87-2.10 (m, 8H), 2.99 (t, *J* = 8 Hz, 8H), 4.21 (t, *J* = 6 Hz, 4H), 4.40 (s, 8H). ^{13}C NMR (100 MHz, MeOD): δ 21.8, 26.5, 29.5, 38.7, 42.5, 52.3, 62.9, 161.4, 161.7, 168.6. Calc $[M]^+$ ($C_{29}H_{60}N_8O_8$) *m/z* = 648.45. Found MALDI-ToF $[M+H]^+$ *m/z* = 649.6.

EA-G_1-Lys(Glu(Bn)Boc)$_8$ (24). Compound **22a** (89 mg, 63 µmol) and BocGlu(OBz)-ONp (290 mg, 632 µmol) were added to a 20 ml reaction vial. Under a nitrogen atmosphere, DMF (1 mL) and triethylamine (140 µL, 1.0 mmol) were added and the reaction was allowed to stir for 4 h. MALDI-ToF analysis showed a single peak corresponding to the fully functionalized dendrimer. *N*,*N*-dimethylethylene diamine (50 µl, 690 µmol) was added to quench excess PNP esters. The reaction was diluted with ethyl acetate (100 mL) and washed with three 50 mL portions of 1M $NaHSO_4$, three 50 mL portions of saturated K_2CO_3, 50 mL of DI water, and 50 mL brine. The organic layer was dried over Na_2SO_4 and evaporated to dryness to give **24** (171 mg, 87% yield) as a white foam. ^{1}H NMR (400 MHz, MeOD): δ 1.41-1.56 (bm, 96H), 1.60-1.75 (m, 4H), 1.70-2.13 (m, 16H), 2.25-2.40 (m, 4H), 2.44-2.51 (m, 12H), 2.58-2.61 (m, 4H), 3.10-3.20 (m, 8H), 4.09-4.25 (m, 12H), 4.35-4.40 (m, 4H) 5.08-5.09 (2s, 16H), 7.28-7.38 (m, 40H). ^{13}C NMR (100 MHz, MeOD): δ 23.8, 28.6, 31.5, 40.8, 44.6, 49.0, 54.4, 64.9, 163.4, 163.8, 170.7. Calc $[M]^+$ ($C_{165}H_{228}N_{16}O_{48}$) *m/z* = 3201.59. Found MALDI-ToF $[M+Na]^+$ *m/z* = 3223.3.

EA-G_1-Lys(Glu(Bn)NH_3TFA)$_8$ (24a). Compound **24** (100 mg, 31 µmol) was dissolved in 1:1 TFA:DCM for 1 h. Quantitative deprotection was confirmed by MALDI-ToF analysis. The solvents were removed under reduced pressure to give **24a** as a gummy solid in quantitative yield. ^{1}H NMR (400 MHz, MeOD): δ 1.19-1.35 (m, 16H), 1.45-1.65 (m, 8H), 2.04-2.20 (m, 16H), 2.38-2.46 (m, 8H), 2.51-2.63 (m, 8H), 2.89-2.93 (m, 4H), 3.09-3.12 (m, 4H), 3.89-3.96 (m, 12H), 4.11 (t, *J* = 4.4 Hz, 4H), 4.30-4.33 (m, 4H), 4.80-5.00 (m, 16H), 7.17-7.26 (m, 40H). ^{13}C NMR (100 MHz, MeOD): δ = 24.1, 27.7, 29.7, 30.3, 30.5, 31.6, 40.2, 53.5, 53.9, 54.1, 63.9, 67.8, 116.7, 119.6, 129.2, 129.3, 129.6, 137.3, 162.8, 163.2, 169.8, 170.3, 172.7, 173.6, 173.8. Calc $[M]^+$ ($C_{125}H_{164}N_{16}O_{32}$) *m/z* = 2402.73. Found MALDI-ToF $[M+Na]^+$ *m/z* = 2424.8.

EA-G_1-Lys(Glu(Bn)PEO)$_8$ (25). PNP-PEG carbonate (986 mg, 192 µmol) and **24a** (81 mg, 25 µmol NH_3) were added to a 20 ml reaction vial. Under a nitrogen atmosphere, DMF (3 mL) was added. After using a warm water bath to dissolve the starting material, triethylamine (120 µL, 0.863 mmol) was added. After stirring for 48 h (reaction monitored by SEC anlaysis), no further increase in the molecular weight was observed and the reaction was considered complete. Piperidine (50 µL, 0.506 mmol) was added to quench remaining PNP carbonate. After 1 h, acetic anhydride (400 µL, 4.24 mmol) was added to acylate any remaining primary amines on the dendrimer that had not reacted with the PNP-PEG carbonate. After stirring an additional hour, the reaction mixture was precipitated into ether (300 mL) and **25** (999 mg) was collected by filtration as a fluffy white solid. In some cases residual 5kDa PEG was observed after the PEGylation was considered complete. This could be removed by dialysis using 100,000 MWCO tubing against water for 24 hours. ^{1}H NMR (500 MHz, D_2O): δ 1.20-1.80 (br m, 24H), 1.80-2.10 (br d, 16H), 2.35-2.55 (br s, 16H), 3.05-3.20 (br s, 8H), 3.38 (s, 24H), 3.40-3.90 (br m, ~3,900H), 4.00-4.40 (br m, 36H), 5.09-5.15 (br s, 16H), 7.25-7.40 (br m, 40H). DMF SEC: Mn: 32,000 Da, Mw: 35,000 Da, PDI: 1.09.

EA-G_1-Lys(GluPEO)$_8$ (25a). Compound **25** (402 mg, 10.1 µmol) was added to a 20 ml reaction vial and dissolved in MeOH (9 mL). Activated Pd/C (10 wt%, 50 mg) was added and the reaction put under hydrogen atmosphere. The reaction was stirred overnight, then filtered and solvent removed via rotary evaporation to give **25a** (387 mg) as a white solid. ^{1}H NMR (500 MHz, D_2O): δ 1.20-1.80 (br m, 24H), 1.80-2.1 (br d, 16H), 2.40-2.51 (m, 16H), 3.15-3.25 (br s, 8H), 3.38 (s, 24H), 3.40-3.90 (br m, ~3,900H), 4.00-4.40 (br m, ~36H).

EA-G_1-Lys(Glu(NNBoc)PEO)$_8$ (26). Compound **25a** (710 mg, 142 µmol COOH), *t*-butyl carbazate (94 mg, 711 µmol), and DMAP (10 mg, 81 µmol) was added to a 20 ml reaction vial. Under a nitrogen atmosphere, DCM (8 mL) was added dropwise. The solution was cooled to 0 ^{o}C followed by the addition of EDC (136 mg, 709 µmol). The reaction was allowed to warm to room temperature and stirred over night. The reaction was dialyzed against MeOH in 12kDa-14kDa MWCO dialysis with 3 solvent changes over 18 h. Concentration of the bag contents *in vacuo* gave **26** (660 mg) as a white solid. ^{1}H NMR (500 MHz, D_2O): δ 1.30-1.60 (br m, 100H), 1.65-2.20 (br m, 20H), 2.30-2.45 (br s, 16H), 3.15-3.25 (br s, 8H), 3.38 (s, 24H), 3.50-3.90 (br m, ~3,900H), 4.00-4.45 (br m, 40H).

EA-G_1-Lys(Glu(NNH$_3$TFA)PEO)$_8$ (26a). Compound **26** (102 mg) was dissolved in 1:1 TFA:DCM for 1 h. The solvents were removed under reduced pressure to give **26a** as a gummy solid. Quantitative deprotection confirmed by ^{1}H NMR.

EA-G_1-Lys(Glu(NNDox)PEO)$_8$ (27). Compound **26a** (72 mg, 14 µmol NNBoc) and doxorubicin (50 mg, 92 µmol) were added to a 20 ml reaction vial and were dissolved in MeOH (3 mL), pyridine (100 µL), and acetic acid (100 µL). The reaction was purged with nitrogen and stirred at 60 ^{o}C in the dark for 18 h. The reaction mixture was loaded directly onto a Sephadex LH-20 column and eluted with methanol. The first dark red band was collected and the solvent removed by rotary evaporation. The solid material was further purified using a Biorad PD-10 column with water as the eluent. After lyophilization 67.2 mg of red powder remained. The Dox loading was quantified using the absorbance at 486 nm (ε = 11,500)[42] to be 9.6%.

PE-G_1-(AspBoc)$_8$ (11). Compound **6** (434 mg) was added to a 20 ml reaction vial and dissolved in MeOH (10 mL). Activated Pd/C (10 wt%, 44 mg) was added and the reaction put under hydrogen atmosphere. After 1 h, the reaction appeared complete by MALDI. Filtration and removal of the solvent via rotary evaporation gave **11** (315 mg) as a white foam. ^{1}H NMR (400 MHz, $CDCl_3$) δ 1.29 (s, 12H), 1.45 (s, 72H), 2.81-3.04 (br d, 16H), 4.16-4.41 (m, 24H), 4.63 (br s, 8H), 5.72 (br s, 6H), 6.52 (br s, 2H); ^{13}C NMR (100 MHz, MeOD) δ 18.3, 28.8, 37.1, 47.7, 51.4, 63.3, 67.0, 80.8, 82.0, 157.5, 172.4, 173.3, 174.0; MS (MALDI-ToF) Calc $[M]^+$ ($C_{97}H_{148}N_8O_{56}$) *m/z* = 2320.9. Found $[M+Na]^+$ *m/z* = 2344.0.

PE-G_1-(Asp(Glu(NNBoc)$_2$)PEO)$_8$ (12). Compound **9** (150 mg, 30 µmol COOH), compound **10** (232 mg, 620 µmol), and pentachlorophenol (164 mg, 620 µmol) were added to a 20 mL reaction vial. Under a nitrogen atmosphere, DMF (600 µL) was added, followed by triethylamine (86 µL, 620 µmol); upon dissolution, EDC (118 mg, 620 µmol) was added and the reaction stirred at room temperature overnight. The reaction was dialyzed against MeOH in 12-14 kDa MWCO dialysis with 3 solvent changes over 24 h. Concentration of the bag contents *in vacuo* gave **12** (140 mg) as a white solid. ^{1}H NMR (400 MHz, $CDCl_3$) δ 1.25 (s, 24H), 1.45 (br s, 110 H), 2.7-3.0 (br m, 66 H), 3.38 (s, 24 H), 3.5-3.9 (br m, 4070 H), 4.1-4.5 (br m, 50H).

PE-G_1-(Asp(Glu(NNDox)$_2$)PEO)$_8$ (14). Compound **12** (15.2 mg, 6.1 µmol NNBoc) was dissolved in 1:1 TFA:DCM for 1 h. The solvent was removed by rotary evaporation. The solid was redissolved in DCM and evaporated twice to remove residual TFA. The solid was dissolved in MeOH (1 mL), pyridine (50 µL), and acetic acid (50 µL), and doxorubicin (10 mg, 17 µmol) was added. The reaction was purged with nitrogen and stirred at 60 ^{o}C in the dark for 16 h. The reaction mixture was loaded directly onto a Sephadex LH-20 column and eluted with methanol. The first dark red band was collected and the solvent removed by rotary evaporation. The solid material was further purified using a Biorad PD-10 column with water as the eluent. After lyophilization, 17 mg of red powder remained. The Dox loading was quantified using the absorbance at 486 nm (ε = 11,500)[42] to be 14.8%.

PLL-G_2-(Asp(NNBoc)PEO)$_8$ (20). Compound **19** (110 mg, 22 µmol COOH) and *t*-butyl carbazate (29.1 mg, 220 µmol) were added to a 20 mL reaction vial. Under a nitrogen atmosphere, DMF (500 µL) was added; upon complete dissolution, HBTU (83.5 mg, 220 µmol) and DIPEA (80 µL, 440 µmol) were added and the reaction stirred at room temperature

overnight. The reaction was dialyzed against MeOH in 3,500 MWCO dialysis with 3 solvent changes over 18 h. SEC analysis of the isolated solid indicated a high degree of polymer degradation.

PLL-G_2-(Asp(Bn)-Amide-PEO)$_8$ (**28**). Deprotected compound **17** (158.4 mg, 0.373 mmol NH_3) and carboxymethyl-PEG (2.14g, 0.428 mmol) were added to a 20 ml reaction vial. Under a nitrogen atmosphere, DMF (4 mL) and DCM (0.6 mL) were added. After using a warm water bath to dissolve the starting material, DMAP (112 mg, 0.92 mmol), EDC (480 mg, 2.50 mmol), and DIPEA (210 µL, 1.21 mmol) were added. After stirring overnight, the reaction was considered complete and acetic anhydride (10 µL, 0.106 mmol) was added to acylate any remaining amines. After 4 h, n-butylamine (200 µL, 2.02 mmol) was added to deactivate any activated PEG chains. The reaction mixture was then precipitated into cold ether (120 mL), dissolved in water and dialyzed against water in 100 kDa MWCO dialysis with one solvent change over 24 h. The retained water was lyophilized to yield a white powder (1.82 g). ^{1}H NMR (D_2O, 500 MHz): δ 1.18 (br s, 15), 1.30 (br s, 13), 1.54 (br s, 8), 1.62 (br s, 6), 2.7-2.9 (br m, 18), 3.01 (br s, 19), 3.32 (s, 24), 3.4-3.8 (br m, ~4200), 4.24 (br m, 25), 4.4-4.6 (br m, 15), 5.1 (br s, 16), 7.3 br (m, 40). DMF SEC: Mn: 33,700 Da, Mw: 37,000 Da PDI: 1.06.

PLL-G_2-(Asp-Amide-PEO)$_8$ (**28a**). Compound **28** (991mg, 1.98 mmol) was added to a 20 ml reaction vial and dissolved in MeOH (6 mL). Activated Pd/C (10 wt%, 210 mg) was added and the reaction put under hydrogen atmosphere. The reaction stirred overnight and then the Pd/C was filtered off. The solution was then precipitated into ether to give **28a (**550 mg) as an off-white solid. ^{1}H NMR (D_2O, 500 MHz) δ 1.18 (br d, 15), 1.36 (br s, 14), 1.57 (br s, 8), 1.66 (br s, 7), 2.7-2.9 (br m, 18), 3.05 (br s, 19), 3.25 (s, 24), 3.4-3.8 (br m, ~4000), 4.0-4.3 (br m, 23).

PLL-G_2-(Asp(NNBoc)-Amide-PEO)$_8$ (**29**). Compound **28a** (691 mg, 0.138 mmol COOH), *t*-butyl carbazate (192 mg, 1.45 mmol), and DMAP (180 mg, 1.47 mmol) were added to a 20 mL reaction vial. Under a nitrogen atmosphere, DMF (5.5 mL) and DCM (1 mL) were added. After using a warm water bath to dissolve the starting material, the solution was cooled to 20 ^{o}C and EDC (268 mg, 1.40 mmol) was added and the reaction was stirred overnight. The reaction was precipitated into cold ether (200 mL), dissolved in water and dialyzed against water in 3500 MWCO dialysis, changing the water after 2 and 8 hours. The retained water was lyophilized to yielda white powder (460 mg). ^{1}H NMR (D_2O, 500 MHz) δ 1.1-1.6 (br m, 94), 1.64 (br s, 8), 1.73 (br s, 7), 2.7-2.9 (br m, 17), 3.12 (br s, 19), 3.32 (s, 24), 3.4-3.8 (br m, ~4200), 4.0-4.3 (br m, 23).

PLL-G_2-Asp(GluNNBoc$_2$)PEG$_8$ (30). Compound **18** (1.0 g, 0.22 mmol COOH) and DMF (4 mL) were added to a 20 mL vial. Under a nitrogen atmosphere, **10** (810 mg, 2.2 mmol) and HBTU (830 mg, 2.2 mmol) were added. The mixture was stirred 5 min, and then DIPEA (760 µL, 4.4 mmol) was added. After 24 h, water was added and the solution was dialyzed against water in 3500 MWCO dialysis for 24 h. The retained water was lyophilized to yield a white powder (1.1 g, quant). ^{1}H NMR (500 MHz, D_2O): δ 1.47 (br s, 180), 1.6-1.9 (br m, 18), 2.2 (br m, 8), 2.4 (br m, 16), 2.7-2.9 (br m, 18), 3.21 (br s, 19), 3.39 (s, 24), 3.5-4.0 (br m, ~4300), 4.24 (br m, 25), 4.4-4.6 (br m, 15).

PLL-G_2-Asp(GluNNDox$_2$)PEG$_8$ (31). Compound **30** (166 mg, 66 μmol NNBoc) was dissolved in 1:1 TFA:DCM for 2 h. The solvent was removed by rotary evaporation, then again by azeotropic distillation twice with toluene under vacuum. The solid was dissolved in MeOH and evaporated twice to remove residual TFA. The solid was dissolved in MeOH (3 mL), pyridine (100 μL), and acetic acid (100 μL), and doxorubicin (100 mg, 170 μmol) was added. The reaction was purged with nitrogen and stirred at 60 ^{o}C in the dark for 16 h. The reaction mixture was loaded directly onto a Sephadex LH-20 column and eluted with methanol. The first dark red band was collected and the solvent removed by rotary evaporation. The solid material was further purified using a Biorad PD-10 column with water as the eluent. After lyophilization 163 mg of red powder remained. The Dox loading was quantified using the absorbance at 486 nm (ε = 11,500) (*1*) to be 16%.

Polymer Degradation Study. Compound **26** (20 mg) was dissolved in 1.5 ml of 1X PBS buffer and incubated at 37 ^{o}C. At t = 0, 1, 2, 3, 6, 15, 20 days, 100 μl aliquots were taken out and immediately frozen followed by lyophilization. At the end of the experiment, each sample was dissolved in 0.5 ml DMF from the System A mobile phase, filtered though a 0.2 μm PVTF filter and measured by the RI detector on system A.

Hydrolysis of Dox from Compound 27 at pH 7.4 and pH 5. Drug release rates were determined by a modified published procedure.[43] Compound **27** was dissolved in either 1X PBS or pH 5 acetate buffer (30 mM with 70 mM $NaNO_3$), at 1 mg/mL. Buffers were preheated to 37 ^{o}C before dissolving polymer and maintained at this temperature throughout the experiment. At each timepoint, 25 μL was injected onto SEC system C for analysis.

Cytotoxicity Studies in Cells. The cytotoxicities of free Dox, **26**, and **27** were determined by using the MTT assay with C26 cells. Cells were seeded onto a 96-well plate at a density of 5.0 × 10^3 cells per well in 100 μl of medium and incubated overnight (37°C, 5% CO_2, and 80% humidity). An additional 100 μl of new medium (RPMI medium 1640, 10% FBS, 1% penicillin-streptomycin, 1% Glutamax) containing varying concentrations of DOX, **26**, or **27** were added to each well. After incubation for 72 h, 40 μl of media containing thiazolyl blue tetrazolium bromide (5 mg/ml) was added. The cells were incubated for 3 h, after which time the medium was carefully removed. To the resulting purple crystals was added 200 μl of DMSO and 25 μl of pH 10.5 glycine buffer (0.1 M glycine/0.1 M NaCl). Optical densities were measure at 570 nm by a SpectraMAX 190 microplate reader (Molecular Devices, Sunnyvale, CA). Optical densities measured for wells containing cells that received neither dendrimer nor drug were considered to represent 100% viability. IC_{50} values were obtained from sigmoidal fits of the data using Origin 7 SR4 8.0552 software (OriginLab, Northhampton, MA).

Biodistribution Study in Xenograph Mice. Six to eight week old female Balb/C mice were injected in the right hind flank with 3 x 10^5 C26 cells. Twelve days after tumor inoculation, mice were randomized into two groups. Mice were injected by means of the tail vein either with DOXIL (8 mg DOX eq/kg; 3 mice) or with **27** (8 mg DOX eq/kg; 6 mice) in ~200 μL of PBS. Blood was collected from half of the mice injected with polymer by submandibular bleeds 60 and 1440 min after dosing (data not shown); after 2880 min, the three mice were sacrificed. The remaining six mice were sacrificed at 1 wk postinjection. The blood (collected by heart

puncture), heart, liver, spleen, kidney, muscle, and tumor were collected for analysis. Each organ was weighed and 200-300 mg of the collected organs were homogenized with zirconium beads and 1 mL acidified isopropyl alcohol (0.075 M HCl, 90% IPA). The samples then incubated at 4 °C for 24 h. Serum was collected using Microtainer serum separator vials and processed in the same manner as the organs. The samples were frozen in a -80 °C freezer until measurements could be made. At measurement time, samples were thawed, briefly vortexed, and centrifuged for 3 min at 8,000 rpm. Then, 80 μL of supernatant was combined with 920 μL of acidified IPA for fluorescence measurements. Dox fluorescence (excitation 490 nm; emission 590 nm) was measured on a PTI fluorimeter (Birmingham, NJ). Calibration curves were made from organ samples collected from an untreated mouse.

Chemotherapy Experiments. While under anesthesia, female Balb/C mice were shaved, and C26 cells (3×10^5 cells in 50 μL) were injected subcutaneously in the right hand flank. At eight days post-tumor implantation, mice were randomly distributed into treatment groups of 10 animals. Mice were injected by means of the tail vein with Doxil (20 mg Dox/kg) or **27** (10, 15, and 20 mg Dox/kg) in approximately 200 μL of solution. Mice were weighed and tumors measured every other day. The tumor volume was estimated by measuring the tumor volume in three dimension with calipers and calculated using the formula tumor volume = length x width x height. Mice were removed from the study when (i) a mouse lost 15% of its initial weight, (ii) any tumor dimension was > 20 mm, or (iii) the mouse was found dead. The mice were followed until day 60 post-tumor inoculation. Statistical analysis was performed as previously described[41] using MedCalc 8.2.1.0 for Windows (MedCalc Software, Mariakerke, Belgium). The tumor growth delay was calculated based upon a designated tumor volume of 400 mm^3.

References

(1) Kopecek, J. **1977,** *Polymers in Medicine 7*, 191-221.
(2) Bader, H., Ringsdorf, H., and Schmidt, B. *Angewandte Makromolekulare Chemie.* **1984**, *123*, 457-485.
(3) Seymour, L. W. *Critical Reviews in Therapeutic Drug Carrier Systems* **1992,** *9*, 135-187.
(4) Matsumura, Y., and Maeda, H. *Cancer Research* **1986,** *46*, 6387-6392.
(5) Liu, S., Maheshwari, R., and Kiick, K. L. *Macromolecules* **2009,** *42*, 3-13.
(6) Kataoka, K., Harada, A., and Nagasaki, Y. *Advanced Drug Delivery Reviews* **2001,** *47*, 113-131.
(7) Guo, X., and Szoka, F. C. *Accounts of Chemical Research* **2003,** *36*, 335-341.
(8) Christian, D. A., Cai, S., Bowen, D. M., Kim, Y., Pajerowski, J. D., and Discher, D. E. *European Journal of Pharmaceutics and Biopharmaceutics* **2009 ,** *71*, 463-474.
(9) Fox, M. E., Szoka, F. C., and Frechet, J. M. J. *Accounts of Chemical Research* **2009,** *42*, 1141-1151.
(10) Li, M. H., and Keller, P. *Soft Matter* **2009,** *5*, 927-937.
(11) Green, J. J., Langer, R., and Anderson, D. G. *Accounts of Chemical Research* **2008,** *41*, 749-759.
(12) Haag, R., and Kratz, F. *Angewandte Chemie-International Edition* **2006,** *45*, 1198-1215.

(13) Peer, D., Karp, J. M., Hong, S., Farokhzad, O. C., Margalit, R., and Langer, R. *Nature Nanotechnology* **2007,** *2*, 751-760.
(14) Medina, S. H., and El-Sayed, M. E. H. *Chemical Reviews* **2009,** *109*, 3141-3157.
(15) Gillies, E. R., and Frechet, J. M. J. *Drug Discovery Today* **2005,** *10*, 35-43.
(16) Lee, C. C., MacKay, J. A., Frechet, J. M. J., and Szoka, F. C. *Nature Biotechnology* **2005,** *23*, 1517-1526.
(17) Lee, C. C., Gillies, E. R., Fox, M. E., Guillaudeu, S. J., Frechet, J. M. J., Dy, E. E., and Szoka, F. C. *Proceedings of the National Academy of Sciences of the United States of America* **2006,** *103*, 16649-16654.
(18) De Jesus, O. L. P., Ihre, H. R., Gagne, L., Frechet, J. M. J., and Szoka, F. C. *Bioconjugate Chemistry* **2002,** *13*, 453-461.
(19) Parrott, M. C., Marchington, E. B., Valliant, J. F., and Adronov, A. *Journal of the American Chemical Society* **2005,** *127*, 12081-12089.
(20) Bellis, E., Hajba, L., Kovacs, B., Sandor, K., Kollar, L., and Kokotos, G. *Journal of Biochemical and Biophysical Methods* **2006,** *69*, 151-161.
(21) Krishna, T. R., Jain, S., Tatu, U. S., and Jayaraman, N. *Tetrahedron* **2005,** *61*, 4281-4288.
(22) Chen, H. T., Neerman, M. F., Parrish, A. R., and Simanek, E. E. *Journal of the American Chemical Society* **2004,** *126*, 10044-10048.
(23) Lim, J. D., and Simanek, E. E. *Organic Letters* **2008,** *10*, 201-204.
(24) Lim, J., Guo, Y., Rostollan, C. L., Stanfield, J., Hsieh, J. T., Sun, X. K., and Simanek, E. E. *Molecular Pharmaceutics* **2008,** *5*, 540-547.
(25) Esfand, R., and Tomalia, D.A. *Drug Discovery Today* **2001,** *6*, 427-436.
(26) Khandare, J. J., Jayant, S., Singh, A., Chandna, P., Wang, Y., Vorsa, N., and Minko, T. *Bioconjugate Chemistry* **2006,** *17*, 1464-1472.
(27) Kono, K., Kojima, C., Hayashi, N., Nishisaka, E., Kiura, K., Wataral, S., and Harada, A. *Biomaterials* **2008,** *29*, 1664-1675.
(28) Bhadra, D., Bhadra, S., Jain, S., and Jain, N. K. *International Journal of Pharmaceutics* **2003,** *257*, 111-124.
(29) Patri, A. K., Myc, A., Beals, J., Thomas, T. P., Bander, N. H., and Baker, J. R. *Bioconjugate Chemistry* **2004,** *15*, 1174-1181.
(30) Malik, N., Evagorou, E. G., and Duncan, R. *Anti-Cancer Drugs* **1999,** *10*, 767-776.
(31) Kaminskas, L. M., Kelly, B. D., McLeod, V. M., Boyd, B. J., Krippner, G. Y., Williams, E. D., and Porter, C. J. H. *Molecular Pharmaceutics* **2009,** *6*, 1190-1204.
(32) Kaneshiro, T. L., Wang, X., and Lu, Z. R. *Molecular Pharmaceutics* **2007,** *4*, 759-768.
(33) Okuda, T., Kawakami, S., Akimoto, N., Niidome, T., Yamashita, F., and Hashida, M. *Journal of Controlled Release* **2006,** *116*, 330-336.
(34) Grinstaff, M. W. *Chemistry-a European Journal* **2002,** *8*, 2838-2846.
(35) Malik, N., Wiwattanapatapee, R., Klopsch, R., Lorenz, K., Frey, H., Weener, J. W., Meijer, E. W., Paulus, W., and Duncan, R. *Journal of Controlled Release* **2000,** *68*, 299-302.
(36) Gillies, E. R., Dy, E., Frechet, J. M. J., and Szoka, F. C. *Molecular Pharmaceutics* **2005,** *2*, 129-138.
(37) Gillies, E. R., and Frechet, J. M. J. *Journal of the American Chemical Society* **2002,** *124*, 14137-14146.
(38) Goodwin, a. P., Lam, S. S., and Frechet, J. M. J. *Journal of the American Chemical Society* **2007,** *129*, 6994-6995.

(39) Guillaudeu, S. J., Fox, M. E., Haidar, Y. M., Dy, E. E., Szoka, F. C., and Frechet, J. M. J. *Bioconjugate Chemistry* **2008,** *19*, 461-469.
(40) King, H. D., Yurgaitis, D., Willner, D., Firestone, R. A., Yang, M. B., Lasch, S. J., Hellstrom, K. E., and Trail, P. A. *Bioconjugate Chemistry* **1999,** *10*, 279-288.
(41) Fox, M. E., Guillaudeu, S., Frechet, J. M. J., Jerger, K., Macaraeg, N., and Szoka, F. C. *Molecular Pharmaceutics* **2009,** *6*, 1562-1572.
(42) Gabbay, E. J., Grier, D., Fingerle, R. E., Reimer, R., Levy, R., Pearce, S. W., and Wilson, W. D. *Biochemistry* **1976,** *15*, 2062-2070.
(43) Lee, C. C., Cramer, A. T., Szoka, F. C., and Frechet, J. M. J. *Bioconjugate Chemistry* **2006,** *17*, 1364-1368.
(44) Martinez, J., and Bodanszky, M. *International Journal of Peptide and Protein Research* **1978,** *12*, 277-283.
(45) Tekade, R. K., Kumar, P. V., and Jain, N. K. *Chemical Reviews* **2009,** *109*, 49-87.
(46) Kaminskas, L. M., Boyd, B. J., Karellas, P., Krippner, G. Y., Lessene, R., Kelly, B., and Porter, C. J. H. *Molecular Pharmaceutics* **2008,** *5*, 449-463.
(47) Denkewalter. *U.S. Patent*, **1982,** 4,360,646.
(48) Seymour, L. W., Duncan, R., Strohalm, J., and Kopecek, J. *Journal of Biomedical Materials Research* **1987,** *21*, 1341-1358.
(49) Kratz, F., Warnecke, A., Schmid, B., Chung, D. E., and Gitzel, M. *Current Medicinal Chemistry* **2006,** *13*, 477-523.
(50) Bae, Y., Nishiyama, N., Fukushima, S., Koyama, H., Yasuhiro, M., and Kataoka, K.. *Bioconjugate Chemistry* **2005,** *16*, 122-130.
(51) Ulbrich, K., Etrych, T., Chytil, P., Jelinkova, M., and Rihova, B. *Journal of Controlled Release* **2003,** *87*, 33-47.

Chapter 3 – Synthesis and Evaluation of Branched Block Copolymers for Platinum (II) Delivery

Abstract

Platinum (II) chemotherapy drugs are effective against a wide range of cancer types. Chapter 3 presents a method for producing PEGylated dendrimers with a high loading of diaminocyclohexane platinate (DACHPt). The PEGylated dendrimer is composed of a lysine core that has oligomers of glutamic acid attached at the periphery. The end groups of the glutamic acid were PEGylated and the glutamic acid side chains are further modified with dicarboxylate chelators that are then loaded with platinum. The platinum release, *in vitro*, and *in vivo* toxicity of the platinum conjugates were measured in comparison to the parent drug, oxaliplatin.

Introduction

The anticancer properties of platinum complexes have made them a powerful addition to the current arsenal of natural product based chemotherapeutics.[1] In addition, platinum drugs show great promise in combination chemotherapy,where two drugs act synergistically together. Platinum drugs are generally more water soluble than natural product-like drugs and therefore tend follow different biodistribution and pharmacokinetic trends.[2] This leads to non-overlapping systemic toxicity profiles with natural product drugs thus their maximum tolerated doses tend to be independent of each other. Cisplatin and other Pt(II) analogues are usually administered as inactive prodrugs composed of platinum atoms bearing two amino ligands *cis* to two leaving groups, most commonly dichloride or dicarboxylate.[3] Upon injection and cellular uptake, the leaving groups begin to dissociate from the Pt complex forming the active mono or diaquo species[4] followed by cross-linking of DNA and ultimately apoptosis or necrosis.[5]

The mechanism of action for platinum (II) chemotherapeutics relies on platinum's affinity for nitrogen containing heterocyclic ligands like those found in the DNA bases.[6] Since the discovery of the cytotoxic properties of Pt(II) compounds[7] there have been thousands of small molecule derivatives studied in academia and industry.[8] There have been extensive chemical and biological studies aimed at elucidating the nature of platinum binding to DNA.[9-11] Generally, 60-65% of platinum adducts are a 1,2GpG intrastrand crosslink, 20-25% are ApG 1,2 intrastran crosslinks, and the remaining 10-20% come from rare 1,3 intrastrand cross lings, interstrand crosslinks, and monodentate platinum adducts.[12]

Despite the benefits of using platinum chemotherapeutics, clinical use of platinates is limited by severe side effects. Cisplatin, which has been a major weapon against ovarian and testicular cancers, is particularly toxic to the kidneys and the gastrointestinal tract. This toxicity has driven research toward the development of less toxic analogues that are still active against tumor cells. Carboplatin was developed under the assumption that a more stable bidentate dicarboxylate leaving group would result in slower drug activation and therefore lower toxicity.[13] Oxaliplatin benefits from the slower drug activation from a dicarboxylate leaving group but also utilizes a bulkier diamine ligand which decreases the cell's ability to repair the Pt-DNA adducts and ultimately improves the drug's efficacy against a broader spectrum of cancer types.[14] The three FDA approved, clinically used platinum drugs are shown in Figure 1.

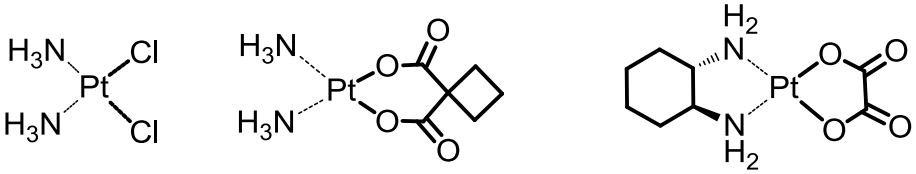

Figure 1. The three major platinum (II) drugs and their year of FDA approval

While much has been done to improve platinum chemotherapeutics there are still limitations. Side effects still do exist, and the more polar nature of platinum complexes causes them enter cells relatively slowly compared to more lipophilic drugs.[15] To this end, there is great interest in developing delivery vehicles for platinum-based drugs. Macromolecular carriers show the greatest potential for drug delivery to solid tumors as a result of the enhanced permeation and retention (EPR) effect.[16] Platinum presents a significant challenge for polymeric drug delivery because it is difficult to attach the drug and have it release in a controlled or triggered manner.

Macromolecular approaches for delivery of platinum prodrugs have shown improvements in drug efficacy, due in large part to the extended circulation half-life of the polymer drug conjugate and the isolation of the polymer bound payload from deactivating agents.[17] The large size and extended circulation time of the macromolecule allows for the conjugated drug to preferentially accumulate at the site of the tumor because of the enhanced permeation and retention (EPR) effect.[16] Polymeric carriers such as linear polymers,[18-20] micellar assemblies,[21-26] dendrimers,[27-29] hyperbranched polymers,[30] and polymeric[31,32] and gold[33] nanoparticles are among the nanoscopic architectures that have been explored for platinum delivery. Our goal in this work was to use our PEGylated dendrimer technology for the delivery of platinum (II) drugs by chelating platinum through the polymer via the leaving group portion of the drug. Figure 2 is a structure representation of the mechanism of platinum drug activation.

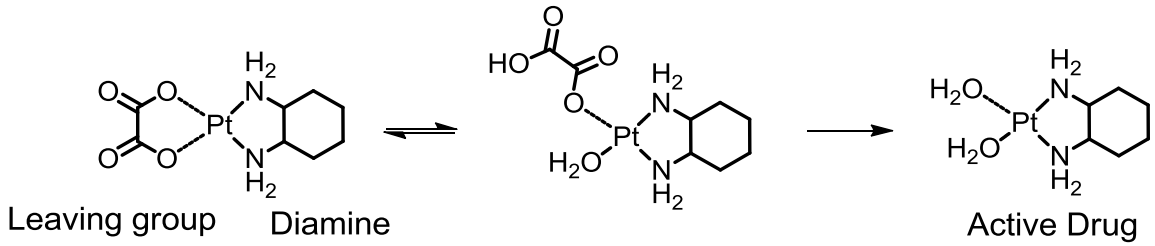

Figure 2. Mechanism of platinum drug activation.

Results and Discussion

Synthesis of Branched Block Copolymer Drug Carrier

A logical approach for the attachment of platinum (II) drugs to a polymeric carrier is to install multiple copies of dicarboxylate chelators onto the polymer and then load the diaminoplatinum drug. Previous work in our group, and the work described in chapter 2, has shown that the number of PEG arms attached to the dendrimer periphery has a profound effect on the biodistribution.[34] We initially envisioned using a 40 kDa PEGylated dendrimer with 8 sites for platinum attachment as shown in Figure 3.

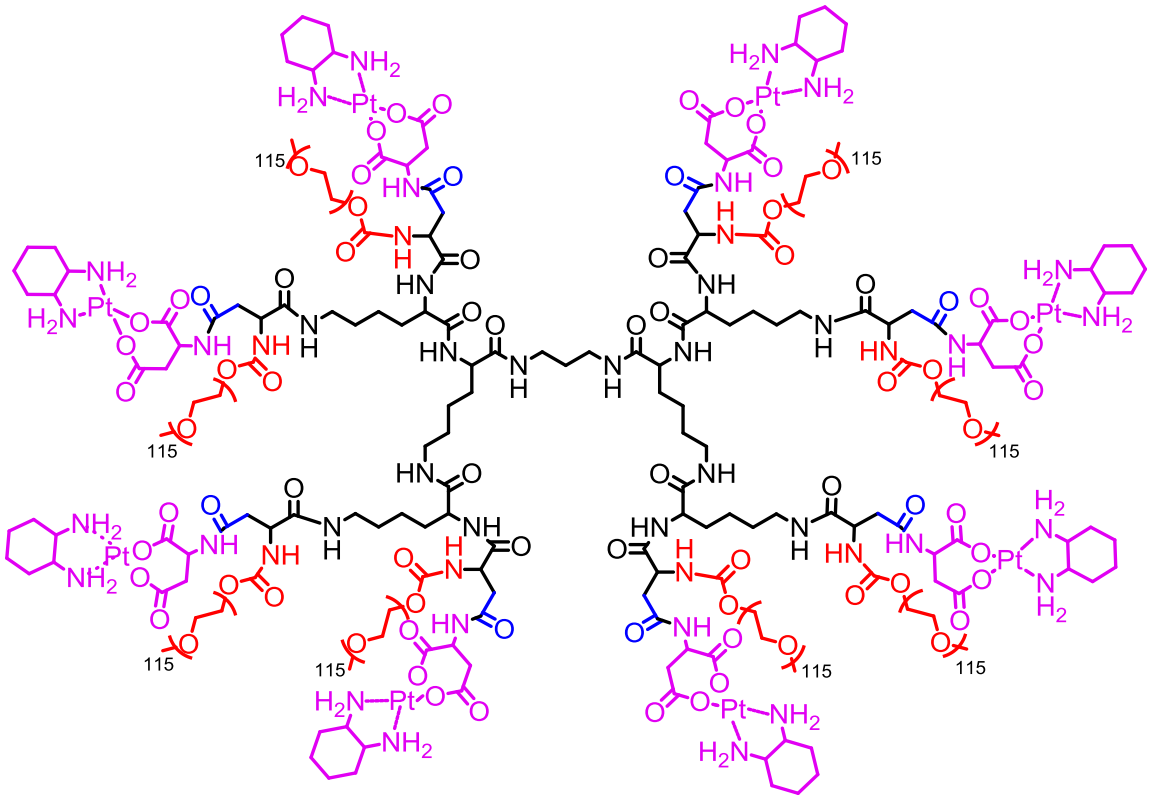

Figure 3. 40 kDa PEGylated dendrimer with eight platinum drugs attached.

While this structure is an attractive polymer support that should provide isolation of the drug payload and favorable pharmokinetics and biodistribution, we were concerned that eight platinum molecules per polymer would only provide a maximum drug loading of approximately 4% wt/wt. This is not ideal as large polymer quantities would be required to injected higher doses of platinum drug. Therefore, we opted to modify the polylysine core by oligomerizing glutamic acid molecules from the primary amine periphery of polylysine via a radial growth polymerization (Scheme 2). The side chain carboxylic acids of glutamic acid provide additional sites for chelator attachment and thus a higher theoretical drug loading. A polylysine dendrimer core was chosen for use in this study because it can be made easily and is very robust due its polyamide structure. The first generation (G1) lysine dendrimer is synthesized by the addition of Boc-Lys(Boc)-ONp to a 1,3-diaminopropane core. Removal of the Boc groups is carried out using 1:1 dichloromethane: trifluoroacetate. Another iteration of these two reactions yields a second generation (G2) dendrimer with eight amine groups at the periphery (Scheme 1).

Scheme 6. Synthesis of polylysine dendrimers.

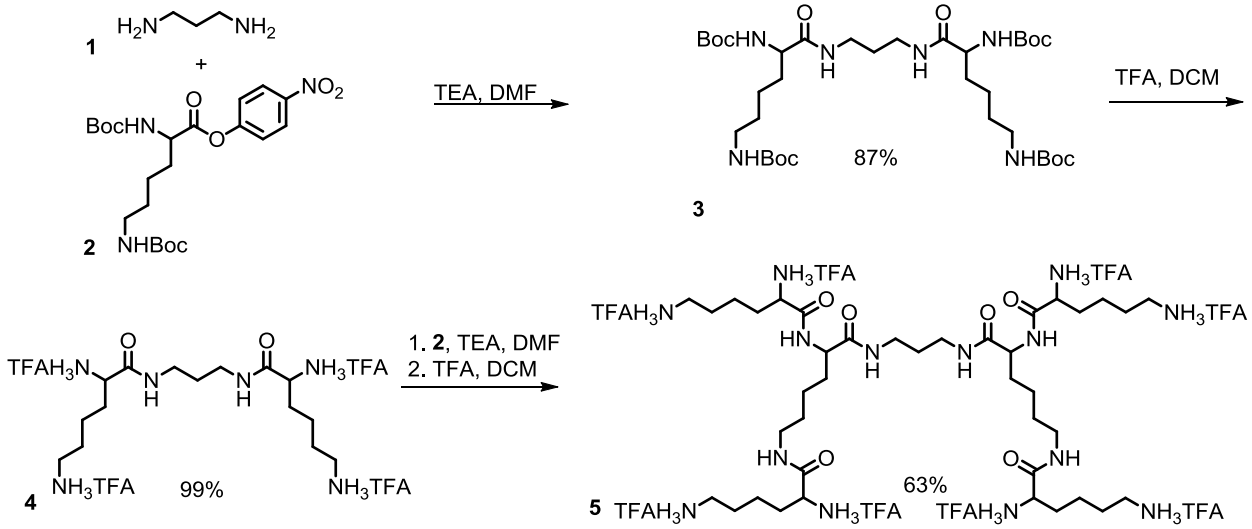

The G2 dendrimer is deprotected to furnish a macroinitiator with eight primary ammonium trifluoroacetate groups. Ten equivalents of the *N*-carboxy anhydride (NCA) of benzyl-L-glutamate are added per ammonium salt of the dendrimer. The result is a radial growth living polymerization in which the equilibrium between the protonated ammonium salt and the free base defines the equilibrium between active and dormant polymer chains (Figure 4a), a concept demonstrated by Shlaad et al.[35]

Scheme 7. Synthesis of PEGylated dendrimer and platinum loading.

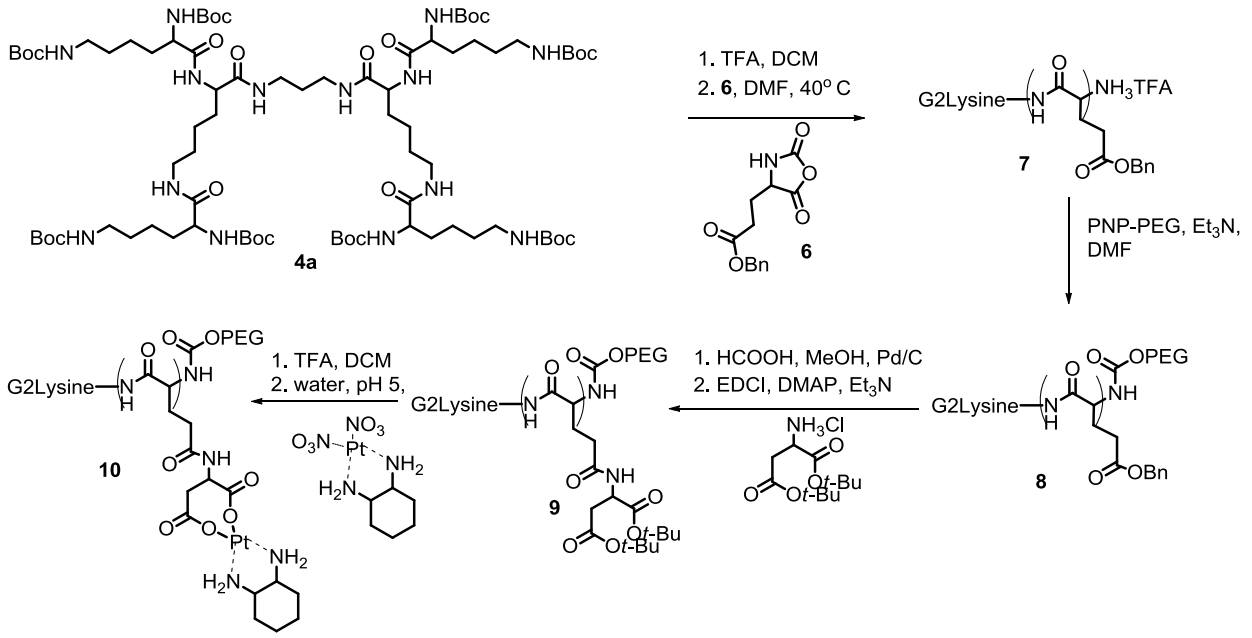

This is an attractive polymerization method because the acidic conditions also suppress cyclization occurring at the chain end that terminate the polymerization (Figure 4b).

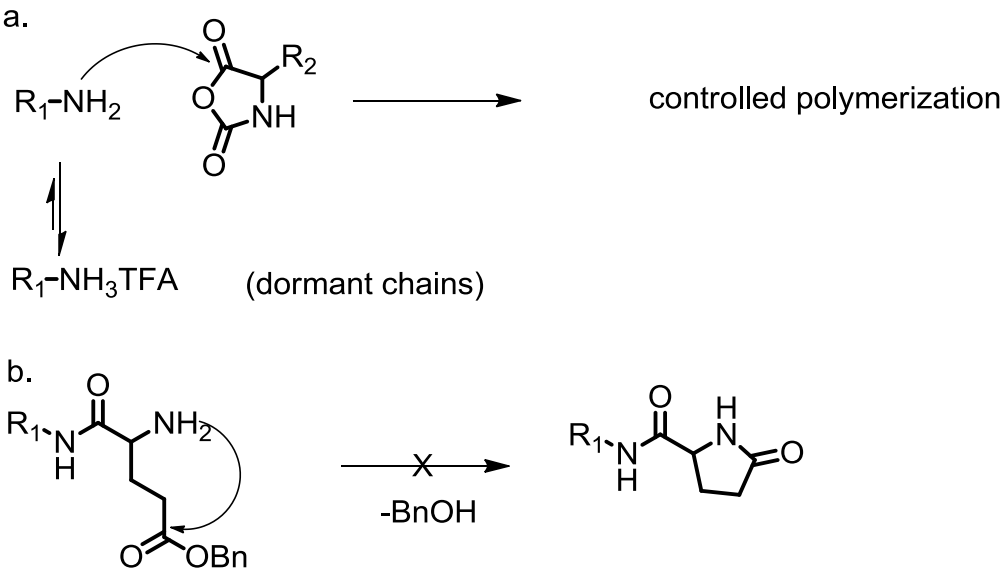

Figure 4. (a) Ammonium salt initiation of a living, ring-opening polymerization of glutamic acid. (b) Chain termination by ring closure aminolysis.

Polymerization of NCA monomers is a well established technique for fabricating polypeptides.[36] Typically, NCA ring opening polymerizations are difficult to control and lead to polymers with high polydispersity indexes (PDI). This is because the NCA monomer is very unstable and can spontaneously decompose back to the starting amino acid, which can then initiate polymerization in the bulk sample. Also, when a primary amine is used as the initiator, there are two competing mechanisms of chain growth as illustrated in Figure 5.

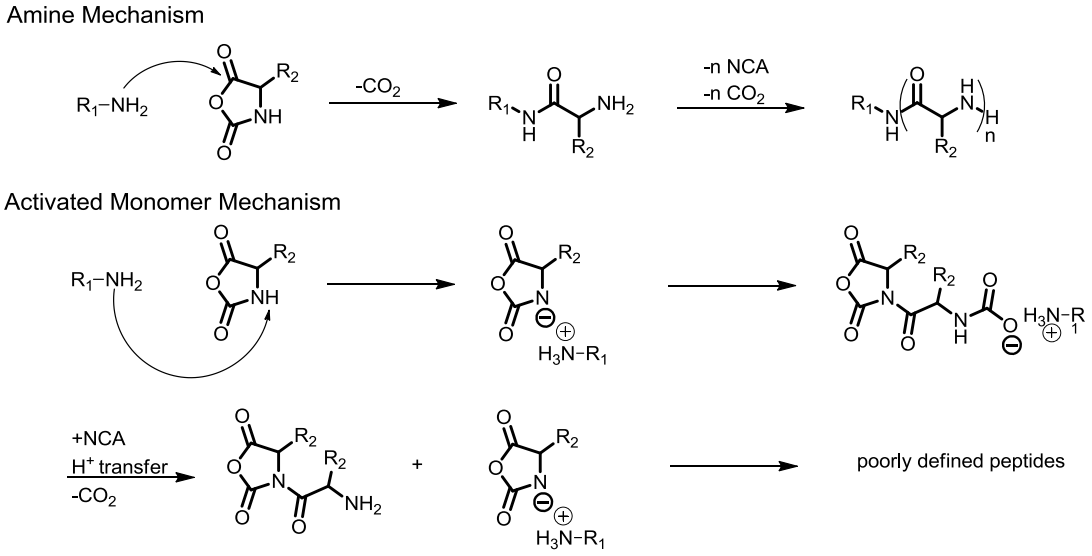

Figure 5. Competing mechanisms for NCA ring opening polymerization initiated by a primary amine (adapted from Deming[37]).

The NCA monomer of glutamic acid is prepared by treating benzylester protected glutamic acid with triphosgene at 90˚C in ethyl acetate. When the trifluoroacetate salt of the lysine dendrimer is used to initiate a radial growth polymerization, we were pleased to observe a fairly narrow distribution of oligomerized product. In our hands, 40˚C was the best temperature to run the polymerization. Figure 6 shows a structural representation of the radial growth polymerization a MALDI-ToF spectrum of the reaction product. The spectrum in Figure 6b is a blowup of spectrum 6a. If the mass of tallest peak is analyzed, we approximate that the average substitution per dendrimer core is 29 monomer units, and average of 3.6 per dendrimer arm.

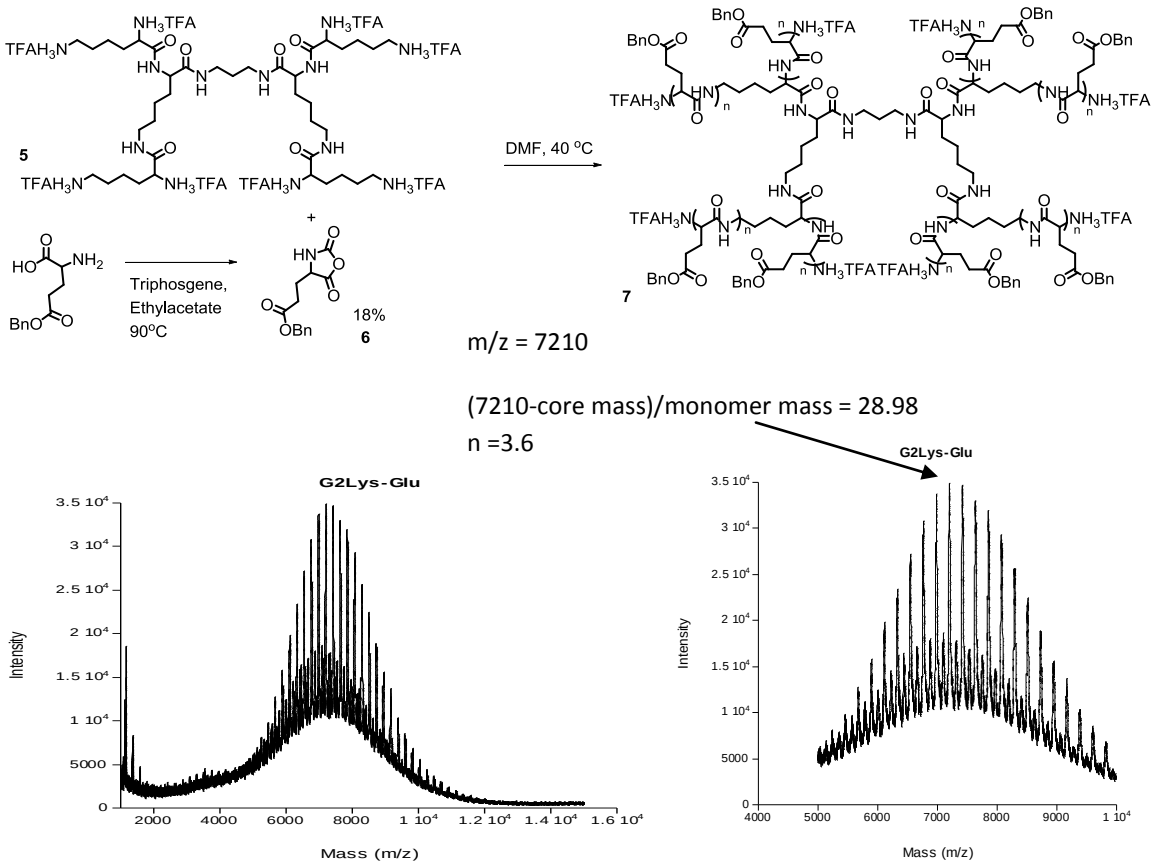

Figure 6. Maldi-ToF of dendrimer after radial growth polymerization at periphery.

After a reaction time of three days, the polymer is precipitated into ether. The polymer is then redissolved and treated with triethylamine as well as *para*-nitrophenyl-activated poly(ethylene) glycol (PNP-PEG). It is important to note that a small amount of linear oligomers are formed during the NCA ring opening polymerization. Since they cannot be quantitatively removed from the dendrimer by any practical means, the crude material is taken forward to PEGylation step. Once PEGylated, the linear oligomers become block copolymers ~6 kDa with multiple sites for drug attachment. It is critical to remove these prior to any biological evaluation of a highly branched, high molecular weight drug carrier. If the linear block copolymers are not removed from the reaction mixture, they will become drug loaded and the resulting sample will have two fundamentally different carriers present. Interestingly, conventional aqueous dialysis

could not remove the 6 kDa copolymers as it can for 5 kDa linear PEG. We propose that the amphiphilic copolymers form micelles in water that are two large to pass through the 100 kDa molecular weight cut off dialysis tubing. Fortunately, fractional precipitation from dichloromethane could efficiently remove the lower molecular weight material as shown in the size exclusion chromatograms in Figure 7. After purification and fractionation, the resulting polymer sample had a Mw = 37.5 kDa and a PDI of 1.07

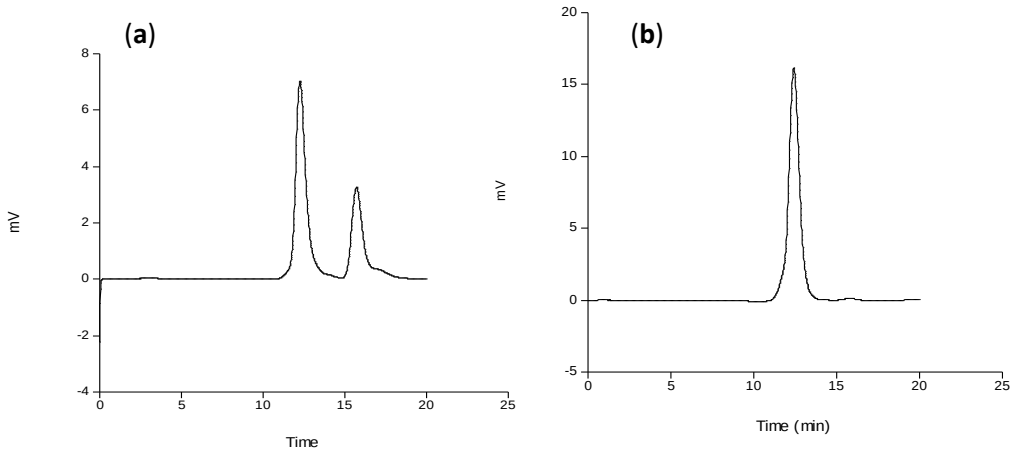

Figure 7. (a) SEC trace of crude PEGylation reaction mixture. (b) SEC trace of PEGylated product after fractional precipitation.

Platinum attachment to the PEGylated dendrimer is shown in Scheme 2. The benzyl ester protected side chains of glutamic acid were deprotected using activated palladium on carbon catalyst and formic acid as a hydrogen source. Quantitative removal of protecting groups was confirmed by ^{1}H NMR and the free acids are subsequently amidated using a di *t*-butyl ester protected aspartatic acid derivative to give **9**. Trifluoroacetic acid was used to furnish a dicarboxylate chelator pendant from the glutamic acid oligomers. Finally, platinum was loaded into the chelators by stirring deprotected **9** in pH 5 water in the presence of a slight excess of the dinitrato salt of diaminocyclohexylplatinum (II) to give the drug loaded polymer, **10**.

In vitro Cytotoxicity and Drug Release

The preliminary biological evaluation for a new polymer drug entity is to assess the cytotoxicity of the conjugate in comparison to the cytotoxicity of the parent drug, which in this case is oxaliplatin. Generally, decreased toxicity on a per drug basis should be observed. This is because small molecule drugs tend to passively diffuse through the cell membrane while the drug conjugate relies on nonspecific endocytosis to enter the cell.[38] Also, the free drug enters a cell in its active form while the polymer bound drug is not active until it has been released. The cytotoxicity of our conjugate was measured alongside oxaliplatin against C26 murine colon carcinoma cells. The IC_{50} observed for oxaliplatin in this experiment was 1.99 ± 0.25 μM and the IC_{50} for our conjugate was 2.52 ± 0.21 μM. This is a very small difference in toxicity which led us to believe that the drug is releasing rapidly and over the course of the three day incubation

period most of the drug is released, either after endocytosis or while the polymer is dissolved in the cell culture media.

The drug release rate was measured using a dialysis technique reported by Kataoka and coworkers.[24] The platinum loaded polymer was dissolved in water and placed inside a dialysis bag. The bag was then placed inside 500 mL of pH 7.4 PBS buffer at 37 ˚C and gently stirred. Aliquots of 5 mL were taken out at each time point and assayed by inductively couple plasma atomic emission spectroscopy. The graph in Figure 8 represents the platinum release versus time.

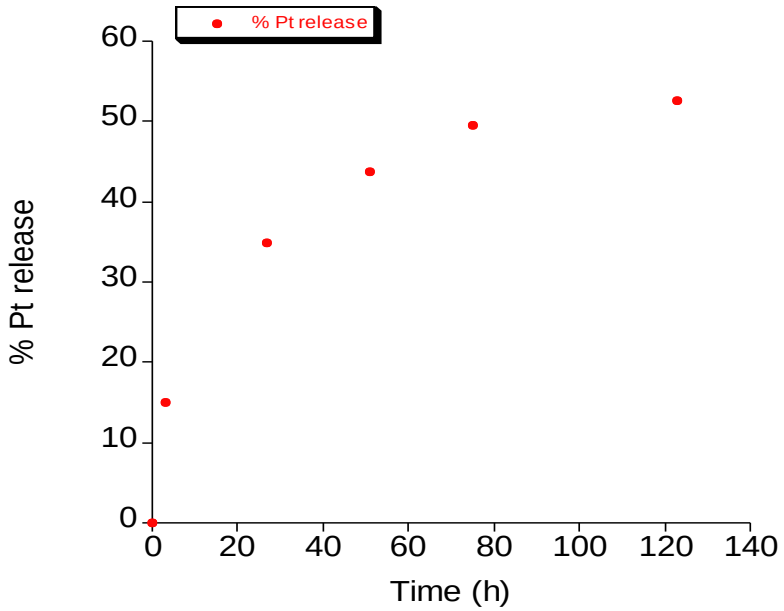

Figure 8. Platinum release versus time at pH 7.4 and 37 ˚C.

***In vivo* toxicity**

The maximum tolerated dose (MTD) of polymer bound platinum was determined by administering the polymer via intra venous (*i.v.*) tail vein injection at a range of platinum equivalents. The level of toxicity was evaluated by the amount of weight lost, level of lethargy and ruffled fur. Mice that exhibit a change in initial body weight greater than 15% are removed from the experiment and euthanized in accordance with the guidelines set forth by the animal protocol at UCSF. Figure 9 shows the percent of initial weight plotted against time for the conjugate as well as oxaliplatin. Both were injected at escalating doses. Interestingly, the MTD for the free drug and the polymer drug was approximately the same. At a dose somewhere between 5-10 mg/kg, the mice exhibit weight loss and toxicity and signs of generally toxicity.

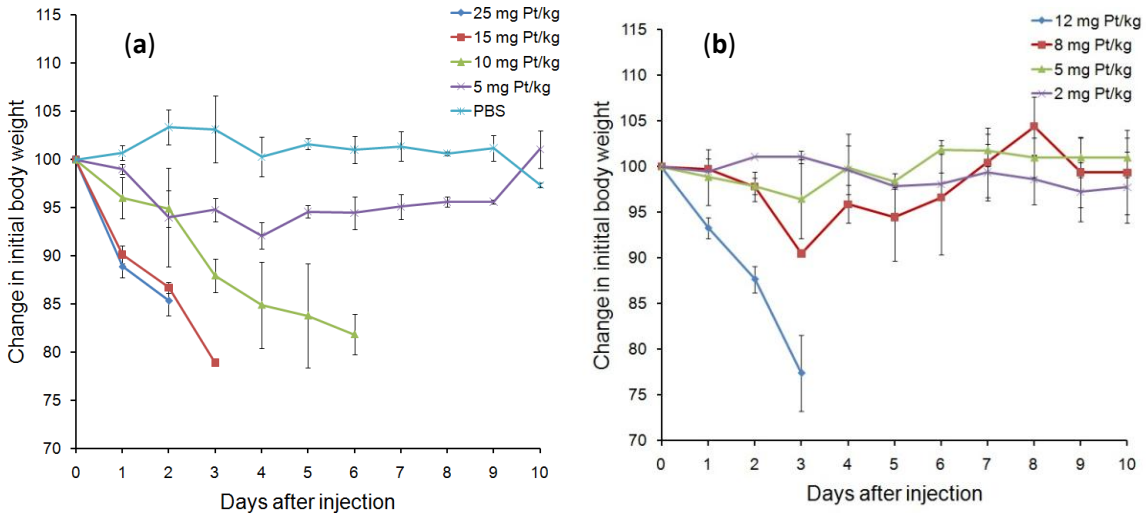

Figure 9. (a) Maximum tolerated dose of **10**. (b) Maximum tolerated dose of oxaliplatin

Conclusion

While the design and synthesis of this polymer represents an interesting approach to Pt (II) delivery, the release, cytotoxity and *in vivo* toxicity indicates that the polymer is not effectively detoxifying the drug payload. For this reason, we believe that too much drug is being released prior to tumor extravasation which will not result in dramatic improvements in efficacy for the polymer drug conjugate. Further *in vivo* evaluation for this polymer was subsequently put on hold while we explored alternative platinum attachment strategies which will be discussed in Chapters 4 and 5.

Materials and Methods

Materials. Materials were used as obtained from commercial sources unless otherwise noted. Dimethylformamide (DMF), pyridine, NEt_3, and CH_2Cl_2 for syntheses were purged 1 h with nitrogen and further dried by passing them through commercially available push stills (Glass Contour). Ethyl acetate used for synthesis was first distilled over calcium hydride. Solvents were removed under reduced pressure using a rotary evaporator or by vacuum pump evacuation. Reactions were performed in dry glassware under an N_2 atmosphere unless otherwise noted.

Characterization. NMR spectra were recorded on Bruker AVB 400, AVQ 400, or DRX 500 MHz instruments. Elemental analyses were performed at the UC Berkeley Mass Spectrometry Facility. Time-of-flight mass spectrometry with electrospray ionization (TOF MS ES+) experiments were performed at the UC Berkeley MS facilities. MALDI-TOF MS was performed on a PerSeptive Biosystems Voyager-DE using the following matrices: *trans*-3-indoleacrylic acid (IAA), 2,5-dihyroxybenzoic acid (DHB), and α-cyanohydroxy cinnamic acid (CHCA). Samples were prepared by diluting dendrimer solutions (~1 M in DMF or CH_2Cl_2) 40-fold in 100 mM matrix solutions in tetrahydrofuran and spotting 0.5 μL on the sample plate. Size exclusion chromatography (SEC) consisted of a Waters 515 pump, a Waters 717 autosampler, a Waters 996 Photodiode Array detector (210-600 nm), and a Waters 2414 differential refractive index (RI) detector. SEC was performed at 1.0 mL/min in a PLgel Mixed B (10 μm) and a PLgel Mixed C (5 μm) column (Polymer Laboratories, both 300 x 7.5 mm), in that order, using DMF

with 0.2% LiBr as the mobile phase and linear PEO (4,200-478,000 MW) as the calibration standards. The columns were kept at 70 °C.

Synthesis of Polylysine Dendrimer. Compounds **3-5** were prepared according to literature procedures.[39]

Synthesis of 3. 1,3-Diaminopropane (720 mg, 9.7 mmol), NEt_3 (3.5 mL, 25.1 mmol), and Boc-Lys(Boc)-ONp (10 g, 21.4 mmol) were added sequentially to 4:1 DMF:Acetonitrile (25 mL). When the reaction was completed as determined by MALDI (40 min, IAA), the heterogeneous mixture was diluted with CH_2Cl_2 (75 mL). *N*,*N*-dimethylethylenediamine (5.5 mL, 50 mmol) was added to quench the remaining active ester. After 10 min, the mixture was washed with 1 M NaOH (3 x 100 mL), 1 M $NaHSO_4$ (3 x 100 mL), and water (100 mL), dried over $MgSO_4$, filtered, and concentrated to yield a white powder (6.14 g, 87%). ^{1}H NMR (500 MHz, $CDCl_3$): δ 1.3-1.55 (br m, 44), 1.6-1.7 (br m, 4), 1.7-1.85 (br m, 2), 3.0-3.3 (br m, 6), 3.4-3.5 (br m, 2), 4.05 (br d, 2, *J* = 6), 4.68 (s, 2), 5.2-5.5 (br m, 2), 6.8-7.2 (br m, 2). ^{13}C NMR ($CDCl_3$, 100 MHz): δ 22.78, 28.32, 28.44, 28.83, 29.63, 32.07, 36.79, 40.01, 54.69, 78.95, 79.75, 156.02, 156.15, 172.96. Calcd: $[M+Na]^+$ ($C_{35}H_{66}N_6O_{10}Na$) *m/z* = 756.4738. Found: TOF MS ES+: $[M+Na]^+$ *m/z* = 753.4727.

Synthesis of 4. Protected dendrimer **3** (3.0 g, 4.1 mmol) was slowly added to 1:1 TFA:CH_2Cl_2 (50 mL) cooled to 0 °C, and then the reaction mixture was allowed to warm to RT. When the reaction was completed (determined by MALDI, DHB), the solvents were removed under reduced pressure. The crude material was dissolved in CH_3OH (6 mL) and added dropwise to rapidly stirred ether (250 mL). A white gummy material stuck to the flask after ~1 h of stirring, so the ether was decanted. The flask was rinsed with ether (25 mL), and residual solvents were removed on a rotary evaporator. This precipitation was repeated twice more, and solvents were thoroughly removed under high vacuum to yield a white foam (3.2 g, 100%). ^{1}H NMR (500 MHz, D_2O): δ 1.45 (m, 4), 1.6-1.8 (m, 6), 1.91 (m, 4), 3.01 (t, 4, *J* = 7.8), 3.29 (m, 4), 3.95 (t, 2, *J* = 6.7).

Synthesis of 4a. Compound 4(3.3 g, 4.2 mmol) and NEt_3 (4.7 mL, 33.7 mmol) were dissolved in CH_2Cl_2 (125 mL), and then Boc-Lys(Boc)-ONp (8.6 g, 18.5 mmol) was added. When the reaction was completed as determined by MALDI (48 h, CHCA), *N*,*N*-dimethylethylenediamine (0.56 mL, 5.1 mmol) was added to quench the remaining active ester. After 10 min, the mixture was washed with 1 M NaOH (3 x 100 mL), 1 M $NaHSO_4$ (3 x 50 mL), water (75 mL), and brine (75 mL), dried over $MgSO_4$, filtered, and concentrated. The crude product was dissolved in minimal $CHCl_3$ until fluid and was then added dropwise to rapidly stirred 9:1 hexanes:ether (1.5 L). The white powder was filtered and rinsed to afford the pure dendrimer (5.5 g, 80%). ^{1}H NMR (400 MHz, $CDCl_3$): δ 1.2-1.9 (m, 110), 3.0-3.5 (m, 16), 4.27 (br s, 6), 4.85 (br s, 2), 5.0-5.5 (br m, 2), 5.6-6.1 (br m, 4), 7.1-7.8 (br m, overlaps solvent, 6). Calcd: $[M+Na]^+$ ($C_{79}H_{146}N_{14}O_{22}Na$) *m/z* = 1666.0634. Found: TOF MS ES+: $[M+Na]^+$ *m/z* = 1666.0570.

Synthesis of 5. Compound **4a** was deprotected using the same method as for **3**. The first precipitation afforded pure product as a white powder that was filtered and rinsed (yield: 88%). ^{1}H NMR (400 MHz, D_2O): δ 1.3-1.6 (m, 16), 1.6-1.8 (m, 14), 1.8-2.0 (m, 8), 3.00 (dd, 8, *J* = 7.1,

7.2), 3.24 (m, 8), 3.92 (t, 2, *J* = 6.7), 4.03 (t, 2, *J* = 6.6), 4.23 (t, 2, *J* = 7.4). ^{13}C NMR (100 MHz, D_2O): δ 21.06, 21.24, 22.43, 26.24, 27.75, 27.88, 30.30, 30.50, 36.73, 38.88, 39.17, 52.62, 53.01, 54.23, 116.22, 162.15, 162.50, 162.86, 163.21, 169.17, 169.42, 173.33. Calcd: $[M+H]^+$ ($C_{39}H_{83}N_{14}O_6$) *m/z* = 843.6620. Found: TOF MS ES+: $[M+H]^+$ *m/z* = 843.6606.

Synthesis of 6. The NCA monomer was preparation was inspired by a procedure reported by Poche et al.[40] Briefly, a 1 L 3-neck flask equipped with a reflux condenser was flame dried and filled with nitrogen. 20 g of H-Glu(OBz)-OH (84.3 mMol) were added. Freshly distilled ethyl acetate was added via a canula transfer and the suspension was heated to reflux. 12.5 g (42.15 mMol) of triphosgene was added to the suspension. The reaction stirred at reflux for 4h. *In some cases, after 4h some of the starting material remained as a solid in the reaction flask. More triphosgene can be added until all the starting material has reacted.* After 4h, the reaction flask was cooled to -10 ^oC and washed with 200 ml of deionized water at 0 ^oC and then with 200 ml of 0 ^oC 0.5% sodium bicarbonate solution. The organic layer was then dried over $NaSO_4$ and concentrated on a rotary evaporator until about 150 ml of solvent remained. Hexane was added to the yellow solution until precipitate began to form. At this point, the flask was capped with a septum and placed in a freezer overnight. The product was recrystallized three times under anhydrous conditions to give 654 mg of crystalline solid in 18% yield. ^{1}H NMR (400 MHz, $CDCl_3$): δ 2.07-2.16 (m, 1H), 2.44-2.33 (m,1H), 2.60 (t, *J* = 6.8 Hz, 2H), 4.38 (t, *J* = 6 Hz, 1H), 5.14 (s, 2H), 6.44 (s, 1H), 7.26-7.40 (m, 5H). m.p. /^oC = 92-93.

Synthesis of 7. Dendrimer **5** (1.189 g, 0.73 mmol) was dissolved in 5 ml of dry, degassed DMF. A 1.5 mL portion of this solution was added of a solution of **6** (6.02 g, 22.87 mmol) dissolved in 35 ml of dry, degassed DMF. The solution stirred for three days at 40 ^oC before being precipitated into diethyl ether. The resulting material was insoluble in most organic solvents and analyzed by MALDI-ToF before being taken on to the next step.

Synthesis of 8. Compound **7** (153 mg, 0.17 mmol of amine) and PNP-PEG (850 mg, 0.18 mmol) were dissolved in 2.5 mL of dry DMF under anhydrous conditions. Triethylamine (120 µL) was added and the reaction stirred at room temperature for 36 h. When the reaction was deemed complete by SEC, 50 µL of piperidine was added to quench and residual PNP-PEG and 2 h later 1 mL acetic anhydride was added to cap any remaining unreacted primary amines. The solution was then precipitated into ether and the recovered 950 mg of white solid were dissolved in 150 mL of DCM. Ether was slowly added in 100 mL to a total volume of 750 mL. The cloudy solution was heated to its boiling point and became clear again. An addition 50 mL portion of ether was added and the solution was allowed to slowly cool to room temperature and sit overnight. The ether was then decanted and the residual solid was redissolved and chloroform and transferred to a new flask. The recovered 600 mg of material had less than 1% low molecular weight product. ^{1}H NMR (400 MHz, $CDCl_3$): δ 1.1-2.6 (br m, ~150H), 3.7 (s, 24H), 3.5-3.8 (br m, ~3700H), 5.1 (br s, ~50H), 7.26 (br m, ~195H). DMF SEC: M_w = 36,000; M_n= 38,700; PDI = 1.07.

Synthesis of 8a. Compound **8** (500 mg) was added to a 100 mL flask and dissolved in 4% formic acid in methanol (10 mL) followed by the addition of Pd/C (50 mg). The solution stirred for 24 hours before being filtered. The solvents were removed under reduced pressure to give a white powder in quantitative yield. ^{1}H NMR (400 MHz, D_2O): δ 1.2-1.4 (br m, 32H), 1.4-1.6 (br m,

16H), 1.6-1.8 (br m, 16H), 1.9-2.2 (br m, 64H), 2.3-2.6 (br m, 64H), 3.2-3.3 (br m 20H), 3.4 (s, 24H), 3.4-3.8 (br m, ~3,600H), 4.1-4.4 (br m, 55H).

Synthesis of 9. Compound **8a** (475 mg), H-Asp(O*t*-Bu)-O*t*-Bu (428 mg, 1.9 mmol), and 4-dimethylaminopyridine (40 mg, 0.3 mmol) were added to a 20 mL reaction vial under nitrogen atmosphere. DMF (8ml) was added followed by triethylamine (400 µL). The solution was cooled to zero degrees and then 1-ethyl-3-(3-dimethylaminopropyl) carbodiimide (290 mg, 1.9 mmol) was added. The reaction stirred for 20 hours as it gradually warmed to room temperature and then it was diluted with methanol and transferred to a dialysis bag (12,000 MWCO). After three solvent changes the contents were transferred to a flask and the solvents were removed by rotary evaporation to give a white solid (395 mg). ^{1}H NMR (400 MHz, $CDCl_3$): δ 1.1-1.2 (br m, 20H), 1.4 (br s, ~430H), 1.8-2.5 (br m, 180H), 2.6-2.9 (br m, 52H), 3.4 (s, 24H), 3.4-3.8 (~3,600H), 4.1-4.4 (br m, 50H), 4.6-4.9 (br m, 25H).

Synthesis of 9a. Compound **9** (375 mg) was added to a 20 mL reaction vial under nitrogen and dissolved 8 mL of 1:1 TFA:DCM. The reaction stirred at room temperature for 6 h and then the solvents were removed under reduced pressure to give 317 mg of white solid. ^{1}H NMR (400 MHz, D_2O): δ 1.1-1.2 (br s, 24H), 1.2-1.6 (br m, 24H), 1.6-1.8 (br m, 12H), 1.9-2.2 (76H), 2.3-2.5 (br m, 50H), 2.7-2.8 (br m, 16H), 2.8-3.0 (br m, 86H), 3.1-3.3 (br m, 40H), 3.4 (s, 24H), 3.5-3.8 (br m, ~3,600H), 4.0-4.5 (br m, 48H).

Synthesis of 10. Platination of **9a** was carried out using a method reported by Sood et al.[18] Briefly, a platinating solution was prepared by dissolving diaminocyclohexyl platinum (II) chloride ($DACHPtCl_2$) (410 mg, 10.8 mmol) and $AgNO_3$ (366 mg, 21.6 mmol) in water (7 mL). The pH is brought to <2 using 5% HNO_3 and the solution was stirred in the dark at 70 ˚C for 15h. The solution was allowed to cool to room temperature and the AgCl salts were filtered off through a 0.2 µm nylon filter. The platinum solution (2.5 mL) was then added to a stirring solution of compound **9a** (380 mg) and the pH is adjusted to 5.4 using 0.5 M NaOH. After 2h of stirring at room temperature, the pH was adjusted to 7.4 and temperature is raised to 38 ˚C for 17h. The solution was purified by dialyzing in 3,500 MWCO dialysis tubing against Millipore water with four water changes over the course of 18h. The material was removed from the dialysis bag and lyophilized to afford a fluffy tan powder. In order to removed and loosely chelated Pt species, the material was redissolved in pH 7.4 buffer at 37 ˚C for four hours. The material is then dialyzed as previously described with only three water changes. The material is lyophilized again to give a final amount of 354 mg of platinum loaded polymer.

Platinum Loading. The Pt content of the resulting polymer is characterized by ICP-AES. To confirm the absence of any small molecule Pt species, 5.34 mg of polymer were dissolved in 550 µl of Millipore water. A 250 µl aliquot was removed and filtered through a 3,000 nominal molecular weight cutoff microcon filter. The filtrate was diluted to a volume of 4.5 ml of 20% HCl matrix. The remaining 300 µl of stock solution was diluted to 10 ml in 20% HCl matrix. A calibration curve was constructed from a Pt standard solution in 20% HCl. Solutions of 500, 100, 50, 10, 5 and 1 µg/ml were prepared from successive dilutions of a 1000 µg/ml standard in 20% HCl. The results of this experiment indicated that no detectible free Pt species are present, and that the final polymer had a Pt loading of 10.5 % (wt/wt).

Platinum Release Measurements. Of the various techniques for platinum release measurements reported, we chose a method inspired by a procedure reported by Cabral et al.[21] A known quantity of polymer bound platinum was dissolved in 1X PBS and placed inside a dialysis bag. The bag was then placed into PBS preheated to 37 ˚C and aliquots are taken out at set time points and measured for platinum content by ICP.

Toxicity of PEG-Pt complexes, Dend-Pt complexes, and oxaliplatin in C26 cells. Cells were seeded onto a 96-well plate at a density of 5.0 x 10^3 cells per well in 100 μl of medium and incubated overnight (37 °C, 5% CO_2, and 80% humidity). An additional 100 μl of new medium (RPMI medium 1640/10% FBS/1% penicillin-streptomycin) containing either **10** or oxaliplatin with concentrations ranging from 4 nM to 5 mM Pt equivalents, was added to the cells. The tests were conducted in replicates of three for each concentration. After incubation for 72 h, 40 μl of media containing thiazolyl blue tetrazolium bromide solution (5 mg/mL) was added. The cells were incubated for 3 h, after which time the medium was carefully removed. To the resulting purple crystals was added 200 μl of DMSO, followed by 25 μl of pH 10.5 glycine buffer (0.1 M glycine/0.1 M NaCl). The optical densities at 570 nm were measured by using a SpectraMAX 190 microplate reader (Molecular Devices, Sunnyvale, CA). Optical densities measured for wells containing cells that received neither polymer nor drug were considered to represent 100% viability. IC_{50} values were obtained from sigmoidal fits of semilogarithmic plots of the percentage of viability versus platinum concentration by using Origin 7 SR4 8.0552 software (OriginLab, Northhampton, MA).

Animal and Tumor Models. All animal experiments were performed in compliance with National Institutes of Health guidelines for animal research under a protocol approved by the Committee on Animal Research at the University of California (San Francisco, CA) (UCSF). C26 colon carcinoma cells obtained from the UCSF cell culture facility were cultured in RPMI medium 1640 containing 10% FBS. Female BALB/c mice were obtained from Simonsen Laboratories, Inc. (Gilroy, CA).

Maximum Tolerated Dose in Healthy Mice. Female Balb/C mice were injected with via tail vein injection with **10** or oxaliplatin. Mice weight and general health was monitored over 9 days. When gross toxicity was observed, loss of greater than 15% of initial body weight, lethargy and ruffled fur, mice were removed from the study.

References

(1) Weiss, R. B.; Christian, M. C. *Drugs* **1993**, *46*, 360-377.
(2) Natile, G.; Coluccia, M. *Coordin Chem Rev* **2001**, *216*, 383-410.
(3) Wang, X. Y.; Guo, Z. J. *Dalton Transactions* **2008**, 1521-1532.
(4) Davies, M. S.; Berners-Price, S. J.; Hambley, T. W. *J Inorg Biochem* **2000**, *79*, 167-172.
(5) Jung, Y. W.; Lippard, S. J. *Chem Rev* **2007**, *107*, 1387-1407.
(6) Kelland, L. *Nat Rev Cancer* **2007**, *7*, 573-584.
(7) Rosenberg, B; Vancamp, L.; Krigas, T. *Nature* **1965**, *205*, 698-&.
(8) Abu-Surrah, A. S.; Kettunen, M. *Curr Med Chem* **2006**, *13*, 1337-1357.
(9) Takahara, P. M.; Rosenzweig, A. C.; Frederick, C. A.; Lippard, S. J. *Nature* **1995**, *377*, 649-652.

(10) Huang, H. F.; Zhu, L. M.; Reid, B. R.; Drobny, G. P.; Hopkins, P. B. *Science* **1995**, *270*, 1842-1845.
(11) Teuben, J. M.; Bauer, C.; Wang, A. H. J.; Reedijk, J. *Biochemistry-Us* **1999**, *38*, 12305-12312.
(12) Fichtingerschepman, A. M. J.; Vanderveer, J. L.; Denhartog, J. H. J.; Lohman, P. H. M.; Reedijk, J. *Biochemistry-Us* **1985**, *24*, 707-713.
(13) Harrap, K. R. *Cancer Treat Rev* **1985**, *12 Suppl A*, 21-33.
(14) Raymond, E.; Faivre, S.; Chaney, S.; Woynarowski, J.; Cvitkovic, E. *Mol Cancer Ther* **2002**, *1*, 227-235.
(15) Gately, D. P.; Howell, S. B. *Brit J Cancer* **1993**, *67*, 1171-1176.
(16) Maeda, H.; Seymour, L. W.; Miyamoto, Y. *Bioconjugate Chem* **1992**, *3*, 351-362.
(17) Haxton, K. J.; Burt, H. M. *Journal of Pharmaceutical Sciences* **2008**, *98,* 2299-2316.
(18) Sood, P.; Thurmond, K. B.; Jacob, J. E.; Waller, L. K.; Silva, G. O.; Stewart, D. R.; Nowotnik, D. P. *Bioconjugate Chem* **2006**, *17*, 1270-1279.
(19) Ye, H. F.; Jin, L.; Hu, R. Z.; Yi, Z. F.; Li, J.; Wu, Y. L.; Xuguang, X. G.; Wu, Z. R. *Biomaterials* **2006**, *27*, 5958-5965.
(20) Song, R.; Jun, Y. J.; Kim, J. I.; Jin, C.; Sohn, Y. S. *J Control Release* **2005**, *105*, 142-150.
(21) Cabral, H.; Nishiyama, N.; Okazaki, S.; Koyama, H.; Kataoka, K. *J Control Release* **2005**, *101*, 223-232.
(22) Mizumura, Y.; Matsumura, Y.; Hamaguchi, T.; Nishiyama, N.; Kataoka, K.; Kawaguchi, T.; Hrushesky, W. J. M.; Moriyasu, F.; Kakizoe, T. *Jpn J Cancer Res* **2001**, *92*, 328-336.
(23) Nishiyama, N.; Kato, Y.; Sugiyama, Y.; Kataoka, K. *Pharmaceut Res* **2001**, *18*, 1035-1041.
(24) Cabral, H.; Nishlyama, N.; Kataoka, K. *J Control Release* **2007**, *121*, 146-155.
(25) Nishiyama, N.; Kataoka, K. *J Control Release* **2001**, *74*, 83-94.
(26) Kaida, S.; Cabral, H.; Kumagai, M.; Kishimura, A.; Terada, Y.; Sekino, M.; Aoki, I.; Nishiyama, N.; Tani, T.; Kataoka, K. *Cancer Res* **2010**, *70*, 7031-7041.
(27) Malik, N.; Evagorou, E. G.; Duncan, R. *Anti-Cancer Drug* **1999**, *10*, 767-776.
(28) Kapp, T.; Dullin, A.; Gust, R. *Bioconjugate Chem* **2010**, *21*, 328-337.
(29) Bellis, E.; Hajba, L.; Kovacs, B.; Sandor, K.; Kollar, L.; Kokotos, G. *J Biochem Bioph Meth* **2006**, *69*, 151-161.
(30) Haxton, K. J.; Burt, H. M. *Dalton Transactions* **2008**, 5872-5875.
(31) Dhar, S.; Gu, F. X.; Langer, R.; Farokhzad, O. C.; Lippard, S. J. *P Natl Acad Sci USA* **2008**, *105*, 17356-17361.
(32) Aryal, S.; Hu, C. M. J.; Zhang, L. F. *Acs Nano* **2010**, *4*, 251-258.
(33) Dhar, S.; Daniel, W. L.; Giljohann, D. A.; Mirkin, C. A.; Lippard, S. J. *J Am Chem Soc* **2009**, *131*, 14652-14653.
(34) Gillies, E. R., Dy, E., Frechet, J. M. J., and Szoka, F. C. *Molecular Pharmaceutics* **2005,** *2*, 129-138.
(35) Dimitrov, I.; Schlaad, H. *Chem Commun* **2003**, 2944-2945.
(36) Kricheldorf, H. R. *Angew Chem Int Edit* **2006**, *45*, 5752-5784.
(37) Deming, T. J. *J Polym Sci Pol Chem* **2000**, *38*, 3011-3018.
(38) Subr, V.; Strohalm, J.; Ulbrich, K.; Duncan, R.; Hume, I. C. *J Control Release* **1992**, *18*, 123-132.

(39) Fox, M. E.; Guillaudeu, S.; Frechet, J. M. J.; Jerger, K.; Macaraeg, N.; Szoka, F. C. *Mol Pharmaceut* **2009**, *6*, 1562-1572.
(40) Poche, D. S.; Moore, M. J.; Bowles, J. L. *Synthetic Commun* **1999**, *29*, 843-854.

Chapter 4 - New Polymeric Chelators for Sustained Release of Platinum (II) Drugs

Abstract

A series of polymer bound platinum (II) chelators were designed to tune platinum release, reduce *in vivo* toxicity, and improve efficacy. Amino acid inspired chelators containing oxygen, nitrogen, and sulfur ligands were loaded with diaminocyclohexane platinate (DACHPt) and then evaluated with respect to drug release rate, cytotoxicity, and *in vivo* antitumor activity. We observed a direct correlation between drug release rate and drug toxicity both *in vitro* and *in vivo*. In the C26 colon carcinoma model, improved survival and reduced tumor growth was achieved with a cysteine chelator over the more traditional dicarboxylate chelator, warranting continued investigation of platinum chelation modes for clinical applications.

Introduction

The anticancer properties of platinum (II) complexes have made them a powerful addition to the current arsenal of chemotherapeutics.[1] These complexes have demonstrated both broad antitumor activity and high efficacy, as well as the potential to be used synergistically in combination with other chemotherapeutic agents.[2] Despite these advantages, clinical use of platinates is often limited by severe side effects. Cisplatin and other Pt(II) analogues are usually administered as inactive prodrugs composed of platinum atoms bearing two amino ligands *cis* to two leaving groups, most commonly dichloride or dicarboxylate.[3] Upon injection and cellular uptake, the leaving groups begin to dissociate from the Pt complex forming the active mono or diaquo species followed by cross-linking of DNA and ultimately apoptosis or necrosis.[4] In practice, this rapid ligand disassociation leads to several challenges for small molecule Pt-drugs. In particular, Pt can interact with sulfur containing molecules and other circulating biomolecules, leading to drug deactivation or unwanted trafficking[5,6] Furthermore, Pt drugs are rapidly excreted from the body due to their low molecular weight[5].

Direct attachment of Pt(II) drugs to a polymeric architecture is most commonly achieved by noncovalent binding of a pendent dicarboxylate[7] or hydroxyl[8,9] containing chelators. While the dicarboxylate leaving group is effective for platinum drugs with a short plasma residence, its rapid release is not optimized, and many of the reported platinum delivery systems do not significantly reduce the systemic toxicity of the platinum compared to small molecule platinum drugs.[7] Access Pharmaceuticals has carried out extensive ^{195}Pt experiments with their AP64595 polymer to investigate the exact Pt binding mode of the aspartic acid moiety. They observed that platinum chelation exists in a pH dependent equilibrium between the (O, O) and (N, O) forms,[10] but the exact nature of this equilibrium *in vivo* is still uncertain.[10-13] It is known that the chelation mode can impact release rates and biological activity of platinum containing polymeric nanoparticles.[14] These studies suggest that the dicarboxylate chelator may not be the most attractive chelator and a more strongly coordinating chelator may improve efficacy. Here we report a new class of Pt(II) drug delivery polymers designed to modulate both *in vivo* toxicity and drug release rates. To the best of our knowledge, this is the first systematic comparison of platinum attached to a single carrier through a variety of coordination modes. A keystone of this work is the development of strong chelators that when paired with a biologically relevant PEGylated dendrimer,[15-17] do not release the active drug until extravasation into tumors has occurred.

Results and Discussion

Synthesis of Platinum-Polymer Library

We initially synthesized the chelators as part of a small library of polyethylene glycol (PEG) conjugated platinum complexes based on FDA approved Oxaliplatin (Scheme 1), and evaluated these molecules with respect to their release rates and *in vitro* toxicity. Differences in ligand strength and ring size were examined in order to correlate toxicity with molecular structure, and ultimately determine the most effective complex for macromolecular delivery. Linear polyethylene glycol (PEG) was chosen as a model polymeric carrier due to ease of fictionalization and characterization allowing for rapid access to a library of PEGylated Pt(II) complexes. Amino acids or amino acid-inspired molecules were chosen as chelating moieties because they provide a variety of chelation modes, are readily available, and are easily

functionalized. Scheme 1 outlines the synthetic approach to a small library of protected chelating derivatives with one free amine available for attachment onto a PEG carrier.

Scheme 8. Synthesis of chelator precursors.

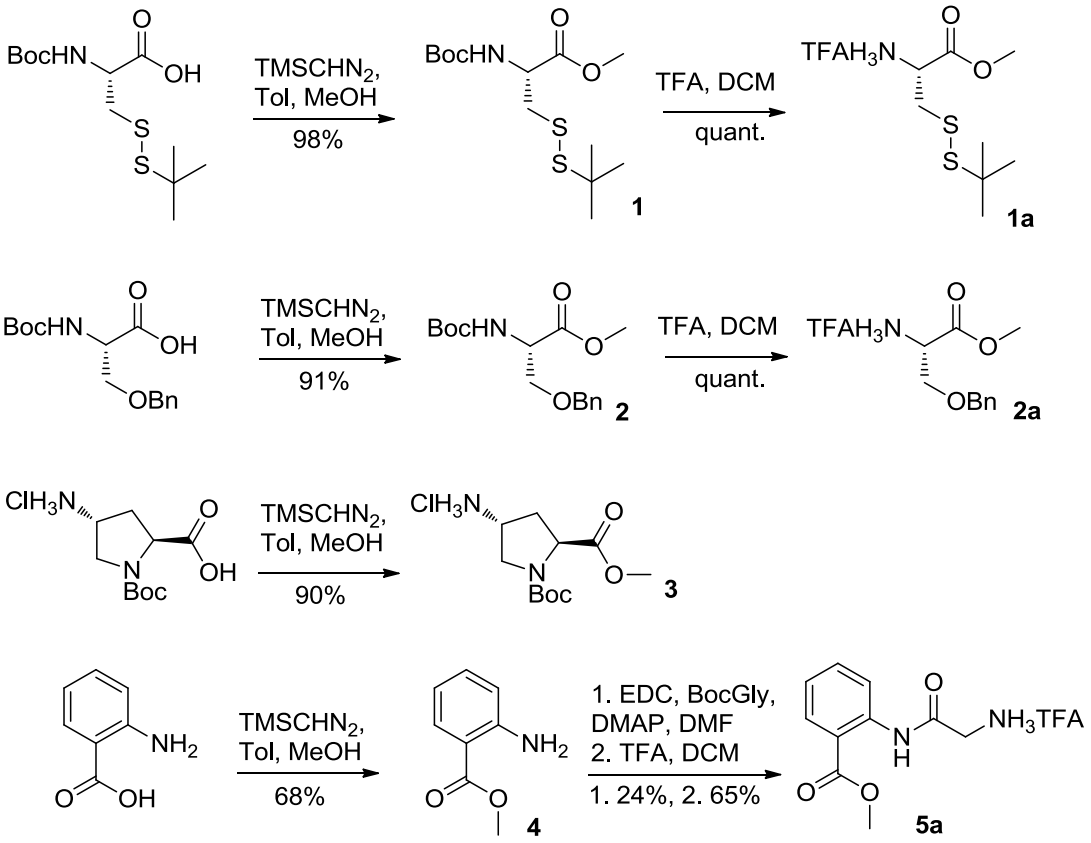

Scheme 2. General synthetic scheme of Pt complexes attached to 5 kDa polyethylene glycol where R represents amino acid inspired chelators with various protecting groups (PG).

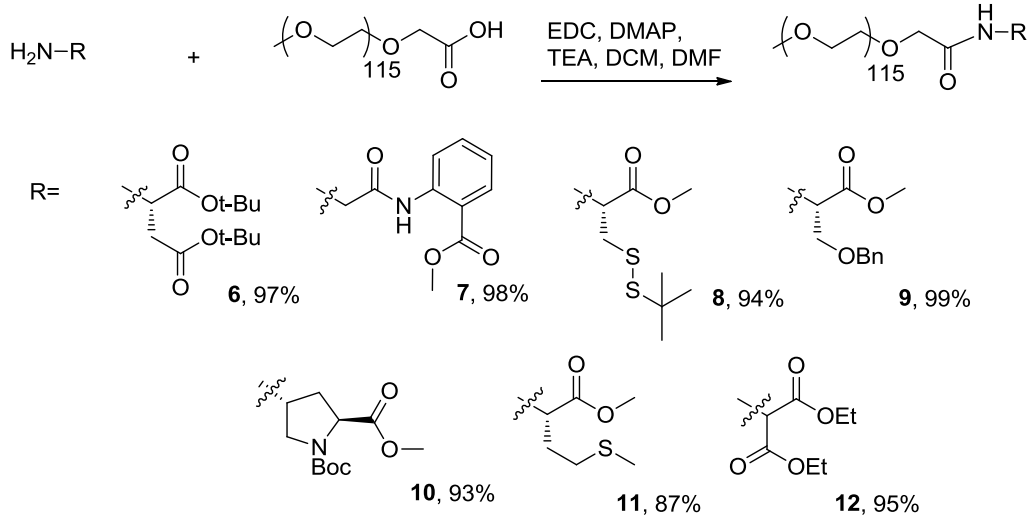

Scheme 3. Chelator deprotection and platinum loading.

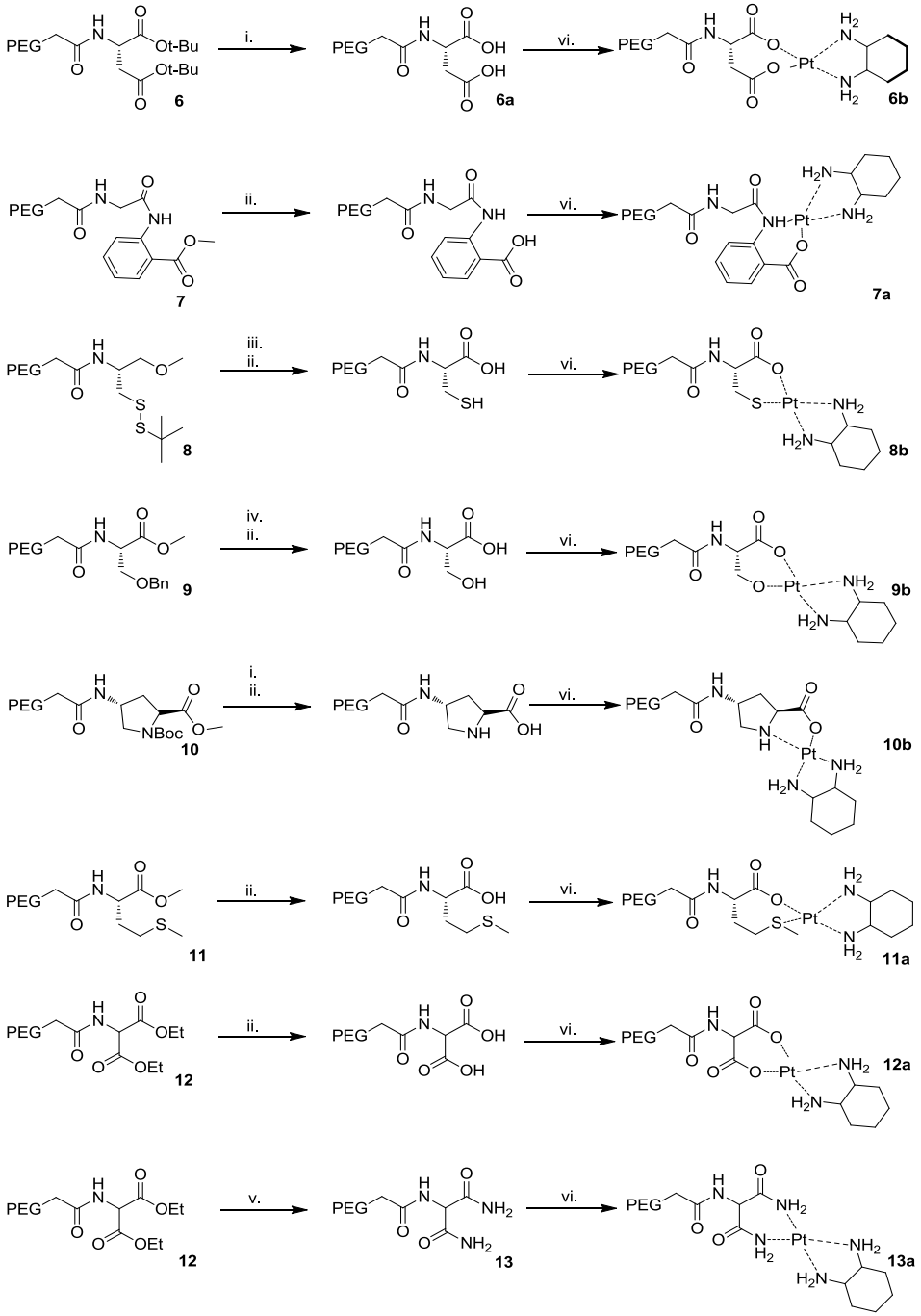

i. TFA, DCM; ii. 2M NaOH; iii. TCEP, H_2O; iv. TFA, Thioanisol, DCM; v. 7N NH_4OH;
vi. DACHPt$(NO_3)_2$, ~pH 5

Using standard carbodiimide-mediated amidation chemistry, the ligand precursors were coupled to PEG (Scheme 2). The chelator molecules were all either commercially available or prepared from commercial materials. In each case, the product was isolated by precipitation into a rapidly stirring 1:1 mixture of diethylether and isopropanol. The PEG-chelator conjugates were

subsequently deprotected and loaded with the dinitrato salt of diaminocyclohexyl palatinate (Scheme 3). The platinum content of each polymer was determined using inductively-coupled plasma atomic emission spectroscopy.

Drug Release Rates and *In vitro* Toxicity of PEG-Pt Conjugates

The cytotoxicity of each PEG-Pt complex was measured against C26 colon carcinoma cells and compared to the cytotoxicity of the parent platinum drug, Oxaliplatin. Table 1 presents IC_{50} and weight percent loading for each derivative. The library was designed to span a range of toxicities as a direct consequence of variation in both ligand strength and ring size, such that soft ligands such as sulfur and nitrogen should bind more tightly to the Pt(II) center than harder oxygen ligands. As expected carboxylate and hydroxyl chelators showed the highest toxicity in our library and the ligands bearing sulfur atoms showed the greatest decrease in toxicity. It has been shown that Pt-S interactions can lead to drug deactivation or unwanted trafficking to healthy tissue;[6] however, even with the high concentration of sulfur ligands present in circulation and inside the cell, platinum drugs are still effective chemotherapy agents. We believe that a sulfur bearing chelator for platinum delivery could improve the state of the art in platinum delivery systems by preventing premature release and ultimately leading to much greater platinum accumulation in tumor tissue and lowering systemic toxicity. Despite concerns of sulfur deactivation, each derivative maintained activity, with the IC_{50} values spanning two orders of magnitude in platinum concentration.

Table 1. Loading and toxicity data for the evaluated polymers

Compound	Pt Loading	IC_{50} (μM)
Oxaliplatin	-	0.6 ± 0.1
PEG-Aspartate (**6b**)	3.6%	6.7 ± 1.4
PEG-Anthranilate (**7a**)	0.7%	7.4 ± 6.1
PEG-Serine (**9b**)	0.9%	8.4 ± 0.1
PEG-Malonate (**12a**)	2.8%	11.2 ± 0.9
PEG-Malonamide (**13a**)	1.3%	26.5 ± 1.4
PEG-Proline (**10b**)	0.9%	29.3 ± 5.0
PEG-Methionine (**11a**)	3.6%	33.3 ± 2.6
PEG-Cysteine (**8b**)	4.8%	126.4 ± 2.4

The rate of platinum release from the polymer is an important parameter in predicting its *in vivo* performance. We expected the cellular toxicity to be directly related to the rate of platinum release because the drug cannot bind to DNA until it has come off the polymer and exposed two open coordination sites. The design criteria for the chelators in our library include, not only the tunability of release rate, but also that the chemistry used to synthesize the molecules be amenable to a variety of more sophisticated and biodegradable delivery systems.

For example, the deprotection conditions should be mild and the platinum loading efficiency should be high. For further study we chose to determine the release profiles of the aspartate, malonate, methionine and cysteine conjugates, as they span a range of toxicities and meet these design requirements. We measured the platinum release using a dialysis procedure that is similar to techniques previously reported.[14,18-22] Release of platinum from the polymer was monitored over a 72 hour period by incubating polymer samples in pH 7.4 buffer at 37 °C in 1000 MWCO tubing and analyzing the platinum content in the solution outside of the dialysis bag. Figure 1 shows the release rates for polymers containing each type of linkage. In all cases, the amount of released platinum began to level off after nine hours which is most likely the result of reaching equilibrium conditions between the high local concentration of bidentate ligand inside the dialysis bag and the released small molecule platinum. The rate and extent of platinum release when measured by this technique is directly related to the chloride concentration of the buffer.[22] Half lives for the release were calculated by fitting the linear portion of a log plot of Pt released as a function of time for early time points ($t \leq 9$ h). As expected, the rate of release was directly related to *in vitro* cytotoxicity. Furthermore, our library shows tunable hydrolysis rates over an order of magnitude, with hydrolysis half-lives from 37 hours to 360 hours. In agreement with previous reports on HPMA carriers, we have found that the aspartate chelator releases small molecule Pt species considerably faster than the malonate chelator due to the decreased chelate stability from the 7-membered ring formed by the aspartate dicarboxylate compared to the 6-membered ring formed by the malonate.[23] The methionine and cysteine linkers both show decreased release rates because of the more favorable Pt-S interactions. It is important to note that the PEGylated complexes in Scheme 1 may exist in additional binding modes in which the proximal amide group acts as a ligand. We were not able to unambiguously establish the presence or absence of multiple binding modes by ^{195}Pt or ^{1}H NMR. However, we feel that the release data and cytotoxicity indicate that the alternative binding modes do not represent a significant portion of the bound platinum.

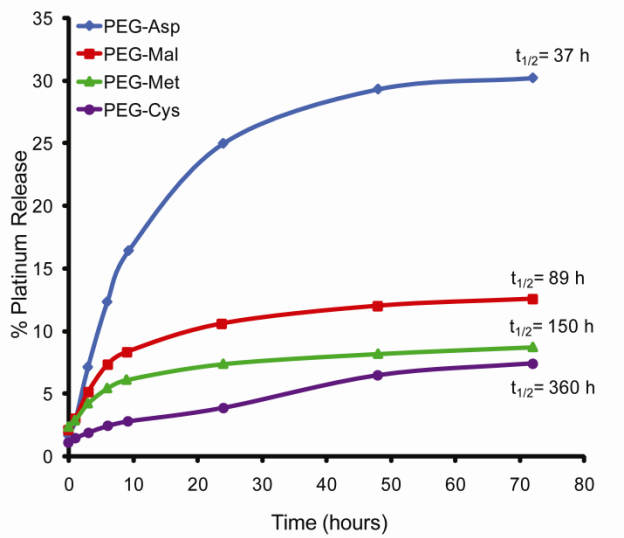

Figure 1. Hydrolysis of platinum from selected polymers at 37°C in 1X PBS. Platinum content analyzed by ICP-AES.

Attachment of Platinum Chelators to PEGylated Dendrimer

After characterizing the platinum chelators with respect to toxicity, rates of hydrolysis, and chemistry, a polymer more suited for *in vivo* applications was selected to replace linear PEG. The PEGylated dendrimer (**14)** chosen is not only biodegradable and nontoxic, but also easily functionalized with drug payloads at its core. A series of the platinum drugs were attached to the dendrimer and their *in vivo* activity evaluated as a function of the drug release rate and *in vitro* toxicity. Specifically, the aspartate, methionine, and cysteine chelators were attached to the dendrimer and loaded with the Pt(II) drug as shown in Scheme 2. The aspartate and methionine precursors were commercially available, while the cysteine derivative **16** was prepared by forming the *t*-butyl ester of BocCys(Trityl)-OH. Selective deprotection of the Boc group was achieved by treating **15** with anhydrous hydrochloric acid in dioxane. The 8 dendrimer carboxylic acids were functionalized with the aspartic acid, methionine and cysteine chelator precursor molecules via amidation reactions. In the case of the cysteine functionlized dendrimer, the more reactive HBTU coupling reagent was used instead of EDC because it provided higher loadings of the bulky, trityl protected ligand onto the dendrimer scaffold. Global cleavage of the protecting groups with trifluoroacetic acid followed by platination gave Dend-Asp (**17**), Dend-Met (**18**), and Dend-Cys (**19**). The excess platinum was removed by aqueous dialysis and platinum loading (wt/wt %) for **17, 18**, and **19** was determined to be 4.0%, 3.4% and 4.4% respectively as determined by ICP. The cytotoxicity of the three dendrimers was measured against C26 cells, giving IC_{50} values of 3.7 $\pm$ 7 µM (**17**), 42.1 $\pm$ 14 µM (**18**), and 62.0 $\pm$ 11 µM (**19**).

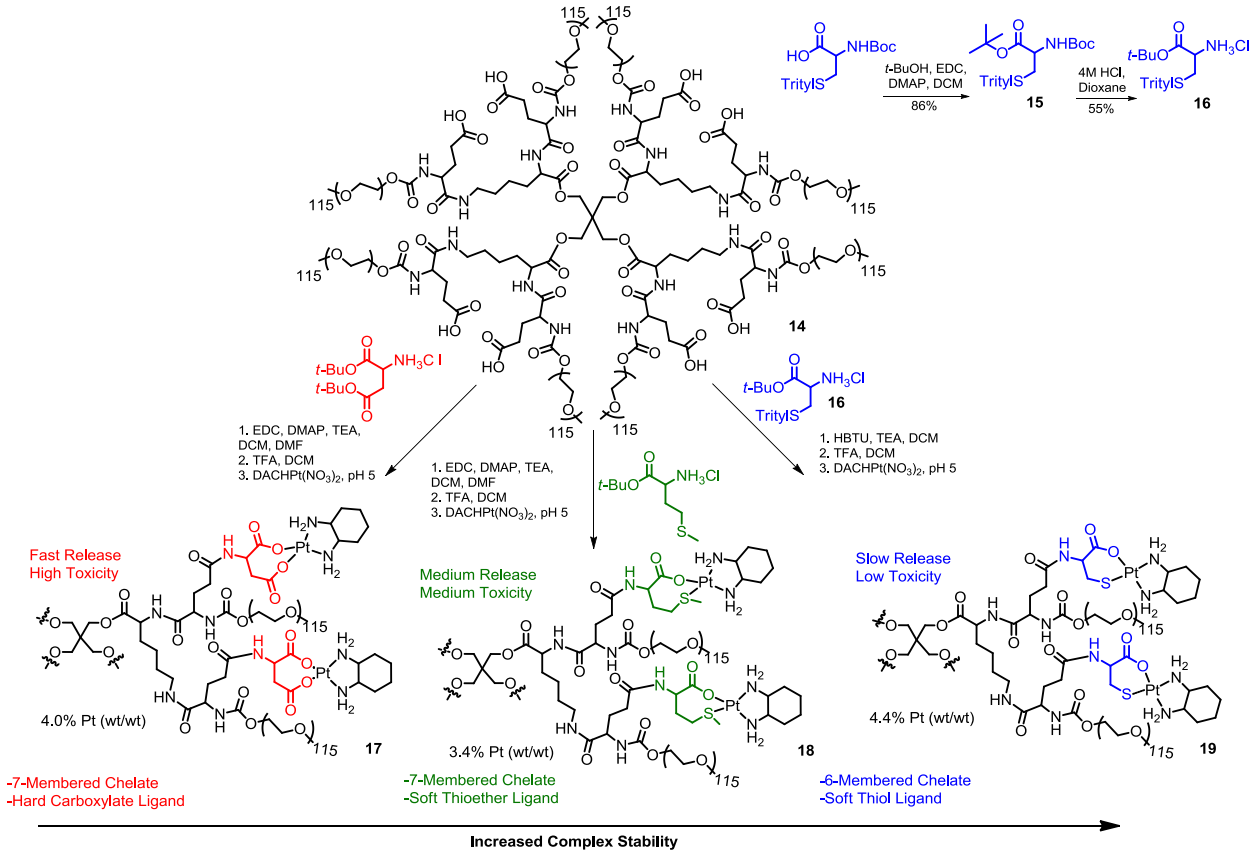

Scheme 4. Conjugation and platination of aspartate, methionine, and cysteine chelators to PEGylated dendrimer.

Maximum Tolerated Dose Experiments

The *in vivo* toxicity of **17**, **18**, and **19** was evaluated in female Balb/C mice. The maximum tolerated dose (MTD) was determined by administering the drug conjugate via tail vein injection at increasing doses, until mice lost >15% of their initial body mass. The *in vivo* toxicity trend followed the *in vitro* toxicity trend (Figure 2). Dend-Asp had the highest toxicity with a MTD somewhere between 5-10 mg/kg. Dend-Met had a maximum tolerated dose of approximately 90 mg/kg and Dend-Cys did not cause a 15% body weight loss even at the highest dose tested, 135 mg/kg.

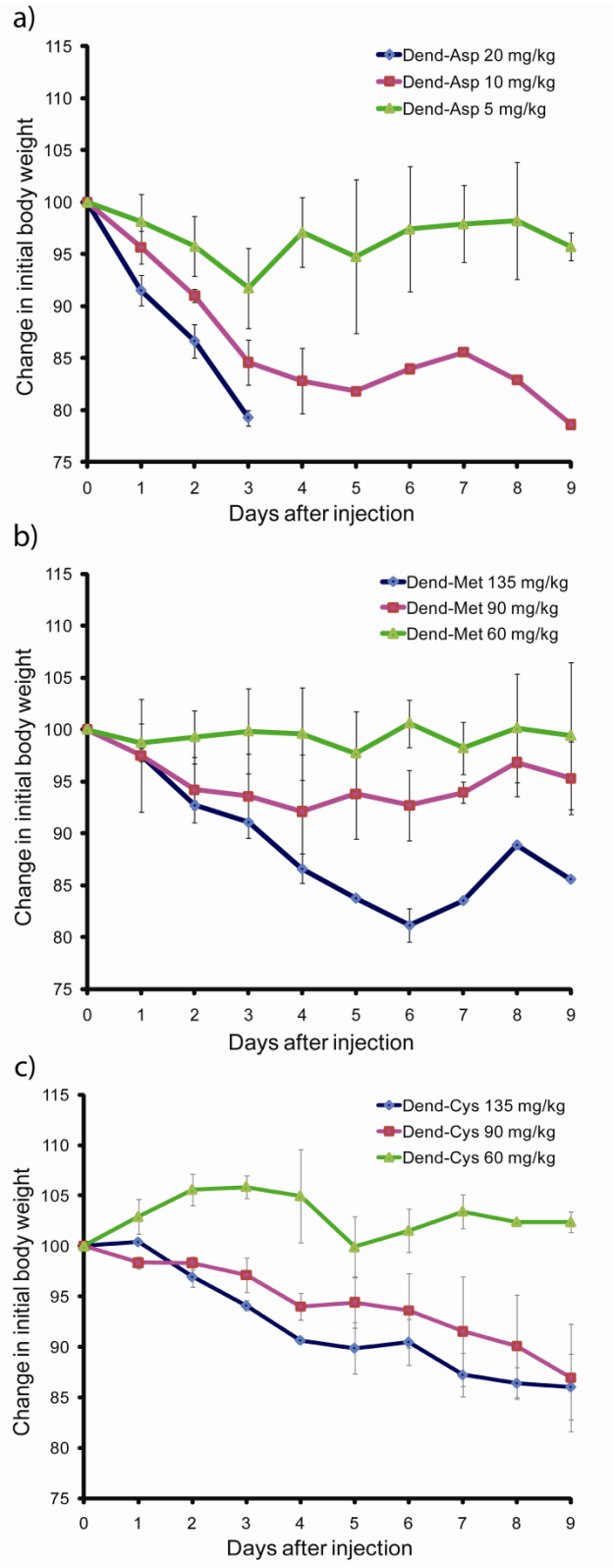

Figure 2. Weight loss observed in healthy Balb/C mice injected with (a) Dend-Asp **17**, (b) Dend-Met **18**, (c) Dend-Cys **19**.

Chemotherapy Study in Tumored Mice

The antitumor efficacy of the three dendrimers was also evaluated in female Balb/C mice bearing C26 murine colon carcinoma. Mice were treated with Cisplatin (6 mg/kg, once a week for 3 weeks), Dend-Asp **17** (6 mg/kg, once a week for 3 weeks), Dend-Met **18** (90 mg/kg), and Dend-Cys **19** (135 mg/kg). As expected due to the fairly rapid release of Pt within the blood by Dend-Asp, and equivalent MTD to Cisplatin, the two treatments exhibited comparable survival efficacy (Figure 3 and Table 2). Each group had one tumor free survivor at the end of the study, however the improved delay in tumor growth and longer average survival time of Dend-Asp, we believe can be attributed to the uptake of dendrimer with bound drug and subsequent release within tumor tissue. Dend-Cys, despite the very slow release of Pt, had the best efficacy of all the treatments. No treatment toxicity was observed, and long term survival and tumor growth was improved over all treatments. Gratifyingly, activity was maintained and similar treatment efficacy observed even with a ten fold range in Pt release rates between Dend-Asp and Dend-Cys.

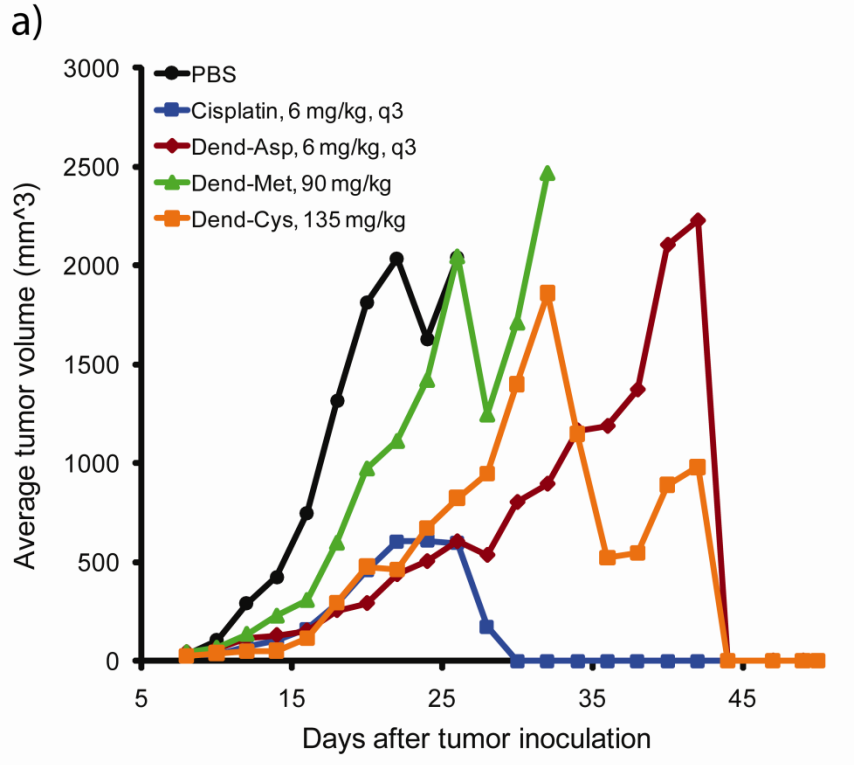

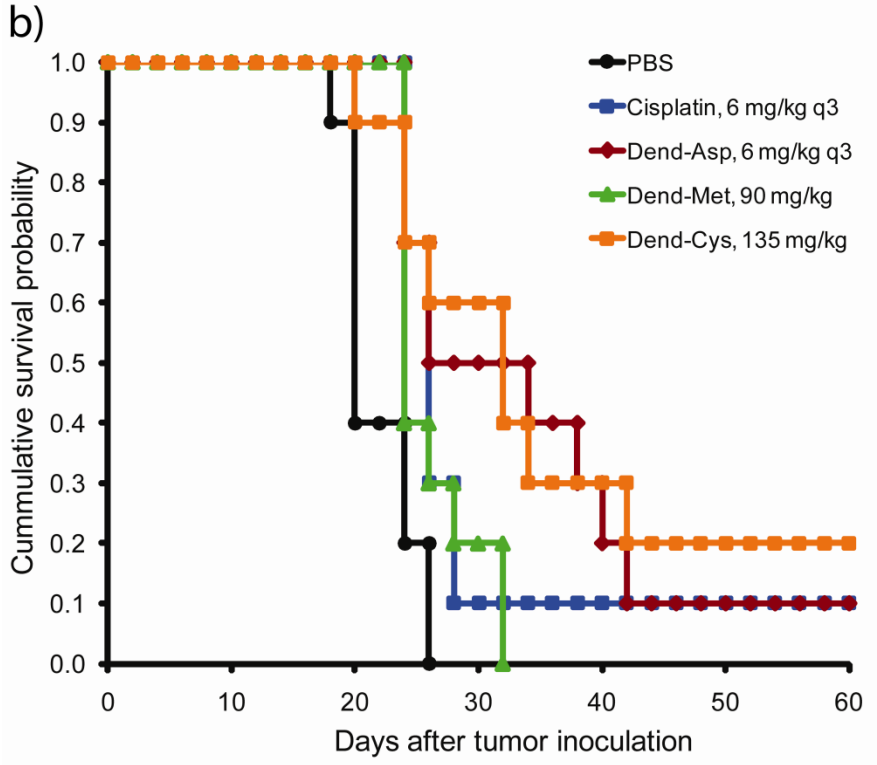

Figure 3. Balb/C mice bearing s.c. C26 colon carcinoma treated on day 8 with Dend-Met **18**, Dend-Cys **19**, and PBS or day 8, 15, 22 with Cisplatin and Dend-Asp **16**. (a) Growth inhibition, (b) Kaplan Meier survival data.

Table 2. In vivo efficacy of dendrimer-Pt and controls against Balb/C mice with C26 colon carcinoma.

Treatment Group	No. mice	Dose (mg/kg)	No. of injections	Treatment days	Mean TGD (%)	Median survival time (days)	LTS
PBS	10		1	8		20	0
Cisplatin	10	6	3	8,15,22	59[c]	26[b]	1
Dend-Asp (**17**)	10	6	3	8,15,22	88[c]	30[b]	1
Dend-Met (**18**)	10	90	1	8	24[a]	24[c]	0
Dend-Cys (**19**)	10	135	1	8	97[c]	32[b]	2

TGD, tumor growth delay, calculate from time of growth to 400 mm^3; LTS, long term survivors; [a] Compared to PBS, $P \leq 0.0001$. [b] Compared to PBS, $P < 0.005$. [c] Compared to PBS, $P < 0.05$.

Conclusion

In conclusion, a family of Pt(II) chelators have been explored for their potential as polymeric platinum delivery agents. A range of *in vitro* toxicities as well as drug release rates was observed. We believe that the prolonged stability of sulfur containing chelator complexes, evidenced by lower toxicity and slower Pt release in the methionine and cysteine chelators, may prevent premature Pt release and reduce uptake by competing endogenous ligands and offers new directions for protecting groups of platinum containing drugs. This study is the first extensive examination of how various attachment modes of a known drug will alter the drug conjugate toxicity, drug release rates and *in vivo* activity. Given the activity observed with these polymer platinum compounds it is also of interest to learn if attachment strategies that provide a burst release of the platinum drug will improve the activity of new platinum drugs.

Materials and Methods

Materials. Materials were used as obtained from commercial sources unless otherwise noted. The platinum ICP standard was purchased from VHG Labs, Manchester, NH. Dimethylformamide (DMF) and CH_2Cl_2 (DCM) for syntheses were purged 1 h with nitrogen and further dried by passing them through commercially available push stills (Glass Contour). Monomethoxypolyethyleneglycol carboxymethyl (mPEG-CM) was purchased from Laysan Bio, Inc. Solvents were removed under reduced pressure using a rotary evaporator or by vacuum pump evacuation.

Characterization. NMR spectra were recorded on Bruker AV 300, AVB 400, AVQ 400, or DRX 500 MHz instruments. Elemental analyses were performed at the UC Berkeley Mass Spectrometry Facility. Size exclusion chromatography (SEC) system A consisted of a Waters 515 pump, a Waters 717 autosampler, a Waters 996 Photodiode Array detector (210-600 nm), and a Waters 2414 differential refractive index (RI) detector. SEC was performed at 1.0 mL/min in a PLgel Mixed B (10 μm) and a PLgel Mixed C (5 μm) column (Polymer Laboratories, both 300 x 7.5 mm), in that order, using DMF with 0.2% LiBr as the mobile phase and linear PEO (4,200-478,000 MW) as the calibration standards. The columns were kept at 70 °C. SEC system C consisted of a B Waters Alliance separation module 2695 and a Waters 410 differential RI detector. SEC was performed in a Shodex SB-804 HQ column at ambient temperature using phosphate buffered saline (pH 7.4) as the mobile phase. Inductively coupled plasma-atomic emission spectroscopy (ICP-AES) was carried out on a Perkin Elmer Optima 7000 DV Optical Emission Spectrometer.

General procedure for esterification of chelator precursors.

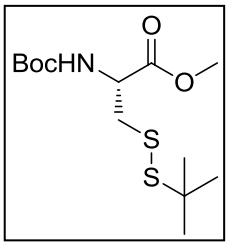

BocCys(S*t*-Bu)OMe (1). BocCys(S*t*-Bu)OH (210 mg, 0.68 mmol) was dissolved in 4 mL of a 3:2 toluene methanol mixture. Trimethylsilyldiazomethane ($TMSCHN_2$) as a 2M solution in diethyl ether was added dropwise (~850 μl) until a faint yellow color persisted and no gas evolution was observed. After 30 min of stirring at room temperature the solvents were removed to give 213 mg of pure product in 97% yield. ^{1}H NMR (400 MHz, $CDCl_3$): δ 1.31 (s, 9H), 1.44 (s, 9H), 3.14 (d, *J*=4.4 Hz, 2H), 4.58 (d, *J*=7.6 Hz, 1H), 5.38 (d, *J* =7.6, 1H). ^{13}C NMR (100 MHz, $CDCl_3$): δ 28.3, 29.7, 42.6, 48.1,

52.5, 53.1, 80.1, 155.0, 171.2. Calcd $[M]^+$ ($C_{13}H_{25}NO_4S_2$) *m/z*= 323.12. Found FAB $[M+Na]^+$ *m/z*= 346.1109.

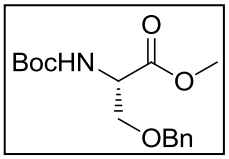

BocSer(OBz)OMe (2). BocSer(OBz)OH (305 mg, 1.03 mmol) was treated as described in the general procedure. 91% yield. ^{1}H NMR (400 MHz, $CDCl_3$) δ 1.45 (s, 9H), 3.73 (s, 3H), 3.76 (dm, *J*=2.8, 2H), 4.43-4.55 (m, 3H), 5.44 (d, *J*=8.4, 1H), 7.25-7.35 (m, 5H). ^{13}C NMR (100 MHz, $CDCl_3$): δ 28.3, 52.4, 53.9, 69.9, 71.8, 73.2, 79.9, 127.6, 127.8, 128.4, 137.5, 155.5, 171.1. Calcd $[M]^+$ ($C_{16}H_{23}NO_5$) *m/z*= 309.16. Found FAB $[M+H]^+$ *m/z*= 332.1468.

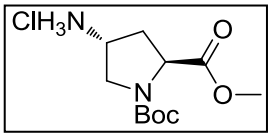

2-Amino proline methylester (3). (2S, 4R)-1-Boc-4-Amino-pyrrolidine-2-carboxylic acid•HCl (300 mg, 1.12 mmol) was dissolved in a 3:2 toluene/methanol mixture (2 mL). $TMSCHN_2$ (2M) (450 µl, 0.89 mmol) was added dropwise to the solution. After 45 min, the solvent was evaporated. The residual oil was then flashed through a silica plug using 10% methanol in DCM (90% yield). Note: If an excess of $TMSCHN_2$ is used under extended reaction times, a small amount (< 3%) of N-methylation is observed. ^{1}H NMR (400 MHz, D_2O rotamers present): δ 1.39, 1.45 (2s, 9H), 2.17-2.20 (m, 2H), 3.23-3.30 (m, 1H), 3.60-3.67 (m, 2H), 3.79 (s, 3H), 4.41-4.5 (m, 1H). ^{13}C NMR (100 MHz, $CDCl_3$ rotamers present): δ 28.3, 28.4, 39.0, 39.6, 49.6, 50.4, 52.0, 52.2, 54.5, 54.8, 57.9, 58.2, 80.1, 153.8, 154.4, 173.3, 173.6. Calcd $[M]^+$ ($C_{11}H_{20}N_2O_4$) *m/z*= 244.14. Found FAB $[M+H]^+$ *m/z*= 245.1497.

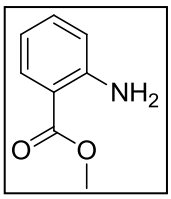

Synthesis of Methyl Anthranoate (4). Anthranilic acid (1 g, 7.3 mmol) was dissolved in a 3:2 toluene/methanol mixture (80 mL). Trimethylsilyldiazomethane (2M) (4 mL, 8 mmol) was added dropwise to the solution until the yellow color in the solution persisted. After 2 h, the solvent was evaporated. A silica gel column was run in 5% ethyl acetate and 95% hexanes to give 754 mg of a yellow oil in 68% yield. ^{1}H NMR (400 MHz, $CDCl_3$): δ 3.85 (s, 3H), 5.66 (bs, 2H), 6.63 (t, *J*=7.6 Hz, 2H), 7.25 (t, *J*=7.2 Hz, 1H), 7.85 (d, *J*=7.2 Hz, 1H). ^{13}C NMR (100 MHz, $CDCl_3$): δ 49.5, 108.7, 114.3, 114.7, 129.2, 132.1, 148.5, 166.6. Calcd $[M]^+$ ($C_8H_9NO_2$) *m/z*= 151.06. Found EI $[M+H]^+$ *m/z*= 152.0712.

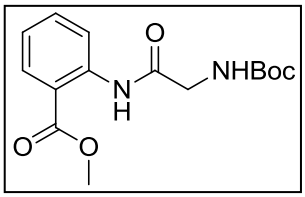

Synthesis of Glycine Boc protected methyl anthranoate (5). Methyl anthranoate (**4**) (356 mg, 2.355 mmol), BocGlyOH (2.475 g, 14.131 mmol), and 4-dimethylaminopyridine (DMAP) (14.4 mg, 0.118 mmol) were dissolved in dry DMF (2 mL). 1-ethyl-3-[3-dimethylaminopropyl]carbodiimide hydrochloride (EDC) (2.708 g, 14.131 mmol) was added. After 16 h, the solution was diluted with ethyl acetate (100 mL) and washed with 1 M $NaHSO_4$ (3 x 100 mL), 1 M NaOH (3 x 100 mL), and water (2 x 100 mL). The organic layer was dried with Na_2SO_4, filtered, and the solvent was evaporated to yield a yellow oil which was recrystallized with ether/hexanes to give 172 mg of a white crystalline solid in 24% yield. ^{1}H NMR (400 MHz, $CDCl_3$) δ 1.50 (s, 9H), 3.91 (s, 3H), 4.01 (d, *J*=5.6 Hz, 2H), 5.27 (bs, 1H), 7.10 (t, *J*=7.6 Hz, 1H), 7.54 (t, *J*=8 Hz, 1H), 7.85 (d, *J*=8 Hz, 1H), 8.71 (d, *J*=8.8 Hz, 1H), 11.55 (bs, 1H). ^{13}C NMR (100 MHz, $CDCl_3$): δ 28.4, 45.4,

52.3, 80.3, 115.3, 120.4, 122.9, 130.8, 134.7, 140.9, 155.9, 168.5, 168.6. Calcd $[M]^+$ ($C_{15}H_{20}N_2O_5$) *m/z*= 308.14. Found EI $[M]^+$ *m/z*= 308.1377.

General procedure for Boc deprotections.

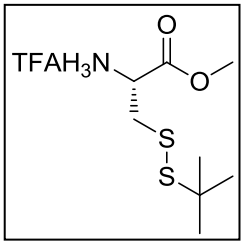

TFA•NH_3Cys(S*t*-Bu)OMe (1a). BocCys(S*t*-Bu)OMe (**1**) (105 mg, 0.32 mmol) was placed in a reaction vial equipped with a Teflon septum. The vial was evacuated and backfilled with nitrogen gas. A solution of 1:1 TFA:DCM (3 mL) was added and the reaction was allowed to stir at room temperature for 1 h. The solvents were removed under reduced pressure to give 104 mg of product as a viscous oil in quantitative yield. ^{1}H NMR (400 MHz, MeOD) δ 1.33 (s, 9H), 3.18-3.31 (m, 2H), 3.85 (s, 3H), 4.38 (t, *J*=4.8 Hz, 1H). ^{13}C NMR (100 MHz, MeOD): δ 28.7, 39.0, 51.6, 52.5, 114.5, 117.4, 159.9, 168.2. Calcd $[M]^+$ ($C_8H_{17}NO_2S_2$) *m/z*= 223.08. Found FAB $[M+H]^+$ *m/z*= 224.0774.

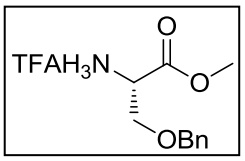

TFA•NH_3BocSer(OBz)OMe (2a). Treated as described in the general procedure. ^{1}H NMR (400 MHz, MeOD) δ 3.80-3.98 (m, 2H), 3.70 (s, 3H), 4.19 (t, *J*=2.4 Hz, 1H), 4.63 (q, *J*=9.6 Hz, 2H), 7.3-7.36 (m, 5H). ^{13}C NMR (100 MHz, MeOD): δ 52.3, 53.0, 66.4, 73.0, 114.4, 117.2, 127.7, 128.1, 136.9, 159.7, 160.1, 167.6. Calcd $[M]^+$ ($C_{11}H_{16}NO_3S$) *m/z*= 209.11. Found FAB $[M+H]^+$ *m/z*= 210.1125.

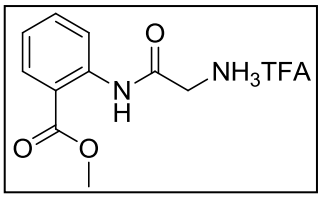

Glycine methyl anthranoate TFA salt (5a). The Boc-protected glycine methyl anthranoate (**5**) (150 mg, 0.487 mmol) was dissolved in a solution of 1:1 TFA:DCM. After 30 min, the solvent was evaporated. The product was recrystallized in methanol/ether to yield a white solid (102 mg, quant). ^{1}H NMR (400 MHz, $CDCl_3$): δ 3.83 (s, 3H), 3.89 (s, 2H), 7.10 (t, *J*=7.6 Hz, 1H), 7.49 (t, *J*=8.4 Hz, 1H), 7.93 (d, *J*=8 Hz, 1H), 8.31 (d, *J*=8.4 Hz, 1H). ^{13}C NMR (100 MHz, $CDCl_3$): δ 43.8, 54.1, 80.3, 119.6, 123.6, 126.2, 133.1, 136.4, 141.6, 166.9, 170.6. Calcd $[M]^+$ ($C_{10}H_{12}N_2O_3$) *m/z*= 208.08. Found EI $[M+H]^+$ *m/z*= 209.0931.

General procedure for coupling chelators to mPEG-COOH. The general procedure for coupling protected chelators onto linear PEG chains was inspired by a procedure reported by Zhao et al.[24]

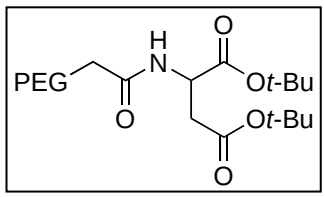

Synthesis of PEG-Asp(Ot-Bu)-OtBu (6). mPEG-CM (300 mg, 0.06 mmol), H-Asp(OtBu)-OtBu•HCl (84 mg, 2.99 mmol) and DMAP (5 mg, 0.04 mmol) were added to a reaction vial equipped with a septum. The vial was evacuated and backfilled with N_2 three times. Via syringes, 100 µl of triethyl amine, 200 µl of DMF, and 1.5 mL of DCM were added. The solution was cooled to 0ºC and EDC (92 mg, 0.48 mmol) was added. The reaction was allowed to warm to room temperature and stirred overnight before being precipitated into 300 mL of 1:1 isopropanol:ether mixture. The product was isolated (290 mg) as a fluffy solid in 97% yield. ^{1}H NMR (500 MHz, $CDCl_3$): δ 1.37-1.39

(2s, 14H), 2.66-2.79 (dd, 1.5 H) 3.31 (s, 3H), 3.42-3.72 (br m, ~500H), 3.97 (d, *J*=8 Hz, 1.65 H), 4.66 (m, 0.75H).

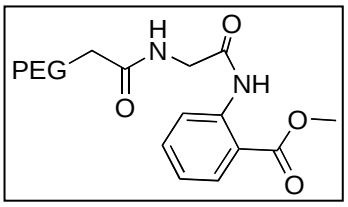

Synthesis of PEG-Glycine methyl anthranoate (7). Compound **5a** (82 mg, 0.255 mmol), 5 kDa PEG (254.5 mg, 0.051 mmol), and DMAP (6.2 mg, 0.051 mmol) were added to a 20 mL reaction vial equipped with a septum. The vial was evacuated under vacuum and backfilled with N_2 three times. Via a syringe, diisopropylethylamine (DIPEA) (0.044 mL, 0.253 mmol), DMF (0.4 mL) and DCM (3 mL) were added. The solution was then cooled to 0ºC and EDC (78.1 mg, 0.407 mmol) was added. After 16 h, the solution was precipitated into a 1:1 ether/isopropyl alcohol mixture and filtered to yield 248 mg of fluffy white solid in 98% yield. ^{1}H NMR (500 MHz, $CDCl_3$): δ 3.30 (s, 3H), 3.42-3.83 (br m, ~500H), 4.09-4.12 (m, 4H), 7.02 (t, *J*=7.5 Hz, 0.6), 7.46 (t, *J*=7.5 Hz, 0.65), 7.88 (s, 0.86H), 7.94 (d, *J*= 8 Hz, 1H), 8.65 (d, *J*=8 Hz, 1H).

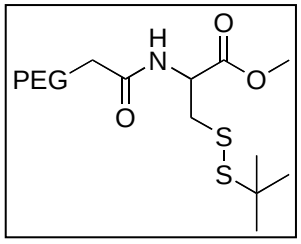

Synthesis of PEG-Cys(St-Bu)-OMe (8). Prepared as according to the general procedure. ^{1}H NMR (500 MHz, D_2O): δ 1.34 (s, 9H), 3.1-3.25 (m, 1.8H), 3.36 (s, 3H), 3.54-3.83 (br m, ~500H), 4.14 (d, *J*=5 Hz, 2H), 4.88 (m, 1H).

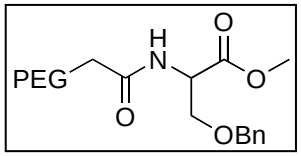

Synthesis of PEG-Ser(OBn)-OMe (9). Prepared as according to the general procedure. ^{1}H NMR (500 MHz, $CDCl_3$): δ 3.31 (s, 3H), 3.42-3.72 (br m, ~500H), 3.97 (d, *J*=3.5 Hz, 1.65 H), 4.54 (m, 2H, 1.60), 4.75 (m, 1H), 7.28-7.34 (m, 5H).

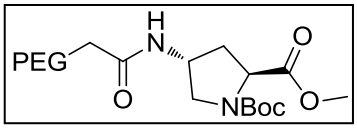

Synthesis of PEG-Boc-Pro-OMe (10). Prepared as according to the general procedure. ^{1}H NMR (500 MHz, D_2O rotamers present): δ 1.39 (s, 6H), 1.44 (s, 3H), 2.35 (m, 2H), 3.37 (s, 3H), 3.54-3.83 (br m, ~500H), 4.07 (s, 1.7H), 4.40-4.50 (m, 1H).

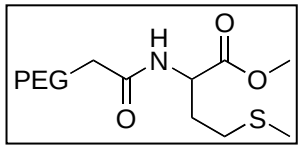

Synthesis of PEG-Met-OMe (11). Prepared as according to the general procedure. ^{1}H NMR (500 MHz, D_2O): δ 1.84-1.90 (m, 0.7 H), 1.93 (s, 3H), 2.01-2.04 (m, 0.7H), 2.51-2.68 (m, 1.5H), 3.37 (s, 3H), 3.55-3.83 (br m, ~500H), 4.13 (s, 1.4H), 4.65 (m, 0.6H).

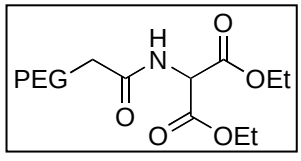

Synthesis of PEG-diethyl Malonate (12). Prepared as according to the general procedure. ^{1}H NMR (500 MHz, $CDCl_3$): δ 1.27 (t, *J*=7 Hz, 6H), 3.36 (s, 3H), 3.54-3.83 (br m, ~500H), 4.18 (s, 2H), 4.29 (m, 4H).

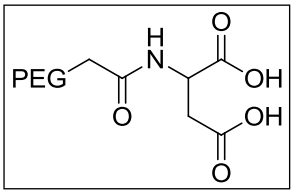

PEG-Asp(OH)-OH Deprotection (6a). PEG-Asp(Ot-Bu)-OtBu (**6**) (250 mg) was dissolved in 1.5 mL of 1:1 DCM: TFA for 3 h at room temperature. The solvents were evaporated and the resulting solid was redissolved in 1 mL of DCM and precipitated into rapidly stirring ether to yield 248 mg of white solid. Complete removal of O*t*-Bu groups confirmed by ^{1}H NMR.

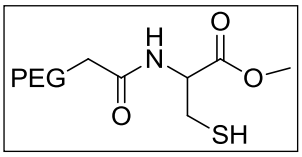

PEG-Cys(SH)-OMe (8a). PEG-Cys(St-Bu)-OMe (**8**) (200 mg) was dissolved in 0.5 mL of Millipore water. Two equivalents of tris-carboxyethyl phosphine (23 mg, 0.08 mmol) were added and the solution was allowed to stir overnight. The resulting solution was dialyzed in methanol using 1000 MWCO regenerated cellulose tubing with three solvent changes over 24 h, and dried to yield 170 mg of white solid. Complete removal of the S*t*-Bu protecting groups was confirmed by ^{1}H NMR.

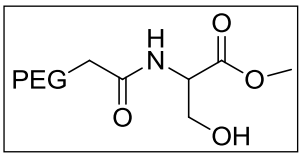

PEG-Ser(OH)-OMe (9a). PEG-Ser(OBn)-OMe (**9**) (203 mg) was dissolved in 2 mL of 1:1 DCM:TFA and 0.2 mL of thioanisole. The solution was allowed to stir for 24 h before being precipitated into rapidly stirring ether, yielding 180 mg of white solid. Complete removal of the OBn protecting groups was confirmed by ^{1}H NMR.

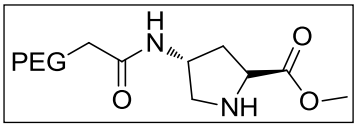

PEG-Pro-OMe (10a). PEG-Boc-Pro-OMe (**10**) (200 mg) was dissolved in 2 mL of 1:1 DCM:TFA and stirred at room temperature for 3 h. The resulting solution was precipitated into rapidly stirring ether, yielding 185 mg of white solid. Complete removal of the Boc protecting groups was confirmed by ^{1}H NMR.

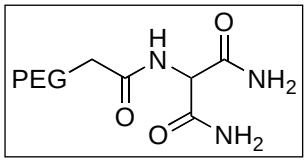

PEG-Malonamide (13).[25] PEG-diethyl malonate (**12**) (90 mg) was dissolved in 7 N NH_4OH and stirred at RT overnight. The resulting solution was precipitated into rapidly stirring ether, yielding 70 mg of white solid. ^{1}H NMR (500 MHz, $CDCl_3$): δ 3.33 (s, 3H), 3.45-3.74 (br m, ~500H), 4.07 (s, 2H), 5.07 (d, *J*=7.5 Hz, 1H), 6.16 (s, 2H), 7.09 (s, 2H), 8.01 (d, *J*=6.5 Hz, 1H).

Dendrimer-Pt synthesis.

Dendrimer **14** was synthesized as previously reported in chapter 2.[17]

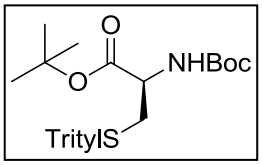

BocCys(STrityl)O*t*-Bu (15). BocCys(STrityl)OH (5 g, 10.8 mmol) and DMAP (658 mg, 5.4 mmol) were added to a 100 mL round bottom flask. The flask was evacuated and backfilled with nitrogen three times before the addition of 25 mL DCM and *t*-butanol (1.199 g, 18.2 mmol). The solution was cooled to 0 ^oC and then the EDC was added (2.678 g, 14.0 mmol). The solution slowly warmed to room temperature and stirred overnight. The DCM was evaporated and the crude material was redissolved in ethyl acetate before being washed with three 100 mL portions of 1M $NaHSO_4$, three 100 mL portions of saturated K_2CO_3, and one 100 mL portion of brine. The organic layer was dried over sodium sulfated and the solvent removed by rotary

evaporation. The residual material was further purified by flash chromatography using 66% hexanes, 33% ethyl acetate as an eluent to give 4.81 grams of white foam in 86% yield. ^{1}H NMR (400 MHz, Acetone *d*-6) δ 1.37 (s, 9H), 1.42 (s, 9H), 2.56 (ddd, *J* = 16.84, 12.09, 6.44 Hz, 2H) 3.99 (dt, *J* = 8.11, 5.03 Hz, 1H), 6.10 (d, *J* = 8.10 Hz, 1H), 7.26 (t, *J* = 7.21 Hz, 3H), 7.34 (t, *J* = 7.59 Hz, 6H), 7.42 (d, *J* = 7.65 Hz, 6H). ^{13}C NMR (100 MHz, $CDCl_3$): δ 29.04, 29.52, 35.61, 55.62, 68.30, 80.35, 82.89, 128.60, 129.77, 131.29, 131.29, 146.53, 156.91, 171.50. Calcd $[M]^+$ ($C_{31}H_{37}NO_4S$) *m/z*= 519.24. Found FAB $[M+Na]^+$ *m/z*= 542.2336.

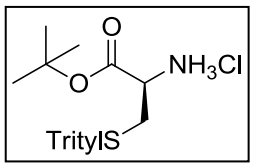

Cl•NH_3Cys(STrityl)O*t*-Bu (16). Compound **16** was prepared as previously reported.[26] Briefly, **15** (1.005 g, 1.9 mmol) was added to a 100 mL round bottom flask evacuated and backfilled with nitrogen. Via syringe, 1.5 mL of 4M HCl in dioxane was added. The solution was stirred at room temperature for 3 h before the solvent was removed by rotary evaporation. The residual material was purified by column chromatography using 15:5:1 mixture of DCM:ethyl acetate:MeOH as an eluent to give 481 mg of a glassy solid in 55% yield. ^{1}H NMR (400 MHz, MeOD *d*-$_4$) δ 1.41 (s, 9H), 2.48 (dq, *J* = 12.23, 6.25 Hz, 1H), 3.04 (t, *J* = 6.19 Hz, 1H), 7.19 (t, *J* = 7.22 Hz, 1H), 7.26 (t, *J* = 7.50 Hz, 1H), 7.41 (d, *J* = 7.66 Hz, 1H). ^{13}C NMR (100 MHz, MeOD *d*-4): δ 28.41, 37.81, 67.95, 82.76, 128.02, 129.14, 130.82, 146.02, 173.87.

General Procedure for chelator attachment to 40,000 Da dendrimer scaffold.

Dendrimer Aspartate protected. Dendrimer **14** (518 mg), Cl•NH_3Asp(O*t*-Bu)O*t*-Bu (292 mg, 1.04 mmol), and DMAP (10 mg, 0.08 mmol) were added to a 20 mL reaction vial equipped with a septum. The vial was evacuated and backfilled with nitrogen before the addition of 4 mL of DCM, 0.6 mL of DMF, and 400 μL TEA. Once all the solids dissolved, the solution was cooled to 0 ^{o}C and EDC (198 mg, 1.04 mmol) was added. The reaction mixture stirred at room temperature overnight before being transferred to a 12,000-14,000 MWCO dialysis bag in methanol. The dialysis solvent was changed four times of 18 hours. The content of the bag was concentrated to give 469 mg of white solid. Product confirmed by ^{1}H NMR (500 MHz, D_2O).

Dendrimer Methionine protected. Dendrimer **14** (526 mg), Cl•NH_3MetO*t*-Bu (254 mg, 1.04 mmol), and DMAP (10 mg, 0.08 mmol). Recovered 488 mg of white solid. Product confirmed by ^{1}H NMR (600 MHz, D_2O).

Cysteine Dendrimer. Dendrimer **14** (400 mg), **16** (365 mg, 0.8 mmol), HBTU (303 mg, 0.8 mmol). Recovered 423 mg of white solid. Product confirmed by ^{1}H NMR (600 MHz, $CDCl_3$).

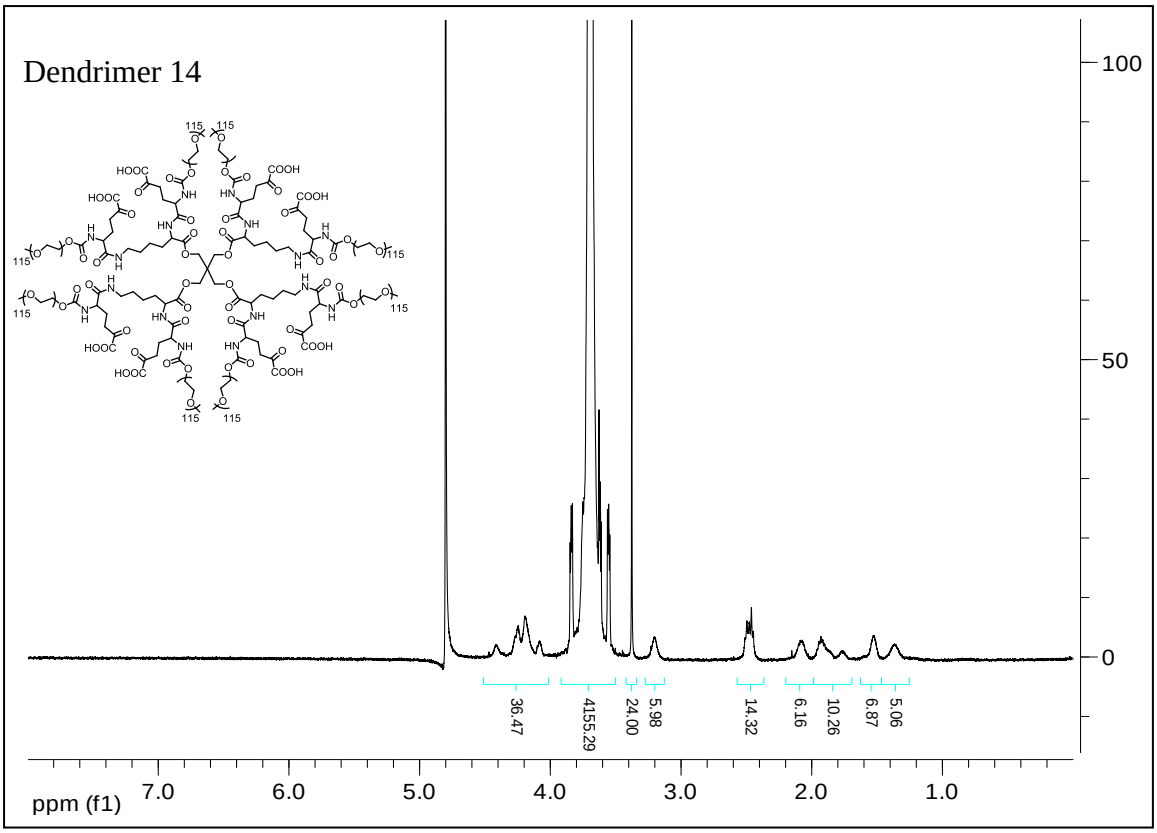
Dendrimer 14
100
50
0
36.47
4155.29
24.00
5.98
14.32
6.16
10.26
6.87
5.06
ppm (f1)
7.0
6.0
5.0
4.0
3.0
2.0
1.0

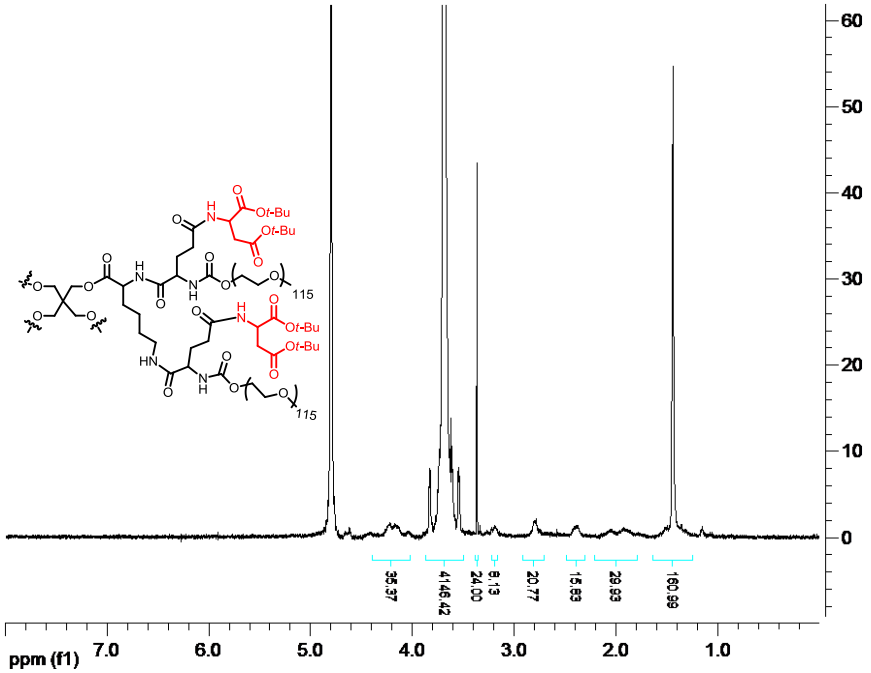
60
50
40
30
20
10
0
35.37
4146.42
24.00
8.13
20.77
15.83
29.93
160.99
ppm (f1)
7.0
6.0
5.0
4.0
3.0
2.0
1.0

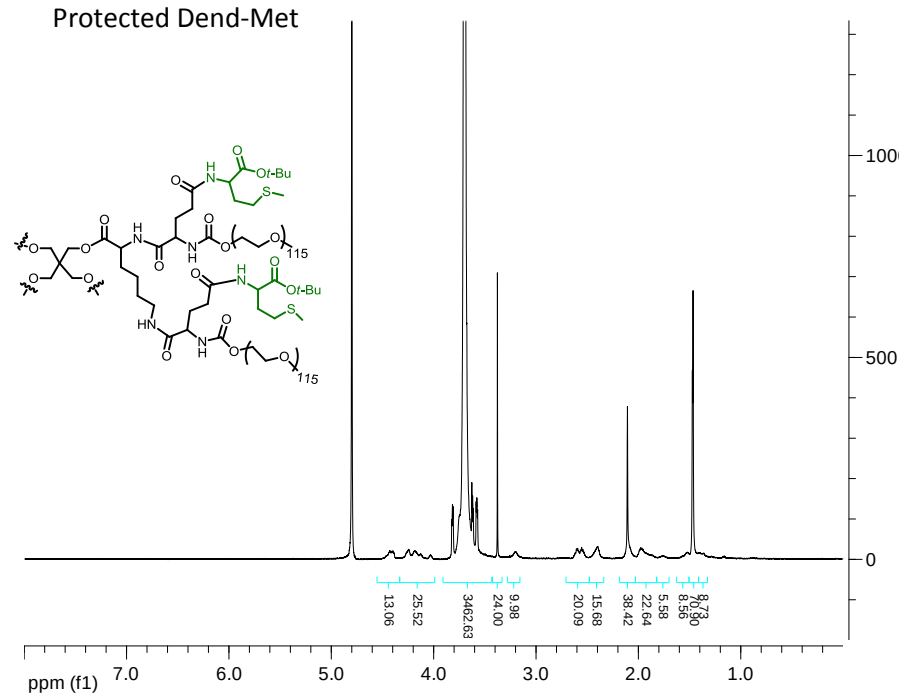

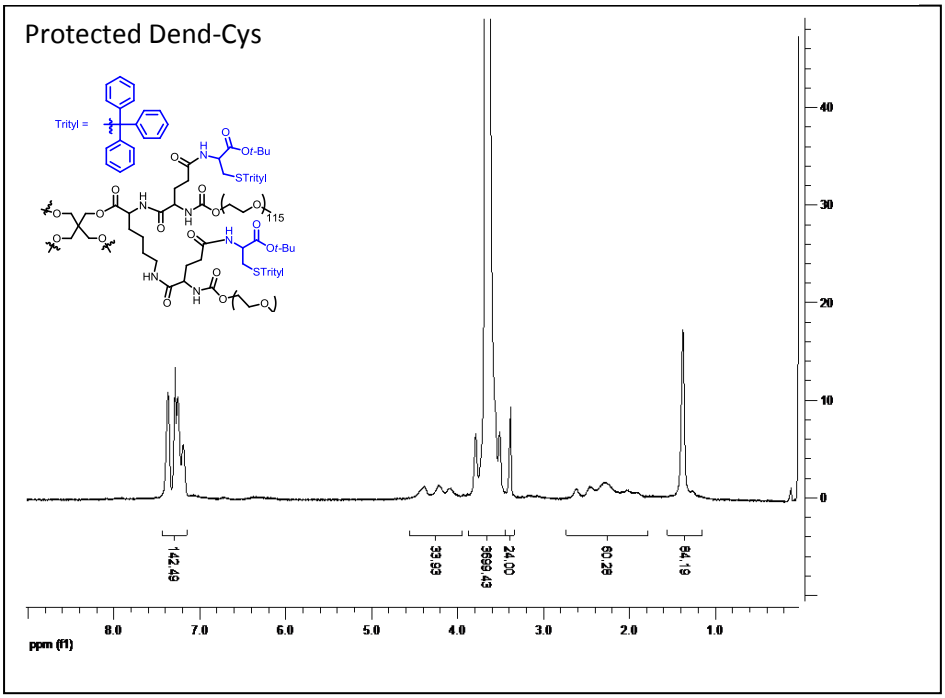

General Procedure for Deprotection of Chelator Precursors. In a typical deprotection, dendrimer Asp (233 mg) was added to a 20 mL reaction vial equipped with a septum. The vial was evacuated and backfilled with nitrogen prior to the syringe addition of a premixed solution of 1.5 mL DCM, 1.5 mL of TFA, and 100 µL of triethyl silane. The reaction was allowed to stir at room temperature for approximately 3 h before being precipitated into rapidly stirring ether.

The product (183 mg) was collected by filtration as a white solid and confirmed by ^{1}H NMR (500 MHz, D_2O).

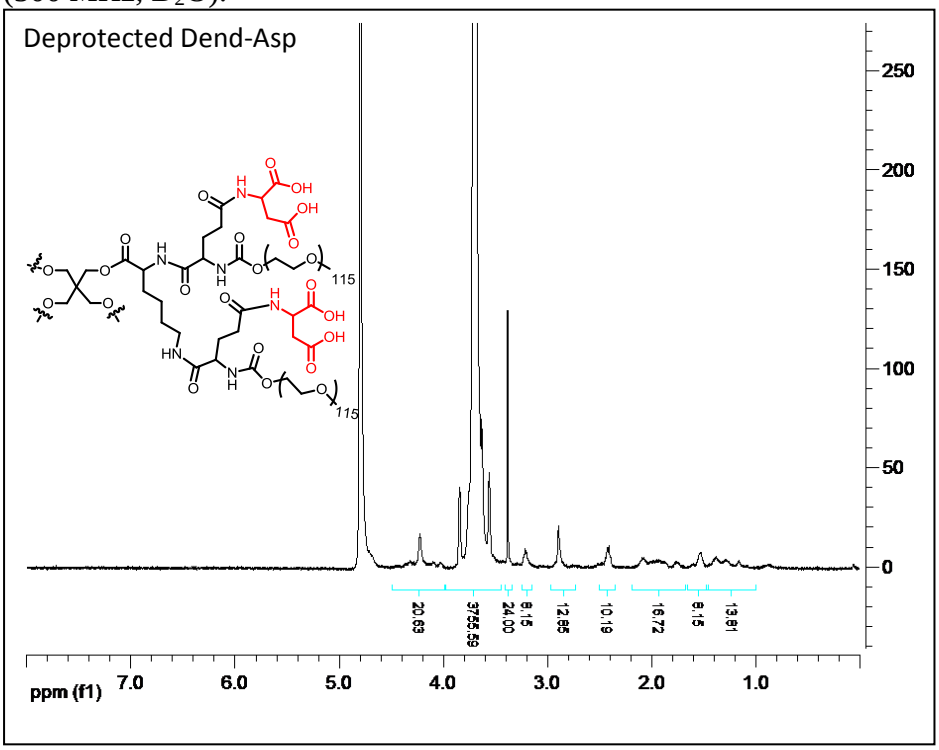

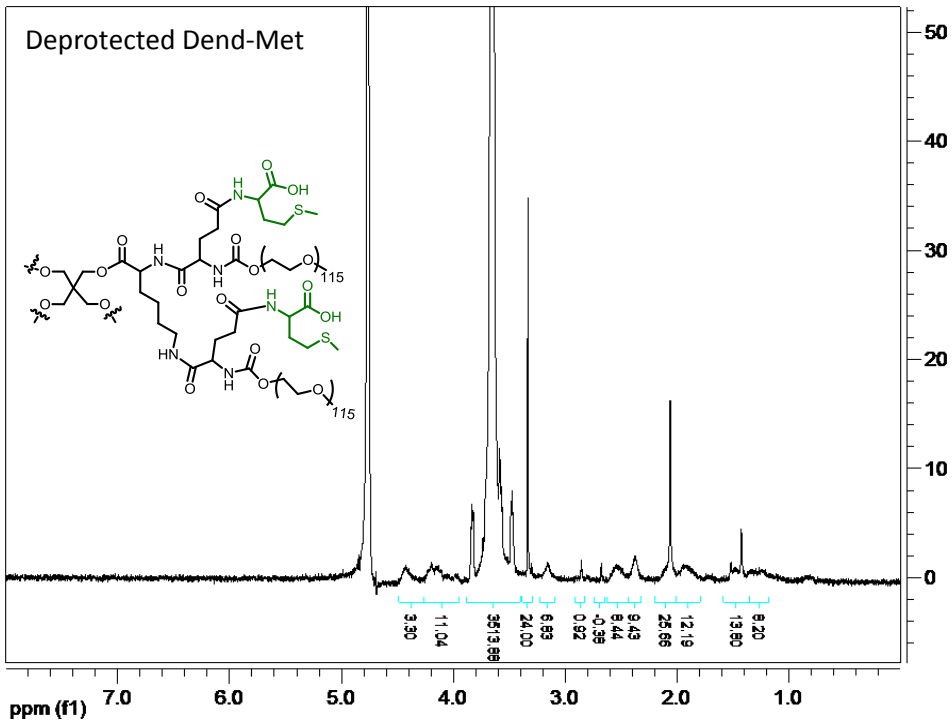

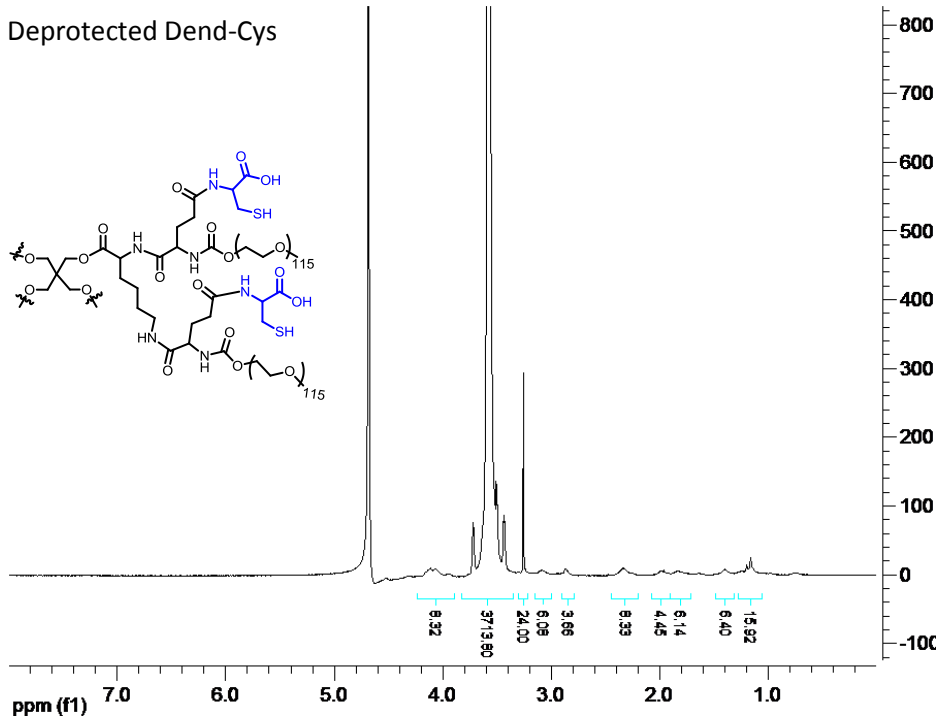

General Procedure for Platinum Loading. Platinum loading was carried out by first preparing a stock solution of the dinitrato salt of DACHPt$(OH_2)_2^{2+}$. This was done by treating DACHPtCl_2 with two equivalents of $AgNO_3$ and a few drops of nitric acid in water at 70°C, a procedure reported by Sood et al.[10] The solution was stirred in the dark for 17 h. The AgCl salts were filtered off through a 0.22 µm Teflon filter. The aspartate (**6a**) and malonamide (**13**) polymers were dissolved in 1 mL Millipore water followed by the addition of two equivalents of the platinum solution. The solutions were maintained at pH 3-5 by the addition of 1M NaOH and 5% HNO_3 and stirred in the dark at room temperature overnight. The anthranilate (**7**), cysteine (**8a**), serine (**9a**), proline (**10a**), methionine (**11**), and malonate (**12**) polymer conjugates were dissolved in 0.5 mL of 2M NaOH for one hour to saponify the methyl ester protecting groups. To the same reaction vials, portions of the platinum solution were added. The solutions were maintained at pH 3-5 by the addition of 5% HNO_3 and 1M NaOH and stirred in the dark at room temperature overnight. To remove excess small molecule species, the reaction solutions were dialyzed in Millipore water using 3500 MWCO regenerated cellulose with three solvent changes over 24 hours. The residual white fluffy solids were passed through PD-10 size exclusion columns to give PEG-Asp (**6b**), PEG-Ant (**7a**), PEG-Cys (**8b**), PEG-Ser (**9b**), PEG-Pro (**10b**), PEG-Met (**11a**), PEG-Mal (**12a**), PEG-Malonamide (**13a**), Dend-Asp (**17**), Dend-Met (**18**), and Dend-Cys (**19**), followed by Pt loading, cytotoxicity and platinum release measurements.

Measurement of Pt content. The platinum content of each polymer was determined using inductively coupled plasma atomic emission spectroscopy (ICP-AES). First, known quantities of polymer are dissolved in a known volume of water and the platinum concentration is measured. This value is used to back calculate the original weight percentage of platinum on the polymer. Platinum content was measured by weighing out ~5 mg polymer samples on a microbalance and

dissolving in 1 mL of Millipore water. The resulting solutions were allowed to sit at room temperature for one hour. From each sample, 400 µl was removed and diluted to 10 mL in a 20% HCl solution. Calibration standards were prepared by successive dilutions 10 mg/L, 5 mg/L, 1 mg/L, 0.1 mg/L and blank in 20% HCl matrix. The resulting calibration curve had a correction coefficient of 0.999993. Samples were measured in triplicate for their emission at 214.423 nm. Free platinum was measured by taking an additional 400 µl of the Pt-PEG solutions and transferred to prewashed Microcon YM-3 ultracentrifugation devices with a nominal molecular weight cut-off of 3 kDa. The devices were centrifuged at 10,000 rpm for 90 min. 275 µl of the filtrate was drawn up and diluted to 10 mL in 20% HCl matrix. The resulting samples were measured for emission at 214.423 nm. In each case, the amount of small molecule platinum species present was less than 0.1%

Platinum Release Measurements. Of the various techniques for platinum release measurements reported, we chose a method inspired by a procedure reported by Cabral et al.[19] A known quantity of polymer bound platinum was dissolved in 1X PBS and placed inside a dialysis bag. The bag was then placed into PBS preheated to 37^{o}C and aliquots are taken out at set time points and measured for platinum content by ICP. As a negative control, an identical experiment was carried out where small molecule oxaliplatin was placed inside the dialysis bag. This was to ensure that the release measurements under diffusion control and sink conditions.

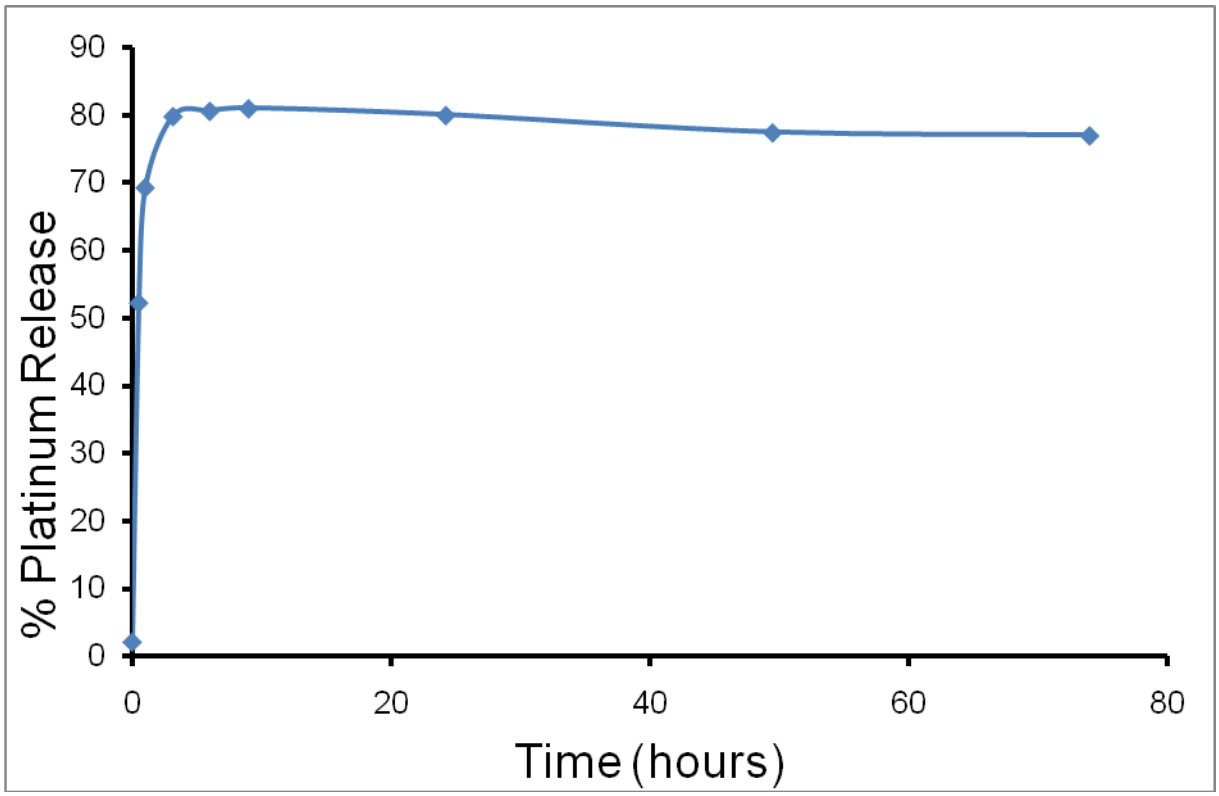

Figure 4. Oxaliplatin diffusion through dialysis tubing into dialysis buffer.

Toxicity of PEG-Pt complexes, Dend-Pt complexes, and oxaliplatin in C26 cells. Cells were seeded onto a 96-well plate at a density of 5.0 x 10^3 cells per well in 100 µl of medium and

incubated overnight (37 °C, 5% CO_2, and 80% humidity). An additional 100 µl of new medium (RPMI medium 1640/10% FBS/1% penicillin-streptomycin) containing either PEG-Pt (**6b, 7a, 8b, 9b, 10b, 11a, 12a, 13a**), Dend-Pt (**17, 18, 19**), or oxaliplatin with concentrations ranging from 4 nM to 5 mM Pt equivalents, was added to the cells. The tests were conducted in replicates of three for each concentration. After incubation for 72 h, 40 µl of media containing thiazolyl blue tetrazolium bromide solution (5 mg/mL) was added. The cells were incubated for 3 h, after which time the medium was carefully removed. To the resulting purple crystals was added 200 µl of DMSO, followed by 25 µl of pH 10.5 glycine buffer (0.1 M glycine/0.1 M NaCl). The optical densities at 570 nm were measured by using a SpectraMAX 190 microplate reader (Molecular Devices, Sunnyvale, CA). Optical densities measured for wells containing cells that received neither polymer nor drug were considered to represent 100% viability. IC_{50} values were obtained from sigmoidal fits of semilogarithmic plots of the percentage of viability versus platinum concentration by using Origin 7 SR4 8.0552 software (OriginLab, Northhampton, MA).

Animal and Tumor Models. All animal experiments were performed in compliance with National Institutes of Health guidelines for animal research under a protocol approved by the Committee on Animal Research at the University of California (San Francisco, CA) (UCSF). C26 colon carcinoma cells obtained from the UCSF cell culture facility were cultured in RPMI medium 1640 containing 10% FBS. Female BALB/c mice were obtained from Simonsen Laboratories, Inc. (Gilroy, CA).

Maximum Tolerated Dose in Healthy Mice. Female Balb/C mice were injected with via tail vein injection with Dend-Asp **17** (5, 10, and 20 mg/kg), Dend-Met **18** (60, 90, 135 mg/kg), Dend-Cyst **19** (60, 60, and 135 mg/kg). Mice weight and general health was monitored over 9 days. When gross toxicity was observed, loss of greater than 15% of initial body weight, lethargy and ruffled fur, mice were removed from the study.

Chemotherapy Experiment in Xenograph Mice. While under anesthesia, female Balb/C mice were shaved, and C26 cells (3×10^5 cells in 50 µL) were injected subcutaneously in the right hand flank. At eight days post-tumor implantation, mice were randomly distributed into treatment groups of 10 animals. Mice were injected by means of the tail vein with Cisplatin (6 mg/kg once a week for 3 weeks), Dend-Asp **17** (6 mg/kg once a week for 3 weeks), Dend-Met **18** (90 mg/kg), or Dend-Cys **19** (135 mg/kg) in approximately 200 µL of solution. Mice were weighed and tumors measured every other day. The tumor volume was estimated by measuring the tumor volume in three dimension with calipers and calculated using the formula tumor volume = length x width x height. Mice were removed from the study when (i) a mouse lost 15% of its initial weight, (ii) any tumor dimension was > 20 mm, or (iii) the mouse was found dead. The mice were followed until day 60 post-tumor inoculation. Statistical analysis was performed as previously described [27] using MedCalc 8.2.1.0 for Windows (MedCalc Software, Mariakerke, Belgium). The tumor growth delay was calculated based upon a designated tumor volume of 400 mm^3.

References

(1) Weiss, R. B.; Christian, M. C. *Drugs* **1993**, *46*, 360-377.
(2) Kelland, L. *Nat Rev Cancer* **2007**, *7*, 573-584.

(3) Wang, X. Y.; Guo, Z. J. *Dalton Transactions* **2008**, 1521-1532.
(4) Jung, Y. W.; Lippard, S. J. *Chem Rev* **2007**, *107*, 1387-1407.
(5) Siddik, Z. H.; Newell, D. R.; Boxall, F. E.; Harrap, K. R. *Biochem Pharmacol* **1987**, *36*, 1925-1932.
(6) Reedijk, J. *Chem Rev* **1999**, *99*, 2499-2510.
(7) Haxton, K. J.; Burt, H. M. *Journal of Pharmaceutical Sciences* **2008**, *98*, 2299-2316.
(8) Johnson, M. T.; Komane, L. L.; N'Da, D. D.; Neuse, E. W. *J Appl Polym Sci* **2005**, *96*, 10-19.
(9) Neuse, E. W.; Mphephu, N.; Netshifhefhe, H. M.; Johnson, M. T. *Polym Advan Technol* **2002**, *13*, 884-895.
(10) Sood, P.; Thurmond, K. B.; Jacob, J. E.; Waller, L. K.; Silva, G. O.; Stewart, D. R.; Nowotnik, D. P. *Bioconjugate Chem* **2006**, *17*, 1270-1279.
(11) Furin, A.; Guiotto, A.; Baccichetti, F.; Pasut, G.; Deuschel, C.; Bertani, R.; Veronese, F. M. *Eur J Med Chem* **2003**, *38*, 739-749.
(12) Kim, Y. S.; Song, R.; Chung, H. C.; Jun, M. J.; Sohn, Y. S. *J Inorg Biochem* **2004**, *98*, 98-104.
(13) Song, R.; Jun, Y. J.; Kim, J. I.; Jin, C.; Sohn, Y. S. *J Control Release* **2005**, *105*, 142-150.
(14) Paraskar, A. S.; Soni, S.; Chin, K. T.; Chaudhuri, P.; Muto, K. W.; Berkowitz, J.; Handlogten, M. W.; Alves, N. J.; Bilgicer, B.; Dinulescu, D. M.; Mashelkar, R. A.; Sengupta, S. *P Natl Acad Sci USA* **2010**, *107*, 12435-12440.
(15) Lee, C. C.; Gillies, E. R.; Fox, M. E.; Guillaudeu, S. J.; Frechet, J. M. J.; Dy, E. E.; Szoka, F. C. *P Natl Acad Sci USA* **2006**, *103*, 16649-16654.
(16) Guillaudeu, S. J.; Fox, M. E.; Haidar, Y. M.; Dy, E. E.; Szoka, F. C.; Frechet, J. M. J. *Bioconjugate Chem* **2008**, *19*, 461-469.
(17) van der Poll, D. G.; Kieler-Ferguson, H. M.; Floyd, W. C.; Guillaudeu, S. J.; Jerger, K.; Szoka, F. C.; Frechet, J. M. *Bioconjugate Chem* **2010**, *21*, 764-773.
(18) Rieter, W. J.; Pott, K. M.; Taylor, K. M. L.; Lin, W. B. *J Am Chem Soc* **2008**, *130*, 11584-11585.
(19) Cabral, H.; Nishiyama, N.; Okazaki, S.; Koyama, H.; Kataoka, K. *J Control Release* **2005**, *101*, 223-232.
(20) Malik, N.; Evagorou, E. G.; Duncan, R. *Anti-Cancer Drug* **1999**, *10*, 767-776.
(21) Haxton, K. J.; Burt, H. M. *Dalton Transactions* **2008**, 5872-5875.
(22) Ohya, Y.; Shirakawa, S.; Matsumoto, M.; Ouchi, T. *Polym Advan Technol* **2000**, *11*, 635-641.
(23) Gianasi, E.; Buckley, R. G.; Latigo, J.; Wasil, M.; Duncan, R. *J Drug Target* **2002**, *10*, 549-556.
(24) Zhao, H.; Rubio, B.; Sapra, P.; Wu, D. C.; Reddy, P.; Sai, P.; Martinez, A.; Gao, Y.; Lozanguiez, Y.; Longley, C.; Greenberger, L. M.; Horak, I. D. *Bioconjugate Chem* **2008**, *19*, 849-859.
(25) Laxer, A.; Major, D. T.; Gottlieb, H. E.; Fischer, B. *J Org Chem* **2001**, *66*, 5463-5481.
(26) West, K. R.; Bake, K. D.; Otto, S. *Org Lett* **2005**, *7*, 2615-2618.
(27) Fox, M. E.; Guillaudeu, S.; Frechet, J. M. J.; Jerger, K.; Macaraeg, N.; Szoka, F. C. *Molecular Pharmaceutics* **2009**, *6*, 1562-1572.

Chapter 5 – Design, Synthesis and Evaluation of pH Sensitive Platinum (II) Drugs for Polymeric Delivery

Abstract

A challenge for polymeric delivery of platinum (II) is to devise a way to attach the organometallic complex to the polymer in a controlled and releasable way. It the complex is not releasable the drug cannot reach the cell's DNA and carry out its cytotoxic effects. If the drug releases very quickly than the cytotoxic drug will distribute throughout the body before tumor extravasation has occurred. Chapter 5 discusses an approach toward pH sensitive release of platinum (II) drugs via a hydrozone linkage. A small library of new platinum (II) drugs containing a ketone were prepared and evaluated with respect to *in vitro* and *in vivo* toxicity as well as antitumor activity.

Introduction

Platinum (II) delivery has been widely explored via a sustained release mechanism by attachment to the polymer through the leaving group portion of the drug (Figure 1a). In Chapter 4 we utilized this mechanism of platinum delivery by exploring chelators with varied release rates. We next became interested in investigating a new mechanism of selective Pt (II) release. Installing a triggered release mechanism for the cytotoxic payload holds great potential to further decrease systemic toxicity and improve the passive targeting of the drug to the tumor via the EPR affect. Significant research has focused on the development of small molecule Pt(IV) prodrugs that are activated to Pt(II) drugs after an intracellular reduction event.[1,2] The Lippard group has collaborated with a number of drug delivery groups to attach the Pt(IV) prodrugs to a polymer support such as peptides,[3] carbon nanotubes,[4] PEG-PLGA nanoparticles[5] and gold nanoparticles.[6] There is also a recent report of incorporating Pt(IV) prodrugs into a nanoparticle via a hydrazone linkage to create a carrier that is redox and pH responsive.[7] Our group has had great success using our PEGylated dendrimer scaffold with doxorubicin attached through a hydrazone.[8-10] We hypothesized that a platinum (II) drug could be attached to a polymer through a hydrazone with a diamine ligand containing a ketone. Figure 1b outlines an approach in which the diamine portion of the drug contains a ketone moiety that can be attached to a polymer with hydrazide moieties. The resulting conjugate will have the drug attached to the polymer through a pH-sensitive linkage which will provide selective drug release inside the lysosome of a cell and not during circulation in the bloodstream. Figure 1c shows a few Pt (II) complexes based on heterocyclic bidentate ligands. The size and shape of the diamine ligand can impact the potency of the drug and predisposition to intrinsic cellular resistance.[11]

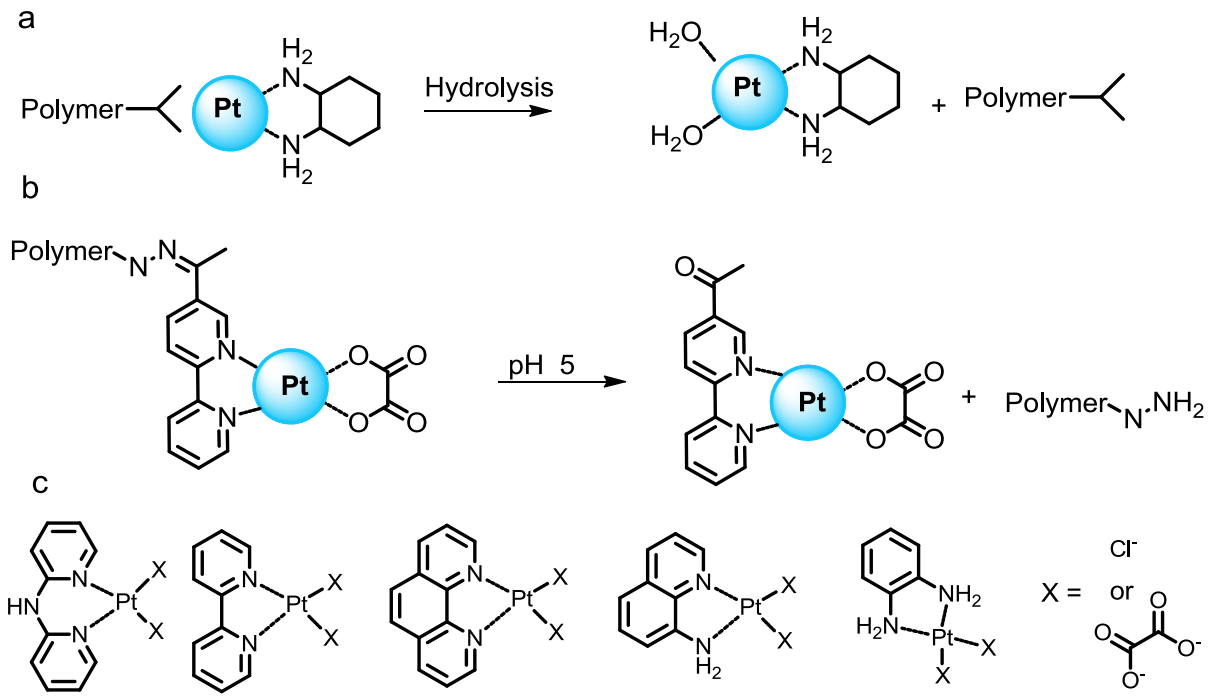

Figure 1. Platinum strategies. (a) sustained platinum release. (b) pH triggered platinum release. (c) representative aromatic ligands for platinum drugs.

These types of ligands are gaining interest in the literature as they show high potency *in vitro* and are sometimes active against cancer lines that are resistant to cisplatin.[12-22] However, their poor solubility and bioavailability limits their success *in vivo.* Fortunately, our polymer delivery system can circumvent these issues because the pharmacokinetic behavior of the polymer will dictate the pharmacokinetic behavior of the drug. For this reason, we anticipate high tumor accumulation and long circulation times for these highly potent platinum constructs.

Results and Discussion

Design of ketone containing ligands

The approach to achieving a highly potent Pt (II) derivative relied on designing a modular synthesis so that many different structural variations of the complexes could be accessed in a straightforward manner. We elected to use 2-bromo-5-acetopyridine as our primary building block because it could easily be cross-coupled to a large variety of heterocycles to create a small library of ketone containing bidentate ligands. Interestingly, 2-pyridine boronic acid could not be coupled to **2** under any of standard Suzuki conditions, a documented challenge.[23] However, the stannyl pyridine (**1**) coupled to **2** in good yield. The 8-quinoline boronic acid could be coupled to **2** by a Suzuki coupling to give **4**. The pyridine-thiazole ligand (**5**) was prepared by a Stille coupling between **2** and the commercially available 2-trimethystannylthiazole. Finally, the pyrazole-pyridine ligand (**6**) was prepared by a copper catalyzed Ullman-like C-N bond formation between **2** and pyrazole. The ligands were dissolved in acetone and added dropwise to a stirring solution of K_2PtCl_4 at 65˚C to form the platinum complexes. The initial screening process for these complexes was to measure their toxicity against C26 murine colon carcinoma cells. The IC_{50} values of the complexes are listed in Scheme 1. As a positive control, oxaliplatin was measured in the same experiment and found to be 1.2 μM. Our best performing complex was the quinoline-pyridine (**8**) which was about three-fold less toxic than oxaliplatin. This is a very promising starting point towards the rational design of highly potent burst release polymer platinum conjugates.

Scheme 1. Synthesis of platinum (II) complexes containing a ketone.

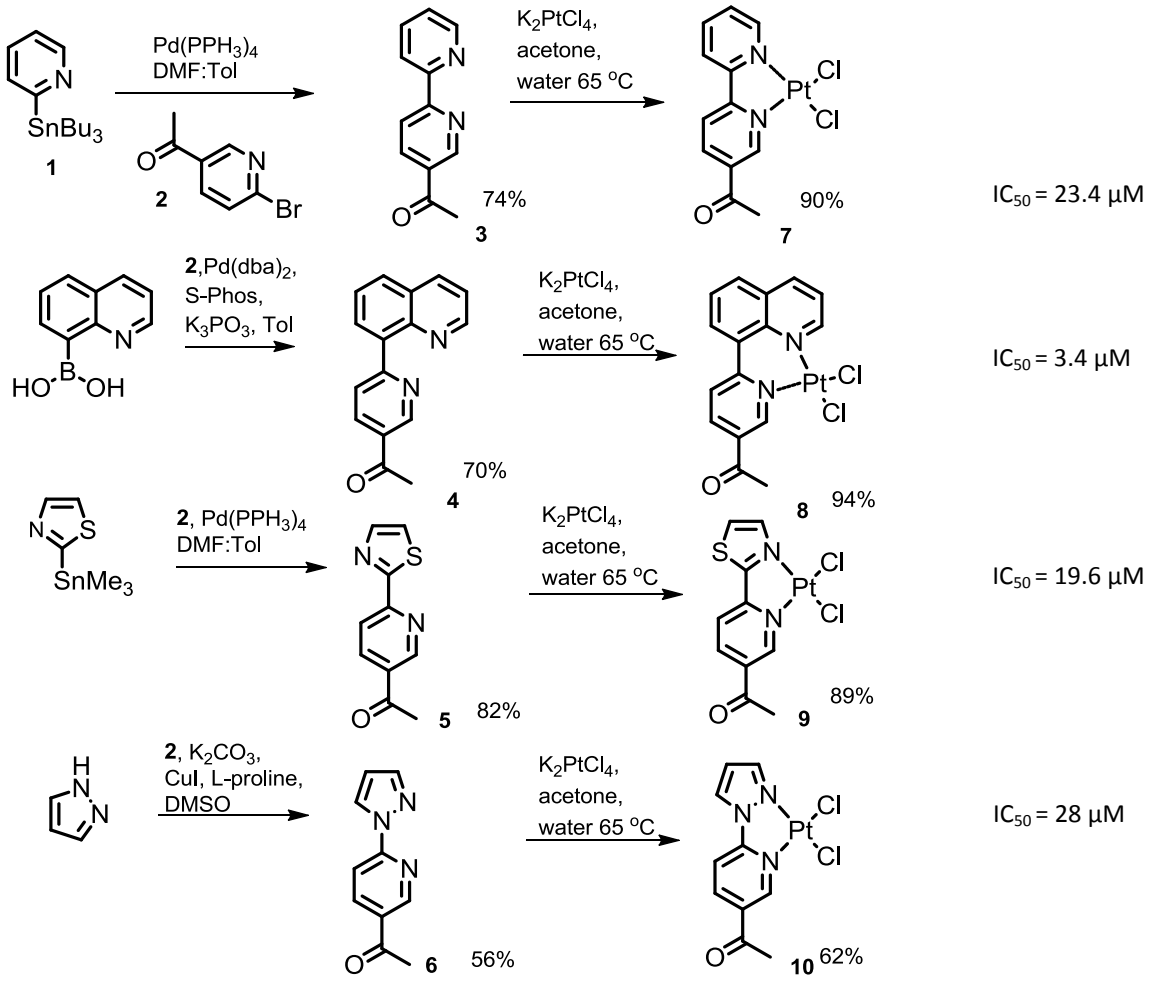

With the synthesis and toxicity screen of these four complexes complete, we verified that subtle changes in the complex shape can indeed impact the potency. We were particularly interested in why the quinoline complex had considerably higher potency than the others. In addition to being the bulkiest ligand, the quinoline complex is the only one that forms a 6-membered chelate to the Pt (II) center. For clues into the differences in potency, computational models of the complexes were generated. A side by side comparison of the quinoline and bipy complexes and their corresponding geometry optimizations is shown in Figure 2. When observing the molecules from the flat face, few differences are observed. However, when the complex is viewed down the plane of the square planar geometry, the 6-membered quinoline has a profound twist about the bond connecting the two portions of the ligand, causing the dichloride coordination sites to be more exposed. In contrast, the bipy ligand maintains a completely planar complex. We rationalized that the more exposed dichloride coordination sites may be more available to bind DNA bases which could explain the higher potency. Also, the bulkier ligand may cause a more severe bend in the Pt-DNA adduct which can affect the cell's ability to excise the platinum lesion on DNA.

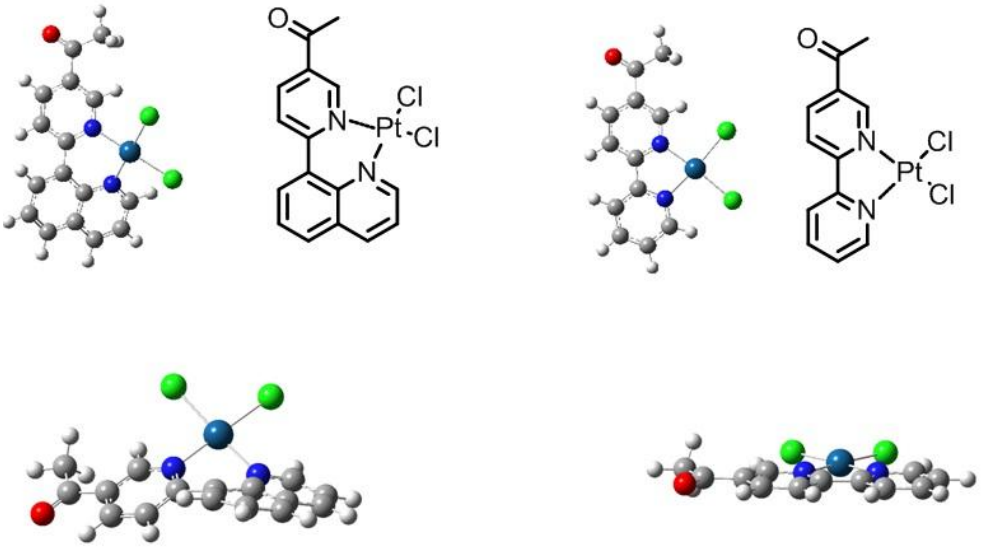

Figure 2. Comparison of complex geometries based on gas phase calculations.

Upon establishing that we could expect drastic differences in potency depending on whether the complex adopts a 5 or 6-membered chelate, we were interested in exploring the effect of steric bulk. The pyrazole complex, **10**, demonstrated low activity in our initial screen. However, we envisioned that the pyrazole could be modified in the 4 position using bromination and subsequent cross-coupling chemistry. Perhaps a *t*-butylphenyl group or a mesitylene group appended onto the complex could potentially increase activity (Figure 3). This is an attractive approach because it is a modular way to access a number of different complexes from a common starting material.

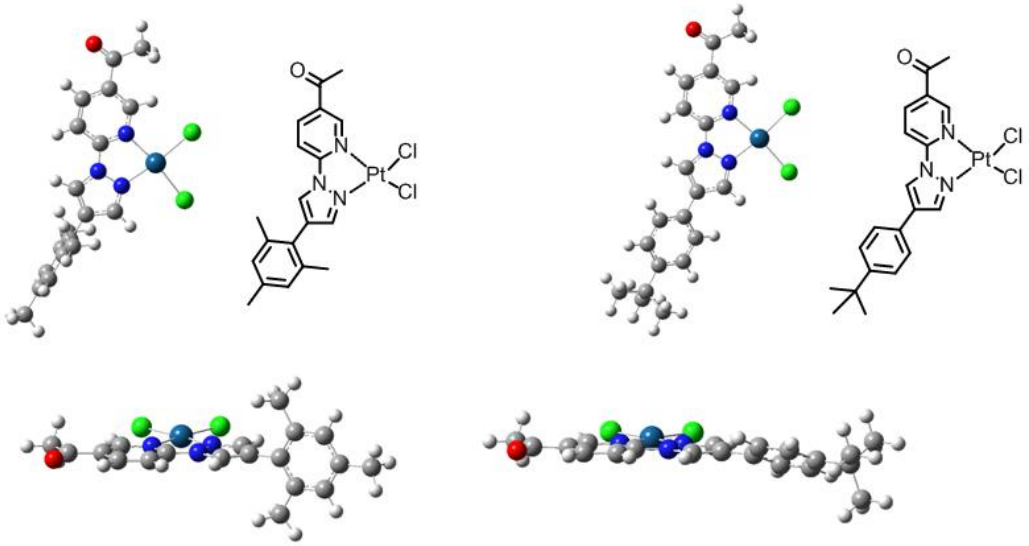

Figure 3. Gas phase calculations of complex **10** with added steric bulk.

One final consideration in the design of a suitable platinum complex that could be attached through a hydrazone is the electronic environment of the ketone complex. Because the

ketone is in conjugation with the ligand, resonance and inductive effects may play a significant role in the hydrolysis of the complex. Therefore, changing the position of the ketone on the complex may offer additional control over the rate of hydrolysis at different pH levels (Figure 4).

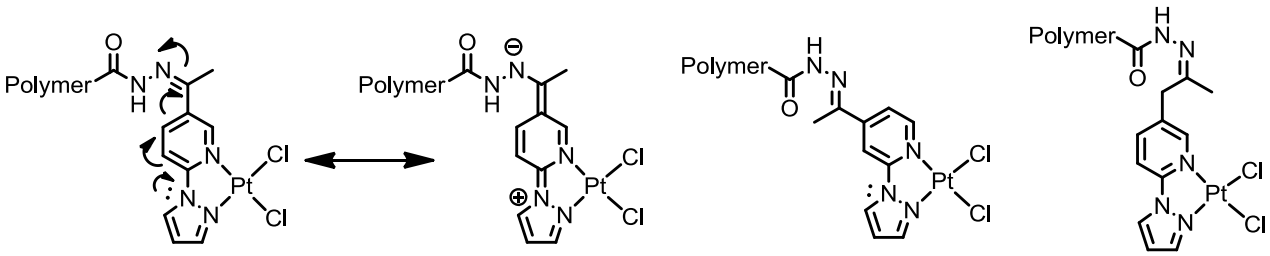

Figure 4. Electronic considerations for hydrazone hydrolysis.

Synthesis of ligands and complexes

Our second generation platinum ligands were inspired by the pyrazole-pyridine ligand, **10** (Scheme 2). Gratifyingly, selective bromination could be achieved using *N*-bromo succinimide to give compound **11**. Next, two different arylboronic acids were Suzuki coupled onto the bromopyrazole to give ligands **12** and **13**. Additionally, 3-trimethylstannyl pyridine was attached using a Stille coupling. The final pyrazole-pyridine ligand, **15**, was made with the same Ullman type coupling between 2-bromo-5-aceto-pyridine and 3,5-dimethylpyrazole. The platinum was loaded as previously described. Each ligand was dissolved in acetone and added dropwise to a solution of K_2PtCl_4 in water at 65˚C.

The cytoxicity of each derivative is listed underneath the final structure on Scheme 2. In control experiments, the toxicity of the free ligands without platinum was measured and found to be effectively nontoxic at the concentrations tested. Also, the toxicity of the K_2PtCl_4 salt was measured to ensure that the observed toxicity was not due any trace amounts of residual platinum starting material. This was found to have an IC_{50} value greater than 40 μM, which ensures that the toxicity of observed was not from either the free ligand, or the starting material platinum salt. Interestingly, in the cases where a bulky phenyl ring was appended to the chelator the potency was improved. However, when a pyridine was installed on the chelator scaffold the potency became much worse. Additionally, the pyrazole bromide complex, **16,** and the dimethyl pyrazole complex, **20**, were less potent than the original pyrazole-pyridine complex. These were also noticeably less soluble than the other, more potent complexes. Encouraged by these findings, we were still eager to discover complexes more potent than the original quinoline-pyridine complex, **8.**

Scheme 2. Second generation of platinum complexes with enhanced steric bulk.

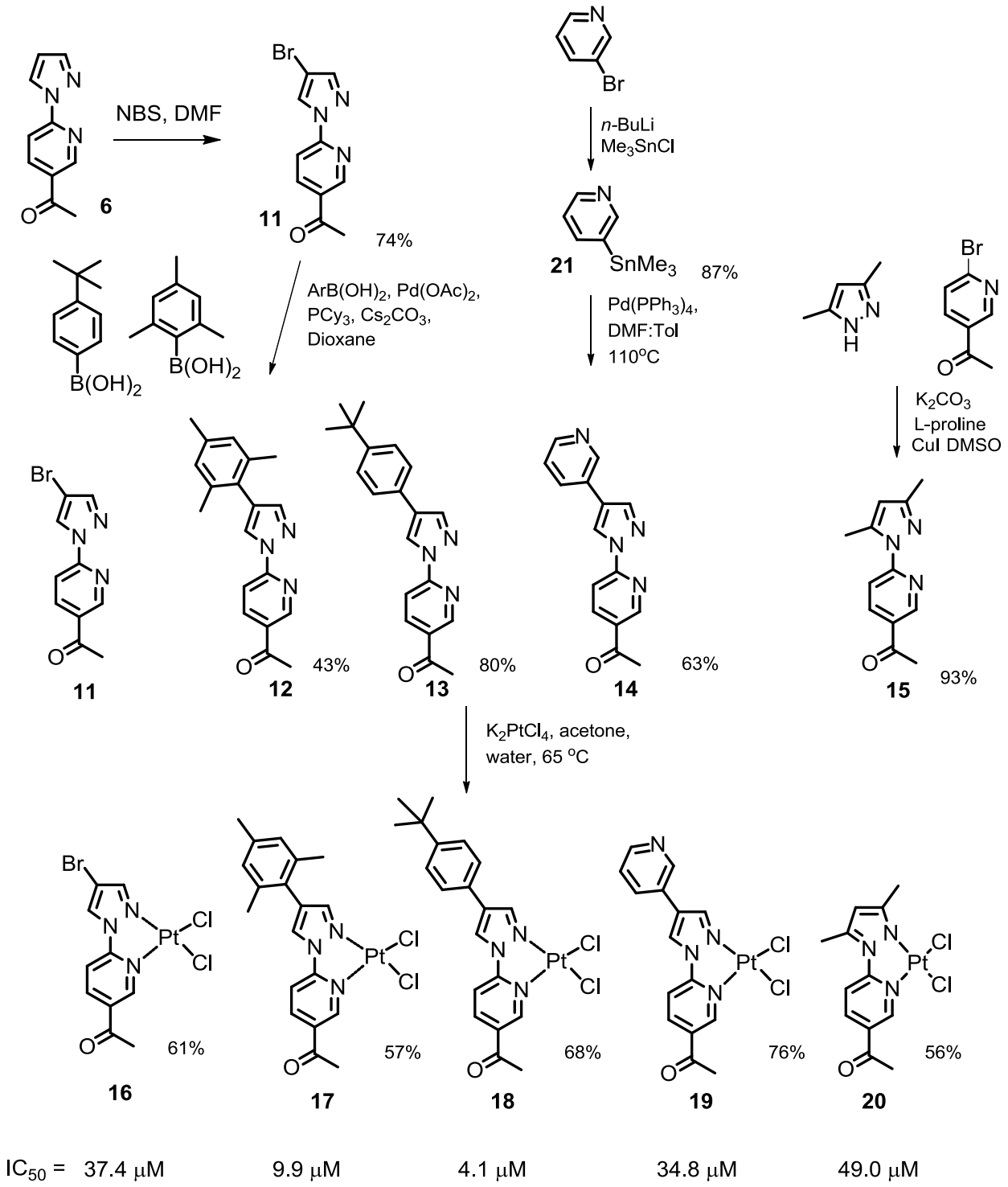

After the importance of ligand bulk was probed, a series of new complexes were synthesized in which the location of the ketone is altered. A pyrazole-quinoline starting material

(**25**) was prepared such that 6-membered chelates could be prepared with varied ketone positions. The purpose here was to investigate the consideration outlined in Figure 4, where electronics may impact the rate of hydrazone hydrolysis. These complexes were prepared by similar chemistry as the complexes prepared in Scheme 2, however, two new building blocks were prepared. Compound **23** was prepared as a building block for ligands **29** and **30**. These ligands are of interest because they are structurally similar to the ligands used to make complexes **17**-**19**, however now the ketone in **29** is more electron rich than the ketone in **30**. Ligands **31**-**33** are analogous to **29** and **30** except that they are made from building block **25**, allowing them to form the empirically more potent 6-membered chelate. The ligand **33** also differs in that there is a methylene spacer between the ketone and the aromatic system. The result is a hydrazone that should be much less affected by electronic resonance and induction. Underneath the structures are the observed IC_{50} values. Interestingly, once again the 6-membered chelate proved to have a more potent cytotoxic effect than there 5-membered ring counterparts.

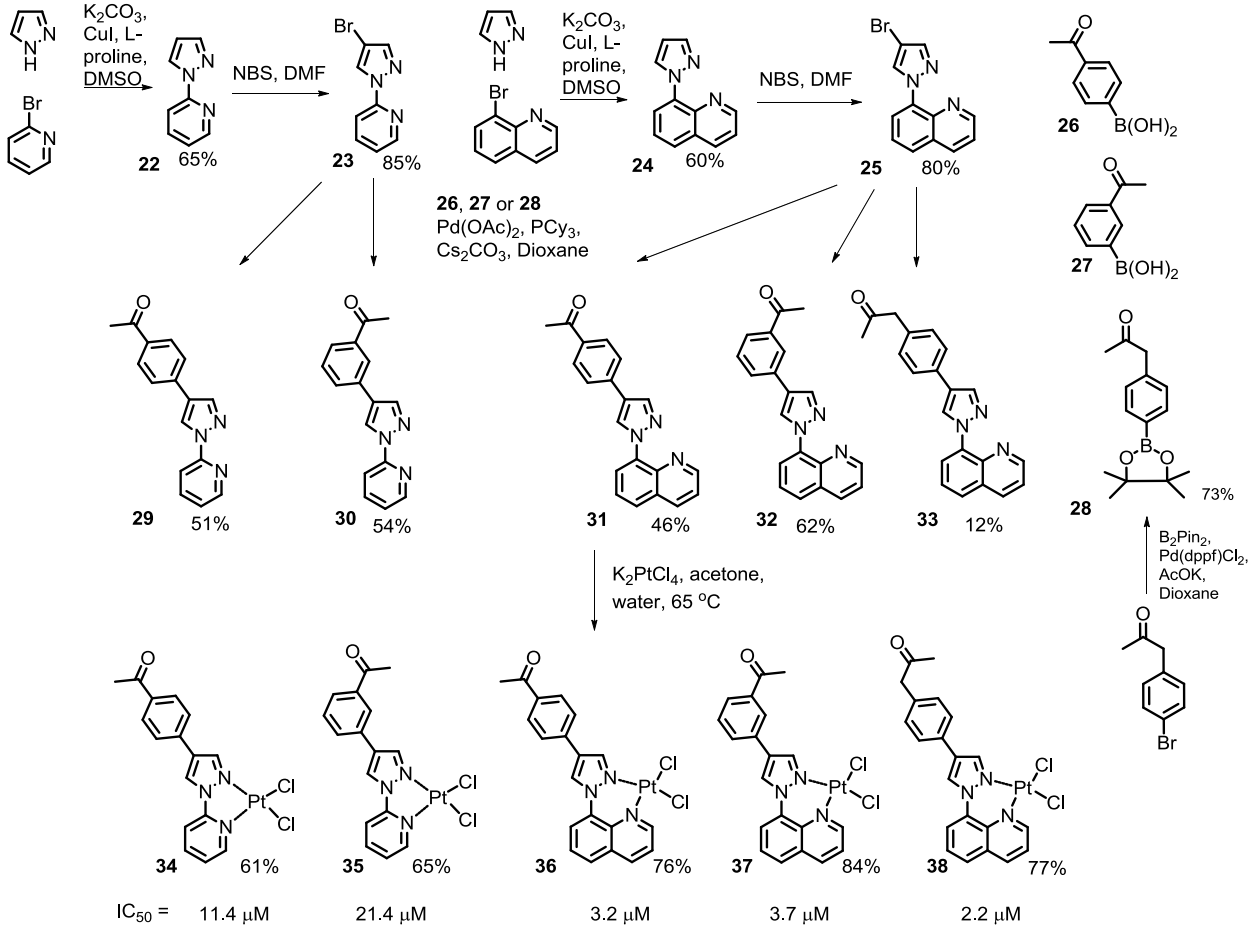

Scheme 3. Synthesis of platinum complexes with different ketone positions.

Complex **37** could be recrystallized by a vapor diffusion crystallization of methanol into dimethylsulfoxide. The crystal structure in Figure 5 shows that the solid state conformation of the quinoline-pyrazole chelate is in agreement with the gas phase calculations of the optimized geometry. The dihedral angle about the C-N biaryl bond connecting the pyrazole and quinoline

rings was found to be -30.38˚ in the crystal structure and -34.0 in the gas phase calculation. The increased planarity in the crystal structure is probably caused by stabilization from the crystal packing.

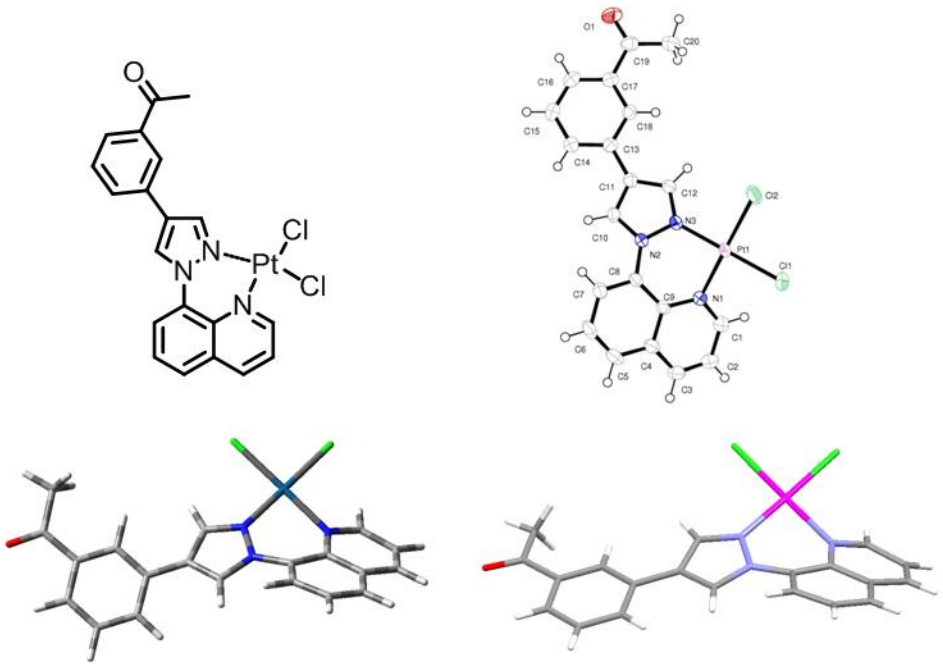

Figure 5. Comparison of gas phase calculations and crystal structure for complex **37**.

Polymer Attachment

After the synthesis and *in vitro* evaluation was complete for the aforementioned fourteen ketone containing platinum complexes, the project moved forward to the polymer attachment and evaluation stage. The original hypothesis of this work was that poorly soluble, potent platinum drugs could be attached to a polymer support via a hydrazone bond. Further, we proposed that we can control the hydrolysis rate of the polymer bound drug by modifying the electronic environment of the ketone. We proceeded to investigate the polymer conjugates of six of the described complexes. From Scheme 1 we chose complexes **7** and **8**. Complex **8** is highly potent while complex **7** is much less potent. We were very interested in learning how differences in potency for the small molecules might translate when they are attached to the polymer support. From Scheme 2 we chose complex **18** due to its high potency despite its very poor solubility. Finally, from Scheme 3 we chose complexes **37**, **38** and **39**. All three of these have toxicities on par with oxaliplatin and we anticipated they would have different drug release rates due to the differences in ketone position.

We elected to attach the complexes to two different polymer supports: a linear 5 kDa PEG chain with an acylhydrazide chain end and the 40 kDa PEGylated ester-amide dendrimer described in Chapter 2. The conjugates were prepared by stirring the dendrimer or PEG with an excess of the complex at 60˚C in dimethylformamide (DMF) overnight (Scheme 4). The resulting polymer was precipitated into ether to remove the DMF. The polymer was redissolved in methanol and filtered again through a 20 μm filter to remove excess small molecule platinum, which is not soluble in methanol. The polymer is then purified by size exclusion chromatography through an LH-20 resin with methanol as the eluent to remove any trace free drug. Finally, the

polymer samples are redissolved in water and passed through PD-10 desalting columns and lyophilized. Removal of the small molecule platinum species was confirmed by size exclusion chromatography (SEC). The resulting solids were soluble in water at concentrations greater than 250 mg polymer/mL. Similarly to the Pt conjugates described in Chapters 3 and 4, the drug loading of the final conjugates was determined by inductively coupled plasma atomic emission spectroscopy.

Scheme 4. Complex loading onto linear PEG and PEGylated dendrimer carriers.

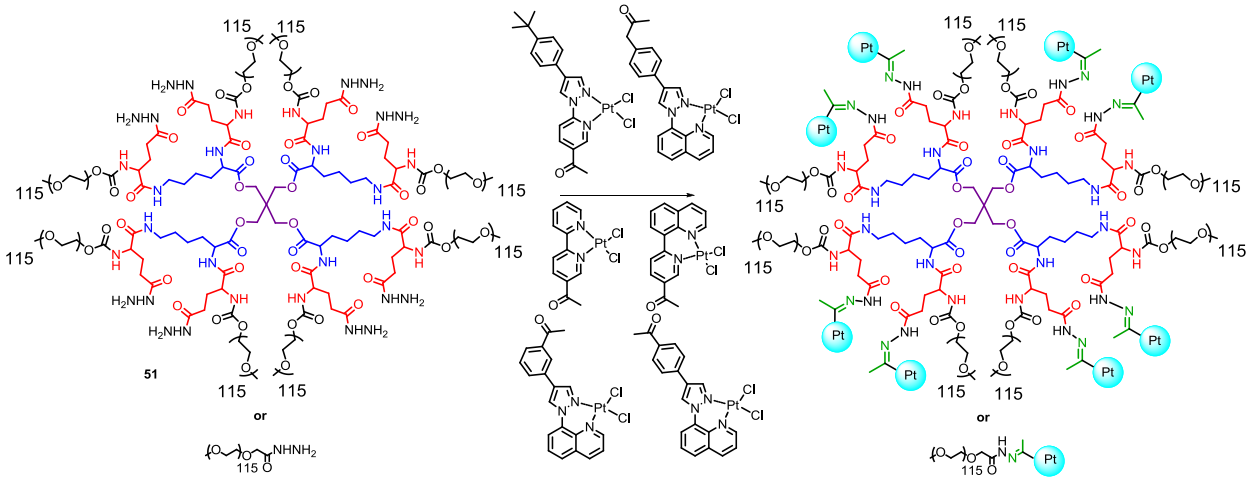

Table 1. Toxicity and drug loading data for polymer platinum conjugates.

	Bipy (**7**)	Quinoline (**8**)	*t*-butyl (**18**)	*m*-quinoline (**37**)	*p*-quinoline (**36**)	Aliphatic (**38**)
IC_{50} Free Drug (μM)	21.4	3.4	4.1	3.7	3.2	2.2
IC_{50} Dendrimer (μM)	800	70	27.8	10.1	61	12.1
51 Pt Loading (wt/wt %)	2.8% (**39**)	2.9% (**40**)	2.0% (**41**)	2.6% (**42**)	2.2% (**43**)	3.0% (**44**)
PEG Pt Loading (wt/wt %)	0.8% (**45**)	2.47% (**46**)	1.5% (**47**)	2.2% (**48**)	2.9% (**49**)	0.9% (**50**)

The cytotoxicity of the polymer-drug conjugates was measured alongside the free drug. In our previous doxorubicin-polymer systems we typically see about a 10-fold decrease in toxicity when the drug is attached to the polymer through a hydrazone. For the 6 polymer conjugates shown in Table 1, there is a range of toxicities observed for the polymer-drugs compared to the free drug. Our hypothesis is that the more toxic drug conjugates are faster releasing than the less toxic polymers.

Drug release experiments proved to be significantly more difficult than for doxorubicin or the platinum release experiments described in Chapters 2-4. We decided to measure the

release from the simplified linear PEG conjugates. The released platinum entities are very insoluble in most organic solvents as well as water. Therefore, conducting release experiments in water is a challenge. The dialysis technique used to measure platinum release in Chapters 3 and 4 failed even when the dialysis buffer was spiked with 20% DMSO. An aqueous size exclusion column with 30% acetonitrile in water was used to measure the drug released from the polymer by monitoring the UV-vis trace of the injected sample at the wavelength at which the given complex absorbs. For each polymer sample there was no release at pH 7.4 after several days. Conversely, there was significant release for most of the polymer samples at pH 5. We were surprised to see no release at pH 5 for the PEG-bipy and PEG-*t*-butyl polymers. The planar bipy and *t*-butly complexes are also the most insoluble of the complexes tested. Their poor solubility may have caused them to precipitate upon hydrolysis leading to no observed signal from released platinum in the SEC trace. The other polymers containing complexes based on the 6-membered quinoline chelate motif showed varied release rates at pH 5 which agrees with our initial hypothesis that varying the ketone position will alter the electronic environment of the subsequent hydrazone and affect their susceptibility to hydrolysis.

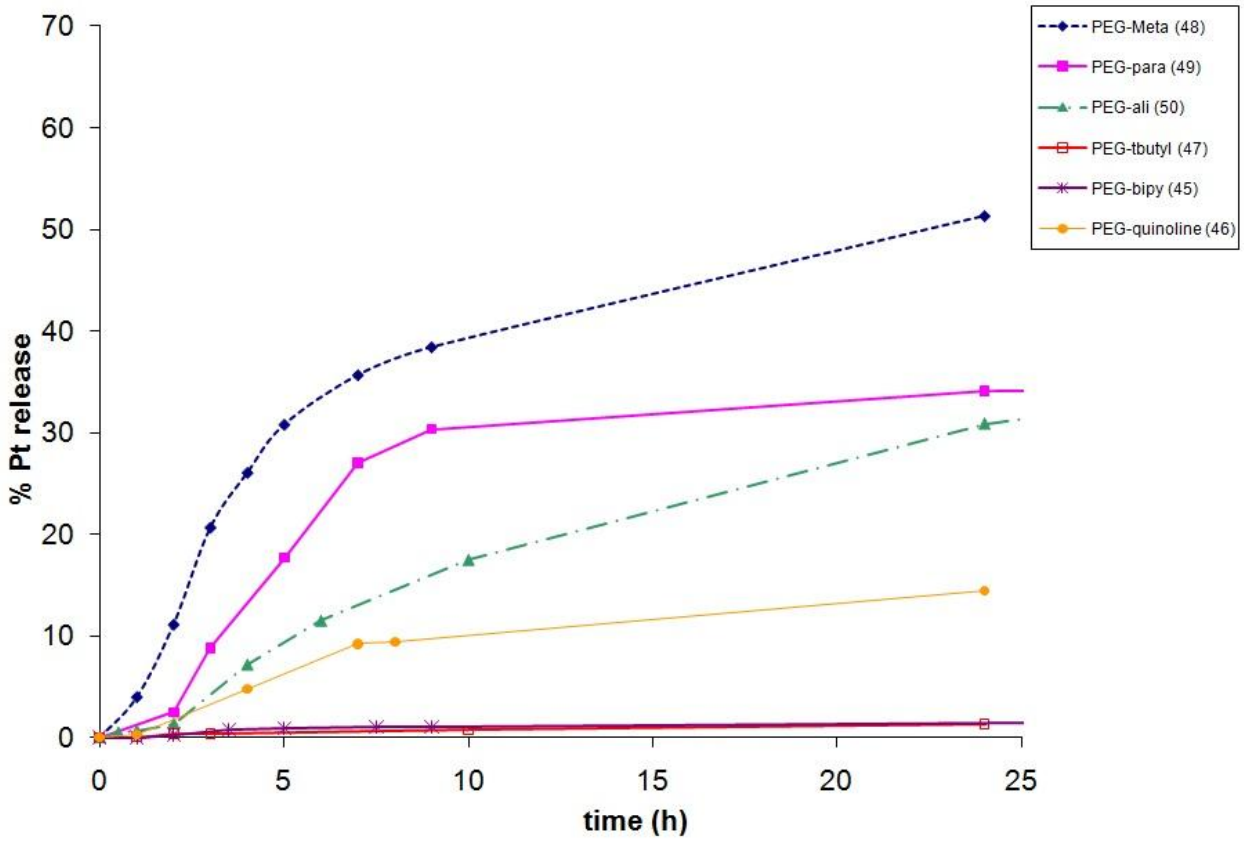

Figure 6. Drug release versus time at pH 5.

In vivo toxicity experiments

The maximum tolerated dose is an important parameter to determine reasonable dosing regimens for a new therapeutic. The drug loaded polymers were injected at doses of 0 (PBS), 15, 45 and 90 mg/kg of platinum equivalents. At 90 mg/kg, it was necessary to inject *i.p.* rather than *i.v.* because the polymer solutions at this concentration are highly viscous and an injection directly into the bloodstream may jeopardize the mouse's health. The weights of the mice were

monitored over a 10 day period. The signs of toxicity induced by the drug include weight loss, lethargy, and ruffled fur. The graphs in Figure 7 show that as the dose increases there is a greater decrease in average mouse weight. Mice receiving injections of PBS show no signs of toxicity over the course of the 10 days. Mice receiving 90 mg/kg did show signs of toxicity. One of the mice in the quinoline group was found dead on day 5. One mouse from each of the bipy and *t*-butyl groups had to be euthanized on day 6 due to excessive weight loss. Mice in the 45 mg/kg group showed some weight loss, but none exceeding the threshold of body weight loss set forth by the animal protocol. In the 15 mg/kg group there is no significant weight loss or signs of toxicity. This data provides an upper boundary for how much drug can be injected in tumored mice during a chemotherapy experiment.

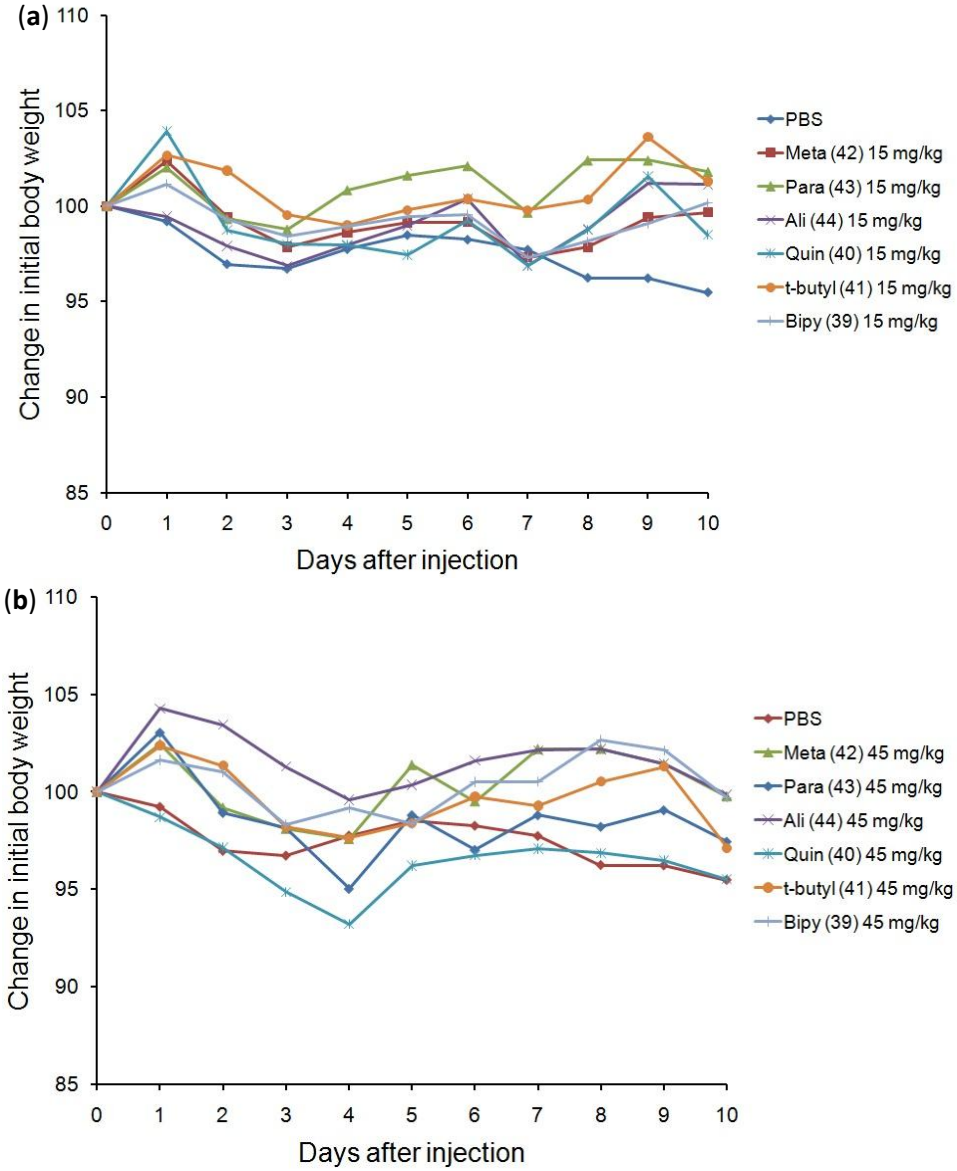

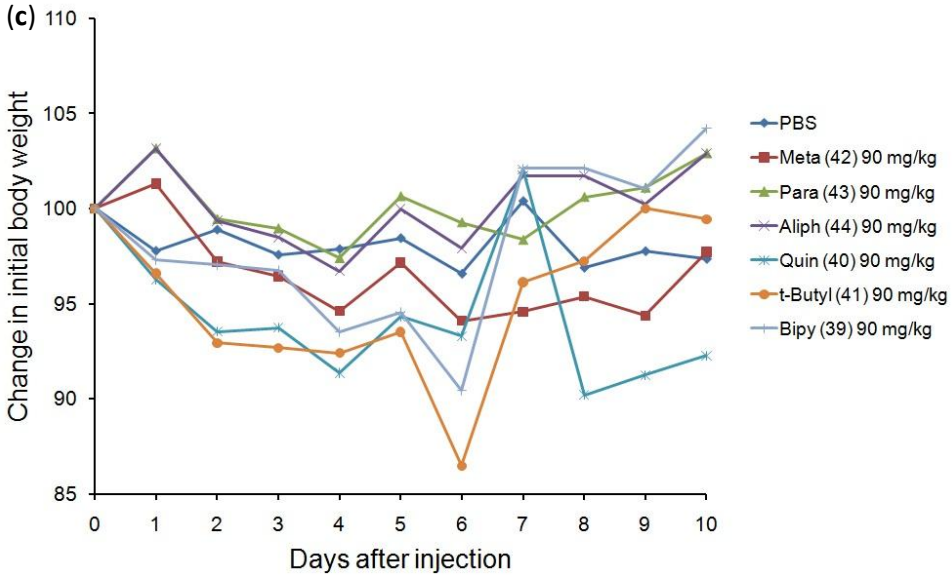

Figure 7. In vivo toxicity of platinum-dendrimer conjugates. (a) mice injected at 15 mg/kg. (b) mice injected at 45 mg/kg. (c) mice injected at 90 mg/kg.

Biodistribution Experiment

A biodistribution study was carried out to confirm that the platinum conjugates have favorable tumor accumulation properties similar to those seen in previous dendrimer-drug conjugates made in our group.[9,24-26] Female Balb/C mice were inoculated with C26 murine colon carcinoma in their right flank. Ten days later the Pt dendrimers **41** and **44** and PEG conjugate **50** was also injected for a comparison. The control samples were the small molecule complex **38** and the drug cisplatin. The measured platinum quantities shown in Figure 8 are indeed comparable to previous experiments in that there is high drug accumulation in the tumor 48 h after a single *i.v.* injection. Also, the dendrimer samples had significantly higher tumor accumulation than the PEG sample and all the polymer samples had higher tumor accumulation than the small molecule platinum species.

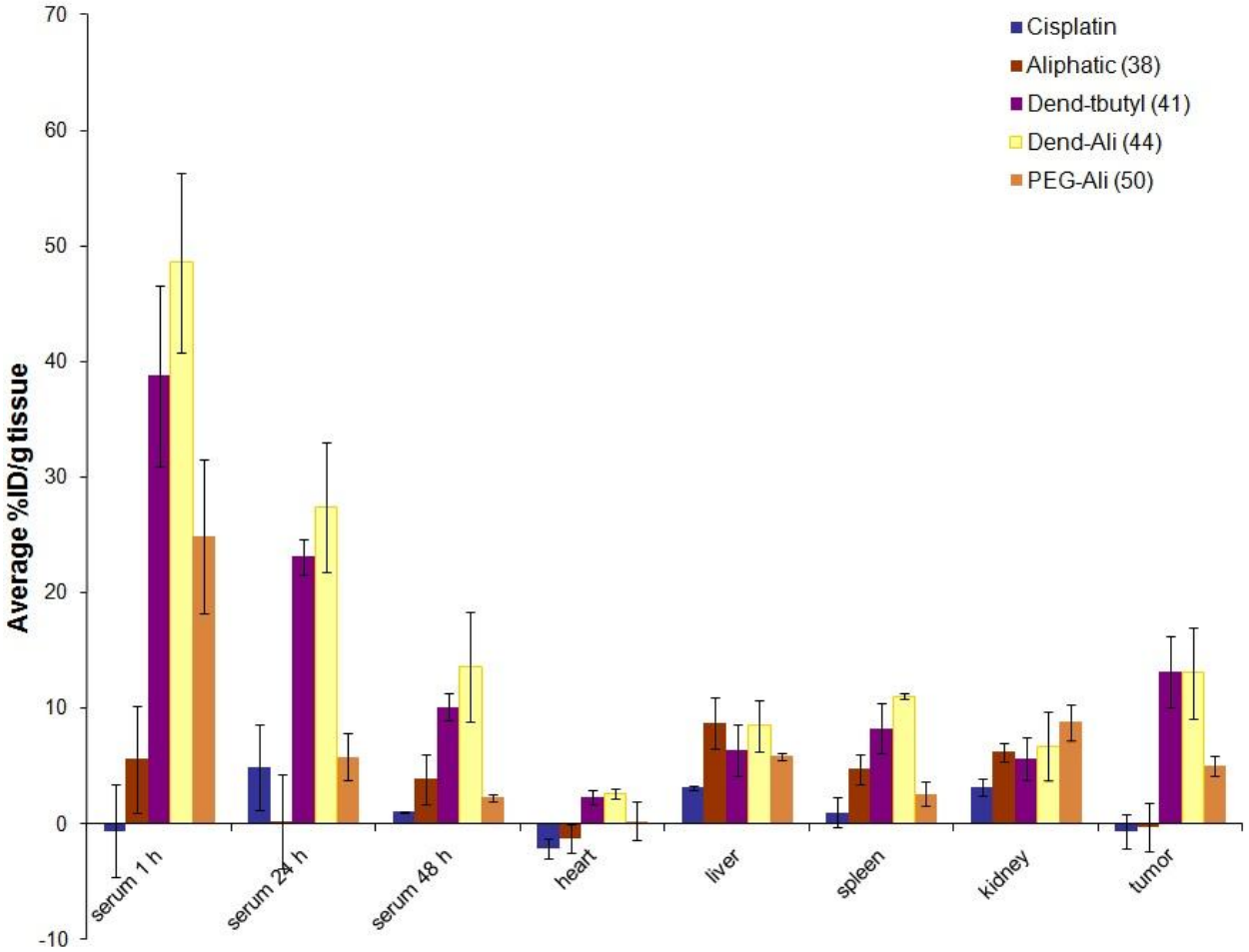

Figure 8. Biodistribution of platinum in tumored mice.

Chemotherapy Experiment

The favorable *in vitro* and *in vivo* toxicity profiles validated further study of these materials. The antitumor activity of the platinum conjugates was tested against the C26 colon carcinoma model. Female Balb/C mice were tumored in the right flank and injected eight days later. The treatment groups (6 mice per group) were PBS (negative control), cisplatin at 6 mg/kg, doxil at 20 mg Dox/kg, small molecule complex **38** and Polymers **39, 41, 42, 43,** and **44** at 36 mg Pt/kg. Polymer **40** was omitted from the experiment because on injection day it was found to contain an unknown contaminant and therefore could not be injected. The liposomal doxorubicin formulation, doxil, was included as a positive control to verify that the tumor model was behaving in a similar manner as in past experiments. This is important because there can be variations in how aggressive the tumors grow from experiment to experiment. As expected, the doxil group had 5/6 long term survivors, almost a full cure. None of the other treatment groups had median survival time (Figure 9a) or tumor growth delay (Figure 9b) that was significantly better than cisplatin or PBS.

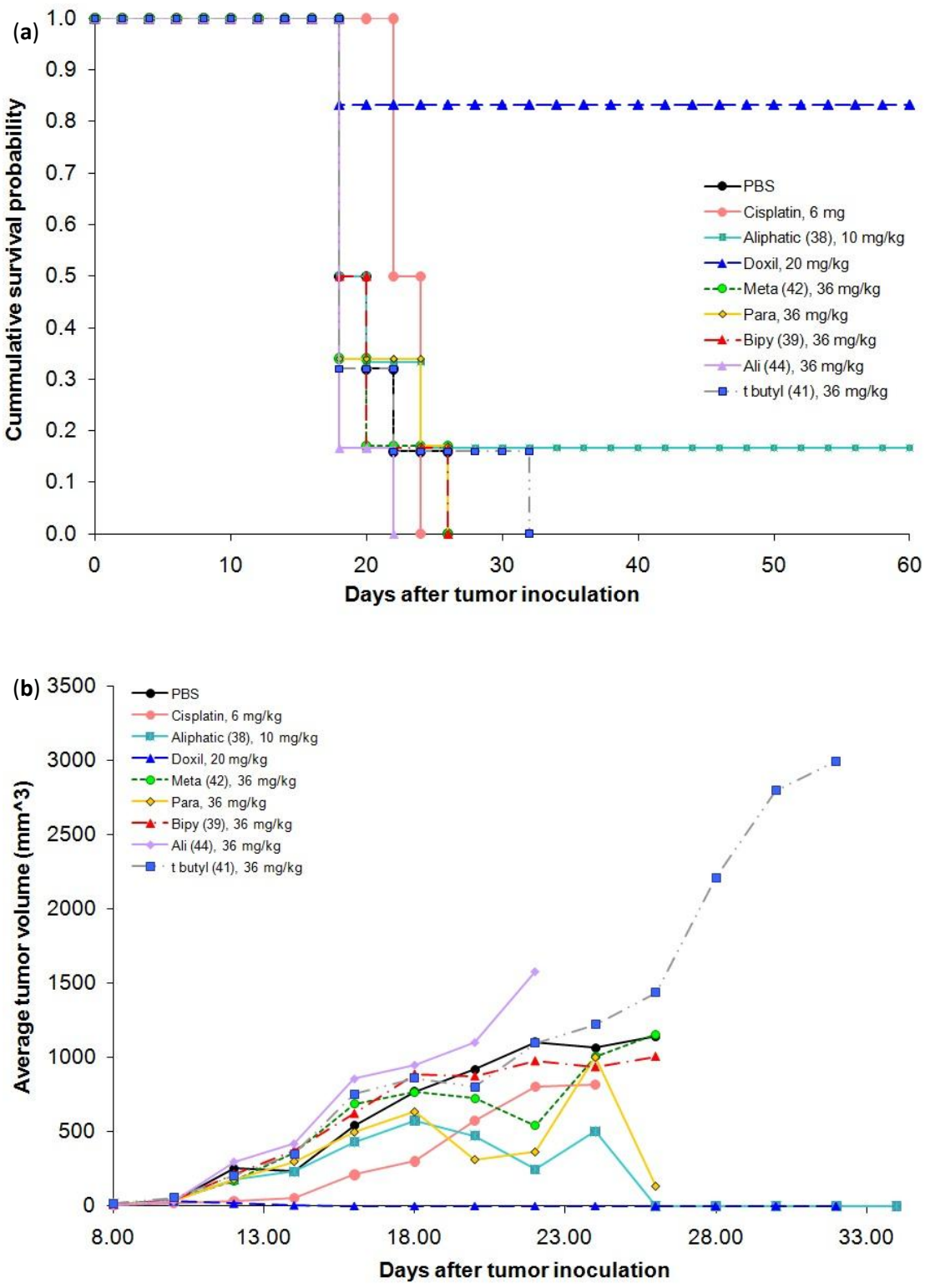

Figure 9. (a) Kaplan-Meyer survival probability plot. (b) average tumor volume vs time for platinum conjugates injected in mice inoculated with C26 colon carcinoma.

Conclusion

The design and synthesis of a small library of heterocyclic diamine ligands containing a ketone functional group has been carried out. These ligands have been used to create Pt (II) drugs inspired by oxaliplatin but specially tailored for polymeric delivery via a pH-sensitive hydrazone bond. The *in vitro* toxicity of these complexes has been evaluated and select complexes were attached to polymeric carriers for further evaluation. The drugs did in fact have pH-sensitive release profile, and the polymer bound payload had promising activity *in vitro*. During the *in vivo* evaluation, we were disappointed to see essentially no anti-tumor activity for these conjugates as we have seen for hydrazone-linked drugs in the past. It may be that the potency of the platinum drugs developed was still not enough to achieve antitumor activity despite selective delivery of large payloads. If work is to be continued on this project, it will be toward the design of similar drugs with higher potency and better solubility than those reported here in Chapter 5.

Materials and Methods

Materials. Materials were used as obtained from commercial sources unless otherwise noted. The platinum ICP standard was purchased from VHG Labs, Manchester, NH. Dimethylformamide (DMF) and CH_2Cl_2 (DCM) for syntheses were purged 1 h with nitrogen and further dried by passing them through commercially available push stills (Glass Contour). Monomethoxypolyethyleneglyco-hydrazide (mPEG-HZ) was purchased from Laysan Bio, Inc. Solvents were removed under reduced pressure using a rotary evaporator or by vacuum pump evacuation.

Characterization. NMR spectra were recorded on Bruker AV 300, AVB 400, AVQ 400, or DRX 500 MHz instruments. Elemental analyses were performed at the UC Berkeley Mass Spectrometry Facility. Size exclusion chromatography (SEC) system A consisted of a Waters 515 pump, a Waters 717 autosampler, a Waters 996 Photodiode Array detector (210-600 nm), and a Waters 2414 differential refractive index (RI) detector. SEC was performed at 1.0 mL/min in a PLgel Mixed B (10 μm) and a PLgel Mixed C (5 μm) column (Polymer Laboratories, both 300 x 7.5 mm), in that order, using DMF with 0.2% LiBr as the mobile phase and linear PEO (4,200-478,000 MW) as the calibration standards. The columns were kept at 70 °C. SEC system C consisted of a B Waters Alliance separation module 2695 and a Waters 410 differential RI detector. Inductively coupled plasma-atomic emission spectroscopy (ICP-AES) was carried out on a Perkin Elmer Optima 7000 DV Optical Emission Spectrometer.

Synthetic Details

Synthesis of 3. Compound **2** (500 mg, 2.5 mmol), 2-(trimethylstannyl) pyridine (725 mg, 3.0 mmol) and tetrakis(triphenylphosphine)palladium (145 mg, 0.13 mmol) were weighed into a 250 mL 3-neck flask equipped with a condenser. The flask was evacuated and backfilled with nitrogen 3 times. Freshly degassed DMF (10 mL) and freshly degassed toluene (40 mL) were added to the flask via syringe. The reaction stirred at 110 ˚C overnight. The reaction was diluted with dichloromethane and washed three times with water. The organic layer was dried over sodium sulfate and concentrated by rotary evaporation. The residue was purified by silica gel chromatography using 60% ethyl acetate 40% Hexanes as an eluent. 367 mg of a white solid were collected in 74% yield. ^{1}H NMR (500 MHz, $CDCl_3$) δ 2.68 (s, 3H), 7.35-7.38 (m, 1H),

7.84-7.87 (m, 1H), 8.34 (d, J =10.5 Hz, 1H), 8.48 (d, J = 8Hz, 1H), 8.53 (d, J = 8 Hz, 1H), 8.72 (d, J = 5 Hz, 1 H), 9.21 (s, 1H). ^{13}C NMR (125 MHz, $CDCl_3$) δ 27.06, 121.00, 122.14, 124.76, 132.05, 136.76, 137.29, 149.64, 149.79, 155.16, 159.68, 196.84. MS (EI) Calc $[M]^+$ ($C_{12}H_{10}N_2O$) *m/z* = 198.08. Found $[M]^+$ *m/z* = 198.0.

Synthesis of 4. Compound **2** (241 mg, 1.2 mMol), quinoline-8-boronic acid (250 mg, 1.45 mmol), Tris(dibenzylideneacetone)dipalladium (7 mg, 0.01 mmol), 2-Dicyclohexylphosphino-2',6'-dimethoxybiphenyl (10 mg, 0.02 mmol) and tribasic potassium phosphate (1.277 g, 6.02 mmol) where weighed into a 100 mL 3-neck flask equipped with a reflux condenser. The flask was evacuated and backfilled with nitrogen 3 times. Freshly degassed toluene (12 mL) was added via syringe and the reaction was left to stir at 100 ˚C for 36 hours. The reaction mixture was then diluted with 100 mL of ether and the solids were filtered off. The filtrate was concentrated by rotary evaporation and loaded onto a silica gel column. A gradient column was run from 0 to 50% ethyl acetate in hexane to give 209 mg of white solid in 70% yield. ^{1}H NMR (400 MHz, $CDCl_3$) δ 2.70 (s, 3H), 7.52-7.44 (m, 1H), 7.76-7.66 (m, 1H), 7.98-7.92 (m, 1H), 8.23-8.19 (m, 1H), 8.31-8.23 (m, 2H), 8.40-8.33 (m, 1H), 8.97 (m , 1H), 9.35-9.31 (m, 1H). ^{13}C NMR (100 MHz, $CDCl_3$) δ 26.81, 121.27, 126.45, 126.82, 128.63, 129.70, 130.46, 131.51, 134.98, 136.55, 137.71, 145.68, 149.76, 150.55, 160.95, 196.84. MS (EI) Calc $[M]^+$ ($C_{16}H_{12}N_2O$) *m/z* = 248.09. Found $[M]^+$ *m/z* = 248.0.

Synthesis of 5. Compound **2** (100 mg, 0.5 mmol), 2-tributylstannyl thiazole (224 mg, 0.6 mmol), and tetrakis(triphenylphosphine)palladium (29 mg, 0.03 mmol) were weighed into a 100 mL 3-neck flask equipped with a condenser. The flask was evacuated and backfilled with nitrogen 3 times. Freshly degassed DMF (2 mL) and freshly degassed toluene (8 mL) were added to the flask via syringe. The reaction stirred at 110 ˚C overnight. The reaction was diluted with dichloromethane and washed three times with water. The organic layer was dried over sodium sulfate and concentrated by rotary evaporation. The residue was purified through a gradient silica gel column from 0% to 30% ethyl acetate in hexanes to give 90 mg of white solid in 82% yield. ^{1}H NMR (400 MHz, $CDCl_3$) δ 2.62 (s, 3H), 7.50 (d, *J* = 3.09 Hz, 1H), 7.94 (d, *J* = 3.07 Hz, 1H), 8.26 (dd, *J* = 18.44, 8.24 Hz, 2H), 9.10 (s, 1H). ^{13}C NMR (100 MHz, $CDCl_3$) δ 26.72, 119.26, 122.82, 132.22, 136.67, 144.57, 149.78, 154.21, 167.78, 195.89. MS (EI) Calc $[M]^+$ ($C_{10}H_8N_2OS$) *m/z* = 204.04. Found $[M]^+$ *m/z* = 204.0.

Synthesis of 6. Compound **2** (1.756 g, 8.8 mmol), pyrazole (896 mg, 13.2 mmol), copper (I) iodide (334 mg, 1.76 mmol), l-proline (405 mg, 3.51 mmol), and potassium carbonate (6.066 g, 43.9 mmol) were added to a 250 mL round bottom flask. The flask was evacuated and backfilled with nitrogen three times. Anhydrous DMSO was added via syringe and the reaction stirred at 100 degrees C overnight. The reaction was diluted with ethyl acetate and washed three times with water. The organic layer was dried over sodium sulfate and concentrated by rotary evaporation. The residue was purified through a silica gel column with 40% ethyl acetate in hexane as the eluent to give 890 mg of white solid in 53% yield. ^{1}H NMR (400 MHz, $CDCl_3$) δ 2.60 (s, 3H), 6.47 (t, J = 1.6 Hz, 1H), 7.74 (s, 1H), 8.05 (d, *J* = 8.65 Hz, 1H), 8.34 (dd, *J* = 8.64, 2.29 Hz, 1H), 8.60 (d, *J* = 2.58 Hz, 1H), 8.95 (d, *J* = 1.86 Hz, 1H). ^{13}C NMR (100 MHz, $CDCl_3$) δ 26.82, 108.91, 112.18, 127.96, 130.38, 138.75, 143.39, 149.56, 153.99, 195.71. MS (EI) Calc $[M]^+$ ($C_{10}H_9N_3O$) *m/z* = 187.07. Found $[M]^+$ *m/z* = 187.0.

Synthesis of 15. Compound **2** (300 mg, 1.5 mmol), 3,5-dimethylpyrazole (288 mg, 3.0 mmol), copper (I) iodide (57 mg, 0.3 mmol), l-proline (69 mg, 0.6 mmol), and potassium carbonate (828 mg, 6 mmol) were added to a 250 mL round bottom flask. The flask was evacuated and backfilled with nitrogen three times. Anhydrous DMSO was added via syringe and the reaction stirred at 130 degrees C for three days. The reaction was diluted with ethyl acetate and washed three times with water. The organic layer was dried over sodium sulfate and concentrated by rotary evaporation. The residue was purified through a silica gel column with 40% ethyl acetate in hexane as the eluent to give 890 mg of white solid in 53% yield. ^{1}H NMR (400 MHz, $CDCl_3$) δ 2.60 (s, 3H), 6.47 (t, J = 1.6 Hz, 1H), 7.74 (s, 1H), 8.05 (d, *J* = 8.65 Hz, 1H), 8.34 (dd, *J* = 8.64, 2.29 Hz, 1H), 8.60 (d, *J* = 2.58 Hz, 1H), 8.95 (d, *J* = 1.86 Hz, 1H). ^{13}C NMR (100 MHz, $CDCl_3$) δ 26.82, 108.91, 112.18, 127.96, 130.38, 138.75, 143.39, 149.56, 153.99, 195.71. MS (EI) Calc $[M]^+$ ($C_{12}H_{13}N_3O$) *m/z* = 215.11. Found $[M]^+$ *m/z* = 215.1.

Synthesis of 11. Compound **6** (870 mg, 4.65 mmol) and *N*-bromosuccinimide (1.241 g, 6.97 mmol) were added to a 20 mL reaction vial. The solids were dissolved in DMF and stirred in the dark at room temperature for 24 hours. The reaction mixture was diluted with 50 mL of ethyl acetate and washed with 10% NaOH in 3 50 mL portions. The organic layer was dried over sodium sulfate and concentrated by rotary evaporation to give 920 mg of white solid in 74% yield. ^{1}H NMR (400 MHz, $CDCl_3$) δ 2.64 (s, 3H), 7.71 (s, 1H), 8.02 (d, *J* = 8.63 Hz, 1H), 8.36 (dd, *J* = 8.62, 1.99 Hz, 1H), 8.63 (s, 1H), 8.95 (s, 1H). ^{13}C NMR (100 MHz, $CDCl_3$) δ 26.91, 97.73, 111.77, 128.09, 130.82, 138.96, 143.79, 149.56, 153.20, 195.63. . MS (EI) Calc $[M]^+$ ($C_{10}H_8N_3O$) *m/z* = 264.99. Found $[M]^+$ *m/z* = 265.0.

Synthesis of 14. Compound **11** (48.5 mg, 0.18 mmol), compound **21** (45 mg, 0.2 mmol), tetrakis(triphenylphosphine)palladium(0) (10.5 mg, 0.01 mmol) were dissolved in degassed dimethylformamide (0.6 mL) and degassed toluene (2.5 mL). The solution was heated to 110˚ C for 24 h and then diluted with ethyl acetate (50 mL) and washed with three 50 mL portions of water. The organic layer was concentrated and loaded on to a silica gel column with 66% ethyl acetate in hexanes as the eluent to give 30 mg of a tan solid in 63% yield. *Note: this sample was contaminated with a small amount of triphenylphosphine* ^{1}H NMR (400 MHz, $CDCl_3$) δ 2.65 (s, 3H), 7.32-7.35 (m, 1H), 7.84-7.84 (m, 1H), 8.35-8.36 (m, 2H), 8.55 (s, 1H), 8.81-9.01 (m, 3H). ^{13}C NMR (100 MHz, $CDCl_3$) δ 26.67, 111.97, 122.24, 123.76, 124.25, 127.50, 128.40, 128.52, 130.45, 132.00, 132.10, 132.92, 138.67, 140.70, 147.14, 148.41, 149.35, 153.32, 195.42. MS (EI) Calc $[M]^+$ ($C_{15}H_{12}N_4O$) *m/z* = 264.10. Found $[M]^+$ *m/z* = 265.0.

Synthesis of 13. Compound **11** (57 mg, 0.21 mmol), 4-*tert*-butylphenylboronic acid (41 mg, 0.23 mmol) and bis(tri-*tert*-butylphosphine) palladium(0) (6 mg, 0.01 mmol) were added to a 20 mL microwave reaction vial under nitrogen atmosphere. Degassed tetrahydrofuran (5 mL) and degassed 2M Na_2CO_3 (1.5 mL) were added and the reaction was irradiated in a microwave reactor at 160˚ C for 45 min. The contents of the vial was diluted with 50 mL of ethyl acetate and washed with three 50 mL portions of water. The organic layer was concentrated and loaded onto a silica column with 40% ethyl acetate in hexanes as an eluent to give 53 mg of white solid in 80% yield. ^{1}H NMR (400 MHz, $CDCl_3$) δ 1.36 (s, 9H), 2.65 (s, 3H), 7.43-7.56 (m, 4H), 8.05-8.10 (m, 2H), 8.34-8.38 (m, 1H), 8.83 (s, 1H), 9.00 (s, 1H). ^{13}C NMR (100 MHz, $CDCl_3$) δ

26.65, 31.29, 34.59, 111.86, 123.58, 125.58, 125.64, 125.91, 128.51, 130.09, 138.51, 141.18, 149.40, 150.41, 153.65, 195.49. MS (EI) Calc $[M]^+$ ($C_{20}H_{21}N_3O$) *m/z* = 319.17. Found $[M]^+$ *m/z* = 319.1.

Synthesis of 12. Compound **11** (61 mg, 0.23 mmol), 2-mesityleneboronic acid (41 mg, 0.25 mmol) and bis(tri-*tert*-butylphosphone) palladium(0) (6 mg,0.01mmol) were added to a 20 mL microwave reaction vial under nitrogen atmosphere. Degassed tetrahydrofuran (5 mL) and degassed 2M Na_2CO_3 (1.5 mL) were added and the reaction was irradiated in a microwave reactor at 160˚ C for 45 min. The contents of the vial was diluted with 50 mL of ethyl acetate and washed with three 50 mL portions of water. The organic layer was concentrated and loaded onto a silica column with 40% ethyl acetate in hexanes as an eluent to give 30 mg of white solid in 43% yield. ^{1}H NMR (400 MHz, $CDCl_3$) δ 2.18 (s, 6H), 2.33 (s, 3H), 2.65 (s, 3H), 6.97 (s, 2H), 7.669 (s, 1H), 8.11-1.13 (m, 1H), 8.38-8.40 (m, 1H), 8.50 (s, 1H), 8.99 (s, 1H). ^{13}C NMR (100 MHz, $CDCl_3$) δ 21.20, 21.31, 111.95, 123.05, 126.75, 128.29, 128.52, 130.27, 137.51, 138.73, 144.35, 149.64, 154.01, 195.70. MS (EI) Calc $[M]^+$ ($C_{19}H_{19}N_3O$) *m/z* = 305.15. Found $[M]^+$ *m/z* = 305.1.

Synthesis of 24. Pyrazole (663 mg, 9.7 mmol) 8-bromoquinoline (1.008 grams, 4.87 mmol), copper (I) iodide (185 mg, 0.97 mmol), l-proline (224 mg, 1.94 mmol), and potassium carbonate (3.365 g, 24.3 mmol) were added to a 250 mL round bottom flask. The flask was evacuated and backfilled with nitrogen three times. Anhydrous DMSO (20 mL) was added via syringe and the reaction stirred at 110 degrees C overnight. The reaction was diluted with ethyl acetate and washed three times with water. The organic layer was dried over sodium sulfate and concentrated by rotary evaporation. The residue was purified through a silica gel column with 33% ethyl acetate in hexane as the eluent to give 570 mg of clear oil in 60% yield. ^{1}H NMR (400 MHz, $CDCl_3$) δ 6.55 (t, *J* = 7.1 Hz, 1H), 7.44 (dd, *J* = 8.32, 4.16 Hz, 1H), 7.62 (t, *J* = 7.87 Hz, 1H), 7.76 (d, *J* = 8.18, 1.24 Hz, 1H), 7.82 (d, *J* = 1.54 Hz, 1H), 8.19 (m, 2H), 8.74 (d, *J* = 2.35 Hz, 1H), 8.95 (dd, *J* = 4.12, 1.66 Hz, 1H). ^{13}C NMR (100 MHz, $CDCl_3$) δ 106.76, 121.62, 124.02, 126.59, 126.86, 129.29, 129.59, 133.71, 136.52, 137.23, 140.81, 150.44. MS (EI) Calc $[M]^+$ ($C_{12}H_9N_3$) *m/z* = 195.08. Found $[M]^+$ *m/z* = 195.1.

Synthesis of 25. Compound **24** (2.62 g, 13.4 mmol) and *N*-bromosuccinimide (3.56 g, 20.0 mmol) were added to a 250 mL reaction vial. The solids were dissolved in DMF (50 mL) and stirred in the dark at room temperature for 24 hours. The reaction mixture was diluted with 300 mL of ethyl acetate and washed with 10% NaOH in 3 50 mL portions. The organic layer was dried over sodium sulfate and concentrated by rotary evaporation to give 2.84 g of white solid in 78% yield. ^{1}H NMR (400 MHz, $CDCl_3$) δ 7.46-7.49 (m, 1H), 7.61-7.64 (m, 1H), 7.75 (s, 1H), 7.78-7.80 (m, 1H), 8.17-8.23 (m, 2H), 8.88 (s, 1H), 8.96 (m, 1H). ^{13}C NMR (100 MHz, $CDCl_3$) δ 94.60, 121.72, 123.30, 126.47, 127.20, 129.15, 133.75, 136.38, 136.53, 140.26, 141.12, 150.42. MS (EI) Calc $[M]^+$ ($C_{12}H_8N_3Br$) *m/z* = 272.99. Found $[M]^+$ *m/z* = 273.0.

Synthesis of 31. Compound **25** (403 mg, 1.47 mmol), 4-acetylphenylboronic acid (361 mg, 2.2 mmol) and cesium carbonate (1.433 g, 4.4 mmol) were added to a 3-neck round bottom flask equipped with a reflux condenser under nitrogen atmosphere. Degassed dioxane (20 mL) was added via syringe followed by the addition of palladium acetate (16 mg, 0.07 mmol) and

tricyclohexylphosphine (41.1 mg, 0.14 mmol). The solution was heated to reflux for 24 h and the reaction mixture was then cooled to room temperature, diluted with ethyl acetate (100 mL) and washed with three 50 mL portions of water. The organic layer was concentrated and loaded onto a silica column with 40% ethyl acetate in hexanes as an eluent to give 220 mg of white solid in 47% yield. ^{1}H NMR (400 MHz, $CDCl_3$) δ 2.55 (s, 3H), 7.39-7.42 (m, 1H), 7.55-7.63 (m, 3H), 7.71-7.73 (m, 1H), 7.91 (d, *J*= 6.8 Hz), 8.08 (s, 1H), 8.17 (q, *J*= 7.8 Hz, 2H), 8.93 (s, 1H), 9.12 (s, 1H). ^{13}C NMR (100 MHz, $CDCl_3$) δ 26.53, 121.63, 122.73, 123.55, 125.37, 126.44, 127.08, 129.09, 129.16, 131.12, 134.93, 136.49, 136.52, 137.45, 138.47, 140.36, 150.38, 197.46. MS (ESI) Calc $[M]^+$ ($20_{20}H15N_3O$) *m/z* = 313.12. Found $[M+H]^+$ *m/z* = 314.1288.

Synthesis of 32. Compound **25** (120 mg, 0.44 mmol), 3-acetylphenylboronic acid (97 mg, 0.59 mmol) and cesium carbonate (284 mg, 0.87 mmol) were added to a 3-neck round bottom flask equipped with a reflux condenser under nitrogen atmosphere. Degassed dioxane (10 mL) was added via syringe followed by the addition of palladium acetate (7 mg, 0.03 mmol) and tricyclohexylphosphine (17 mg, 0.06 mmol). The solution was heated to reflux for 24 h and the reaction mixture was then cooled to room temperature, diluted with ethyl acetate (100 mL) and washed with three 50 mL portions of water. The organic layer was concentrated and loaded onto a silica column with 40% ethyl acetate in hexanes as an eluent to give 85 mg of white solid in 62% yield. ^{1}H NMR (400 MHz, $CDCl_3$) δ 2.60 (s, 3H), 7.41-7.42 (m, 2H), 7.65-7.66 (m, 1H) 7.80-7.82 (m, 3H), 8.12-8.24 (m, 4H), 9.00 (s, 1H), 9.12 (s, 1H). ^{13}C NMR (100 MHz, $CDCl_3$) δ 26.63, 121.43, 122.75, 123.04, 124.95, 126.26, 126.33, 126.80, 128.87, 128.98, 130.09, 130.52, 133.01, 136.31, 136.46, 137.39, 138.15, 140.24, 150.21, 198.06. MS (ESI) Calc $[M]^+$ ($20_{20}H15N_3O$) *m/z* = 313.12. Found $[M+H]^+$ *m/z* = 314.1288.

Synthesis of 33. Compound **25** (503 mg, 1.82 mmol), **28** (569 mg, 2.19 mmol) and cesium carbonate (1.786 g, 5.48 mmol) were added to a 3-neck round bottom flask equipped with a reflux condenser under nitrogen atmosphere. Degassed dioxane (20 mL) was added via syringe followed by the addition of palladium acetate (21 mg, 0.09 mmol) and tricyclohexylphosphine (51 mg, 0.18 mmol). The solution was heated to reflux for 24 h and the reaction mixture was then cooled to room temperature, diluted with ethyl acetate (100 mL) and washed with three 50 mL portions of water. The organic layer was concentrated and loaded onto a silica column with 40% ethyl acetate in hexanes as an eluent to give 318 mg of white solid in 53% yield. ^{1}H NMR (400 MHz, $CDCl_3$) δ 2.19 (s, 3H), 3.73 (s, 2H), 7.24-7.26 (m, 2H), 7.48-7.51 (m, 1H), 7.48-7.68 (m, 3H), 7.80-7.82 (m, 1H), 8.09 (s, 1H), 8.25 (d, *J* = 7.6 Hz, 2H), 9.01 (s, 1H), 9.07 (s, 1H). ^{13}C NMR (100 MHz, $CDCl_3$) δ 25.02, 29.48, 50.91, 71.99, 121.76, 123.68, 123.78, 126.34, 126.71, 127.02, 129.40, 130.06, 130.53, 131.69, 132.54, 136.75, 136.97, 138.61, 140.65, 150.51, 206.74. Calc $[M]^+$ ($C_{21}H_{17}N_3O$) *m/z* = 327.14. Found Hi Res ESI [M+Na] = 350.1264.

Synthesis of 30. Compound **23** (213 mg, 0.95 mmol), 3-acetylphenylboronic acid (210 mg, 1.28 mmol) and cesium carbonate (771 mg, 2.37 mmol) were added to a 3-neck round bottom flask equipped with a reflux condenser under nitrogen atmosphere. Degassed dioxane (15 mL) was added via syringe followed by the addition of palladium acetate (11 mg, 0.05 mmol) and tricyclohexylphosphine (26.5 mg, 0.1 mmol). The solution was heated to reflux for 24 h and the reaction mixture was then cooled to room temperature, diluted with ethyl acetate (100 mL) and washed with three 50 mL portions of water. The organic layer was concentrated and loaded onto

a silica column with 40% ethyl acetate in hexanes as an eluent to give 136 mg of white solid in 54% yield. ^{1}H NMR (400 MHz, $CDCl_3$) δ 2.64 (s, 3H), 7.18-7.22 (m, 1H), 7.46-7.50 (m, 1H), 7.74-7.77 (m, 3H), 7.80-7.84 (m, 1H), 8.06 (s, 1H), 8.15 (s, 1H), 8.42-8.44 (m, 1H), 8.88 (s, 1H). ^{13}C NMR (100 MHz, $CDCl_3$) δ 26.86, 112.46, 121.81, 123.83, 123.97, 125.35, 126.97, 129.31, 130.28, 132.57, 137.73, 138.93, 139.75, 148.16, 151.25, 198.31. MS (EI) Calc $[M]^+$ ($C_{16}H_{13}N_3O$) *m/z* = 263.1. Found $[M]^+$ *m/z* = 263.1.

Synthesis of 29. Compound **23** (200 mg, 0.90 mmol), 4-acetylphenylboronic acid (210 mg, 1.28 mmol) and cesium carbonate (771 mg, 2.37 mmol) were added to a 3-neck round bottom flask equipped with a reflux condenser under nitrogen atmosphere. Degassed dioxane (15 mL) was added via syringe followed by the addition of palladium acetate (10 mg, 0.04 mmol) and tricyclohexylphosphine (25mg, 0.08 mmol). The solution was heated to reflux for 24 h and the reaction mixture was then cooled to room temperature, diluted with ethyl acetate (100 mL) and washed with three 50 mL portions of water. The organic layer was concentrated and loaded onto a silica column with 40% ethyl acetate in hexanes as an eluent to give 90 mg of white solid in 38% yield. ^{1}H NMR (400 MHz, $CDCl_3$) δ 2.61 (s, 3H), 7.20-7.23 (m, 1H), 7.65-7.71 (m, 2H), 7.81-7.85 (s, 1H), 7.97-8.06 (m, 4H), 8.43-8.44 (m, 1H), 8.90 (s, 1H). MS (EI) Calc $[M]^+$ ($C_{16}H_{13}N_3O$) *m/z* = 263.1. Found $[M]^+$ *m/z* = 263.1.

Synthesis of 21. 3-Bromopyridine (1.78 g, 11.3 mmol) was added to a flame dried, 500 mL one neck flask. 100 mL of dry ether was added via syringe and the solution was cooled to -78˚C. n-Butyl lithium (5.41 mL, 13.5 mmol) was added via syringe as 2.5M solution in hexane. The mixture stirred at -78˚C for one hour and then trimethyltin chloride (2.694 g, 13.5 mmol) was added. The reaction was allowed to stir for 4 hours and gradually warm to room temperature and then washed with three 50 mL portions of 10% NaOH. The organic layer was dried over sodium sulfate and concentrated by rotary evaporation to give 2.38 g of clear oil in 87% yield. ^{1}H NMR (400 MHz, $CDCl_3$) δ 0.3 (s, 9H), 7.19-7.24 (m, 1H), 7.68-7.82 (m, 1H), 8.48-8.53 (m, 1H), 8.56-8.65 (m, 1H). ^{13}C NMR (100 MHz, $CDCl_3$) δ -9.45, 124.01, 137.26, 143.58, 149.51, 155.69.

Synthesis of 1. Prepared using the identical procedure described above with 2-bromopyridine as a starting material. ^{1}H NMR (400 MHz, $CDCl_3$) δ 0.33 (s, 9H), 7.09-7.13 (m, 1H), 7.40-7.52 (m, 2H), 8.72-8.73 (m, 1H).

Synthesis of 28. 4-bromophenylacetone (1.234 g, 5.79 mmol), bis(pinacolato)diboron (1.550 g, 6.08 mmol), dichloro 1,1'-bis(diphenylphosphino)ferrocene palladium(II) (94 mg, 0.12 mmol), and potassium acetate (1.563 g, 15.93 mmol) were suspended in 30 mL of degassed dioxane and heated at 110˚C overnight. The reaction mixture was then diluted with 100 mL of ethyl acetate and washed with water in three 100 mL portions. The organic layer was dried over sodium sulfate and concentrated by rotary evaporation. The residue was purified through a silica gel column with 25% ethyl acetate in hexane as the eluent to give 1.104 g of yellow oil in 73% yield. ^{1}H NMR (400 MHz, $CDCl_3$) δ 1.33 (s, 12H), 2.12 (s, 3H), 3.69 (s, 2H), 7.20 (d, *J* = 7.86 Hz, 2H), 7.78 (d, *J* = 7.85 Hz, 2H). ^{13}C NMR (100 MHz, $CDCl_3$) δ 24.96, 29.37, 51.35, 71.94, 83.89, 128.90, 135.34, 137.50, 206.18. MS (EI) Calc $[M]^+$ ($C_{15}H_{21}BO_3$) *m/z* = 260.16. Found $[M]^+$ *m/z* = 260.1.

Synthesis of 22. Pyrazole (776 mg, 11.4 mmol), 2-bromopyridine (1.5 g, 9.5 mmol), copper (I) iodide (362 mg, 1.9 mmol), l-proline (437 mg, 3.8 mmol) and potassium carbonate (6.56 g, 47.5 mmol) were added to a 100 mL round bottom flask. The flask was evacuated and backfilled with nitrogen followed by the addition of 30 mL of anhydrous DMSO via syringe. The reaction mixture stirred at 90˚C overnight and was then diluted with 200 mL of ethyl acetate and washed with three 100 mL portions of water. The organic layer was dried over sodium sulfate and concentrated by rotary evaporation. The residue was purified through a silica gel column with 25% ethyl acetate in hexane as the eluent to give 702 mg of white solid in 51% yield. ^{1}H NMR (400 MHz, $CDCl_3$) δ 6.45 (s, 1H), 7.10-7.25 (m, 1H), 7.14-7.77 (m, 2H), 7.94-7.96 (m, 1H), 8.73 (s, 1H), 8.55 (s, 1H). ^{13}C NMR (100 MHz, $CDCl_3$) δ 107.88, 112.48, 121.46, 127.09, 138.78, 142.12, 148.09, 151.64. MS (EI) Calc $[M]^+$ ($C_8H_7N_3$) *m/z* = 145.06. Found $[M]^+$ *m/z* = 145.1.

Synthesis of 23. Compound **22** (607 mg, 4.18 mmol) and *N*-bromosuccinimide (1.116 g, 6.29 mmol)) were added to a 250 mL reaction vial. The solids were dissolved in DMF (50 mL) and stirred in the dark at room temperature for 24 hours. The reaction mixture was diluted with 300 mL of ethyl acetate and washed with 10% NaOH in three 50 mL portions. The organic layer was dried over sodium sulfate and concentrated by rotary evaporation to give 800 mg of white solid in 85% yield. ^{1}H NMR (400 MHz, $CDCl_3$) δ 7.19-7.22 (m, 1H), 7.67 (s, 1H), 7.79-7.84 (m, 1H), 7.93 (d, *J* = 8 Hz, 1H), 8.38-8.40 (m, 1H), 8.58 (s, 1H). ^{13}C NMR (100 MHz, $CDCl_3$) δ 96.33. 111.85, 121.83, 127.22, 138.76, 142.34, 148.03, 150.79. MS (EI) Calc $[M]^+$ ($C_8H_6BrN_3$) *m/z* = 222.97. Found $[M]^+$ *m/z* = 223.0.

General Procedure for preparing platinum complexes. Complexes were prepared according to a procedure reported by Newkome et al.[27] Briefly, potassium tetrachloroplatinate (II) is dissolved in water at 65 ˚C and then an equimolar amount of the ligand is added dropwise in a solution of acetone. The solution is maintained at 65 ˚C for 6h and then cooled to room temperature and filtered. The precipitate is washed excessively with water and acetone. The solids were screened for their in vitro toxicity. Only the complexes that were taken forward to polymer attachment and *in vivo* evaluation were fully analyzed.

Synthesis of 7. ^{1}H NMR (500 MHz, DMSO-d_6) δ 2.69 (s, 3H), 7.89 (s, 1H), 8.43 (s, 1H), 8.63-8.67 (m, 2H), 8.21-8.24 (m, 1H), 9.56 (s, 1H), 10.00 (s, 1H). Anal. Calcd for $C_{12}H_{10}Cl_2N_2OPt$: C, 31.05; H, 2.17; N, 6.03. Found: C, 31.27; H, 1.98; N, 5.88.

Synthesis of 8. ^{1}H NMR (500 MHz, DMSO-d_6) δ 2.70 (s, 3H), 7.74-7.76 (m, H), 8.02 (t, *J* = 7.5 Hz, 1H), 8.25 (d, *J* = 8.5 Hz, 1H), 8.48 (d, *J* = 8 Hz, 1H), 8.68 (d, *J* = 8.5 Hz, 1H), 8.87-8.92 (m, 2H), 9.46 (d, *J* = 5 Hz, 1H), 9.98 (s, 1H). Anal. Calcd for $C_{16}H_{12}Cl_2N_2OPt$: C, 37.37; H, 2.15; N, 5.45. Found: C, 36.79; H, 2.09; N, 5.15.

Synthesis of 18. ^{1}H NMR (500 MHz, DMSO-d_6) δ 1.32 (s, 9H), 2.67 (s, 3H), 7.51-7.79 (m, 4H), 8.37 (d, *J* = 8.5 Hz, 1H), 8.70 (s, 1H), 8.99 (d, *J* = 7 Hz, 1H), 9.56 (s, 1H), 9.86 (s, 1H). Anal. Calcd for $C_{16}H_{12}Cl_2N_2OPt$: C, 41.03; H, 3.62; N, 7.18. Found: C, 40.15; H 3.07; N, 7.76.

Synthesis of 36. ^{1}H NMR (500 MHz, DMSO-d_6) δ 2.60 (s, 3H), 7.69-7.71 (m, 1H), 7.78 (t, *J* = 7.5 Hz, 1H), 7.88-8.01 (m, 4H), 8.08 (d, *J* = 5 Hz), 8.17 (d, *J* = 6 Hz, 1H), 8.41 (s, 1H), 8.55-8.57

(m, 1H), 9.05-9.06 (m, 1H), 9.26 (s, 1H). Anal. Calcd for $C_{20}H_{15}Cl_2N_3OPt$: C, 41.46; H, 2.44; N, 7.25. Found: C, 41.84; H, 2.55; N, 6.92.

Synthesis of 37. ^{1}H NMR (500 MHz, DMSO-d_6) δ 2.66 (s, 3H), 7.58 (t, J = 8 Hz, 1H), 7.69-7.71 (m, 1H), 7.78 (t, J = 8 Hz, 1H), 7.99-8.01 (m, 1H), 8.16-8.18 (m, 1H), 8.26 (s, 1H), 8.55-8.57 (m, 1H), 9.06-9.07 (m, 1H), 9.25 (s, 1H). Anal. Calcd for $C_{20}H_{15}Cl_2N_3OPt$: C, 41.46; H, 2.44; N, 7.25. Found: C, 41.52; H, 2.55; N, 7.29.

Synthesis of 38. ^{1}H NMR (500 MHz, DMSO-d_6) δ 2.15 (s, 3H), 3.78 (s, 2H), 7.23-7.25 (m, 2H), 7.66-7.71 (m, 3H), 7.77 (t, J = 7 Hz, 1H), 8.06 (d, J = 8 Hz, 1H), 8.17 (d, J = 7.5 Hz, 1H), 8.27 (s, 1H), 8.55 (d, J = 8.5 Hz, 1H), 9.04-9.05 (m, 1H), 9.15 (s, 1H). Anal. Calcd for $C_{21}H_{17}Cl_2N_3OPt$: C, 42.51; H, 2.89; N, 7.08. Found: C, 40.99; H, 2.11; N, 7.25.

General Procedure for Platinum Attachment to Polymer. Dendrimer **51** was prepared by the exact procedure outlined in Chapter 2. The hydrazide terminated poly(ethylene) glycol was purchased from Laysan Bio Inc (Arab, Alabama). The polymer and three equivalents of complex per hydrazide were weighed into a 20 mL reaction vial that is under nitrogen atmosphere. The solids are dissolved in dry dimethylformamide at a concentration of ~100 mg/mL with respect to the polymer. The solution was stirred at 60˚ C for 18h and then precipitated into ether. The polymer was redissolved in methanol and filtered again through a 20 μm filter to remove excess small molecule platinum, which is not soluble in methanol. The polymer is then purified by size exclusion chromatography through an LH-20 size exclusion resin with methanol as the eluent to remove any trace free drug. Finally, the polymer samples are redissolved in water and passed through PD-10 desalting columns and lyophilized. The drug loading of the final conjugates was determined by inductively coupled plasma atomic emission spectroscopy.

Toxicity of Platinum Complexes in C26 cells. Cells were seeded onto a 96-well plate at a density of 5.0 x 10^3 cells per well in 100 μl of medium and incubated overnight (37 °C, 5% CO_2, and 80% humidity). An additional 100 μl of new medium (RPMI medium 1640/10% FBS/1% penicillin-streptomycin) containing the platinum complexes, or oxaliplatin and cisplatin controls, was added to the cells. Small molecule drugs were tested at concentrations ranging from 450 μM to 0.2 μM Pt equivalents, PEG-Pt from 900 μM to 0.4 μM, and dendrimer-Pt from 1.1 mM to 0.3 μM. The tests were conducted in triplicate for each concentration. After incubation for 72 h, 40 μl of media containing thiazolyl blue tetrazolium bromide solution (2.5 mg/mL) was added. The cells were incubated for 2 h, after which time the medium was carefully removed. To the resulting purple crystals was added 200 μl of DMSO, followed by 25 μl of pH 10.5 glycine buffer (0.1 M glycine/0.1 M NaCl). The optical densities at 570 nm were measured by using a SpectraMAX 190 microplate reader (Molecular Devices, Sunnyvale, CA). Optical densities measured for wells containing cells that received neither polymer nor drug were considered to represent 100% viability. IC_{50} values were obtained from sigmoidal fits of semilogarithmic plots of the percentage of viability versus platinum concentration by using Origin 7 SR4 8.0552 software (OriginLab, Northhampton, MA).

Drug Release Experiments. Hydrolysis of the platinum drug was monitored by HPLC with SEC system C and a Shodex SB-804 HQ column maintained at 37 °C. An isocratic flow rate of

0.7 mL/min was used with a 70%/30%/0.05% water/acetonitrile/TFA mobile phase. Each sample was dissolved in 37 °C acetate buffer (pH 5, 100 mM) at a concentration of ~ 2 mg/ml and filtered. Samples were kept at 37 °C for the duration of the study with 25 μL aliquots injected over 48 h.

Animal and Tumor Models. All animal experiments were performed in compliance with National Institutes of Health guidelines for animal research under a protocol approved by the Committee on Animal Research at the University of California (San Francisco, CA) (UCSF). C26 colon carcinoma cells obtained from the UCSF cell culture facility were cultured in RPMI medium 1640 containing 10% FBS. Female BALB/c mice were obtained from Simonsen Laboratories, Inc. (Gilroy, CA).

Biodistribution Study in Xenograph Mice. Six- to eight week-old female Balb/C mice were injected in the right hind flank with $3x10^5$ C26 cells. Twelve days after tumor inoculation, mice were randomized into five groups of two mice each. Mice were injected by means of the tail vein either with Cisplatin (6 mg/kg), **38** (6 mg/kg), **50** (6 mg Pt/kg), **41** (6 mg Pt/kg) or **44** (6 mg Pt/kg) ~200 μL of PBS. Blood was collected by submandibular bleeds 60 min and 24 h after dosing; mice were sacrificed 48 h postinjection. The blood (collected by heart puncture), heart, liver, spleen, kidney, and tumor were collected for analysis. Blood was collected in vials coated with 10 μL heparin (50 mg/mL) to prevent clotting and centrifuged for 10 min at 5,000 rpm to allow for serum removal. Each organ was weighed and 200-300 mg of the collected organs were homogenized with zirconium beads and 250 μL deionized water. The tissue and 48 h serum samples were diluted with 583 μL concentrated HNO_3 and the remaining serum samples were diluted with 200 μL dI water and 466 μL HNO_3 (~70% acid solution). Samples were gently heated at 40 °C overnight. Supernatant (500 μL) was added to 3.5 mL 20% HCl and briefly centrifuged to remove any insoluble particulates. Platinum content in each sample was analyzed by ICP at 265 nm.

Maximum Tolerated Dose in Healthy Mice. Female Balb/C mice were injected with via tail vein injection (15 mg Pt/kg and 45 mg Pt/kg) or via intraperitoneal (90 mg Pt/kg) with polymers **39**-**44**. Mice weight and general health was monitored over 10 days. When gross toxicity was observed, loss of greater than 15% of initial body weight, lethargy and ruffled fur, mice were removed from the study.

Chemotherapy Experiment in Xenograph Mice. While under anesthesia, female Balb/C mice were shaved, and C26 cells (3×10^5 cells in 50 μL) were injected subcutaneously in the right hand flank. At eight days post-tumor implantation, mice were randomly distributed into treatment groups of 6 animals. Mice were injected by means of the tail vein with Cisplatin (6 mg/kg), **38** (10 mg/kg), Doxil (20 mg Dox/kg), and polymers **39**-**44** (36 mg Pt/kg) in approximately 200 μL of solution. Mice were weighed and tumors measured every other day. The tumor volume was estimated by measuring the tumor volume in three dimension with calipers and calculated using the formula tumor volume = length x width x height. Mice were removed from the study when (i) a mouse lost 15% of its initial weight, (ii) any tumor dimension was > 20 mm, or (iii) the mouse was found dead. The mice were followed until day 60 post-tumor inoculation.

Computational Modeling. Molecular geometries were optimized to an energy minimum using Gaussian 09 at the DFT B3LYP level with lanl2dz basis set on Pt and 6-31G(d,p) on all other atoms.[28] Optimized geometries were confirmed as energy minima through a vibration calculation at the same level which yielded no negative frequencies. Bond distances and angles were taken from these optimized geometries.

Crystallography. A yellow rod 0.25 x 0.10 x 0.10 mm in size was mounted on a Cryoloop with Paratone oil. Data were collected in a nitrogen gas stream at 153(2) K using phi and omega scans. Crystal-to-detector distance was 60 mm and exposure time was 10 seconds per frame using a scan width of 0.3°. Data collection was 100.0% complete to 25.00° in θ. A total of 19953 reflections were collected covering the indices, -9<=*h*<=9, -16<=*k*<=16, -20<=*l*<=20. 3412 reflections were found to be symmetry independent, with an R_{int} of 0.0224. Indexing and unit cell refinement indicated a primitive, monoclinic lattice. The space group was found to be P2(1)/c (No. 14). The data were integrated using the Bruker SAINT software program and scaled using the SADABS software program. Solution by direct methods (SIR-2008) produced a complete heavy-atom phasing model consistent with the proposed structure. All non-hydrogen atoms were refined anisotropically by full-matrix least-squares (SHELXL-97). All hydrogen atoms were placed using a riding model. Their positions were constrained relative to their parent atom using the appropriate HFIX command in SHELXL-97.

Table 2. Crystal data and structure refinement for **37**.

X-ray ID	**37**	
Sample/notebook ID	DV-5-76	
Empirical formula	C20 H15 Cl2 N3 O Pt	
Formula weight	579.34	
Temperature	153(2) K	
Wavelength	0.71073 Å	
Crystal system	Monoclinic	
Space group	P2(1)/c	
Unit cell dimensions	a = 7.9363(13) Å	α= 90°.
	b = 13.778(2) Å	β= 101.499(2)°.
	c = 17.356(3) Å	γ = 90°.
Volume	1859.8(5) $Å^3$	
Z	4	
Density (calculated)	2.069 Mg/m^3	
Absorption coefficient	7.848 mm^{-1}	
F(000)	1104	
Crystal size	0.25 x 0.10 x 0.10 mm^3	
Crystal color/habit	yellow rod	

Theta range for data collection	1.90 to 25.35°.
Index ranges	-9<=h<=9, -16<=k<=16, -20<=l<=20
Reflections collected	19953
Independent reflections	3412 [R(int) = 0.0224]
Completeness to theta = 25.00°	100.0 %
Absorption correction	Semi-empirical from equivalents
Max. and min. transmission	0.5075 and 0.2444
Refinement method	Full-matrix least-squares on F^2
Data / restraints / parameters	3412 / 0 / 245
Goodness-of-fit on F^2	1.033
Final R indices [I>2sigma(I)]	R1 = 0.0184, wR2 = 0.0439
R indices (all data)	R1 = 0.0193, wR2 = 0.0445
Largest diff. peak and hole	1.503 and -0.842 e.Å^{-3}

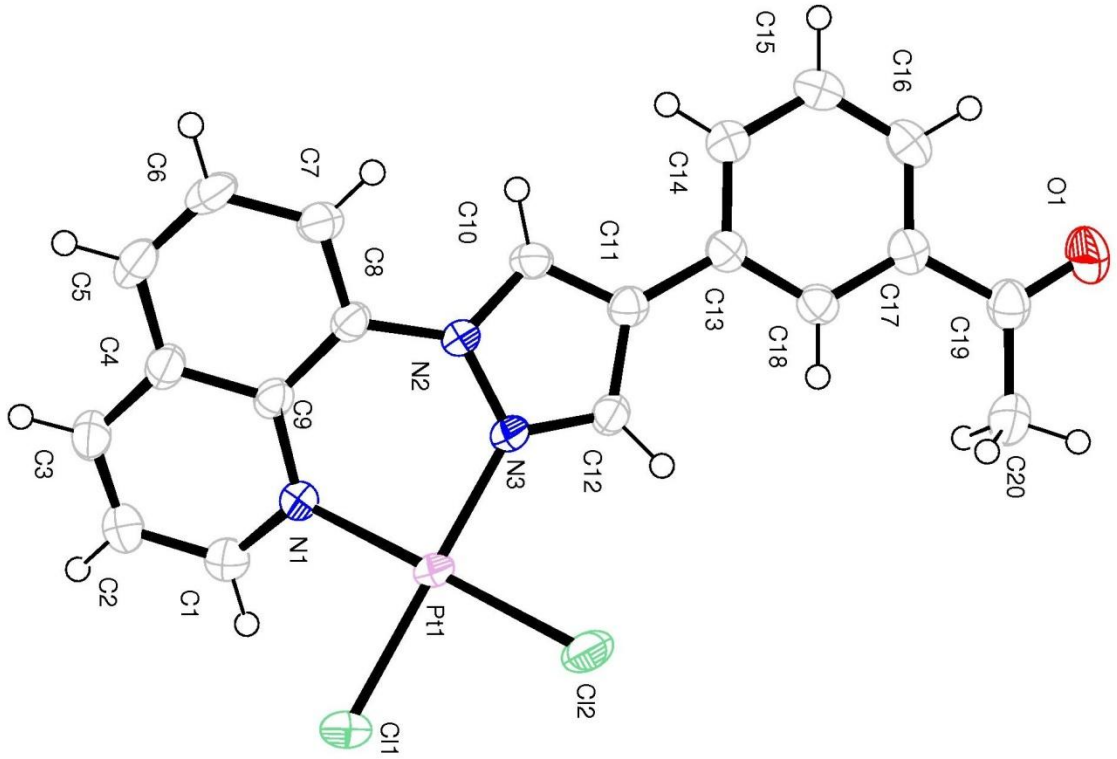

Figure 10. Crystal Stucture of **37.**

Table 3. Atomic coordinates (x 10^4) and equivalent isotropic displacement parameters ($Å^2$x 10^3) for **37**. U(eq) is defined as one third of the trace of the orthogonalized U^{ij} tensor.

	x	y	z	U(eq)
C(1)	12850(5)	980(3)	1803(2)	40(1)
C(2)	13950(5)	325(3)	1530(2)	48(1)
C(3)	13598(5)	66(3)	763(2)	42(1)
C(4)	12275(4)	534(2)	240(2)	33(1)
C(5)	11906(5)	316(3)	-578(2)	37(1)
C(6)	10700(5)	822(3)	-1080(2)	38(1)
C(7)	9835(5)	1594(3)	-800(2)	34(1)
C(8)	10148(4)	1829(2)	-16(2)	27(1)
C(9)	11305(4)	1270(2)	535(2)	28(1)
C(10)	8896(4)	3464(2)	-294(2)	29(1)
C(11)	8194(4)	4161(2)	115(2)	28(1)
C(12)	8346(4)	3780(2)	872(2)	28(1)
C(13)	7434(4)	5091(2)	-208(2)	28(1)
C(14)	7305(4)	5303(3)	-1003(2)	36(1)
C(15)	6568(5)	6164(3)	-1316(2)	42(1)
C(16)	5937(5)	6820(3)	-848(2)	37(1)
C(17)	6063(4)	6627(2)	-54(2)	31(1)
C(18)	6816(4)	5762(2)	264(2)	29(1)
C(19)	5328(5)	7359(3)	422(2)	38(1)
C(20)	5592(6)	7227(3)	1293(3)	52(1)
N(1)	11526(3)	1402(2)	1337(2)	29(1)
N(2)	9413(3)	2710(2)	196(2)	26(1)
N(3)	9072(3)	2905(2)	921(2)	26(1)
O(1)	4531(4)	8049(2)	104(2)	51(1)
Cl(1)	10142(1)	884(1)	2836(1)	42(1)
Cl(2)	7426(1)	2592(1)	2356(1)	44(1)
Pt(1)	9611(1)	1979(1)	1817(1)	27(1)

Table 4. Bond lengths [Å] and angles [°] for **37**.

C(1)-N(1)	1.326(4)	C(1)-C(2)	1.403(5)

C(1)-H(1)	0.9500	C(12)-H(12)	0.9500
C(2)-C(3)	1.353(5)	C(13)-C(18)	1.387(5)
C(2)-H(2)	0.9500	C(13)-C(14)	1.395(5)
C(3)-C(4)	1.401(5)	C(14)-C(15)	1.385(5)
C(3)-H(3)	0.9500	C(14)-H(14)	0.9500
C(4)-C(5)	1.422(5)	C(15)-C(16)	1.376(5)
C(4)-C(9)	1.429(4)	C(15)-H(15)	0.9500
C(5)-C(6)	1.351(5)	C(16)-C(17)	1.387(5)
C(5)-H(5)	0.9500	C(16)-H(16)	0.9500
C(6)-C(7)	1.405(5)	C(17)-C(18)	1.397(5)
C(6)-H(6)	0.9500	C(17)-C(19)	1.495(5)
C(7)-C(8)	1.373(5)	C(18)-H(18)	0.9500
C(7)-H(7)	0.9500	C(19)-O(1)	1.213(4)
C(8)-C(9)	1.414(5)	C(19)-C(20)	1.495(6)
C(8)-N(2)	1.426(4)	C(20)-H(20A)	0.9800
C(9)-N(1)	1.379(4)	C(20)-H(20B)	0.9800
C(10)-N(2)	1.354(4)	C(20)-H(20C)	0.9800
C(10)-C(11)	1.376(4)	N(1)-Pt(1)	2.035(3)
C(10)-H(10)	0.9500	N(2)-N(3)	1.364(4)
C(11)-C(12)	1.399(4)	N(3)-Pt(1)	1.991(3)
C(11)-C(13)	1.478(4)	Cl(1)-Pt(1)	2.2983(9)
C(12)-N(3)	1.332(4)	Cl(2)-Pt(1)	2.2903(9)

N(1)-C(1)-C(2)	123.2(3)	C(6)-C(5)-H(5)	119.6
N(1)-C(1)-H(1)	118.4	C(4)-C(5)-H(5)	119.6
C(2)-C(1)-H(1)	118.4	C(5)-C(6)-C(7)	120.0(3)
C(3)-C(2)-C(1)	118.8(4)	C(5)-C(6)-H(6)	120.0
C(3)-C(2)-H(2)	120.6	C(7)-C(6)-H(6)	120.0
C(1)-C(2)-H(2)	120.6	C(8)-C(7)-C(6)	121.1(3)
C(2)-C(3)-C(4)	119.8(3)	C(8)-C(7)-H(7)	119.4
C(2)-C(3)-H(3)	120.1	C(6)-C(7)-H(7)	119.4
C(4)-C(3)-H(3)	120.1	C(7)-C(8)-C(9)	120.5(3)
C(3)-C(4)-C(5)	121.9(3)	C(7)-C(8)-N(2)	117.0(3)
C(3)-C(4)-C(9)	118.8(3)	C(9)-C(8)-N(2)	122.2(3)
C(5)-C(4)-C(9)	119.3(3)	N(1)-C(9)-C(8)	123.0(3)
C(6)-C(5)-C(4)	120.9(3)	N(1)-C(9)-C(4)	119.1(3)

C(8)-C(9)-C(4)	117.9(3)
N(2)-C(10)-C(11)	108.3(3)
N(2)-C(10)-H(10)	125.8
C(11)-C(10)-H(10)	125.8
C(10)-C(11)-C(12)	104.8(3)
C(10)-C(11)-C(13)	125.9(3)
C(12)-C(11)-C(13)	129.3(3)
N(3)-C(12)-C(11)	110.7(3)
N(3)-C(12)-H(12)	124.6
C(11)-C(12)-H(12)	124.6
C(18)-C(13)-C(14)	118.7(3)
C(18)-C(13)-C(11)	121.3(3)
C(14)-C(13)-C(11)	120.0(3)
C(15)-C(14)-C(13)	120.6(3)
C(15)-C(14)-H(14)	119.7
C(13)-C(14)-H(14)	119.7
C(16)-C(15)-C(14)	120.5(3)
C(16)-C(15)-H(15)	119.8
C(14)-C(15)-H(15)	119.8
C(15)-C(16)-C(17)	119.8(3)
C(15)-C(16)-H(16)	120.1
C(17)-C(16)-H(16)	120.1
C(16)-C(17)-C(18)	119.8(3)
C(16)-C(17)-C(19)	117.5(3)
C(18)-C(17)-C(19)	122.7(3)
C(13)-C(18)-C(17)	120.6(3)
C(13)-C(18)-H(18)	119.7
C(17)-C(18)-H(18)	119.7
O(1)-C(19)-C(20)	120.7(4)
O(1)-C(19)-C(17)	120.2(4)
C(20)-C(19)-C(17)	119.1(3)
C(19)-C(20)-H(20A)	109.5
C(19)-C(20)-H(20B)	109.5
H(20A)-C(20)-H(20B)	109.5
C(19)-C(20)-H(20C)	109.5
H(20A)-C(20)-H(20C)	109.5
H(20B)-C(20)-H(20C)	109.5
C(1)-N(1)-C(9)	118.9(3)
C(1)-N(1)-Pt(1)	119.2(2)
C(9)-N(1)-Pt(1)	120.6(2)
C(10)-N(2)-N(3)	109.7(3)
C(10)-N(2)-C(8)	125.4(3)
N(3)-N(2)-C(8)	124.8(3)
C(12)-N(3)-N(2)	106.5(3)
C(12)-N(3)-Pt(1)	130.7(2)
N(2)-N(3)-Pt(1)	122.87(19)
N(3)-Pt(1)-N(1)	89.54(11)
N(3)-Pt(1)-Cl(2)	91.19(8)
N(1)-Pt(1)-Cl(2)	178.67(8)
N(3)-Pt(1)-Cl(1)	178.01(8)
N(1)-Pt(1)-Cl(1)	91.23(8)
Cl(2)-Pt(1)-Cl(1)	88.02(3)

Table 5. Anisotropic displacement parameters ($Å^2 x\ 10^3$)for **37**. The anisotropic displacement factor exponent takes the form: $-2\pi^2[\ h^2 a^{*2} U^{11} + ... + 2\ h\ k\ a^*\ b^*\ U^{12}\ ]$

	U^{11}	U^{22}	U^{33}	U^{23}	U^{13}	U^{12}
C(1)	44(2)	44(2)	31(2)	2(2)	7(2)	10(2)
C(2)	51(2)	48(2)	45(2)	8(2)	13(2)	23(2)
C(3)	47(2)	35(2)	47(2)	4(2)	19(2)	13(2)
C(4)	40(2)	26(2)	37(2)	-1(1)	17(2)	1(1)
C(5)	46(2)	31(2)	41(2)	-8(2)	23(2)	-3(2)
C(6)	53(2)	37(2)	27(2)	-10(2)	17(2)	-7(2)
C(7)	43(2)	34(2)	27(2)	0(1)	10(2)	1(2)
C(8)	30(2)	28(2)	27(2)	-2(1)	11(1)	0(1)
C(9)	32(2)	25(2)	29(2)	0(1)	13(1)	-1(1)
C(10)	32(2)	32(2)	23(2)	3(1)	7(1)	0(1)
C(11)	24(2)	33(2)	29(2)	0(1)	7(1)	-1(1)
C(12)	28(2)	30(2)	27(2)	-4(1)	6(1)	3(1)
C(13)	22(2)	30(2)	32(2)	3(1)	6(1)	-1(1)
C(14)	40(2)	37(2)	33(2)	2(2)	11(2)	5(2)
C(15)	49(2)	45(2)	31(2)	8(2)	6(2)	6(2)
C(16)	36(2)	30(2)	41(2)	8(2)	3(2)	1(1)
C(17)	26(2)	29(2)	39(2)	2(1)	7(1)	-2(1)
C(18)	27(2)	30(2)	30(2)	3(1)	6(1)	-1(1)
C(19)	37(2)	30(2)	47(2)	2(2)	12(2)	1(2)
C(20)	64(3)	44(2)	52(2)	3(2)	24(2)	20(2)
N(1)	33(1)	30(2)	27(1)	2(1)	9(1)	6(1)
N(2)	29(1)	28(1)	22(1)	0(1)	8(1)	4(1)
N(3)	29(1)	29(1)	20(1)	-2(1)	6(1)	3(1)
O(1)	61(2)	33(2)	58(2)	2(1)	10(2)	16(1)
Cl(1)	58(1)	45(1)	26(1)	8(1)	14(1)	7(1)
Cl(2)	38(1)	69(1)	25(1)	-1(1)	11(1)	12(1)
Pt(1)	32(1)	32(1)	19(1)	-1(1)	7(1)	4(1)

Table 6. Hydrogen coordinates (x 10^4) and isotropic displacement parameters ($Å^2$x 10^3) for **37**.

	x	y	z	U(eq)
H(1)	13065	1130	2348	48
H(2)	14925	67	1878	57
H(3)	14246	-432	579	50
H(5)	12514	-191	-773	44
H(6)	10439	655	-1621	45
H(7)	9018	1960	-1159	41
H(10)	9001	3505	-829	34
H(12)	7980	4101	1295	34
H(14)	7727	4852	-1334	43
H(15)	6498	6302	-1858	50
H(16)	5416	7405	-1068	44
H(18)	6906	5632	808	35
H(20A)	5031	7759	1521	78
H(20B)	6826	7230	1520	78
H(20C)	5092	6607	1410	78

References

(1) Giandomenico, C. M.; Abrams, M. J.; Murrer, B. A.; Vollano, J. F.; Rheinheimer, M. I.; Wyer, S. B.; Bossard, G. E.; Higgins, J. D. *Inorg Chem* **1995**, *34*, 1015-1021.

(2) Dhar, S.; Lippard, S. J. *P Natl Acad Sci USA* **2009**, *106*, 22199-22204.

(3) Mukhopadhyay, S.; Barnes, C. M.; Haskel, A.; Short, S. M.; Barnes, K. R.; Lippard, S. J. *Bioconjugate Chem* **2008**, *19*, 39-49.

(4) Dhar, S.; Liu, Z.; Thomale, J.; Dai, H. J.; Lippard, S. J. *J Am Chem Soc* **2008**, *130*, 11467-11476.

(5) Dhar, S.; Gu, F. X.; Langer, R.; Farokhzad, O. C.; Lippard, S. J. *P Natl Acad Sci USA* **2008**, *105*, 17356-17361.

(6) Dhar, S.; Daniel, W. L.; Giljohann, D. A.; Mirkin, C. A.; Lippard, S. J. *J Am Chem Soc* **2009**, *131*, 14652-14653.

(7) Aryal, S.; Hu, C. M. J.; Zhang, L. F. *Acs Nano* **2010**, *4*, 251-258.

(8) Lee, C. C.; Gillies, E. R.; Fox, M. E.; Guillaudeu, S. J.; Frechet, J. M. J.; Dy, E. E.; Szoka, F. C. *P Natl Acad Sci USA* **2006**, *103*, 16649-16654.

(9) van der Poll, D. G.; Kieler-Ferguson, H. M.; Floyd, W. C.; Guillaudeu, S. J.; Jerger, K.; Szoka, F. C.; Frechet, J. M. *Bioconjugate Chem* **2010**, *21*, 764-773.
(10) Floyd, W. C., 3rd; Datta, G. K.; Imamura, S.; Kieler-Ferguson, H. M.; Jerger, K.; Patterson, A. W.; Fox, M. E.; Szoka, F. C.; Frechet, J. M.; Ellman, J. A. *ChemMedChem* **2010,** doi: 10.1002/cmdc.201000377.
(11) Kelland, L. *Nat Rev Cancer* **2007**, *7*, 573-584.
(12) Gangopadhyay, S. B.; Roendigs, A.; Kangarloo, S. B.; Krebs, B.; Wolff, J. E. A. *Anticancer Res* **2001**, *21*, 2039-2043.
(13) Wilson, J. J.; Lopes, J. F.; Lippard, S. J. *Inorg Chem* **2010**, *49*, 5303-5315.
(14) Puscasu, I.; Mock, C.; Rauterkus, M.; Rondigs, A.; Tallen, G.; Gangopadhyay, S.; Wolff, J. E. A.; Krebs, B. *Z Anorg Allg Chem* **2001**, *627*, 1292-1298.
(15) Mansouri-Torshizi, H.; I-Moghaddam, M.; Divsalar, A.; Saboury, A. A. *Bioorgan Med Chem* **2008**, *16*, 9616-9625.
(16) Mansuri-Torshizi, H.; Ghadimy, S.; Akbarzadeh, N. *Chem Pharm Bull* **2001**, *49*, 1517-1520.
(17) Jin, V. X.; Ranford, J. D. *Inorg Chim Acta* **2000**, *304*, 38-44.
(18) Keter, F. K.; Kanyanda, S.; Lyantagaye, S. S.; Darkwa, J.; Rees, D. J.; Meyer, M. *Cancer Chemother Pharmacol* **2008**, *63*, 127-38.
(19) Elwell, K. E.; Hall, C.; Tharkar, S.; Giraud, Y.; Bennett, B.; Bae, C.; Carper, S. W. *Bioorgan Med Chem* **2006**, *14*, 8692-8700.
(20) Vo, V.; Kabuloglu-Karayusuf, Z. G.; Carper, S. W.; Bennett, B. L.; Evilia, C. *Bioorgan Med Chem* **2010**, *18*, 1163-1170.
(21) Marverti, G.; Cusumano, M.; Ligabue, A.; Di Pietro, M. L.; Vainiglia, P. A.; Ferrari, A.; Bergomi, M.; Moruzzi, M. S.; Frassineti, C. *J Inorg Biochem* **2008**, *102*, 699-712.
(22) Lovejoy, K. S.; Todd, R. C.; Zhang, S. Z.; McCormick, M. S.; D'Aquino, J. A.; Reardon, J. T.; Sancar, A.; Giacomini, K. M.; Lippard, S. J. *P Natl Acad Sci USA* **2008**, *105*, 8902-8907.
(23) Deng, J. Z.; Paone, D. V.; Ginnetti, A. T.; Kurihara, H.; Dreher, S. D.; Weissman, S. A.; Stauffer, S. R.; Burgey, C. S. *Org Lett* **2009**, *11*, 345-347.
(24) Guillaudeu, S. J.; Fox, M. E.; Haidar, Y. M.; Dy, E. E.; Szoka, F. C.; Frechet, J. M. J. *Bioconjugate Chem* **2008**, *19*, 461-469.
(25) Gillies, E. R.; Frechet, J. M. J. *J Am Chem Soc* **2002**, *124*, 14137-14146.
(26) Fox, M. E.; Guillaudeu, S.; Frechet, J. M. J.; Jerger, K.; Macaraeg, N.; Szoka, F. C. *Mol Pharmaceut* **2009**, *6*, 1562-1572.
(27) Newkome, G. R.; Theriot, K. J.; Fronczek, F. R.; Villar, B. *Organometallics* **1989**, *8*, 2513-2523.
(28). Gaussian 09, Revision **A.1**, Frisch, M. J.; Trucks, G. W.; Schlegel, H. B.; Scuseria, G. E.; Robb, M. A.; Cheeseman, J. R.; Scalmani, G.; Barone, V.; Mennucci, B.; Petersson, G. A.; Nakatsuji, H.; Caricato, M.; Li, X.; Hratchian, H. P.; Izmaylov, A. F.; Bloino, J.; Zheng, G.; Sonnenberg, J. L.; Hada, M.; Ehara, M.; Toyota, K.; Fukuda, R.; Hasegawa, J.; Ishida, M.; Nakajima, T.; Honda, Y.; Kitao, O.; Nakai, H.; Vreven, T.; Montgomery, Jr., J. A.; Peralta, J. E.; Ogliaro, F.; Bearpark, M.; Heyd, J. J.; Brothers, E.; Kudin, K. N.; Staroverov, V. N.; Kobayashi, R.; Normand, J.; Raghavachari, K.; Rendell, A.; Burant, J. C.; Iyengar, S. S.; Tomasi, J.; Cossi, M.; Rega, N.; Millam, N. J.; Klene, M.; Knox, J. E.; Cross, J. B.; Bakken, V.; Adamo, C.; Jaramillo, J.; Gomperts, R.; Stratmann, R. E.; Yazyev, O.; Austin, A. J.; Cammi, R.; Pomelli, C.; Ochterski, J. W.; Martin, R. L.;

Morokuma, K.; Zakrzewski, V. G.; Voth, G. A.; Salvador, P.; Dannenberg, J. J.; Dapprich, S.; Daniels, A. D.; Farkas, Ö.; Foresman, J. B.; Ortiz, J. V.; Cioslowski, J.; Fox, D. J. Gaussian, Inc., Wallingford CT, 2009.

Chapter 6 – Synthesis of Hyaluronic Acid Targeted Liposomes

Abstract

Hyaluronic acid (HA), is a natural occurring polysachharide that is a major component of the extracellular matrix. HA interacts with surface bound receptors to regulate cell proliferation and movement. HA is the major ligand for the CD44 receptor and expression of CD44 is upregulated during carcinogenesis. This makes HA a promising targeting ligand for cancer cells. Attachment of HA to a drug loaded carrier is difficult due to the solubility and functionality of HA. In Chapter 6, a new protocol for attaching distearoylphosphatidylethanolamine (DSPE) to the reducing end of HA oligomers in a site specific manner is described. Glycolipids containing HA oligomers of 10 and 24 monosaccharides in length were used to make liposomes which were then evaluated for cell binding and internalization *in vitro.*

Introduction

Since their discovery, liposomes have received great attention as drug carriers.[1] PEGylated stealth liposomes are spherical lipid bilayers with aquoues interiors that can encapsulate drug molecules. Their large size (~100 nm) gives liposomes extended blood circulation times, allowing them to passively target tumor tissue by the enhanced permeation and retention (EPR) effect. Liposomal formulations have been FDA approved for the treatment of certain tumors and fungal diseases in humans. An advantage of liposomal delivery over polymeric delivery is that they can be prepared from natural phospholipids instead of synthetic polymers. Their simple preparation has allowed liposomes to become a platform technology in drug delivery research. One active area of liposome research is in the development of liposomes with targeting ligands displayed on their surface. Such targeting ligands show promise to further improve the efficacy of liposomal drugs by facilitating cellular uptake in specific cells of interest. Active tumor targeting can only be successful if the receptor being targeted is significantly overexpressed on cells of interest. To this end, the CD44 receptor is an attractive target since it is found at elevated levels on various cancer types and at low levels on epithelial, hemopoietic and neuronal cells. Hyaluronic acid (HA) is a poly(disaccharide) that is the main binding ligand for CD44. Hyaluronic acid is a component of the extracellular matrix and its interaction with CD44 is implicated in regulate cell proliferation and movement. CD44 ligation can induce cell transformation, unregulated cell growth, resistance to apoptosis and increased cell migration.[2]

A number of strategies have been employed to create HA targeted delivery vehicles with chemotherapeutic playloads.[3] These include high molecular weight HA-Taxol conjugates[4,5], and HA-HPMA-Doxorubicin conjugates.[6] There have also been reports of conjugating high molecular weight HA via amide bond formation between the phosphatidylethanolamine surface of a liposome and the carboxylates of the D-glucoronic acid repeat unit of HA.[7,8] The Szoka group has prepared HA functionalized liposomes using a reductive amination between the reducing end of HA and amine functionalized phospholipids.[9-11] The advantage of this approach is that HA oligomers of a defined size were attached in a site-specific manner, which guarantees batch-to-batch reproducibility and easy characterization. High molecular weight HA can be digested with hyaluronidase and the resulting oligomers can be fractionated and isolated as nearly monodisperse entities.[12,13] This is significant because it allows for HA-lipids to be prepared with different lengths of HA oligomer. An important consideration when designing an HA targeted liposome is the fact that there are receptors other than CD44 that will recognize circulating high molecular weight HA.[14-16] Our goal is to determine an appropriate length of HA oligomer that when expressed on a liposome surface will bind CD44 but none of the other receptors capable of recognizing the naturally occurring high molecular weight HA.

Reductive amination between a primary amine and an aldehyde or ketone has found wide application in bioconjugation methods in large part due to its chemoselectivity. Reductive amination at the reducing end of a sugar or polysaccharide is less straightforward. Unlike proteins that can have an aldehyde or ketone artificially introduced, the aldehyde functionality in sugars exists as a transient species in equilibrium between the open and closed form. Furthermore, the imine formation under acidic conditions between the amine and carbonyl is in an equilibrium that favors the free carbonyl. The irreversible covalent linkage is finally formed when an excess of the reducing agent, sodium cyanoborohydride, is added to the reaction and traps the imine to result in a secondary alkyl amine. This reaction pathway is outlined in Scheme 1.

Scheme 9. Reductive amination at the reducing end of hyaluronic acid.

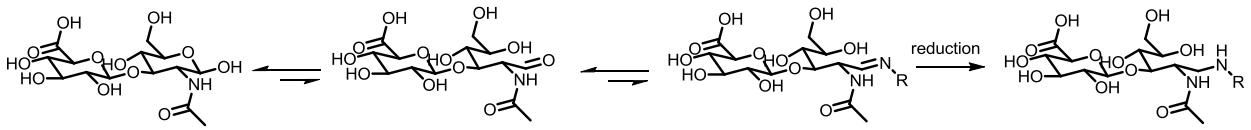

This process is further complicated when trying to create an amphilic lipid-HA conjugate. The lipid has very poor solubility in water and sparing solubility in most organic solvents. Conversely, HA is soluble in water or water-DMF and water-DMSO mixtures at elevated temperatures. Ultimately, conjugation between HA and a lipid such as distearoylphosphatidyl ethanol amine relies on the capture of a transient species by a molecule with poor solubility in the reaction medium. The result is a complex mixture of product, starting material, and byproduct that is difficult to purify and analyze. Alternative approaches to improving the efficiency of this reaction have been reported by the Szoka group wherein the HA is subjected to ozonolysis treatment to generate multiple permanent aldehyde moieties on the HA.[12] This is a valuable methodology that allows for reductive amination to occur at the nonreducing end of the sugar. However, it is still of great interest to find a robust and efficient reaction for forming lipid-HA conjugates only at the reducing end.

Oxime chemistry employs a similar mechanism to reductive amination chemistry except that α-effect nitrogen atoms such as those found in alkoxyamines and hydrazides tend to favor the imine form.[17] Many impressive feats in bioconjugation have been accomplished using this chemistry to link large and sophisticated biomolecules[18-20] and sugars.[21,22] Furthermore, recent efforts in organocatalysis have uncovered reaction conditions that favor rapid and efficient oxime formation.[23,24] In chapter 6, progress toward three different approaches for HA-lipid formation using oxime chemistry is discussed. The key design criteria for an avenue to HA-lipids are that the reactions are high yielding, site selective, simple to purify, and simple to characterize. HA-liposome carriers have shown tremendous promise thus far; but, a remaining obstacle preventing their clinical translation is the development of efficient and reproducible synthetic protocol. Once the synthetic protocol is established, a systematic investigation of the ability of different HA oligomer lengths to bind the CD44 receptor will be possible. This information will provide valuable insight in the design of an HA-targeted liposome with few and well-defined components.

Results and Dicussion

Synthesis of Alkoxyamine-Thiol Linker

In our initial approach toward HA targeted liposomes, the goal was to design a small molecule alkoxyamine containing a sulfhydryl moiety. The rationale for this target is that liposomes with maleimide groups on their surface are commercially available and commonly used for creating functionalized liposomes via the Michael addition between a sulfydryl and maleimde. Additionally, a small molecule HA label is attractive because a large excess can be used to quantitatively functionalize the reducing end of HA and the excess small molecule can be easily removed from the polysaccharide. Scheme 2 illustrates the synthetic pathway to an alkoxyamine-sulfhydryl molecule.

Scheme 2. Synthesis of thiol labeled HA.

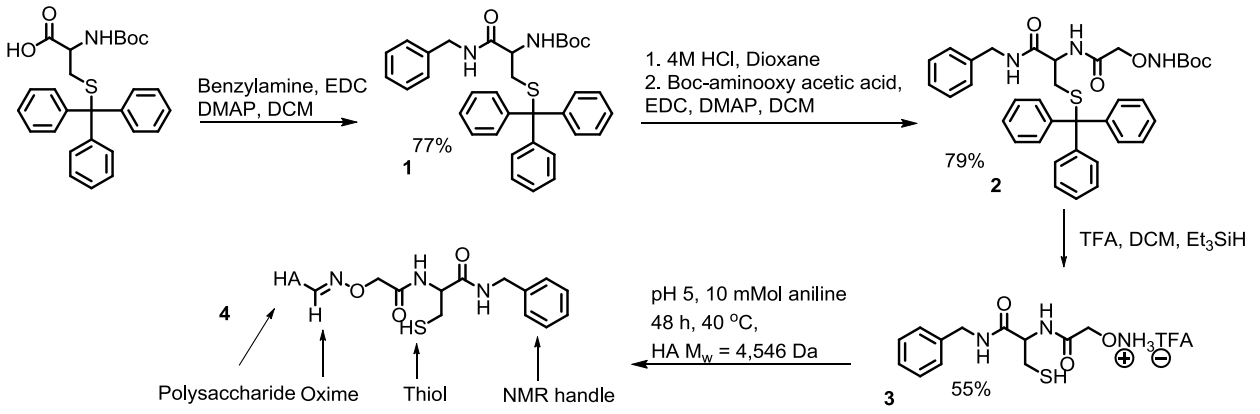

BocCys(Trityl)-OH was functionalized with benzylamine via an EDC mediated amidation reaction. Benzylamine was chosen because its aromatic protons would provide easy quantification of oxime formation by ^{1}H NMR. However, it should be noted that in future applications this carboxylic acid could be functionalized with a drug or imaging probe such as a tryrosine for PET imaging. The Boc group in compound **1** was cleaved using 4M HCl in anhydrous dioxane and then Boc-aminoxyacetic acid coupled onto the primary amine with an EDC mediated amidation reaction to give compound **2**. Global deprotection was achieved by treating **2** with trifluoroacetic acid in dichloromethane with triethylsilane as a cation scavenger. Compound **4** was prepared by reacting 15 equivalents of **3** with HA (M_w = 4,546) in a 100 mMol pH 5 acetate buffer spiked with 10 mMol aniline as a catalyst at 40 ˚C for 48 h. The reaction was then precipitated into methanol twice and then redissolved in water and passed through a PD-10 desalting column. The extent of HA functionalization was approximated to be 70% by comparing the NMR integrations of the acetamide methyl groups and the aromatic peaks on compound **3**. The proton attached to the sp^2 carbon of the oxime can also be integrated; however, because the oxime exists in the *syn* and *anti* comformations this proton's signal is spread over two resonances and ultimately too close to the baseline noise to be accurately integrated.

The sulhydryl functionalized HA molecule, **4**, was passed onto collaborators at UCSF to carry out the conjugation between the HA and the maleimide functionalized liposomes. The sulfhydryl functional group reacts rapidly and efficiently with a maleimide at pH 6-8. Unfortunately, no reaction took place between **4** and the functional liposomes. This was evidenced by no change in the surface charge the liposomes after the reaction and no enhanced internalization by cells with overexpressed CD44 receptors. If the liposome is functionalized with even a low density of the polyanionic targeting ligand, we would expect a negative surface charge on the liposome and enhanced binding to the cells overexpressing CD44. Possible reasons for not observing any HA conjugation include that the thiol on **4** had oxidized upon storage, or perhaps in aqueous media **4** adopts a rigid conformation that shields the sulfhydryl group and thereby limits access to the reactive maleimide groups on the surface of the liposomes.

Synthesis of Lipid-PEG-HA Conjugates

In a second approach, we aimed to prefabricate an HA-lipid conjugate prior to liposome formulation. This will guarantee HA incorporation onto the liposome. One way to improve the reaction between the lipid, distearoylphosphatidylethanolamine (DSPE) and HA is to somehow

enhance their solubilities. This is achieved by installing a poly(ethylene) glycol (PEG) spacer between the lipid and the alkoxyamine as outlined in Scheme 3.

Scheme 3. Synthesis of DSPE-PEG-Alkoxyamine.

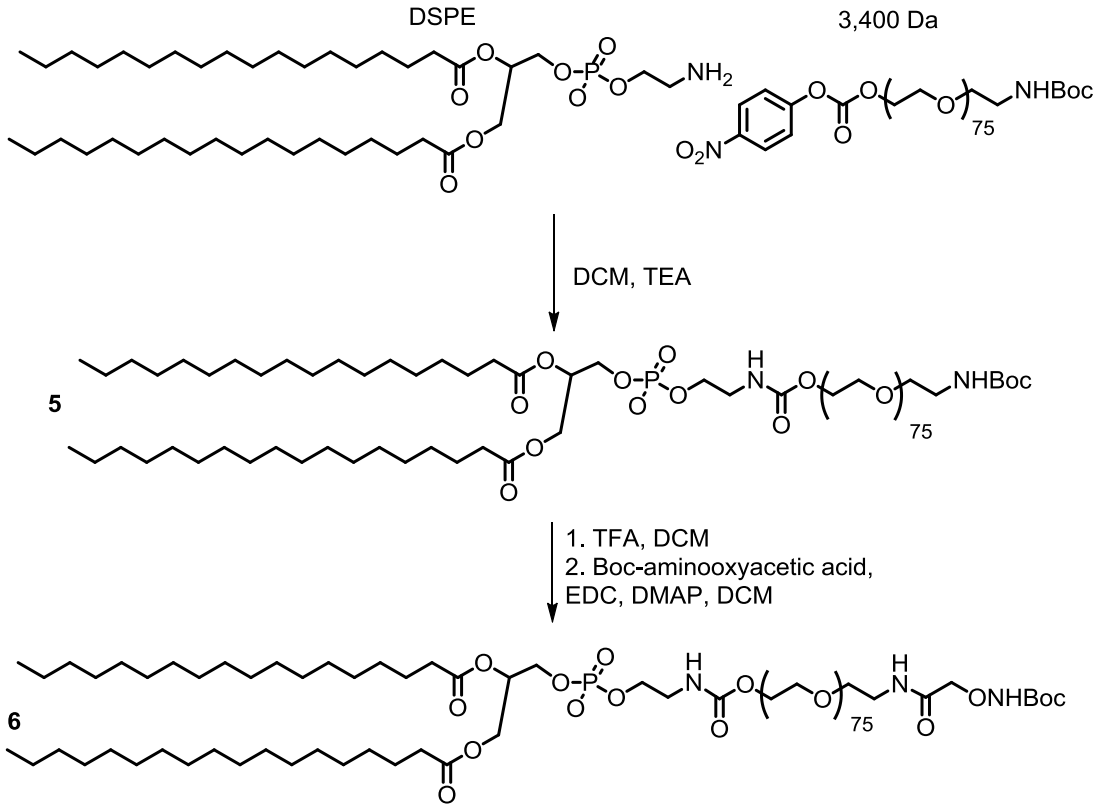

The primary amine on DSPE reacted very efficiently with the *para*-nitrophenyl activated carbonate of heterobifunctional PEG to give **5**. The Boc group on the other end of the PEG chain was subsequently deprotected and the protected alkoxyamine was installed using a carbodiimide coupling. The protecting group on the alkoxyamine of **6** was removed to give compound **6a**, a water soluble lipid-PEG-alkoxyamine well suited to form an oxime with the reducing end of HA under aqueous conditions. We chose to use an HA oligomer of 24 monosaccharides in length for our initial studies. This is shown in Scheme 4, where the oxime formation conditions are very similar to the conditions used in Scheme 2.

Scheme 4. Attachment of lipid-PEG-alkoxy amine to HA Mw 4,546.

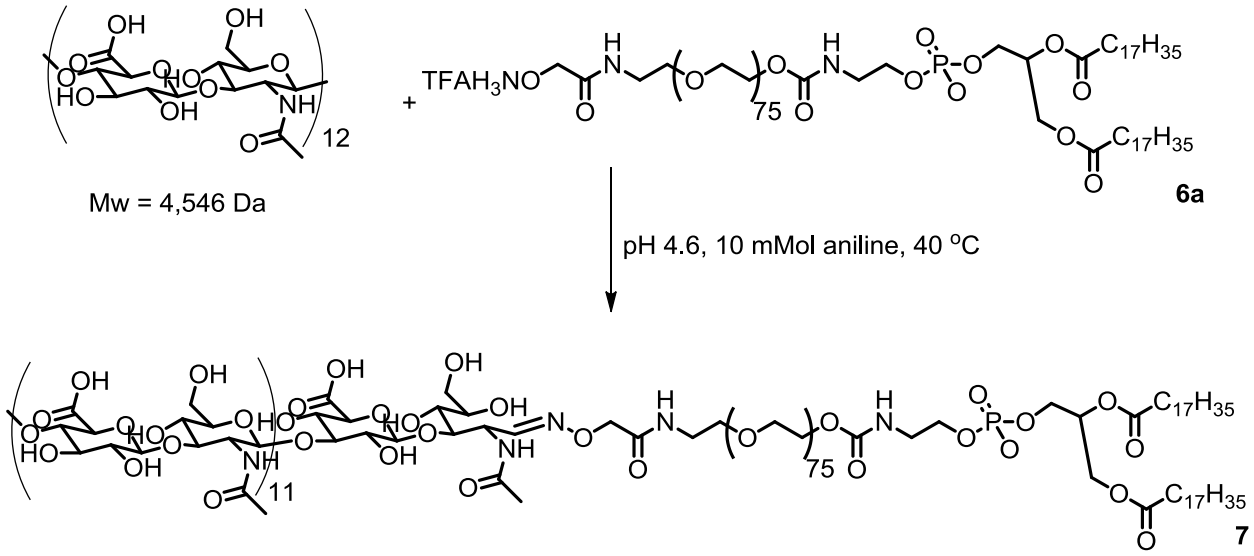

Characterization of lipid-PEG-HA and in vitro cell binding assay

The size and surface charge characterization of compound **7** was measured using dynamic light scattering in pH 7.1 2-(*N*-morpholino)ethanesulfonic acid (MES) buffer. As a comparison, the amphiphile **6a** was tested under the same conditions. Compound **6a** had an average particle size of 118 nm and a zeta potential of -2.97 mV. Compound **7** had an average particle size of 161 nm and a zeta potential of -25.83 mV. This large shift toward a more negative surface charge is strong evidence that liposomes with polyanionic HA at their surface have been produced.

It was of great interest to prepare actual liposomes with a low density of **7** incorporated and determine if there was enhanced cell binding and uptake. This was done by preparing liposomes with rhodamine dye and 1% of **7** incorporated and incubating C26 tumor cells for 2 hours. The cells were then washed and viewed under a red fluorescence field. Control liposomes were prepared with dipalmitoyl phosphatidylglycerol (DPPG) instead of **7**. Figure 1 shows the control and targeted liposomes at 20x magnification. Figure 1a is the non-targeted liposome control under normal field to view the cells. When viewed under red fluorescence field (Figure 1b) the cells are no longer visible, which suggests that the rhodamine labeled liposomes have not bound to the surface or been internalized by the cancer cells. However, the cells shown in Figure 1c and Figure 1d show compelling evidence that the HA targeted liposomes are bound and internalized by the cancer cells after only 2 hours of exposure.

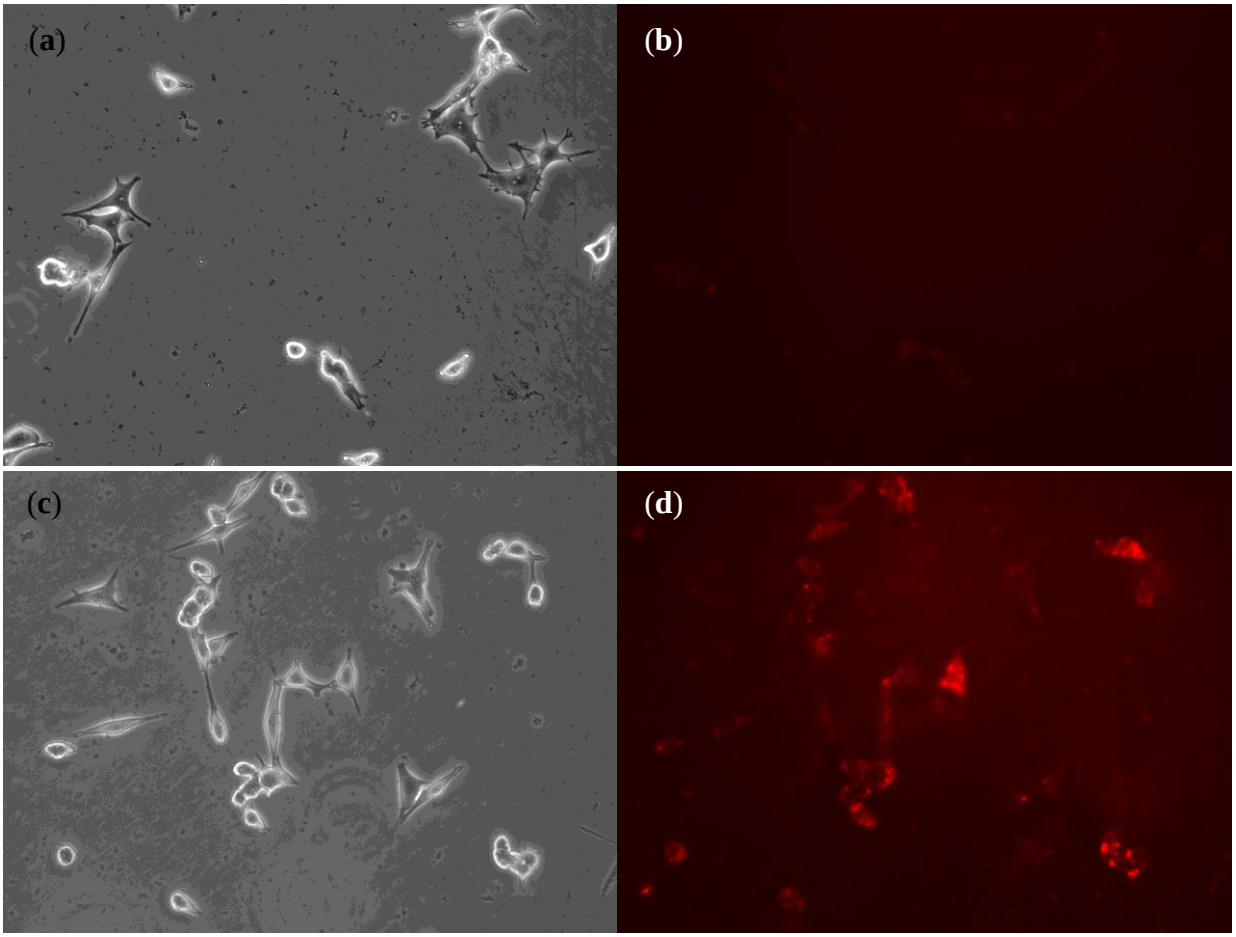

Figure 3. Images of cells incubated with liposomes containing a rhodamine tracer at 20x magnification. (a) DPPG labeled lipsome under normal field. (b) DPPG labeled liposome under red field. (c) **7** labeled liposomes under normal field. (d) **7** labeled liposomes under red field.

Synthesis of DSPE-HA Conjugates

The synthesis of DSPE-PEG-alkoxyamine **6** is a valuable molecule because it allows access to many different potential glycolipid constructs. However, we were also interested in exploring direct attachment of a lipid-alkoxyamine to HA (Scheme 5). This approach is potentially more attractive as it requires fewer synthetic steps and does not require a sophisticated heterobifunctional PEG starting material. This was accomplished by preparing the *N*-hydroxy succinate of Boc-aminoxyacetic acid, **8**. Compound **9** was prepared by treating **8** with DSPE in chloroform with triethylamine at 40 ˚C. The Boc group on **9** was deprotected to furnish an alkoxyamine-lipid suited to react with the reducing end of HA M_w = 1,535 Da. This is done using the similar conditions as those used to prepare **7** except that one drop of the phase transfer catalyst, Aliquat 336, was added to aid in solubilizing the lipid alkoxy amine. The reaction mixture is then loaded directly onto a PD-10 desalting column, eluted with water and lyophilized. The resulting lipid was dissolved in pH 7.1 MES buffer and the particle size and surface potential were measured to be 146 nm and -32.2 mV respectively.

Scheme 5. Direct attachment of DSPE to HA using oxime ligation.

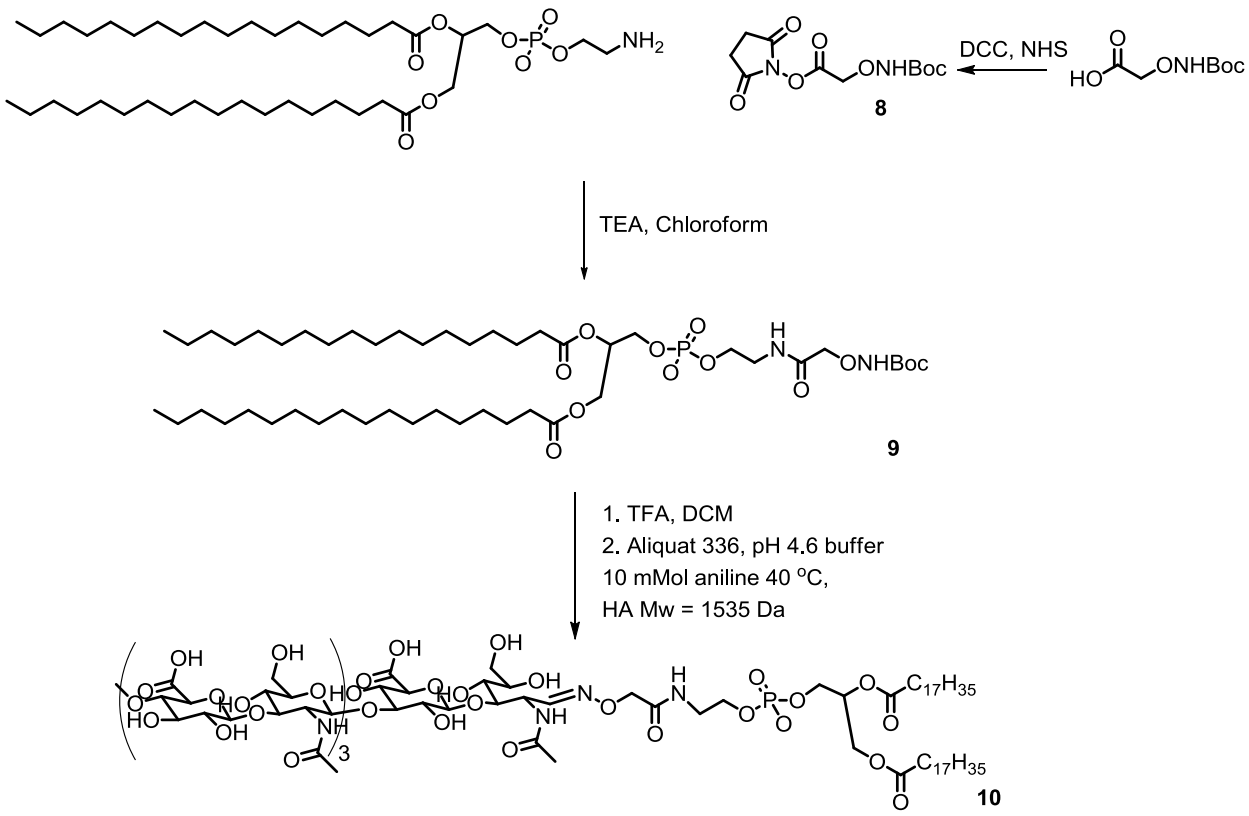

The cell binding experiment for **10** was carried using the same procedure as for **7**. However, in this case the HA is shorter and there is no PEG spacer to increase how far the HA ligand extends beyond the surface of the liposome. Figure 2a and Figure 2b are the images from the control liposomes containing no HA. As expected, there is not a significant amount of cell binding or internalization. Figure 2c and 2d are the images from liposomes containing the HA-lipid **10**. These images indicate that there is no enhanced cell uptake when the liposome is decorated with HA lipids that are only eight monosaccharides in length.

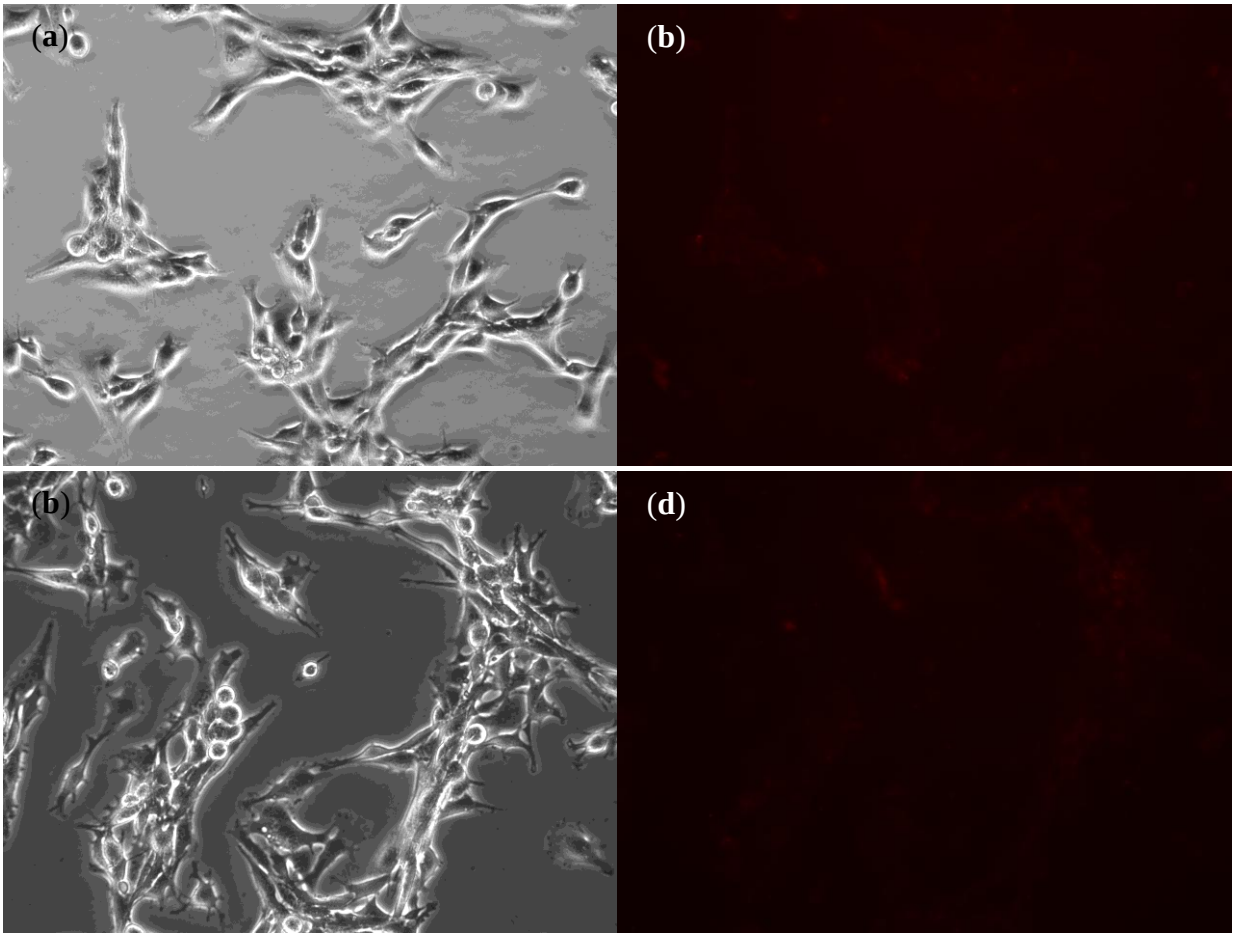

Figure 2. Images of cells incubated with liposomes containing a rhodamine tracer at 20x magnification. (a) DPPG labeled lipsome under normal field. (b) DPPG labeled liposome under red field. (c) **10** labeled liposomes under normal field. (d) **10** labeled liposomes under red field.

Conclusion

The research described in Chapter 6 represents a promising start toward developing clinically relevant HA-targeted liposomes. A low loading of glycolipid **7** incorporated into a liposome increases cellular uptake by C26 colon carcinoma cells. This system benefits not only from extended circulation and high tumor accumulation via the EPR effect, but also the ability to avidly bind and enter a wide range of cancer types that are known to overexpress CD44. The next phase of this project will involve making more DSPE-PEG-HA conjugates with HA lengths between 8 and 24 monosaccharides in length in order to find the shortest HA that will provide enhanced binding to cells that over express CD44 but not bind to normal cells. The collaboration between the Fréchet and Szoka groups toward this goal is ongoing.

Materials and Methods

Materials. Reagents and solvents were purchased from commercial suppliers without further purification. Hyaluronic acid oligomers were kindly provided by the Szoka group at UCSF where they were produced according to a literature procedure.[12]

Characterization. NMR spectra were recorded on Bruker AV 300, AVB 400, AVQ 400, or DRX 500 MHz instruments. MALDI-TOF MS was performed on a PerSeptive Biosystems Voyager-DE using 2,5-dihyroxybenzoic acid (DHB) as a matrix. Samples were prepared by diluting lipid solutions (~1 M) 40-fold in 100 mM matrix solutions in chloroform:methanol 70:30 and spotting 0.5 μL on the sample plate. DLS experiments were carried out on a Zetasizer (Malvern Instruments, UK).

Synthesis of HA-lipid molecules

Synthesis of 1. BocCys(Trityl)-OH (1 g, 2.2 mmol) and 4-dimethylaminopyridine (DMAP) (26 mg, 0.22 mmol) were added to a 20 mL reaction vial under nitrogen atmosphere and dissolved in dichloromethane (5 mL). Benzylamine (353 μL, 3.24 mmol) was added via syringe and the solution was cooled to 0˚ C. 1-ethyl-3-(3-dimethylaminopropyl) carbodiimide) (EDC) (536 mg, 2.80 mmol) was added and the reaction stirred overnight as it gradually warmed to room temperature. The reaction was then diluted with 100 mL of ethyl acetate and washed with two 50 mL portions of 1M $NaHSO_4$ and one 50 mL portion of brine. The organic layer was then concentrated under reduced pressure and purified by flash chromatography with 33% ethyl acetate in hexanes as an eluent to give 970 mg of a white foam in 81% yield. ^{1}H NMR (400 MHz, $CDCl_3$): δ 1.44 (s, 9H), 2.61-2.81 (m, 2H), 4.35-4.54 (m, 2H), 5.80 (d, *J* = 6.8 Hz, 1H), 6.57 (s, 1H), 7.23-7.34 (m, 14H), 7.47-7.49 (m, 6H). ^{13}C NMR (100 MHz, $CDCl_3$): δ 28.32, 34.06, 43.42, 53.70, 67.17, 80.20, 126.91, 127.42, 127.66, 128.10, 128.61, 129.63, 137.96, 144.51, 155.44, 170.49.

Synthesis of 1a. Compound **1** (870 mg, 1.57 mmol) was added to a 20 mL reaction vial under nitrogen atmosphere. Hydrochloric acid 4M in anhydrous dioxane (5 mL) was added via syringe and the reaction stirred at room temperature for 3h. The solvent was then removed under reduced pressure and the residual glassy solid was used in the next step without further purification. ^{1}H NMR (400 MHz, MeOD): δ 2.55-2.67 (m, 2H), 3.71-3.75 (m, 1H), 4.27-4.54 (m, 2H), 7.21-7.37 (m, 20H).

Synthesis of 2. Compound **1a** (186 mg, 0.38 mmol), Boc-aminooxy acetic acid (67 mg, 0.35 mmol), and DMAP (17 mg, 0.014 mmol) were added to a 20 mL reaction vial under nitrogen atmosphere. Dichloromethane (3mL) was added and the solution was cooled to 0˚ C. EDC (84 mg, 0.44 mmol) was added and the reaction was allowed to warm to room temperature and stirred overnight. The reaction was then diluted with 50 mL of ethyl acetate and washed with three 50 mL portions of 1M $NaHSO_4$, three 50 mL portions of saturated $NaHCO_3$ and one 50 mL portion of brine. The organic layer was dried over Na_2SO_4 and the solvent was removed by rotary evaporation to give 188 mg of white solid in 79% yield. ^{1}H NMR (400 MHz, $CDCl_3$): δ 1.40 (s, 9H), 2.67-2.85 (m, 2H), 4.09-4.36, (m, 5H), 6.67 (s, 1H), 7.17-7.28 (m, 14H), 7.41-7.50 (m, 6H), 8.00 (s, 1H). ^{13}C NMR (100 MHz, $CDCl_3$): δ 27.97, 43.22, 52.32, 67.00, 75.92, 82.95, 126.68, 127.17, 127.39, 127.76, 127.89, 128.41, 129.51, 137.81, 144.34, 157.48, 168.88, 169.64.

Synthesis of 3. Compound **2** (5 g, 8.0 mmol) was added to a 100 mL round bottom flask under nitrogen atmosphere. A premixed solution containing dichloromethane (15 mL) trifluoroacetic acid (15mL) and triethylsilane (1 mL) was added via syringe and the reaction stirred at room temperature for 3 h. The solvents were removed under rotary evaporation and the residual solid was purified by column chromatography using a gradient eluent from 0% to 10% methanol in

dichloromethane to give 1.550 g of a glassy solid in 51% yield. ^{1}H NMR (400 MHz, MeOD): δ 2.89-2.99 (m, 2H), 4.17 (s, 2H), 4.36-4.40 (m, 2H), 4.57-4.64 (m, 1H), 7.23-7.30 (m, 5H). ^{13}C NMR (100 MHz, MeOD): δ 26.52, 43.64, 55.92, 74.62, 127.71, 127.98, 129.00, 139.05, 171.41, 172.66.

Synthesis of 4. Hyaluronic acid (50 mg, 11 µmol), and compound **3** (67 mg, 176 µmol) were added to a 20 mL reaction vial and dissolved in 100 mM acetate and 10 mM aniline buffer (pH 5, 2 mL) the reaction was heated to 40˚ C and stirred for 2 days. Methanol (10 mL) was added and the precipitate was collected by filtration. The solid was redissolved in water and precipitated into methanol again. The solid was then dissolved in distilled water and passed through a PD-10 desalting column to give 48 mg of a fluffy white solid. ^{1}H NMR (400 MHz, D_2O): δ 1.99 (s, 36H), 2.93-2.95 (m, 1.33H), 3.31-3.34 (m, 21H), 3.46-3.90 (m, 128H), 4.45-4.54 (m, 28H), 6.85 (d, *J* = 4.8 Hz, 0.3H), 7.29-7.38 (m, 3.6H), 7.71 (d, *J* = 4.4 Hz, 0.5H).

Synthesis of 5. Distearoylphosphatidylethanolamine (16.7 mg, 22 µmol) and *para*-nitrophenyl-$PEG_{3,400Da}$-Boc (68.8 mg, ~20.2 µmol) were added to a 20 mL reaction vial under nitrogen atmosphere and dissolved in dichloromethane (2 mL) and triethylamine (100 µL) and stirred at 40˚ C overnight. The reaction was then cooled to room temperature and precipitated into diethyl ether. The white solid (84.4 mg) was collected and used without further purification. ^{1}H NMR (400 MHz, $CDCl_3$): δ 0.81 (t, *J* = 4.8 Hz, 6H), 1.14-1.84 (br m, 60H), 1.37 (s, 16H), 1.52 (br s, 4H), 2.22-2.23 (m, 4H), 3.24-3.92 (br m, 550H), 3.93-3.98 (br m, 2H), 4.01-4.1 (br s, 1H), 4.30-4.33 (m, 2H), 4.94-5.16 (m 3H).

Synthesis of 5a. Compound **5** (50 mg, 12.2 µmol) was added to a 20 mL reaction vial under nitrogen atmosphere and a premixed solution containing dichloromethane (1 mL) and trifluoroacetic acid (1 mL) was added via syringe. The reaction stirred at room temperature for 1 h before the solvents were removed under reduced pressure. ^{1}H NMR (400 MHz, $CDCl_3$): δ 0.86 (t, *J* = 4.8 Hz, 6H), 1.14-1.84 (br m, 60H), 1.56 (br s, 4H), 2.26-2.31 (m, 4H), 3.24-3.92 (br m, 550H), 3.93-3.98 (br m, 2H), 4.01-4.1 (br s, 1H), 4.30-4.33 (m, 2H), 4.94-5.16 (m 3H).

Synthesis of 6. Compound **5a** (86.6 mg, 21 µmol), Boc-aminooxy acetic acid (24.3 mg, 121 µmol), and DMAP (5 mg, 41 µmol) were added to a 20 mL reaction vial under nitrogen atmosphere. Dichloromethane (2 mL) was added and the solution was cooled to 0˚ C. EDC (24 mg, 121 µmol) was added and the reaction was allowed to warm to room temperature and stirred overnight. The reaction mixture was transferred to a 3,500 MWCO dialysis bag in stirred in 1:1 methanol:dichloromethane with 4 solvent changes over 18 h. The contents were removed from the bad and the solvent was evaporated under reduced pressure to give 50 mg of white solid. ^{1}H NMR (400 MHz, $CDCl_3$): δ 0.85 (t, *J* = 5.6 Hz, 6H), 1.2- 1.28 (m, 58H), 1.33-1.36 (m, 6H), 1.43-1.47 (br m, 12H), 1.48-1.51 (m, 6H), 2.25-2.29 (m, 4H), 2.76 (br s, 2H), 3.05-3.09 (m, 4H), 3.43-3.79 (br m, 430H), 3.91-4.00 (m, 4H), 4.12-4.20 (m, 2H), 4.35-4.40 (m, 3H).

Synthesis of 6a. Compound **6** (79 mg, 19 µmol) was added to a 20 mL reaction vial under nitrogen atmosphere and a premixed solution containing dichloromethane (1 mL) and trifluoroacetic acid (1 mL) was added via syringe. The reaction stirred at room temperature for 1 h before the solvents were removed under reduced pressure. NMR (400 MHz, $CDCl_3$): δ 0.87 (t,

J = 6 Hz, 6H), 1.22- 1.28 (m, 58H), 1.33-1.36 (m, 4H), 1.58 (br s 4H), 2.28-2.32 (m, 4H), 2.86 (br s, 2H), 3.15 (br m, 2H), 3.44-3.84 (br m, 500H), 4.10-4.35 (14H).

Synthesis of 7. Hyaluronic acid (35 mg, 7.7 µmol), and compound **6a** (28.1 mg, 6.9 µmol) were added to a 20 mL reaction vial and dissolved in 100 mM acetate and 50 mM aniline buffer (pH 4.6, 1 mL) the reaction was heated to 40˚ C and stirred for 2 days. Methanol (10 mL) was added and the precipitate was collected by filtration. The solid was redissolved in water and precipitated into methanol again. The solid was then dissolved in distilled water and passed through a PD-10 desalting column to give 40 mg of a fluffy white solid. NMR *note:the lipid peak intensities were attenuated as they were not well solvated in water* (500 MHz, D_2O): δ 1.28 (s, 5H). 2.01 (36H), 3.34-4.12 (br m, 200H), 4.45-4.55 (m, 24H).

Synthesis of 8. Boc-aminooxy acetic acid (515 mg, 2.69 mmol), *N*-hydroxy succinimide (325 mg, 2.83 mg), and dicyclohexyl carbodiimide were added to a 20 mL reaction vial under nitrogen atmosphere. A 1:1 premixed solution of ethyl acetate and dioxane was added via syringe. After 4 H at room temperature, the reaction mixture was filtered through a celite pad. Some dicyclohexyl urea was still present in the filtrate so it was filtered again through a 0.2 µm filter. ^{1}H NMR (400 MHz, $CDCl_3$): δ 1.39 (s, 9H), 2.77 (s, 4H), 4.77 (2H), 7.95 (s, 1H). ^{13}C NMR (100 MHz, $CDCl_3$): δ 25.67, 28.22, 70.87, 82.64, 156.44, 165.17, 168.90.

Synthesis of 9. Compound **8** (64 mg, 0.22 mmol) and DSPE (174 mg, 0.23 mmol) were added to a 20 mL reaction vial under nitrogen atmosphere. Chloroform (3 mL) and triethlyamine (90 µL) were added and the reaction stirred at 40 ˚C over night. The reaction mixture was diluted with ehtyl acetate and cooled to -20˚ C and then centrifuged at 10,000 RMP for 15 min. The supernatant was decanted and the residual pellet was analyzed by ^{1}H NMR. Interestingly, the precipitate was the unreacted DSPE and the supernatant contained the product as well as free *N*-hydroxy succinimide. ^{1}H NMR (400 MHz, $CDCl_3$): δ 0.84 (t, *J* = 7.2 Hz, 6H), 1.22- 1.28 (m, 58H),1.41 (s, 9H), 1.53 (br s, 4H), 2.21-2.27 (m, 4H), 3.44-3.49 (m, 2H), 4.0-4.5 (br m, 10H), 5.15-5.20 (m, 1H), 8.25 (s, 1H), 8.58 (s, 1H). Calc $[M]^+$ ($C_{48}H_{93}N_2O_{12}P$) *m/z* = 921.23. Found MALDI-ToF $[M+Na]^+$ *m/z* = 943.1.

Synthesis of 9a. Compound **9** (114 mg, 0.12 mmol) was added to a 20 mL reaction vial under nitrogen atmosphere and a premixed solution containing dichloromethane (1 mL) and trifluoroacetic acid (1 mL) was added via syringe. The reaction stirred at room temperature for 1 h before the solvents were removed under reduced pressure. ^{1}H NMR (400 MHz, $CDCl_3$): δ 0.83 (t, *J* = 7.2 Hz, 6H), 1.22- 1.28 (m, 58H), 1.54 (br s, 4H), 2.27-2.32 (m, 4H), 3.54 (br s, 2H), 4.01-4.16 (br m, 5H), 4.29-4.33 (m, 1H), 4.71 (s, 2H), 5.20 (m, 1H), 7.93 (s, 1H), 8.35 (s, 1H). Calc $[M]^+$ ($C_{43}H_{85}N_2O_{10}P$) *m/z* = 821.12. Found MALDI-ToF $[M+Na+K]^+$ *m/z* = 884.4

Synthesis of 10. Hyaluronic acid (Mw = 1,535 Da) (8 mg, 12.7 µmol), and compound **9a** (11.6 mg, 12.6 mmol) were added to a 20 mL reaction vial and dissolved in 100 mM acetate and 50 mM aniline buffer (pH 4.6, 1 mL). One drop of Aliquat 336 was added and then reaction was heated to 40˚ C and stirred for 2 days. The reaction mixture loaded directly onto a PD-10 desalting column and lyophilized to give 10 mg of a fluffy white solid. NMR *note:the lipid peak intensities were attenuated as they were not well solvated in water* (500 MHz, D_2O): δ 0.87-0.98

(br m, 6H),), 1.22- 1.28 (m, 30H), 2.03 (s, 12H), 3.2-4.1 (overlapping multiplets, (50H), 4.46-4.57 (m 8H), 6.85 (br d, 0.64H), 7.28 (br t, 0.38H).

Dynamic Light Scattering Experiments. HA-lipid samples were dissolved at 1 mg/ml in 25 mM MES buffer at pH 7.1 and filtered through a 0.45 μm filter and measured for zeta potential and size.

Preparation of Liposomes. Liposomes composed of 1,2 dipalmitoyl-*sn*-glycero-3-phosphotidaylchloine (DSPC):cholesterol:Targeting lipid 60:40:1 with 0.2% of the fluorescent label, Rhodamine-dipalmitoylphosphatidylethanolamine. The targeting lipids used were compound **7**, compound **10**, or dipalmitoyl phosphatidylglycerol as a negative control. The liposomes were rehydrated in 1 mL of 20 mM HEPES buffer, 130 mM Sodium Chloride pH 7.4, followed by vortexing for 1 min and sonifaction at 65 ˚C for 30 min under argon. The liposomes were extruded through 0.2 and 0.1 μm polycarbonate membranes successively to produce liposomes of approximately 110 nm.

Cell Binding Experiments. C26 colon carcinoma cells were cultured in MEM Eagle's with Earle's BSS containing 1% fetal bovine serum, 1% non-essential amino acids, and 1% sodium pyruvate. Cells (2×10^5) were placed in each well of a 6 well plate and grown overnight at 37 ˚C and 5% CO_2 in complete medium. The cells should be at 50-80% confluency before starting. The cells were rinsed once with FBS free medium. Medium containing liposomes was added and the cells were incubated at 37 ˚C for 2 h. The medium was then removed and the cells were washed with three successive aliquots of 1 mL ice cold PBS. The same medium was then added but without phenol red and FBS. The cells were then visualized under a fluorescence microscope (Eclipse TS100, Nikon, Japan). Images were taken with a SPOT RT camera (Diagnostic Instruments, Sterling Heights, MI) and processed using SPOT RT softare.

References

(1) Bangham, A. D. *Nature* **1961**, *192*, 807-808.
(2) Naor, D.; Nedvetzki, S.; Golan, I.; Melnik, L.; Faitelson, Y. *Crit Rev Clin Lab Sci* **2002**, *39*, 527-79.
(3) Platt, V. M.; Szoka, F. C. *Mol Pharmaceut* **2008**, *5*, 474-486.
(4) Luo, Y.; Prestwich, G. D. *Bioconjugate Chem* **1999**, *10*, 755-763.
(5) Luo, Y.; Ziebell, M. R.; Prestwich, G. D. *Biomacromolecules* **2000**, *1*, 208-18.
(6) Luo, Y.; Bernshaw, N. J.; Lu, Z. R.; Kopecek, J.; Prestwich, G. D. *Pharmaceut Res* **2002**, *19*, 396-402.
(7) Peer, D.; Margalit, R. *Neoplasia* **2004**, *6*, 343-353.
(8) Peer, D.; Margalit, R. *Int J Cancer* **2004**, *108*, 780-789.
(9) Eliaz, R. E.; Szoka, F. C., Jr. *Cancer Res* **2001**, *61*, 2592-601.
(10) Eliaz, R. E.; Nir, S.; Szoka, F. C., Jr. *Methods Enzymol* **2004**, *387*, 16-33.
(11) Eliaz, R. E.; Nir, S.; Marty, C.; Szoka, F. C., Jr. *Cancer Res* **2004**, *64*, 711-8.
(12) Ruhela, D.; Riviere, K.; Szoka, F. C. *Bioconjugate Chem* **2006**, *17*, 1360-1363.
(13) Mahoney, D. J.; Aplin, R. T.; Calabro, A.; Hascall, V. C.; Day, A. J. *Glycobiology* **2001**, *11*, 1025-33.

(14) Banerji, S.; Ni, J.; Wang, S. X.; Clasper, S.; Su, J.; Tammi, R.; Jones, M.; Jackson, D. G. *J Cell Biol* **1999**, *144*, 789-801.
(15) Zhou, B.; Weigel, J. A.; Fauss, L. A.; Weigel, P. H. *J Biol Chem* **2000**, *275*, 37733-37741.
(16) Fraser, J. R. E.; Laurent, T. C.; Laurent, U. B. G. *J Intern Med* **1997**, *242*, 27-33.
(17) Sander, E. G.; Jencks, W. P. *J Am Chem Soc* **1968**, *90*, 6154-6155.
(18) Gaertner, H. F.; Rose, K.; Cotton, R.; Timms, D.; Camble, R.; Offord, R. E. *Bioconjugate Chem* **1992**, *3*, 262-268.
(19) Canne, L. E.; Ferredamare, A. R.; Burley, S. K.; Kent, S. B. H. *J Am Chem Soc* **1995**, *117*, 2998-3007.
(20) Mahal, L. K.; Yarema, K. J.; Bertozzi, C. R. *Science* **1997**, *276*, 1125-1128.
(21) Richard, A.; Barras, A.; Ben Younes, A.; Monfilliette-Dupont, N.; Melnyk, P. *Bioconjugate Chem* **2008**, *19*, 1491-1495.
(22) Beaudette, T. T.; Cohen, J. A.; Bachelder, E. M.; Broaders, K. E.; Cohen, J. L.; Engleman, E. G.; Frechet, J. M. J. *J Am Chem Soc* **2009**, *131*, 10360-10361.
(23) Dirksen, A.; Hackeng, T. M.; Dawson, P. E. *Angew Chem Int Edit* **2006**, *45*, 7581-7584.
(24) Thygesen, M. B.; Munch, H.; Sauer, J.; Clo, E.; Jorgensen, M. R.; Hindsgaul, O.; Jensen, K. J. *J Org Chem* **2010**, *75*, 1752-1755.